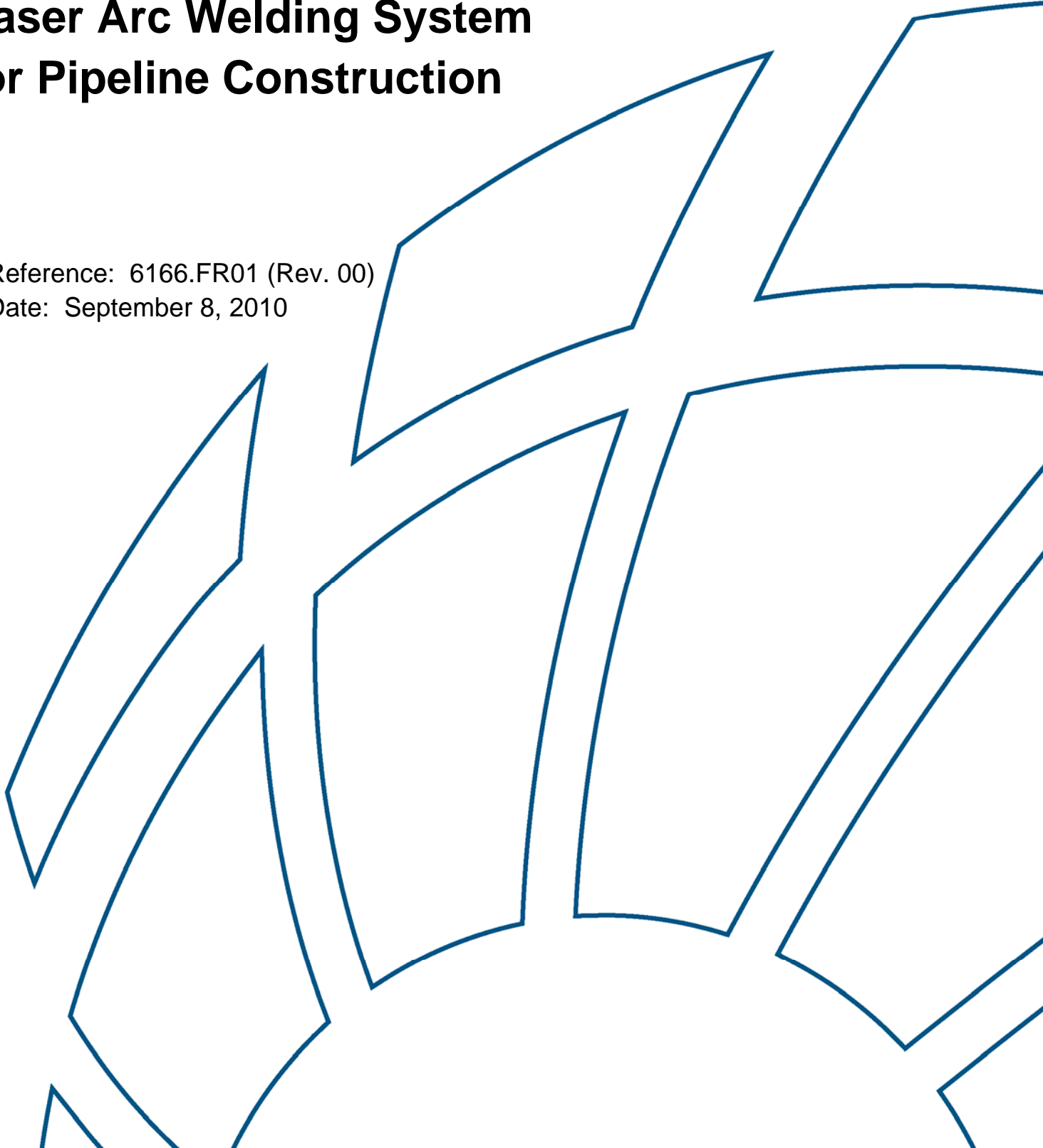


Development of a Hybrid Laser Arc Welding System for Pipeline Construction

Reference: 6166.FR01 (Rev. 00)
Date: September 8, 2010



DEVELOPMENT OF A HYBRID LASER ARC WELDING SYSTEM FOR PIPELINE
CONSTRUCTION

September 8, 2010

Submitted to:

US DEPARTMENT OF TRANSPORTATION
Pipeline and Hazardous Materials Safety Administration
1200 New Jersey Avenue, SE, 22-229
Washington, D.C. 20590-0001
U.S.A.

Submitted by:

BMT FLEET TECHNOLOGY LIMITED
311 Legget Drive
Kanata, ON
K2K 1Z8

BMT Contact: Darren Begg
Tel: 613-592-2830, Ext.229
Fax: 613-592-4950
Email: dbegg@fleetch.com

BMT Fleet Technology Limited accepts no liability for any errors or omissions or for any loss, damage, claim or other demand in connection with the usage of this report, insofar as those errors and omissions, claims or other demands are due to any incomplete or inaccurate information supplied to BMT Fleet Technology Limited for the purpose of preparing this report.

BMT DOCUMENT QUALITY CONTROL DATA SHEET

REPORT: Development of a Hybrid Laser Arc Welding System for Pipeline Construction

DATE: September 8, 2010

PREPARED BY:



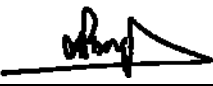
Darren Begg
Program Manager, Welding and Inspection

REVIEWED BY:



Rian Holdstock
Welding Engineer

APPROVED BY:



Nick Pussegoda
Senior Metallurgist

REVISION HISTORY RECORD

Revision No.	Date of Issue	Description of Change
00	September 8, 2010	Initial draft issue for team comment.

TABLE OF CONTENTS

ACRONYMS AND ABBREVIATIONS	x
1 INTRODUCTION	1
2 OBJECTIVES	2
3 BENEFITS	3
4 MARKET ASSESSMENT	4
5 PROGRAM OF WORK AND DELIVERABLES	5
5.1 Phase One (1) Work Plan.....	5
5.1.1 Task 1.1: Develop HLAW Equipment Specification and Design System and Components for a Full Production HLAW System	5
5.1.2 Task 1.2: Assemble the HLAW System Prototype.....	5
5.1.3 Task 1.3: Integrate System with the ALUT Components.....	5
5.1.4 Task 1.4: Evaluation of ALUT Effectiveness.....	5
5.1.5 Task 1.5: Welding Process Development	5
5.1.6 Task 1.6: System Activation and Testing	5
5.2 Phase Two (2) Work Plan.....	5
5.2.1 Task 2.1: HLAW Process Optimization and Procedure Qualification	5
5.2.2 Task 2.2: Implement and Validate HLAW System	6
5.2.3 Task 2.3: Develop Final System Specifications and Users Guide.....	6
5.2.4 Task 2.4: Calculate Return on Investment (ROI) of HLAW Compared to Current Practice	6
5.2.5 Task 2.5: Prepare and Submit Draft and Final Reports	6
6 RESULTS	7
6.1 Phase 1	7
6.1.1 Task 1.1 – Develop System Design and Equipment Specifications	7
6.1.2 Task 1.2 –Design and Acquire Primary System Components	8
6.1.3 Task 1.2 – Fabricate Project Specific Equipment and Software.....	8
6.1.4 Task 1.2 – Design and Implement Seam Tracking System	9
6.1.5 Task 1.2 – Design and Implement In-situ Process Monitoring, Control and Acquisition	9
6.1.6 Task 1.2 – Integrate and Test HLAW System	9
6.1.7 Task 1.3 – Acquire Primary Integration Components	11
6.1.8 Task 1.4 – Define Inspection System Requirements	11
6.1.9 Task 1.4 – Evaluate Weld Joint Inspection Capabilities.....	11
6.1.10 Task 1.4 – Develop Interpass, Surface, and Non-Contact UT Volumetric Inspection and Defect Detection.....	13
6.1.11 Task 1.5 – Welding Procedure Development Preliminary Lab Trials on Plate.....	14
6.1.12 Task 1.6 – Finalize Design of Field Deployable HLAW System.....	14
6.1.12.1 Clamp Assembly	15
6.1.12.2 Weld Head Assembly	18
6.1.12.3 Laser Safety Enclosure	29
6.1.12.4 Overall Integration and Cable Management.....	31

6.1.12.5	Detailed Drawings and Parts List	34
6.1.12.6	Conceptual Trailer Design.....	38
6.1.13	System Activation and Testing	48
6.2	Phase 2	50
6.2.1	Task 2.1 - HLAW Process Optimization	51
6.2.2	Task 2.1 – HLAW Procedure Qualification Testing and Research	56
6.2.2.1	Nick Break Results.....	57
6.2.2.2	Side Bend Results	57
6.2.2.3	Cross Weld Tensile Testing Results	57
6.2.2.4	All Weld Metal Tensile Testing Results	58
6.2.2.5	Charpy Impact Results – API 1104.....	70
6.2.2.6	Non-Standard Charpy Impact Test Development and Results	73
6.2.2.7	Crack Tip Opening Displacement (CTOD) Testing	107
6.2.2.8	Frontic Testing	136
6.2.2.9	Microhardness Testing	151
6.2.2.10	Microstructure Assessment	154
7	REFERENCES	161

LIST OF FIGURES

Figure 6.1:	Robotic Test Set-up for Plate and Pipe Welding	9
Figure 6.2:	Full Head Arrangement for Testing.....	10
Figure 6.3:	HLAW Head Flange	11
Figure 6.4:	Information Plot from Real Time Inspection.....	12
Figure 6.5:	Weld and Surface Inspection Test Report	13
Figure 6.6:	Macro of Root Passes in X80 – Left GMAW (CV) @ 65ipm Travel, Right GMAW (pulsed) @ 85ipm Travel.....	14
Figure 6.7:	HLAW Clamping Mechanism	16
Figure 6.8:	Adaptor Housing and Motor Coupling Designed to Connect to Rotary Actuator and Clamp	18
Figure 6.9:	ESAB Water-Resistant Jacket.....	20
Figure 6.10:	Brackets Designed for Mounting the Torch.....	22
Figure 6.11:	Mounting of Wire Feed to Clamp Assembly and Spool Feed Mount	24
Figure 6.12:	Seam Tracking and Weld Inspection Mount Brackets	26
Figure 6.13:	Local Light Shielding Design	29
Figure 6.14:	Laser Safety Enclosure	30
Figure 6.15:	Concept Orbital Energy Chain Designed by IGUS	32
Figure 6.16:	Full Integration of Orbital HLAW System with Laser Safety Enclosure	34
Figure 6.17:	TNT-ABB Default (Sheet 2 of 3)	35
Figure 6.18:	TNT-ABB Default (Sheet 3 of 3)	36
Figure 6.19:	TNT-ABB (BMT Orbital System Complete Parts List) (Sheet 1 of 3).....	37
Figure 6.20:	ESAB Tube Welding Trailer General Dimension and Layout Orbital Welder	39
Figure 6.21:	ESAB Tube Welding Trailer Driver Side General Dimension and Layout.....	40
Figure 6.22:	ESAB Tube Welding Trailer Top View General Dimension and Layout.....	41
Figure 6.23:	ESAB Tube Welding Trailer Rear Isometric View General Layout	42
Figure 6.24:	ESAB Tube Welding Trailer Rear Isometric View General Layout	43
Figure 6.25:	ESAB Tube Welding Trailer Resonator Containment Room General Dimension	44
Figure 6.26:	ESAB Tube Welding Trailer Resonator and Dampening System Layout.....	45
Figure 6.27:	ESAB Tube Welding Trailer Tent Saddle and Laser Alignment Tube Steel Construction.....	46
Figure 6.28:	ESAB Tube Welding Trailer Chiller Canopy General Setup	47
Figure 6.29:	Orbital Welding Set-up.....	48
Figure 6.30:	Orbital Set-up with ALUT Attachment	49
Figure 6.31:	Validation Test in the Lab.....	50
Figure 6.32:	Girth Weld Development.....	52
Figure 6.33:	Depth of Fill per Pass for X80	53
Figure 6.34:	Depth of Fill per Pass for X100	53
Figure 6.35:	Typical Face Bead Profile for X80	54
Figure 6.36:	Typical Root Bead Profile for X80.....	54
Figure 6.37:	Typical Face Bead Profile for X100	55
Figure 6.38:	Typical Root Bead Profile for X100.....	55
Figure 6.39:	Ten Pipe Sections Manufactured for Testing (Pipe Samples 498 to 508)	56
Figure 6.40:	Location of Test Specimens.....	57
Figure 6.41:	HLAW Weld Macros for (a) X80 and (b) X100 Pipe	59
Figure 6.42:	CAD drawing showing the tensile test specimen dimensions	60

Figure 6.43:	Views of Machined X80 Strip Tensile Test Specimens	61
Figure 6.44:	Machine Hounsfield Specimen	61
Figure 6.45:	Weld Root Side of an AWM Tensile Coupon	62
Figure 6.46:	Weld Metal Anomalies Inherent in Strip Tensile Specimens	62
Figure 6.47:	Etched End of Coupon/Hounsfield Specimen Centred Around Cross Hair	63
Figure 6.48:	Tensile Test Configuration	64
Figure 6.49:	Strip Tensile Stress-strain Curves for X100 Pipe Weld.....	66
Figure 6.50:	Strip Tensile Stress-strain Curves for X80 Pipe Weld.....	67
Figure 6.51:	Fracture Surface of Specimen 502-2 (X100)	67
Figure 6.52:	Fracture Surface of Specimen 507-2 (X80)	68
Figure 6.53:	Fracture Surface of X100 Hounsfield Specimen	69
Figure 6.54:	Weld 508 Impact Test Results – X80 (Subsize Specimens 8.3 mm).....	72
Figure 6.55:	Macrographs of the Sectioned Charpy Specimens from Weld 497	72
Figure 6.56:	Macrographs of the Sectioned Charpy Specimen from Weld 508	73
Figure 6.57:	HLAW Weld Cross Section for (a) X80 and (b) X100 Sample Materials	74
Figure 6.58:	Impacted Specimen Showing Both Shear (Outside) and Cleavage (Centre).....	75
Figure 6.59:	Illustration of Knife Edge Specifications for X80 Pressed Notch Trials.....	77
Figure 6.60:	Four Clock Positions Evaluated for Both X80 and X100 HLAJoints	78
Figure 6.61:	Notch Location of Weld Centreline Sample (Left) and HAZ (Right)	79
Figure 6.62:	Notch Location for HAZ (Left) and Weld Centreline (Right), as Seen from Root	79
Figure 6.63:	Conventional HAZ Charpy V-notch Testing.....	82
Figure 6.64:	Conventional WCL Charpy V-notch Testing	83
Figure 6.65:	Relationship Between HAZ Absorbed Energy and Percent Shear (X) for X80 Sample Material	84
Figure 6.66:	Relationship Between WCL Absorbed Energy and Percent Shear (X) for X80 Sample Material	85
Figure 6.67:	Pressed Notch HAZ Charpy V-notch Testing	86
Figure 6.68:	Pressed Notch WCL Charpy V-notch Testing.....	87
Figure 6.69:	Relationship Between HAZ Absorbed Energy and Percent Shear (X) for X80 Sample Material	88
Figure 6.70:	Relationship Between WCL Absorbed Energy and Percent Shear (X) for X80 Sample Material	89
Figure 6.71:	Conventional HAZ Charpy V-notch Testing for X100 HLAJoints	91
Figure 6.72:	Conventional WCL Charpy V-notch Testing for X100 HLAJoints.....	92
Figure 6.73:	Relationship between HAZ Absorbed Energy and Percent Shear (X) for X100 Sample Material	93
Figure 6.74:	Relationship between WCL Absorbed Energy and Percent Shear (X) for X100 Sample Material	94
Figure 6.75:	Inspected Surface Area	97
Figure 6.76:	Typical Notch Placement for Weld Centreline Samples	98
Figure 6.77:	Typical Notch Placement for Heat Affected Zone Samples.....	99
Figure 6.78:	Fracture Path Deviation from Weld Metal into Heat Affected Zone.....	100
Figure 6.79:	Fracture Path Deviation from Weld Metal into Base Material	101
Figure 6.80:	Fracture Path Deviation from Weld Metal into Heat Affected Zone and Base Metal	102

Figure 6.81:	Fracture Path Deviation from Heat Affected Zone.....	103
Figure 6.82:	Example – Weld Centreline Specimens where Test Results Were Not Consistent with Other Results for Same Material and Test Temperature	104
Figure 6.83:	H LAW Weld Macros for (a) X80 and (b) X100 Pipes.....	107
Figure 6.84:	Weld Fracture Toughness Specimen Geometry	108
Figure 6.85:	Notch Location Marked on the Through-thickness Plane of CTOD Specimen Blanks	110
Figure 6.86:	Typical EDM Notch Profile.....	110
Figure 6.87:	CTOD Test Set up.....	112
Figure 6.88:	Fracture Surface of Specimens 3W (left) and 6W (right) from X80 Pipe Weld	114
Figure 6.89:	Load-CMOD Plots of Specimens 3W (Left) and 6W (Right) from X80 Pipe Weld	114
Figure 6.90:	Macrographs of Specimens 3W (Left) and 6H (Right) from X100 Pipe Weld ..	115
Figure 6.91:	Fracture of Specimen 12-H5.....	117
Figure 6.92:	Macrograph of Specimen 12-H5 Showing Fatigue Crack Location.....	117
Figure 6.93:	Fracture of Specimens 3-W6 (Left) and 9-W1D (Right).....	119
Figure 6.94:	Macrographs of Specimens 3-W6 (Left) and 9-W1D (Right).....	120
Figure 6.95:	Fracture (Left) and Load-CMOD Plot (Right) of Specimen 3-H6	121
Figure 6.96:	Macrographs of Specimen 3-H6 – Fatigue Crack Location (Left) and Tracture Initiation Plane (Right)	122
Figure 6.97:	A Specimen from 9 O’clock Location	123
Figure 6.98:	Fracture (Left) and Load-CMOD Plot (Right) of Specimen 6-H5	125
Figure 6.99:	CTOD Transition Results from Pipe Weld 498 at 3 O’clock Location.....	126
Figure 6.100:	CTOD Transition Results from Pipe Welds 498 and 500 at 3 O’clock Location.....	127
Figure 6.101:	Fracture (Left) and Load-CMOD Plot (Right) of Specimen 6-H1	128
Figure 6.102:	Fracture (Left) and Load-CMOD Plot (Right) of Specimen 6-H3	129
Figure 6.103:	Macrographs of Specimen 6-H1	129
Figure 6.104:	Fracture (Left) and Load-CMOD Plot (Right) of Specimen 6-H2	130
Figure 6.105:	Macrographs of Specimen 6-H2	131
Figure 6.106:	Fracture (Left) and Load-CMOD Plot (Right) of Specimen 3-W3	132
Figure 6.107:	Fracture (Left) and Load-CMOD Plot (Right) of Specimen 3-H5	133
Figure 6.108:	Macrographs at Fatigue Crack (Left) and Fracture Initiation (Right) Planes of Specimen 3-H5.....	134
Figure 6.109:	Micrographs of Fracture Initiation Location in Specimen 3-H5 at Two Magnifications	134
Figure 6.110:	Measurement Location for 2h in Figure 11 [1].....	135
Figure 6.111:	X80, 1:30 Location Macro.....	136
Figure 6.112:	Plot for Layer 1-4, X80, 1:30 Location.....	137
Figure 6.113:	Plot for Layer 5, X80, 1:30 Location.....	138
Figure 6.114:	Plot for X80 BM, WM, GRHAZ, 1:30 Location.....	138
Figure 6.115:	X80, 4:30 Location Macro.....	139
Figure 6.116:	Plots of Layers 1-4, X80, 4:30 Location.....	140
Figure 6.117:	Plot for Layer 5, X80, 4:30 Location.....	141
Figure 6.118:	Plot for X80 BM, WM, GRHAZ, 4:30 Location.....	142
Figure 6.119:	X80, 7:30 Location Macro.....	143
Figure 6.120:	Plots for Layers 1-4, X80, 7:30 Location	144

Figure 6.121: Plot for Layer 5, X80, 7:30 Location	145
Figure 6.122: Plot for X80 BM, WM, GRHAZ, 7:30 Location	146
Figure 6.123: X80, 10:30 Macro	147
Figure 6.124: Plots for Layers 1-4, X80, 10:30 Location	148
Figure 6.125: Plots for layer 5, X80, 10:30 Location.....	149
Figure 6.126: Plot for X80 BM, WM, GRHAZ, 10:30 Location.....	150
Figure 6.127: Microhardness Mapping, X80, 1:30 and 4:30 Clock Positions	151
Figure 6.128: Microhardness Mapping, X80, 7:30 and 10:30 Clock Positions	152
Figure 6.129: Microhardness Mapping, X100, 1:30 and 4:30 Clock Positions	153
Figure 6.130: Microhardness Mapping, X100, 7:30 and 10:30 Clock Positions	154
Figure 6.131: Sample X80 1:30 Location	155
Figure 6.132: Sample X80 1:30 Location	156
Figure 6.133: Sample X80 7:30 Location	157
Figure 6.134: Sample X80, 7:30 Location	158
Figure 6.135: Sample X100, 1:30 Location	159
Figure 6.136: Sample X100, 7:30 Location	160

LIST OF TABLES

Table 6.1:	Welding Parameters for Flat Plate	14
Table 6.2:	Cables and Hoses to Traverse Conduit between Trailer and Safety Enclosure	31
Table 6.3:	Service Requirements	33
Table 6.4:	Cross Weld Tensile Results for Pipes 497 (X100) and 508 (X80).....	58
Table 6.5:	X80 and X100 Chemical Composition	65
Table 6.6:	X80 and X100 Tensile Test Results.....	65
Table 6.7:	X80 and X100 Yield and Tensile strength (UTS) from Micro-hardness Measurements, (MPa).....	70
Table 6.8:	Weld 497 Impact Test Results – X100 (Full Size Specimens 10 mm).....	71
Table 6.9:	Weld 508 Impact Test Results – X80 (Subsize Specimens 8.3 mm).....	71
Table 6.10:	Test Results for Conventional HAZ X80 Testing.....	85
Table 6.11:	Test Results for Conventional WCL X80 Testing.....	86
Table 6.12:	Test Results for Pressed Notch HAZ X80 Testing.....	90
Table 6.13:	Test Results for Pressed Notch WCL X80 Testing	90
Table 6.14:	Test Results for X100 HAZ Charpy Impact Testing	95
Table 6.15:	Test Results for X100 WCL Charpy Impact Testing.....	96
Table 6.16:	CTOD Results for X80 Pipe at -5°C for API 1104 Test Locations	113
Table 6.17:	CTOD Results for X100 Pipe at -5°C for API 1104 Test Locations	113
Table 6.18:	CTOD Results at -5°C for WCL Test Location.....	116
Table 6.19:	CTOD Results at -5°C for HAZ Test Location	116
Table 6.20:	CTOD Results at -40°C for WCL Test Location.....	118
Table 6.21:	CTOD Results at -40°C for HAZ Test Location	118
Table 6.22:	CTOD Results from 3 o'clock Location from X100 Weld.....	121
Table 6.23:	CTOD Results from 3 o'clock location from X80 Weld.....	124
Table 6.24:	Results for X80, 1:30 Location.....	137
Table 6.25:	Results of X80, 4:30 Location	139
Table 6.26:	Results of X80, 7:30 Location	143
Table 6.27:	Results, X80, 10:30 Location.....	147

ACRONYMS AND ABBREVIATIONS

δ_c	Failure type – fracture event from fatigue crack tip
δ_c^*	Failure type – pop-in detected
δ_m	Failure type – maximum load plateau reached
δ_u	Failure type – crack growth or stretch zone observed in fracture face
2D	Two Dimensional
3D	Three Dimensional
5G	Pipe Welding - Horizontal
ALUT	Automated Laser Ultrasonic Inspection
a_{min}	Minimum fatigue crack depth
amp	Ampere(s)
ANGTS	Alaska Natural Gas Transportation System
a_o	Average total crack length
API	American Petroleum Institute
Ar	Argon
AR	Accumulation of Relevant Indications
ASTM	American Society for Testing and Materials
AWM	All Weld Metal
BM	Base Material
BT	Burn Through
C	Cracks
CAD	Computer Aided-Design
CANMET	Canada Centre for Mineral and Energy Technology
CCD	Charge-Coupled Device
CCTV	Closed Circuit Television
cm	Centimetre(s)
CMOD	Crack Mouth Opening Displacement
CMOS	Complimentary Metal-Oxide Semiconductor
CO ₂	Carbon Dioxide
CP	Cluster Porosity
CSA	Canadian Standards Association
CTOD	Crack Tip Opening Displacement
DoT	Department of Transport
DT	Destructive Testing
EDM	Electro-Discharge Machining
ESI	Elongated Slag Inclusion
EU	Undercutting Adjacent to the Cover Pass
FOV	Field of View
FPD	Fracture Path Deviation
FTL	Fleet Technology Limited (now BMT Fleet Technology Limited)
GMA	Gas Metal Arc
GMAW	Gas Metal Arc Welding
GMAW-P	Pulsed Gas-Metal Arc Welding
H	Height
HAZ	Heat-Affected Zone

HB	Hollow Bead Porosity
HLAW	Hybrid Laser Arc Welding
Hz	Hertz
IC	Internal Concavity
ICP	Inadequate Cross Penetration
ID	Identification
ID	Inside Diameter
IEC	International Electrotechnical Commission
IF	Incomplete Fusion
IFD	Incomplete Fusion due to Cold Lap
IP	Inadequate Penetration without High-Low
IPD	Inadequate Penetration due to High-Low
ipm	Inches Per Minute
ISI	Isolation Slag Inclusions
IU	Undercutting Adjacent to the Root Pas
J	Joule(s)
JIP	Joint Industry Project
K _f	Maximum stress intensity factor
kg	Kilogram(s)
kJ	Kilojoule(s)
km	Kilometre(s)
ksi	Kips per Square Inch
KVA	Kilovolt-Ampere(s)
kW	Kilowatt(s)
L	Length
LB	Linear Buried
LOF	Lack of Fusion
LPH	Litre(s) per Hour
LS	Linear Surface
m	Metre(s)
MGP	Mackenzie Gas Pipeline
min.	Minute(s)
mm	Millimetre(s)
MPa	MegaPascal(s)
ms	Millisecond(s)
MTR	Materials Testing Reports
MTS	Clip Gauge Manufacturer
NDE	Non-Destructive Evaluation
NDT	Non-Destructive Testing
NIST	National Institute of Standards and Technology
NSC	Nippon Steel Corporation
OD	Outside Diameter
P	Porosity
PC	Personal Computer
ppm	Parts Per Million
psi	Pounds per Square Inch

R&D	Research and Development
ROI	Return on Investment
R-ratio	Minimum to maximum load ratio
RT	Radiographically Inspected
scfm	Standard Cubic Feet per Minute
sec	Second(s)
SOW	Scope of Work
T	Transverse
USDOT	United States Department of Transport
UT	Ultrasonic Testing
UTS	Ultimate Tensile Strength
V	Volt(s)
VAC	Volts Alternating Current
VC	Volumetric Cluster
VDC	Volts Direct Current
VI	Volumetric Indications
VR	Volumetric Root
VT	Visual Inspection
W	Watt(s)
W	Width
WCL	Weld Centreline
YS	Yield Strength
µm	Micrometre(s)

1 INTRODUCTION

The construction cost of large welded pipeline systems can represent half the project expenditures, and in many instances the welding costs are a major component. The control or reduction of these costs and rework to eliminate weld faults has been the focus of productivity enhancement efforts across a wide range of industries. To this end, laboratory research has investigated and made use of a number of technologies to improve weld quality and efficiency and facilitate inspection including:

- The use of lasers for cutting and joining of plate elements, in particular Hybrid Laser Arc Welding (HLAW) systems;
- Robotic systems with seam tracking technology to automate and control high speed welding processes; and
- Automated Laser Ultrasonic Inspection (ALUT) to detect, size, characterize, and assess the significance of weld defects at high speed and document the inspection results.

BMT Fleet Technology Limited assembled a Joint Industry Project (JIP) sponsorship team to support the integration of a mechanized HLAW system with ALUT (companion USDOT project) for the welding and inspection of pipeline systems. The project sponsors for this JIP include:

- US Department of Transportation (regulator);
- TransCanada Pipelines Limited (pipeline company);
- CHEVRON (oil and gas major);
- ExxonMobil (oil and gas major);
- Nippon Steel (steel maker);
- ESAB (welding equipment manufacturer);
- Applied Thermal Sciences (laser welding/seam tracking equipment consultant/R&D);
- Comau (robotics manufacturer);
- ABB (robotics manufacturer);
- Trumpf Inc (laser manufacturer);
- HighYAG (laser head manufacturer); and
- Intelligent Optical Systems (ALUT manufacturer).

2 OBJECTIVES

The technical objective of this program was to take lessons learned from the lab and input from industry sponsors to develop, test, and validate a “field ready” HLAW system for full circumferential girth welding of large diameter (NPS30 and above) high strength pipelines. Specific requirements were to produce welds:

- At high speeds to improve the economics of pipeline construction;
- For a narrow groove design with a high-quality geometry enhancing pipeline integrity;
- With strength and toughness properties that will support damage tolerance; and
- Maximizing joint-to-joint consistency with low defect repair rates for economy and integrity.

3 BENEFITS

The HLAW system, which includes a fibre delivered laser welding head, presents opportunities for cost savings from reductions in labour content, consumable consumption, joint preparation costs, and enhanced weld completion rates. The disc laser, such as the one used in this project, is particularly suitable for pipeline girth welding because the beam is delivered to the workstation through a single optical fibre, delivering high efficiency and thus enabling the development of more portable welding systems capable of single pass thick section welding. The power and penetration of laser welding systems present the opportunity to deposit high quality welds at high speeds and thus influence the economic viability of remote gas fields through lower cost pipeline construction. The value of this system can be improved through the integration of the ALUT equipment that will further automate and increase the efficiency of the welding system being developed and, therefore, allow for the increased speed of construction.

4 MARKET ASSESSMENT

The use of natural gas is growing worldwide and is expected to represent an increasing portion of the total energy supply. The gas resources that will be needed to accommodate this growing demand are in remote areas such as the Mackenzie Delta and Prudhoe Bay. Discussions on development of these gas reserves have been ongoing since the 1970s, and many factors have slowed or delayed those developments. One of the factors has been the high cost of pipeline construction, estimated at greater than \$4 billion for the Mackenzie Gas Pipeline (MGP, 1,200 km, Mackenzie Delta to northern Alberta) and \$16 billion for the Alaska Natural Gas Transportation System (ANGTS, 2,800 km, Prudhoe Bay to northern Alberta). Pipeline owners and operators have been pursuing a number of next generation pipeline technologies including; higher strength pipeline steels and fittings, multi-wire mechanized/automated welding, ultrasonic inspection, advanced coating systems, and alternative integrity validation processes.

The construction costs for a northern pipeline will represent approximately half the project costs. Construction of the northern pipelines will be extremely challenging with much of the work being carried out in harsh winter conditions at temperatures as low as -55°C . The welding costs are a major component of the overall construction costs and industry continues to seek future generation pipeline welding technologies to achieve additional improvements in productivity and enable significant cost savings. The financial support of this project by industry operators, fabricators, equipment vendors, and regulators illustrates the need or desire by the industry to develop this technology for pipeline construction.

HLAW is a technology that promises to increase the efficiency of welded fabrication. By incorporating automation and integrating an automated inspection system, the HLAW system will produce high-quality welds more quickly with fewer passes. This type of technological advancement is considered an essential requirement for the construction of pipelines to transport oil and gas from remote locations. It is also noted that shortages of trained welders and inspectors requires that tools, such as the HLAW system, be smarter and more efficient in order to make these projects viable.

5 PROGRAM OF WORK AND DELIVERABLES

The program was broken down into two phases of work as follows:

5.1 Phase One (1) Work Plan

5.1.1 Task 1.1: Develop HLAW Equipment Specification and Design System and Components for a Full Production HLAW System

This included the design and integration of the HLAW head, mechanized travel, seam tracking or torch positioning control design (software and hardware), closed loop feedback and process control systems, procedure data acquisition, and safety protocols and controls.

5.1.2 Task 1.2: Assemble the HLAW System Prototype

This included acquiring primary components; fabricating project application specific equipment and developing/implementing software; designing and implementing the seam tracking system for robotic manipulation; and designing and implementing in-situ process monitoring, control, and acquisition as part of the quality assurance and reporting system.

5.1.3 Task 1.3: Integrate System with the ALUT Components

This involved integrating the HLAW system with the custom-mounting hardware and testing the assembled components and software to ensure component communication as well as the effectiveness of system limit controls and safety systems.

5.1.4 Task 1.4: Evaluation of ALUT Effectiveness

This task confirmed previously defined performance of the ALUT system operating in tandem with the HLAW system by evaluating weldment inspection results on laboratory produced HLAW weldments.

5.1.5 Task 1.5: Welding Process Development

This task conducted preliminary lab trials of the HLAW system to evaluate the operation of the assembled system for a range of weld configurations and welding speeds.

5.1.6 Task 1.6: System Activation and Testing

This task completed full pipe welds in position, test clamping, test welding procedures on pipes to measure the efficiency of the welding system and the quality of the deposited welds.

5.2 Phase Two (2) Work Plan

5.2.1 Task 2.1: HLAW Process Optimization and Procedure Qualification

This task focused on defining the optimal HLAW procedures for 36 inch diameter grade X80 and X100 pipe. Weld quality was confirmed by standard testing procedures as well as through various research activities to determine if modifications to the standard testing specifications are required for the HLAW type of welds.

5.2.2 Task 2.2: Implement and Validate HLAW System

This task is an optional USDOT phase to modify the current HLAW system for field deployment, installing the system in custom field enclosures, and conducting full production girth welds in a production environment. This task will only be completed and reported when the additional funds are secured from the pipeline operators and other industry contributors, as well as from the USDOT.

5.2.3 Task 2.3: Develop Final System Specifications and Users Guide

A set of system specifications, including a detailed parts list of the HLAW system, were assembled and are included herein.

5.2.4 Task 2.4: Calculate Return on Investment (ROI) of HLAW Compared to Current Practice

This task will use project data to estimate the weld completion rates and thus the potential to improve productivity in pipeline construction using the HLAW process. It will extract data as acquired from Task 2.2 to produce a report showing the benefits and cost improvements when using HLAW over traditional pipeline welding processes and techniques.

5.2.5 Task 2.5: Prepare and Submit Draft and Final Reports

In addition to the final report, project results will be presented both to the project team and industry at related technical conferences.

6 RESULTS

6.1 Phase 1

As discussed above, Phase 1 was divided into a series of milestones as outlined below:

- Task 1.1 – Develop System Design;
- Task 1.1 – Develop Equipment Specification;
- Task 1.2 –Design and Acquire Primary System Components;
- Task 1.2 – Fabricate Project Specific Equipment and Software;
- Task 1.2 – Design and Implement Seam Tracking System;
- Task 1.2 – Design and Implement In-situ Process Monitoring, Control and Acquisition
- Task 1.2 – Integrate and Test HLAW System;
- Task 1.3 – Acquire Primary Integration Components;
- Task 1.4 – Define Inspection System Requirements;
- Task 1.4 – Evaluate Weld Joint Inspection Capabilities;
- Task 1.4 – Develop Non-Contact Ultrasonic Test (UT) Volumetric Inspection and Defect Detection;
- Task 1.5 – Welding Procedure Development Preliminary Lab Trials on Plate; and
- Task 1.6 – Finalize Design of Orbital HLAW System, System Activation, and Testing.

6.1.1 Task 1.1 – Develop System Design and Equipment Specifications

The first step into developing the HLAW system was to identify the design requirements for its operation. This system would need to be operated in harsh environments within a large temperature span; and in order to survive and operate in these conditions consistently, it would require a detailed engineering assessment of the components. The specification developed is included as Annex A.

With the completion of the equipment specification, details of the HLAW system design were finalized.

6.1.2 Task 1.2 –Design and Acquire Primary System Components

Solid models for an orbital drive unit were developed. All necessary additional components for the conversion of the system to orbital motion were acquired and/or fabricated. The intent was that the HLAW head could be changed out between an orbital drive and a robotic manipulator.

6.1.3 Task 1.2 – Fabricate Project Specific Equipment and Software

All the mounting hardware for the HLAW head assembly was completed and installed for the flat plate development. The software interface for the linear motion system was also completed. Modifications of tooling and software for out-of-position 1G welding of pipe sections were also completed.

Installation of a new ABB robotic platform was completed including the addition of an integrated rotational fixture. In addition, fixtures and mounting hardware for out-of-position 1G welding of pipe sections were fabricated and installed for lab trials. Figure 6.1 shows a solid model and actual test set-up of the robotic system used in the flat plate and pipe welding procedure development phases.

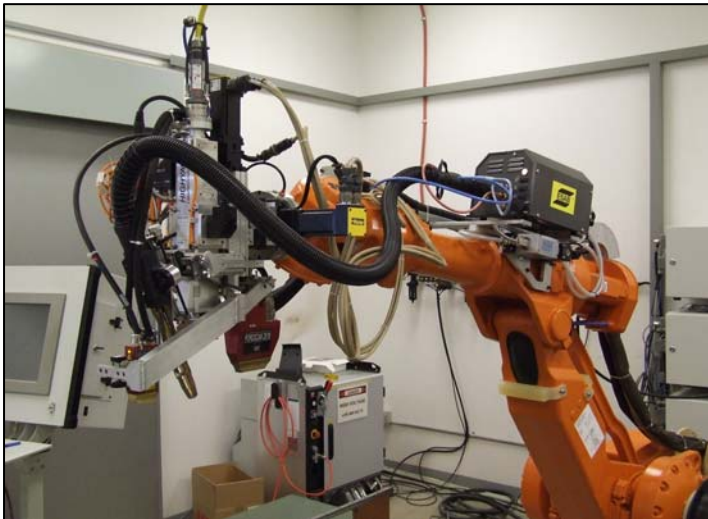
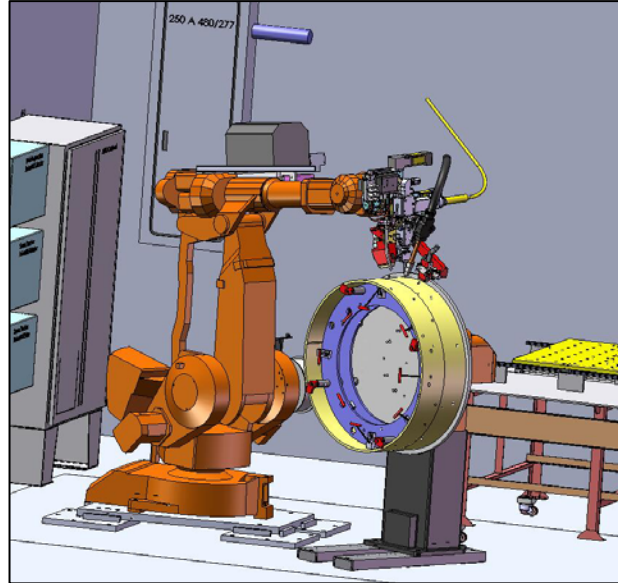


Figure 6.1: Robotic Test Set-up for Plate and Pipe Welding

6.1.4 Task 1.2 – Design and Implement Seam Tracking System

Full system testing of the seam tracking hardware was completed.

6.1.5 Task 1.2 – Design and Implement In-situ Process Monitoring, Control and Acquisition

Customizing of the control system software specifically for pipe welding was completed.

6.1.6 Task 1.2 – Integrate and Test HLAW System

Initial system start-up of the basic HLAW welding system was completed and all components were installed and verified with exception to the final motion system. Figure 6.2 shows the weld setup during testing.

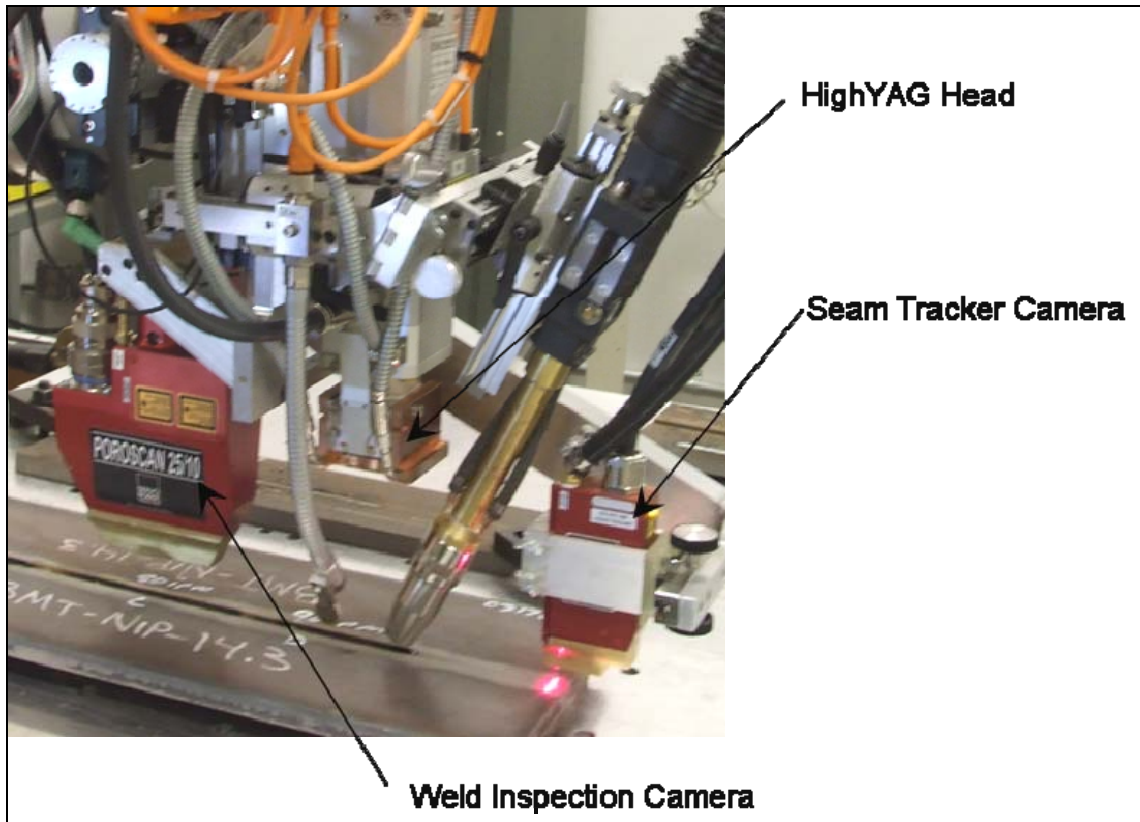


Figure 6.2: Full Head Arrangement for Testing

During the course of system runup, a number of laser operational faults occurred during trial weld operations. These eventually resulted in damage to the main delivery fibre optic cable. A test program was initiated to determine the cause of the fibre optic cable failure and to confirm that longer duration runs (~15 minutes) at 10 kW would not be a problem. Test data taken on HighYAG's BIMO-HP head suggests that there might have been excessive heating of the head in the flange area of the delivery fibre connection (see Figure 6.3). Temperatures of approximately 160°F were measured at 10 kW after running the system for a few minutes. After consultation with both HighYAG and Trumpf, it was revealed that the delivery fibre has a temperature limitation of 140°F. Whether this thermal heating result from head back reflection which causes the fibre optic cable tip to overheat, or whether problems from within the fibre optic cable caused the thermal heating was unknown. Similar measurements were made on an older model HighYAG head design with better cooling in this region. Temperature measurements under identical operations were below 120°F. HighYAG provided a design modification to the existing head, which subsequently provided better control of temperatures near the top.

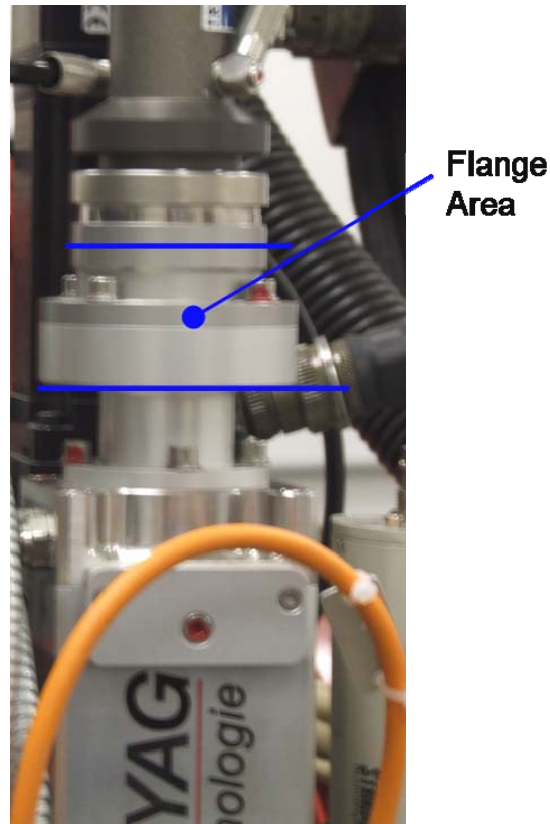


Figure 6.3: HLAW Head Flange

6.1.7 Task 1.3 – Acquire Primary Integration Components

Primary integration components for the weld system were acquired and installed. The weld head system interface for the orbital motion system was designed to be identical to that of the robotic system.

6.1.8 Task 1.4 – Define Inspection System Requirements

This task was completed with the finalization of the overall system specification.

6.1.9 Task 1.4 – Evaluate Weld Joint Inspection Capabilities

Hardware and software integration of the post weld inspection camera was completed for offline mode. This allows the system to scan the joint in a separate pass after the weld is completed.

Integration of the weld inspection system was tested. Figure 6.4, upper left, shows a photograph of a short butt weld with a crater at the end of the weld process where a real-time inspection was simulated. This was done by the system running through a simulated weld process while acquiring weld inspection data. The lower right image shows the weld information recorded by the system. The first column shows the real-time inspection result at a particular point in time, in this case, corresponding to the section of the weld located 1-inch from the start of the weld (whose cross-sectional view of the weld is shown in the lower left) and the second column shows the mean values of the inspection results over the entire length. Joint angle here refers to angular

deflection of the right plate relative to the left plate. For example, if both plates were perfectly flat the joint angle would be 0 degrees. The upper right image shows a 3D plot after reconstructing the weld inspection data gathered in real-time. The 3D reconstruction is an accurate representation of the weld including the crater fill defect at the end. 3D images like this are not usually displayed or saved, but serve to show the fidelity of the inspection system.

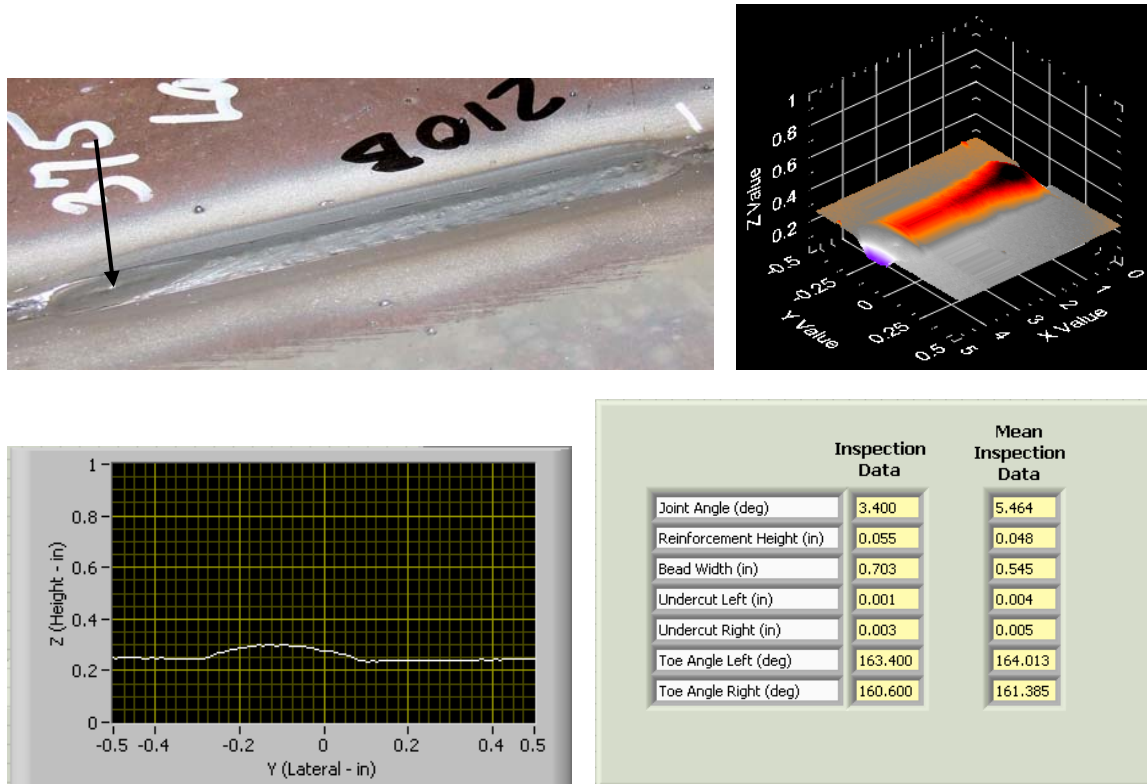


Figure 6.4: Information Plot from Real Time Inspection

The post weld surface inspection equipment was fully integrated and demonstrated. Weld surface features such as crown or fill height, undercut, surface porosity, cracks, etc. can be logged and referenced to the weld position while in process. Reporting features can be easily customized using templates. Figure 6.5 shows a proposed sample report including all relevant weld information. The final form is pending group input.



Weld Summary Report

General Information

Weld ID	P-354-A			
Date of Manufacture	11/26/2008			
Welding Operator	Darrell Rondeau			
Welding Process	LBW/GMAW			

Weld Parameters

Type of Weld	Root Pass			
Material	X100 : X100			
Thickness	0.5600			in
Length of Weld	119.1			in

	Setpoint		Actual		Pass/Fail
Travel Speed	95.0	ipm	90.8	ipm	Pass
Laser Power	9.5	kW	8.5	kW	Pass
GMAW Voltage	32.0	V	30.7	V	Pass
GMAW Wire Feed	500	ipm	500	ipm	Pass
GMAW Amperage	---	A	209.8	A	Pass
Heat Input	---	kJ/in	9.9	kJ/in	

Pre Weld Joint Inspection Data

	Mean	Min	Max		Pass/Fail
Gap	0.0050	0.0000	0.0350	in.	Pass
Mismatch	0.0150	0.0000	0.0250	in.	Pass

Post Weld Surface Inspection Data

	Mean	Min	Max		Pass/Fail
Crown/Fill Height	NaN	NaN	NaN	in.	
Weld Width	0.2500	0.220	0.3000	in.	Pass
Depth of Fill (Left)	0.1190	0.1080	0.1340	in.	Pass
Depth of Fill (Right)	0.2100	0.1990	0.2250	in.	Pass

Comments

Signatures

	Level	Date
Operator		
Inspector		
Supervisor		

Figure 6.5: Weld and Surface Inspection Test Report

6.1.10 Task 1.4 – Develop Interpass, Surface, and Non-Contact UT Volumetric Inspection and Defect Detection

This task is being completed in a separate USDOT project. The results will not be discussed herein.

6.1.11 Task 1.5 – Welding Procedure Development Preliminary Lab Trials on Plate

Welding and initial process development of flat plate X80 material was completed. Samples were welded on 10.5 mm X80 plate using an IPG Gantry. The purpose of these tests was to have a conservative starting point for future development on the orbital pipe welding system. For this series, the plate was prepared in a single-V configuration with a 0.25 inch (6.35 mm) land and a 60 degree included bevel. Two weld passes were made to fill the joint. A total of two plates were welded for examination with the only difference being the wire type. Both Thyssen NiMo80 and ESAB Spoolarc 95 wires were utilized. Details of the weld parameters are shown in the following Table 6.1.

Table 6.1: Welding Parameters for Flat Plate

	Travel Speed	Laser Power	MIG Voltage	WFS
Root Pass	80	9.0	18.0	300
Fill Pass	40	0	26.5	300

Once the pipeline system was commissioned, a test program was undertaken to maximize the root pass. A similar 60 degree single-V preparation was used with varying land thickness ranging from 0.313 inch (7.94 mm) to 0.425 inch (10.8 mm). Consistent backside bead quality was achieved at 0.375 inch (9.5 mm) at 9.5 kW with both a short arc and pulsed parameter set. Figure 6.6 shows the results of these parameters.

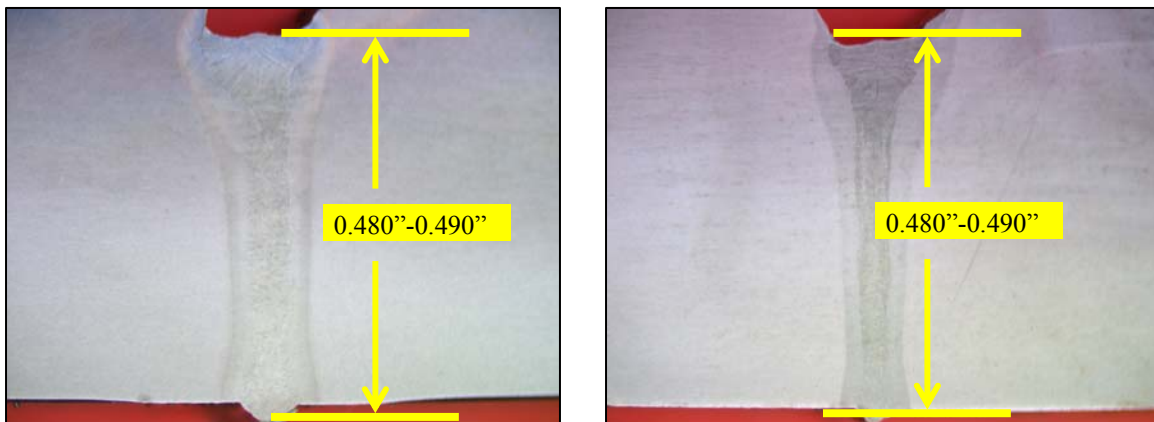


Figure 6.6: Macro of Root Passes in X80 – Left GMAW (CV) @ 65ipm Travel, Right GMAW (pulsed) @ 85ipm Travel

6.1.12 Task 1.6 – Finalize Design of Field Deployable HLAW System

The conceptual field deployable HLAW system was designed to withstand operating conditions from -45°C to +45°C. Where possible, system components had been chosen to withstand the rigors of these conditions. Where components were not available for operation in this temperature range, ESAB Welding & Cutting proposed to use the available components and provide plans for risk mitigation to operate these components in the said environment.

The proposed risk mitigations have not been tested and ESAB Welding & Cutting makes no guarantees that the proposed solutions will be effective at this time. Before an actual system could be manufactured extensive testing of systems components will be required to assure component performance. The Scope of Work (SOW) for this phase did not include provisions for such testing.

The system was divided into the following subcategories:

- Clamp Assembly;
- Weld Head Assembly;
- Laser Safety Enclosure;
- Laser/Chiller Packaging (Transport Trailer Design); and
- System Integration and Cable Management.

6.1.12.1 Clamp Assembly

Motion System

ESAB/ATS utilized a TRI TOOL 636SB to provide the motion system for the orbital HLAW system. The 636SB is designed to be a portable externally mounted pipe cutting and bevelling system. The standard model provides a low clearance split frame design, which allows the machine to quickly be installed around the outside diameter of in-line pipe. The self-centering feature, along with the low friction bearing system, makes the 636SB a stable platform for HLAW.

Subsequently, ESAB worked with TRI TOOL to customize the 636SB design to be better suited for HLAW. Listed below are the design criteria given to TRI Tool for the HLAW clamp:

- New design would have fully automated clamping/unclamping.
- A pre-installed saddle would be used to locate the clamp at the weld joint.
- The clamp would be designed to accept an A/C Servo Drive and planetary gear reducer.
- The clamshell needs to be free of grease lubrication. The natural seeping of lube grease is an issue for the weld and location environment.
- The target is for the machine to weld a single weld joint every 5 minutes over (2) consecutive 8 hour shifts.
- Must be able to work properly in environments ranging from +40°C to -40°C.
- Maximum welding speed of 110 inches/minute.

Servo Motor Drive System

For the servo drive system, ESAB worked with Yaskawa/Wittenstein to provide a drive solution which is compact, accurate, and powerful enough to drive the TRI TOOL clamp with the HLAW equipment onboard. Based on the design criteria provided to Yaskawa/Wittenstein, a TPM rotary actuator was recommended. The TPM Series is Wittenstein's most compact rotary actuator. TPM series actuators provide outstanding dynamics, two-stage gear heads, and extremely short response time.

TPM-025S-091 was recommended for the application. Several modifications will be required to the standard TPM rotary actuator to accommodate the temperature extremes. The modifications will be as follows:

- Aeroshell lubricant in gearbox – working temp -50°C to 50°C;
- All steel construction to prevent dissimilar expansion/contraction rates; and
- Sealed body and outputs for operation in wet environments.

Adapters were designed to connect the rotary actuator to the TRI TOOL clamp.

Figure 6.8 shows the adaptor housing and motor coupling that were designed to connect the rotary actuator and the clamp.

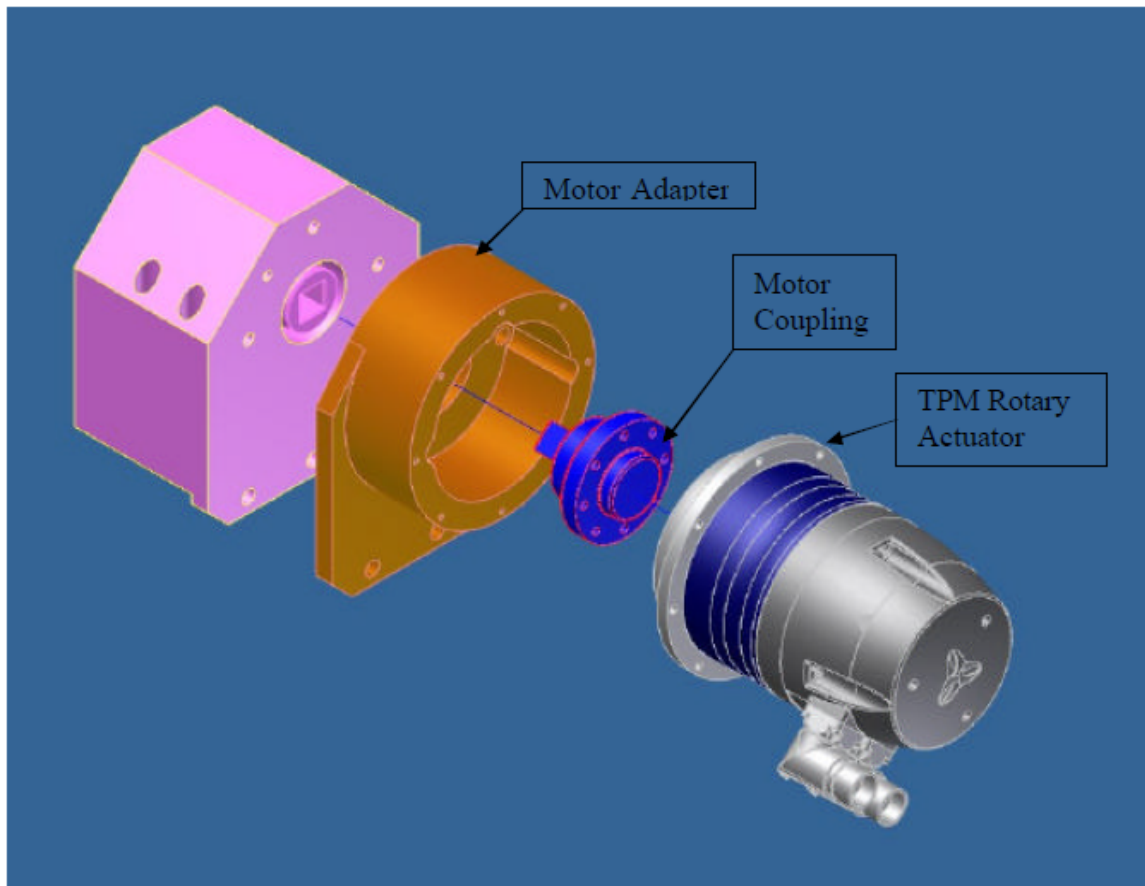


Figure 6.8: Adaptor Housing and Motor Coupling Designed to Connect to Rotary Actuator and Clamp

6.1.12.2 Weld Head Assembly

The weld head assembly design was divided into subcategories. Specifications for each of the following focus areas are discussed:

- Fibre optic cable;
- Gas Metal Arc Welding (GMAW) torch;
- Wire feeder;
- Prismatic joints;
- Seam tracking and weld inspection;
- Focus optics;
- Crash protection; and
- Local light shielding.

Fibre Optic Cable

For this application, ESAB had chosen an II-VI Infrared, Inc. fibre optic cable.

HIGHYAG High Power Laser Light Cable HY-LLK.0300.30:

- Fibre diameter – core (cladding): 300 (720) μm
- Numerical aperture 0.12 – 0.21
- Laser light cable for Nd:YAG, fiber or disc laser
- Suitable for laser power up to 10 kW

Connectors:

- Laser side: (Automobile Standard, compatible with Trumpf LLK-D)
- Optic side: (Automobile Standard, compatible with Trumpf LLK-D)
- Integrated plug-in, temperature and breakage monitoring system (Automobile Standard)
- Pre-aligned for plug in without realignment
- Length: 30 m
- Suitable for robotic applications (150 mm bend radius)

ESAB believes the fibre optic cable could be operated at these temperatures if it is housed in an insulated flexible conduit, with heating/cooling lines to maintain the operating temperature between 5°C and 30°C. ESAB had also developed a water-resistant jacket that can be installed on the fibre optic connector. Figure 6.9 shows an example of this jacket.



Figure 6.9: ESAB Water-Resistant Jacket

GMAW Torch

An Abicor Binzel robotic welding torch was chosen for the GMAW process.

Abicor Binzel WH – 965.2007 coupled with a ROBO WH 652 D TS Swan neck:

- Provides 100 percent duty cycle at 500A with mixed gases
- Wire size capacities 1.0-1.6 mm
- Water cooled for reliable service

- Lead Length - 2.5 m
- Swan neck angle 0°
- For shield gas control, a Burket 8626 Mass Flow controller was used for closed loop control of gas flow. Providing up to 200 SL/M with maximum inlet pressure of 145 psig

Brackets were designed to place the GMAW torch at an angle of 26 degrees off of vertical from the focus optic. Provisions were made for adjustment of the torch normal to the weld parallel to the torch and transverse to the joint. Access to the cover-slide on the focus was also included in the design. Figure 6.10 shows the brackets designed for mounting the torch.

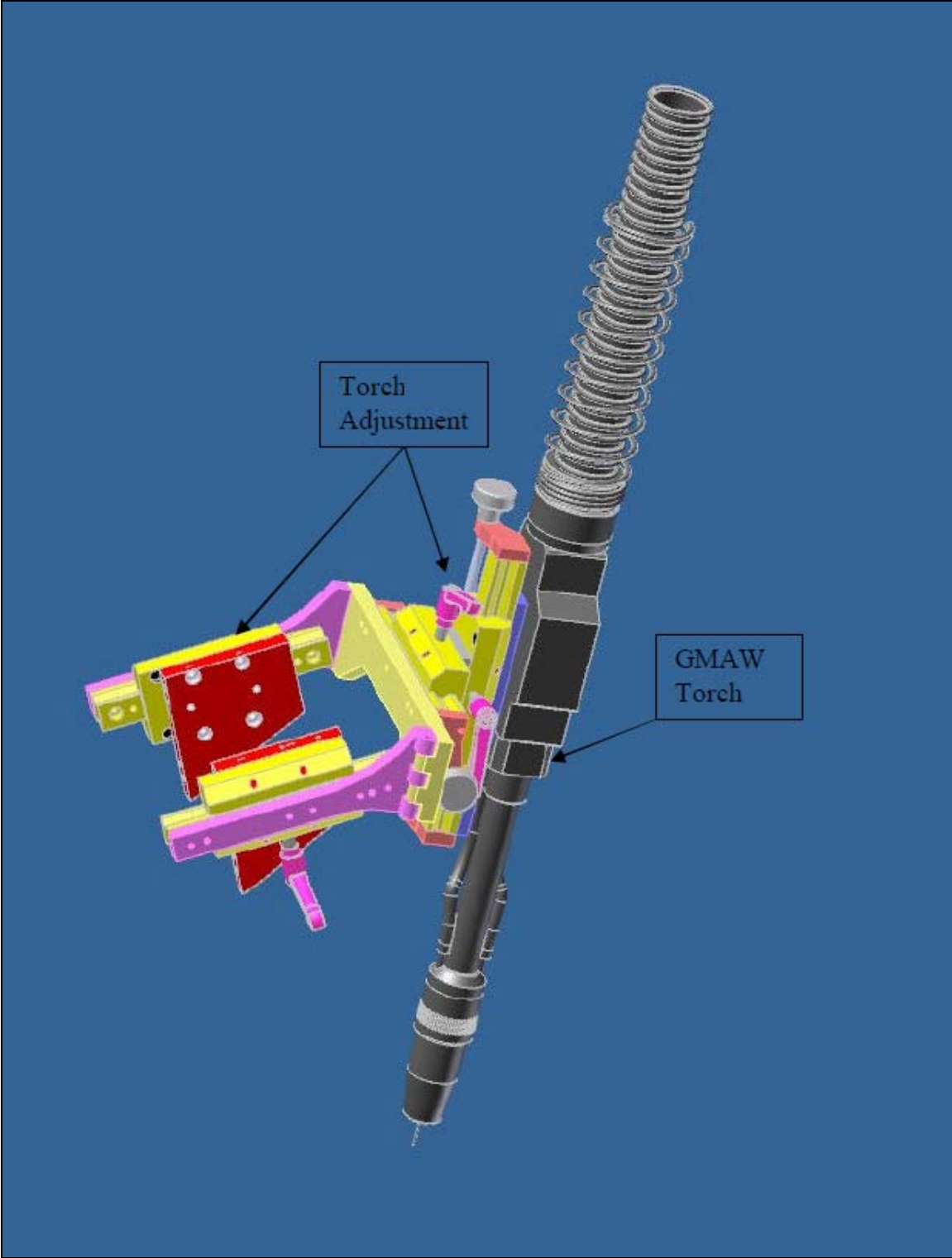


Figure 6.10: Brackets Designed for Mounting the Torch

Wire Feed

For the wire feed control an ESAB Robofeed 3004w was chosen. The Robofeed has a sturdy and reliable design, with aluminum casing for reduced weight and ideal for use in tough environments. The digitally controlled feed units perform accurate speed control with the aid of a pulse encoder on speeds ranging from 0.8 to 25.0 m/min. The four-roll feed mechanism with grooves in both feed and pressure rolls give stable feeding and low wear of the wire, all of which help to ensure reliable wire feeding.

ESAB Robofeed 3004w:

- Robofeed 3004w
- Power supply, 42 VAC, 50/60 Hz
- Drive mechanism 4 WD
- Drive rollers, 30 mm
- Wire feed speed, m/min 0.8-30.0
- Dimensions L x W x H, mm 362 x 246 x 235 383
- Weight 7.3 kg
- Speed control Pulse encoder
- Wire dimensions:
 - steel 0.6-1.6 mm
 - stainless steel 0.6-1.6 mm
 - aluminum 1.0-1.6 mm
 - cored wire 0.8-1.6 mm
- Enclosure class IP 23 IP 2X
- Standards IEC 60974-5

Spool wire feed was chosen over the use of a Marathon pack. A 30 pound spool of 0.045 inch wire will provide approximately 45 root passes. The use of a marathon pack introduces problems with wire management and possible need for wire straightening. Figure 6.11 depicts the mounting of the wire feed to the clamp assembly and the spool feed mount.

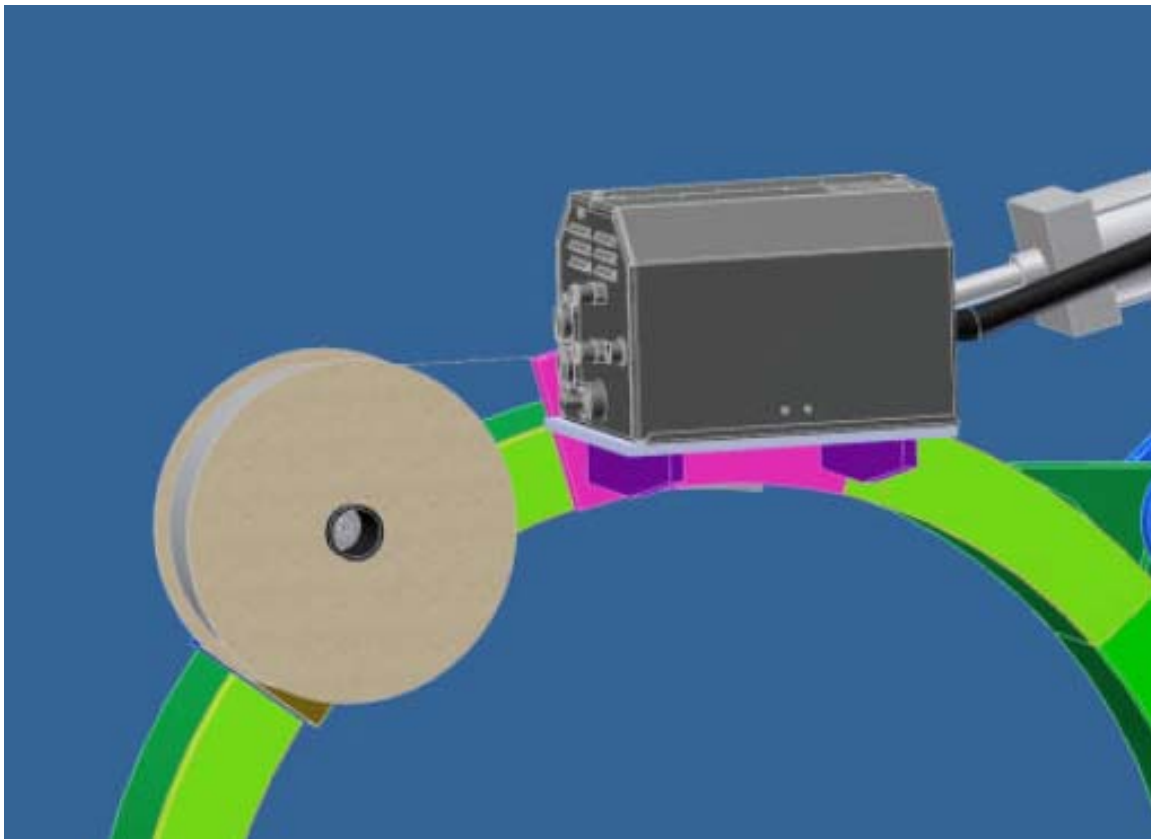


Figure 6.11: Mounting of Wire Feed to Clamp Assembly and Spool Feed Mount

Prismatic Joints

The seam tracking feature of the HLAW requires two prismatic joints for motion correction in 2 axes, one normal to the weld joint and one transverse to the weld joint. For this motion the actuators must be capable of supporting the load, both static and dynamic the head assembly will impose during welding. They must also provide precise and smooth motion.

To provide this motion Danaher DS4 Series position series were chosen, for their load carrying capacity and accuracy class.

Danaher Model DS4-150-C-5G-X23-PL6E-L0-H0-BS-E0:

- 150 mm travel;
- Positional accuracy 12 μm ;
- Bi-directional repeatability +/- 3 μm ;
- Load Capacity, Normal (max) 170 kg;
- Axial Load Capacity 95 kg; and
- Acceleration (max) 20 m/sec^2 ;

- Moving mass 0.75 kg;
- Total Mass 3.3 kg, and
- Ball-screw Lead 5.0 mm

Based on load and inertia data, a 500 W Servo drive was chosen to drive the prismatic joints.

Seam Tracking and Weld Inspection System

Servo Robot Inc. was chosen to provide both the seam tracking and weld inspection systems.

Seam tracking, also known as joint tracking, involves real-time tracking just ahead of where the weld is being deposited. This system allows for trajectory correction of the HLAW system to maintain the laser within the joint. For seam tracking, ESAB has chosen to use a Rafal camera, which provides a compact design, high frame rate, high resolution, and a wide field of view. The features of the Rafal are as follows:

- Laser Class IIIb
- Standoff distance 17 mm
- Sensor type: digital CMOS
- Max Frame Rate 2000 Hz
- Max field of view width 16 mm
- Max field of view depth 10 mm
- Dimensions 60 x 30 x 122 mm
- 40 m cable assembly

The weld inspection system was used to help quantify variation within the welding process. For weld inspection ESAB had chosen LAS-SCAN / IT system from Servo-robot.

A Poroscan-25/10 Laser camera was used for simultaneous weld geometry inspection and pinhole detection. The features of the Poroscan 25 are as follows:

- Laser class: IIIb
- Standoff distance: 44 mm
- Max field of view width: 27 mm
- Max field of view depth: 16 mm
- Dimensions 135 x 50 x 170 mm
- Cable length 40 m

Brackets were designed to mount the seam tracking and weld inspection cameras to the welding head assembly. The brackets provide adjustment of the cameras standoff distance and lateral offset of the camera width field of view. Figure 6.12 depicts the brackets designed to mount the seam tracking and weld inspection cameras.

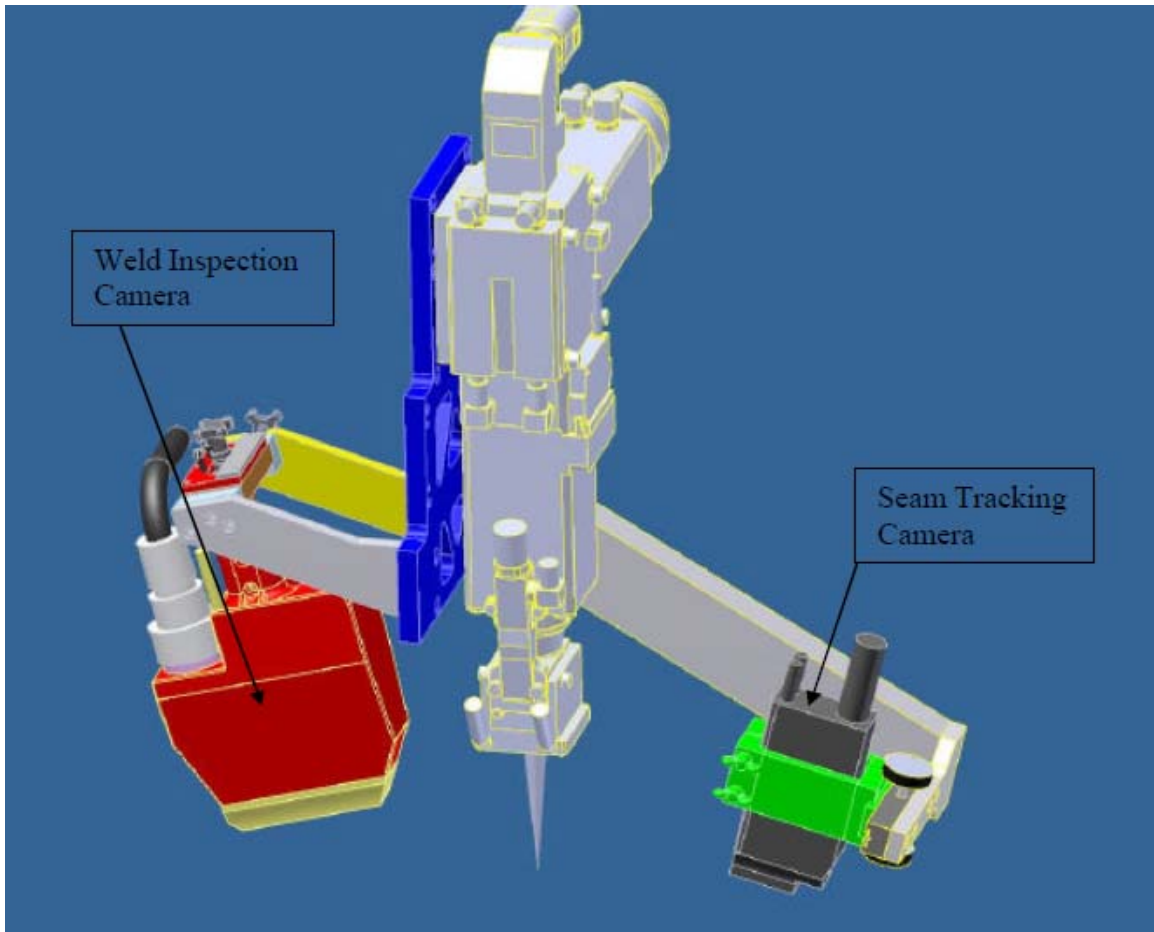


Figure 6.12: Seam Tracking and Weld Inspection Mount Brackets

Along with the cameras, process equipment was necessary to control the prismatic actuators with the data collected from the seam tracking. Due to environments limitations of this equipment, it must be housed in the climate controlled operators station.

The cameras have an operating temperature range of 0°- 45°C. To operate the cameras at lower temperatures, ESAB plans to provide warm dry air through the cameras existing cooling circuit. This has not been tested to-date; therefore ESAB can make no guaranties of the potential effectiveness.

Focus Optics

For the laser processing head, HighYAG a division of II-VI Infrared was chosen.

HighYAG BIMO line of processing heads provides a flexible and modular platform, which allows the processing head to be configured specifically for the application.

Listed below are the specifications of the BIMO used for this project.

- HighYAG Laser Processing Head BIMO –
 - Base Module
- HighYAG Laser Light Cable Receiver Auto –
 - Receiver Auto for HighYAG laser light cable connector (Automobile Standard, compatible to Trumpf LLK-D), others on request
- HighYAG Cover Slide Module before Collimation Module –
 - Cover slide holder with quick change mechanism
 - Without monitoring system
- HighYAG Collimation Module –
 - Integrated optical collimation system for the laser light exiting the fibre
 - Correction of the optical aberrations
 - Optical properties: Magnification MCol, focal length f and beam parameter
 - MCol = 1.33, f = 150 mm, NA = 165 mrad
 - Average laser power up to max. 6 kW, peak power up to 200 kW
 - Wavelength of laser light E = 1025 - 1080 nm (Nd:YAG, fibre or disc laser)
- HighYAG Focusing Module –
 - For HighYAG laser processing head BIMO
 - Focusing module with integrated optical system
 - Magnification MFoc = 1.50 (equivalent focal length 300 mm)
 - The focus diameter ØFoc is the product of the magnification of collimation module MCol,
 - Wavelength of laser light E = 1,025 – 1,080 nm (Nd:YAG, fibre or disc laser)
- HighYAG HP-Extension Module –
 - High laser power up to 20 kW, peaks up to 200 kW
 - Wavelength of laser light = 1025-1080 nm (Nd:YAG, fibre or disc laser)

- HighYAG Preparation for CCTV Viewing System –
 - Beam splitting for monitoring (e.g., behind bending mirror)
 - Integrated optical system for imaging the focal plane on the camera chip
 - Interface for CCD camera (C-Mount or others)
- HighYAG Cover Slide Monitor KSGM 2 with Sensor Adaptation –
 - Compact device for measuring the cover slide status and contamination
 - Digital I/O for warning and alarm (according to status of cover slide)
 - Power supply 24V

ESAB has worked with HighYAG to provide a processing head that is capable of using an antifreeze type coolant for operation in extreme temperatures. Other provision may be necessary for operating the process head at extreme temperatures. Neither ESAB nor HighYAG can at this time make any guaranties that the BIMO can operate over the specified temperature range, although it is believed the risk of operation in extreme temperatures can be mitigated through the use of a heating/cooling fluid circulated through the optic, along with nitrogen purge through the optic.

Crash Protection

Crash protection is provided through an Applied Robotics Quick Stop collision sensor.

The Quick Stop operates through a pressurized pneumatically sealed chamber.

When a collision occurs, the seal is broken and the loss of pneumatic pressure is sensed by a pressure switch, which sends an e-stop signal to the system stopping all motion.

Applied Robotics model QS-800 was chosen as the appropriate size for this system, based on the load and acceleration data. The QS-800 specifications are as follows:

- Operating pressure: 1-6 bar
- Moment trip point: 53-255 N-m
- Compression trip point: 210-960 kg
- Repeatability +/-0.025 mm
- Repeatability rotational +/-0.419 x 10⁻³ radians
- Mass 3.72 kg
- Response time <18 ms
- 40 m cable

Local Light Shielding

Local light shielding was designed to capture as much of the diffuse laser radiation close to the processing head. Sheet metal shielding was used to enclose as much of the head assembly as practical. Local light shielding coupled with a laser enclosure will help minimized the risk associated with the laser power levels required for HLAW. Figure 6.13 displays the local light shielding design. Brush and fin seals will be used to seal the local light shielding to the pipe during welding to further reduce the potential for exposure to laser radiation.

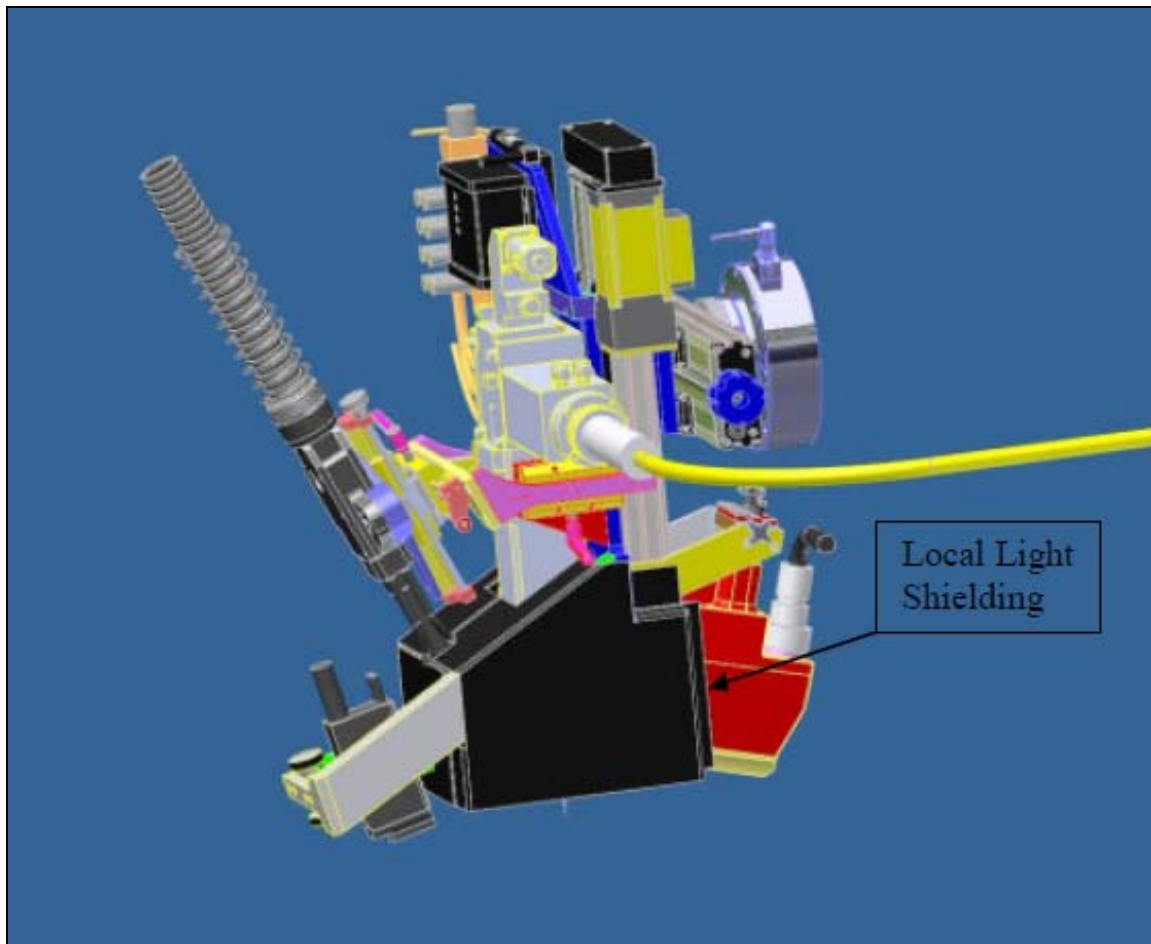


Figure 6.13: Local Light Shielding Design

6.1.12.3 Laser Safety Enclosure

ESAB conceptualized a Class 1 Enclosure for the Field Deployable Orbital HLAW system. The design consists of an aluminum frame covered with Ever-guard® laser barrier material, which provides a light tight design. Ever-guard® Barriers provide 1,200 watts/cm² protection for three minutes. The safety enclosure has hinged sides with pneumatic actuation to provide automated closing around the pipe. Safety interlocking is provided to assure complete closure around the pipe. Provisions were also made to include personnel sensors inside of the safety enclosure. CCTV cameras are included to allow the operators to view the process during welding and transport from weld to weld.

Figure 6.14 depicts the laser safety enclosure. Before actual manufacture of the laser safety enclosure ESAB requires that a third party laser safety contractor review the design and certify it as an acceptable Class 1 enclosure.

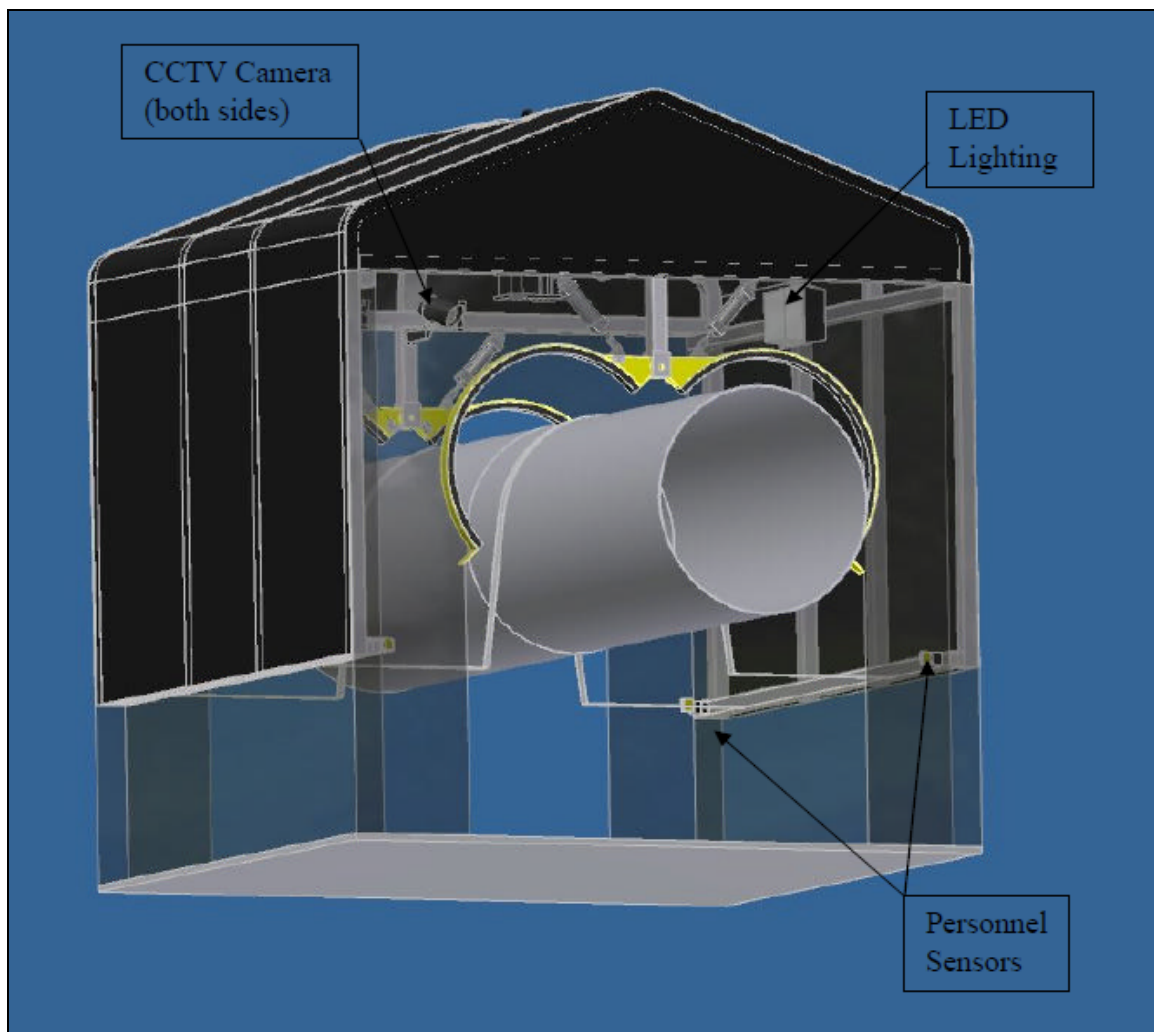


Figure 6.14: Laser Safety Enclosure

Enclosure features include the following:

- Bosch EX14N Series Extreme Environment Day/Night Camera
- Shoebox style LED lighting: 3800 Candela 147 watts
- Parker Viking Extreme Pneumatic Valves and cylinders to control enclosure opening and closing
- Ever-guard® Laser radiation barriers
- Omron OS3101 Operator Presence Detector

- Honeywell 5 VDC Sourcing Hall switches (for detecting enclosure door position)
- Igus Energy Chain cable management

Laser/Chiller Packaging

ESAB worked with Trumpf Laser to design a field ready resonator and chiller. The field ready laser resonator and chiller included a sealed cooling water reservoir and a smaller foot print.

6.1.12.4 Overall Integration and Cable Management

Final integration of the orbital HLAW system required considerations for cable management from the auxiliary equipment location to the welding assembly and for the orbital unit as it orbits around the pipe during welding.

Cable management from the equipment trailer to welding safety enclosure will be accomplished through flexible conduit. Murrplastik, Murrflex EW-PRF-95 would be used between the safety enclosure and the equipment trailer. Murrflex provides continuous operation in temperature ranges from -50°C to 221°C. It is particularly suited for dynamic routing such as robotic applications. The conduit will be wrapped with an insulated material. Heated fluid will be circulated through 0.5 inch diameter polypropylene lines to maintain the encased cables and hoses above 0°C. Table 6.2 lists the cables and hoses that will traverse the conduit between the trailer and the safety enclosure.

Table 6.2: Cables and Hoses to Traverse Conduit between Trailer and Safety Enclosure

HLAW CABLE/HOSE LIST					
CABLE #	QUANTITY	OD (IN)	DESCRIPTION	BEGINNING LOCATION	TERMINATING LOCATION
1	1	1.125	Servo Robot Control Cable	Servo Robot Control Cabinet	Junction box near Laser Head
2	1	0.66	Weld Inspection Camera Cable	Servo Robot Control Cabinet	Weld Inspection Camera
3	2	0.5	Cooling water to RoboFeed	AristoMIG U5000I	Back of RoboFeed
4	1	0.68	Weld Power Lead	AristoMIG U5000I	Back of RoboFeed
5	1	0.4	Shield Gas	AristoMIG U5000I	Back of RoboFeed
6	1	0.3	Shield Gas Purge	AristoMIG U5000I	Back of RoboFeed
7	1	0.52	RoboFeed Control	AristoMIG U5000I	Back of RoboFeed
8	2	0.44	Mass Flow Control Cable	ATS Control Cabinet	MFC near RoboFeed
9	1	0.44	Wire Feed Speed Encoder Cable	ATS Control Cabinet	Back of RoboFeed
10	1	0.44	Crash Sensor Cable	ATS Control Cabinet	Crash Sensor on Laser Head
11	4	0.31	Coolant Lines Fiber/Optics	Trumpf Laser	Laser head
12	1	0.5	Fiber	Trumpf Laser	Laser head
13	1	0.66	CrossJet Air Line	Regulated air supply	Laser head
14	1	0.44	Laser Head Monitoring Cable	ATS Control Cabinet	Laser head
15	1	0.51	Crash Sensor Air Supply	Regulated air supply	Crash Sensor on Laser Head
16	1	0.5	Seam Tracking Control Cable	Servo Robot Control Cabinet	Seam Tracking Camera
17	2	0.5	Seam Tracking Cooling Air	Servo Robot Cooling Unit	Seam Tracking Camera

Cable management within the safety enclosure will be accomplished through an IGUS orbital energy chain. ESAB has worked with IGUS to design an orbital energy chain that can be automatically clamped on the pipe and will follow the orbital welder during welding. Figure 6.15 shows the concept orbital energy chain designed by IGUS.

Based on the conceptual design, estimates have been made for service requirements for the orbital HLAW system. These estimates may change based on the final design and risk mitigation plans for components that could not operate within the full temperature range. Table 6.3 includes the estimates for machine service requirements.

Table 6.3: Service Requirements

Service	Description	Comments
Electrical	200 KVA 460 V 3 Phase	
Air	34 SCMH @ 5.5 BAR	Filtered to 40 microns, 1.66° C Dewpoint
Shield Gas	12 SCMH @8.6 bar	Dry and Free of Oil

Power generation will be provided from a portable generator. The generator shall be located on a separate trailer or skid. This will allow the end user the option of providing the power unit of their choice. This will also facilitate easy replacement in the event of power equipment failure.

ESAB recommended a MQ Power WhisperWatt DCA220SSJ as an acceptable power generator. The WhisperWatt provides 220 KVA of continuous power and a standby rating of 242 KVA. Voltage and frequency are regulated to +/- 0.5 percent and +/-0.25 percent, respectively. The WhisperWatt is powered by a 315 horsepower direct injected, liquid cooled, turbo charged Diesel engine. The WhisperWatt full load fuel consumption is 51.6 LPH.

Compressed air shall be provided through an Ingersoll Rand electric-driven duplex compressor. The duplex compressor offers two individual compressor pumps and motors mounted on a single unit. This provides a 100 percent backup or additional air at peak demands.

The duplex compressor provides 24 hour continuous duty cycle. Ingersoll Rand model 2-2545E10 provides 59.5 SCMH flow at 12 bar.

Final integration was achieved by designing brackets that attach the head assembly to the TriTool clamshell and the orbital welding unit to the safety enclosure. Figure 6.16 shows the full integration of the orbital HLAW system with the laser safety enclosure.

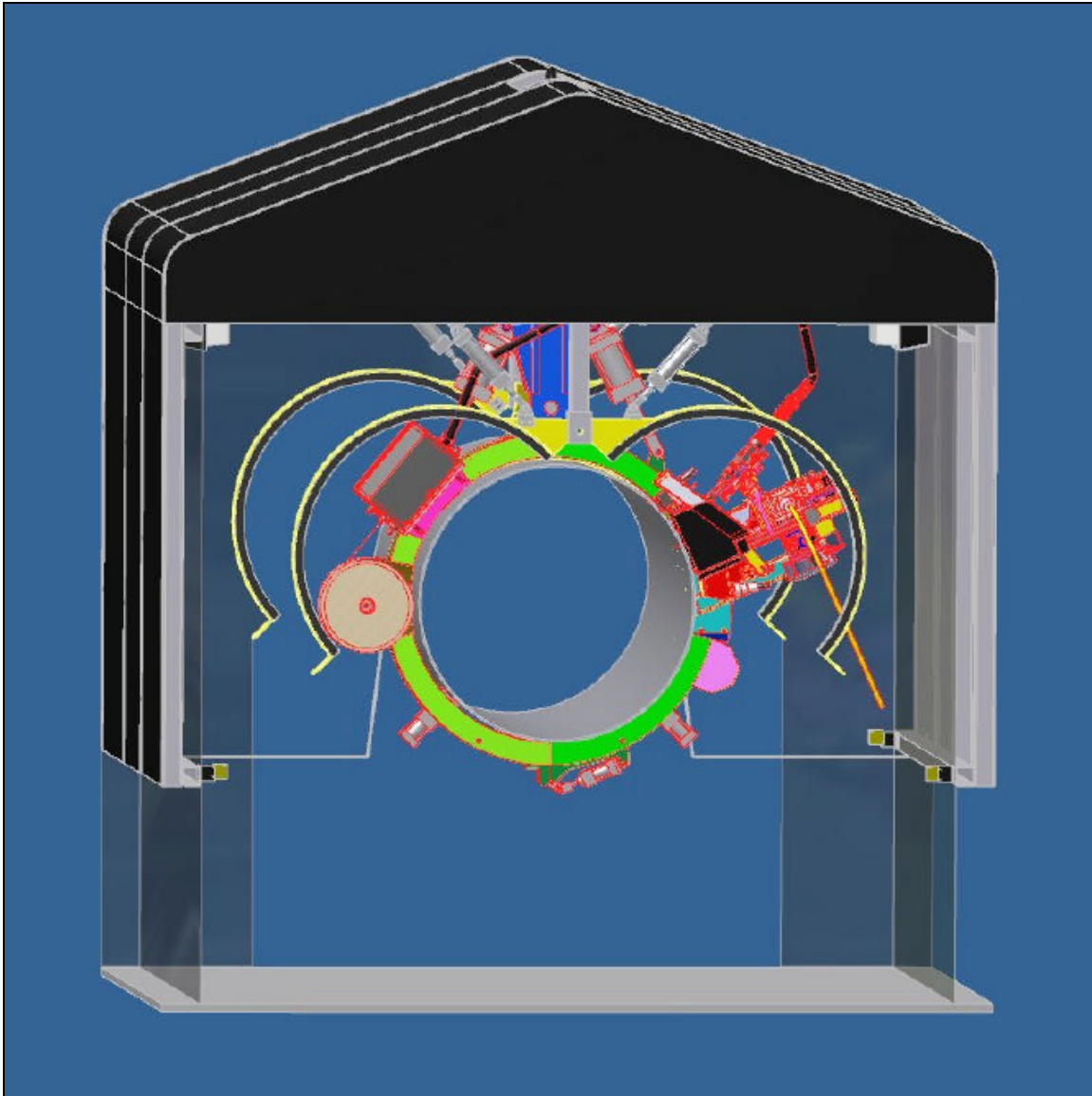


Figure 6.16: Full Integration of Orbital HLAW System with Laser Safety Enclosure

6.1.12.5 Detailed Drawings and Parts List

A set of detailed drawings, along with full parts list, is provided for the HLAW system and clamping mechanism in Figure 6.17 to Figure 6.19.

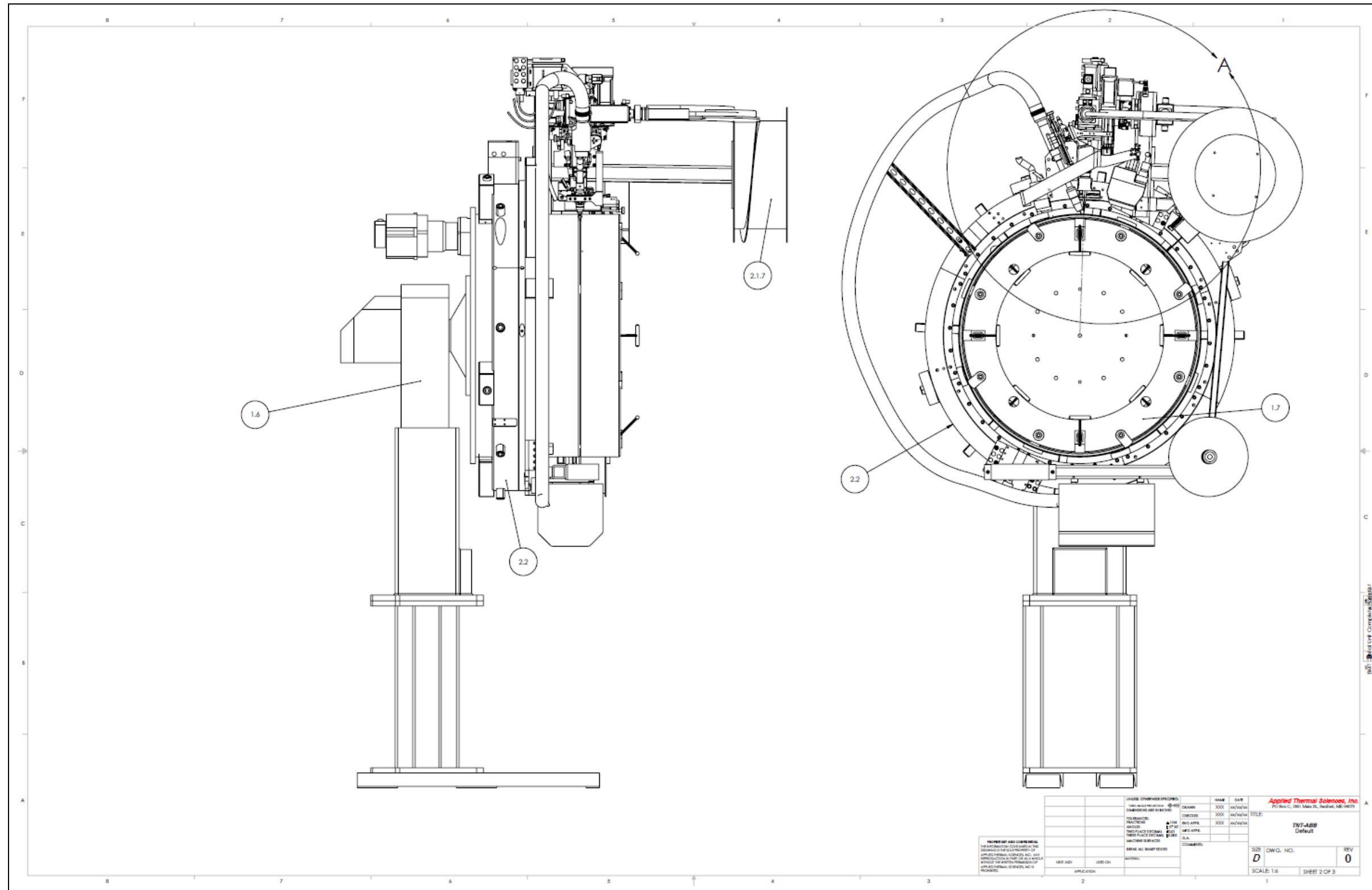


Figure 6.17: TNT-ABB Default (Sheet 2 of 3)

6.1.12.6 Conceptual Trailer Design

Although not a requirement of the USDOT contract, ESAB subcontracted East Trailer Manufacturing to design a transport trailer. The design included a vibration dampening system for the resonator, environmental temperature controlled enclosure for the resonator, a climate-controlled operators and electronics area, deployment crane, and a transport area for the laser safety enclosure.

Figure 6.20 to Figure 6.28 provide illustrations of what the trailer could look like to transport the HLAW system to and from the work site. Once arriving on site, then the system would require loading onto a modified dozer and/or skid to make it along the pipeline from pipe to joint to joint.

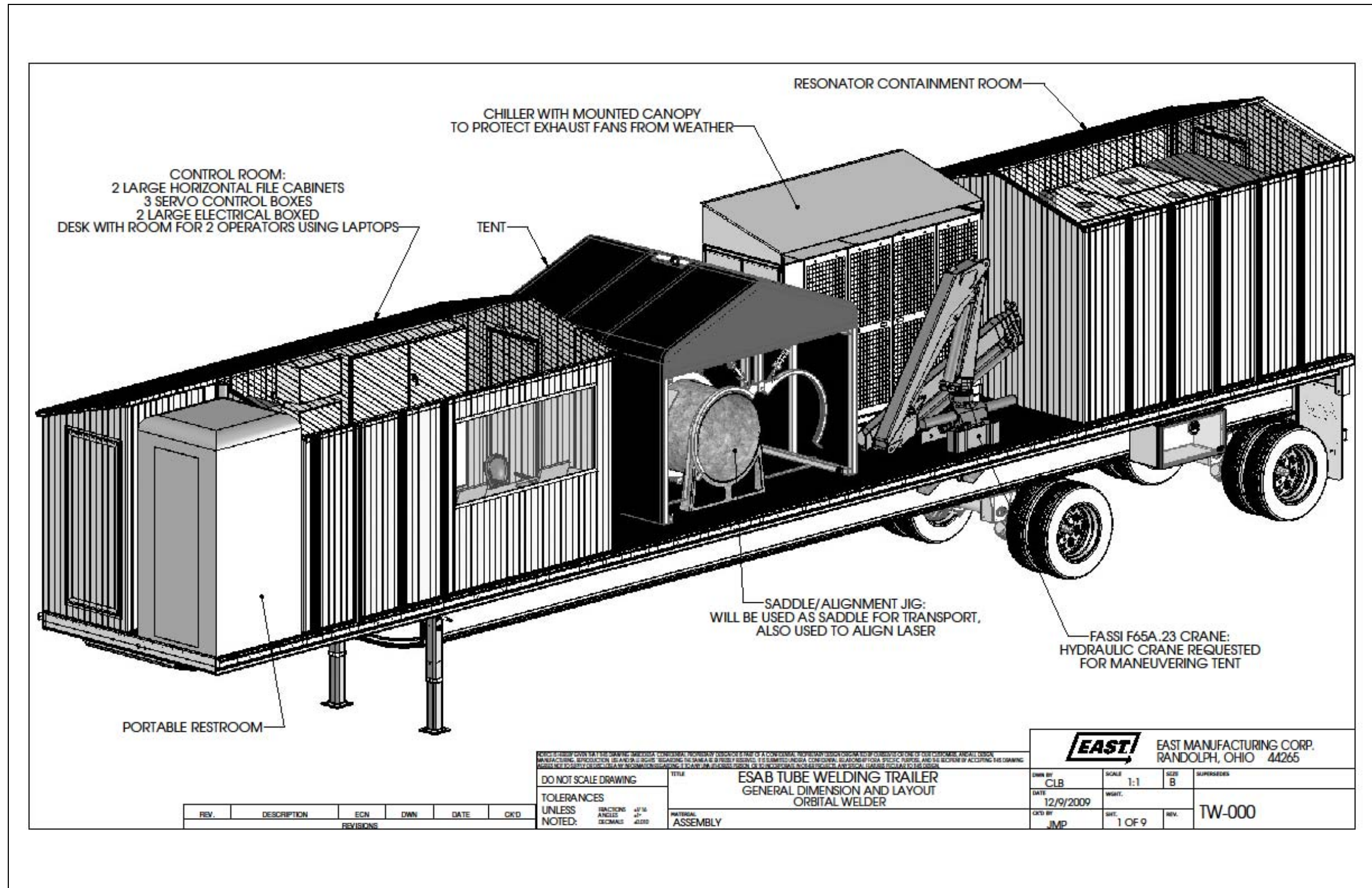


Figure 6.20: ESAB Tube Welding Trailer General Dimension and Layout Orbital Welder

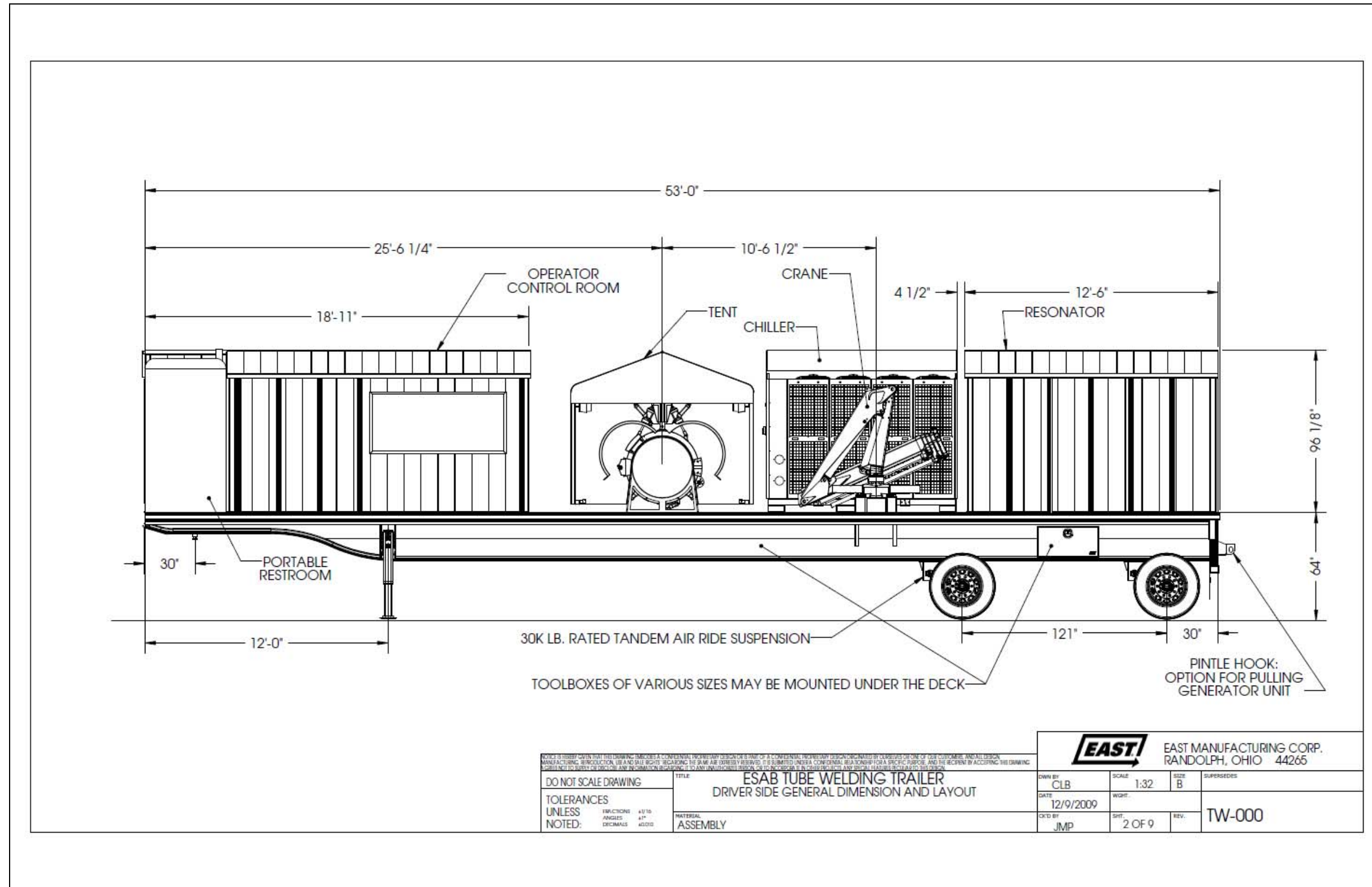


Figure 6.21: ESAB Tube Welding Trailer Driver Side General Dimension and Layout

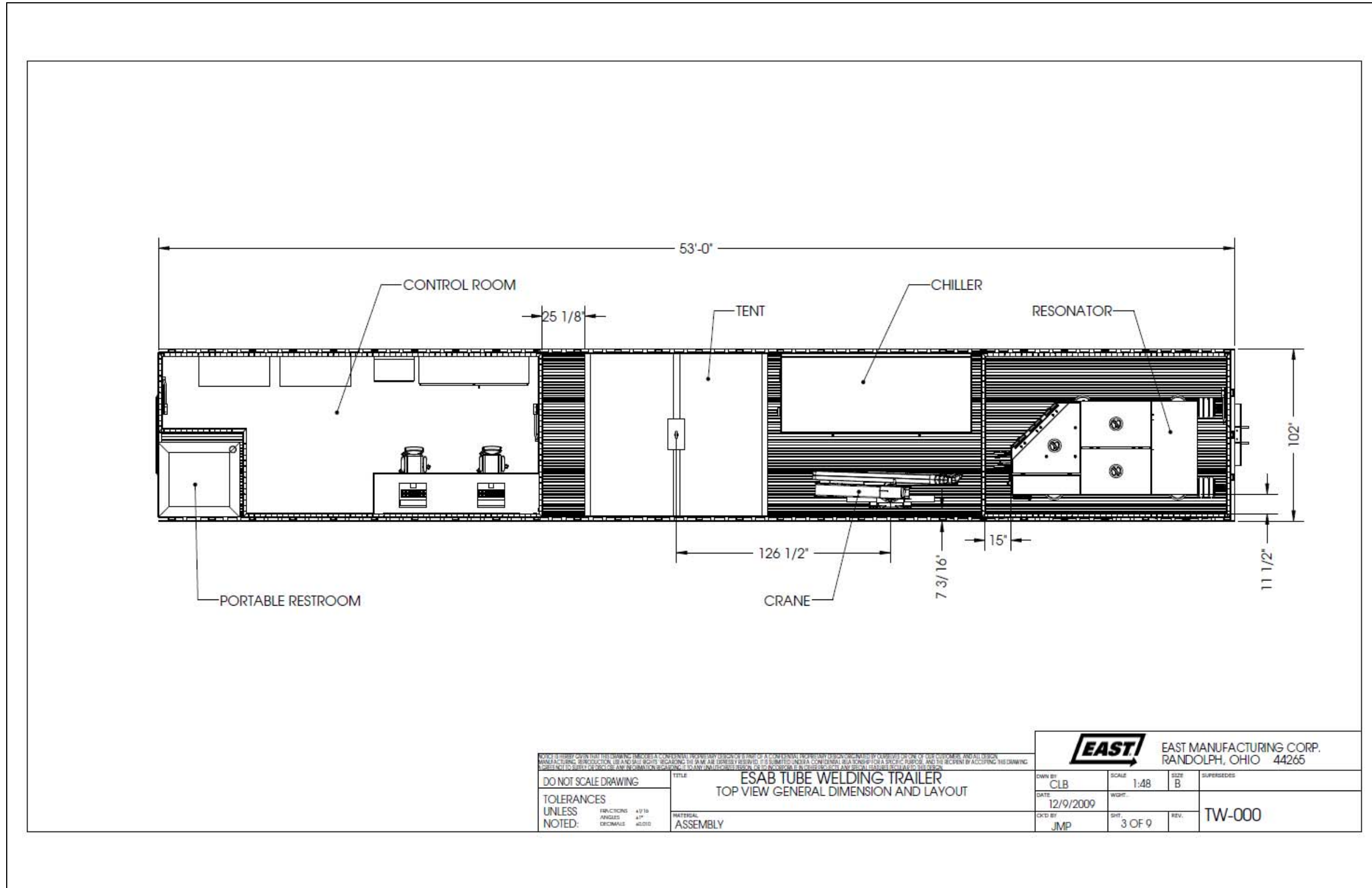


Figure 6.22: ESAB Tube Welding Trailer Top View General Dimension and Layout

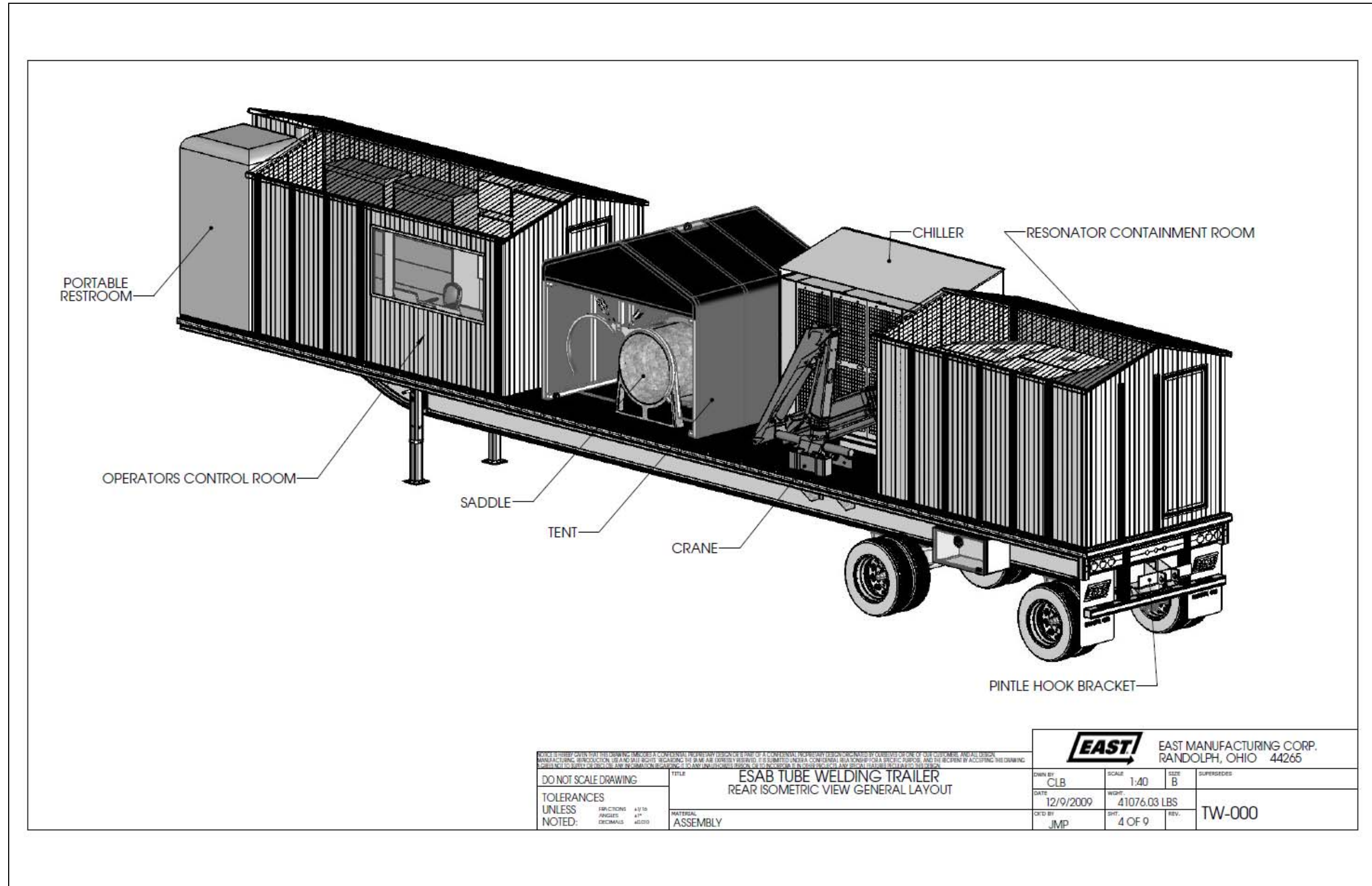


Figure 6.23: ESAB Tube Welding Trailer Rear Isometric View General Layout

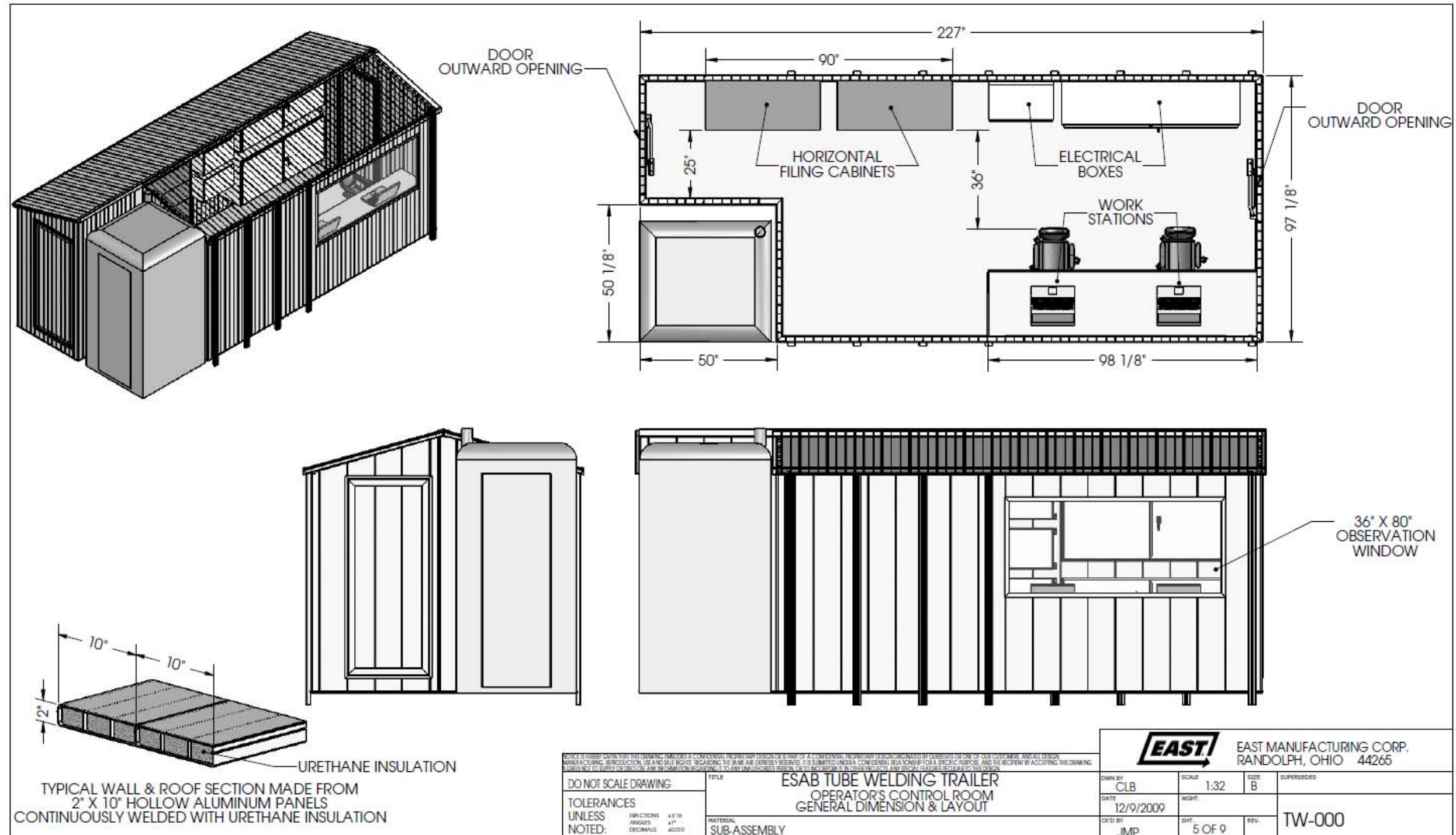


Figure 6.24: ESAB Tube Welding Trailer Rear Isometric View General Layout

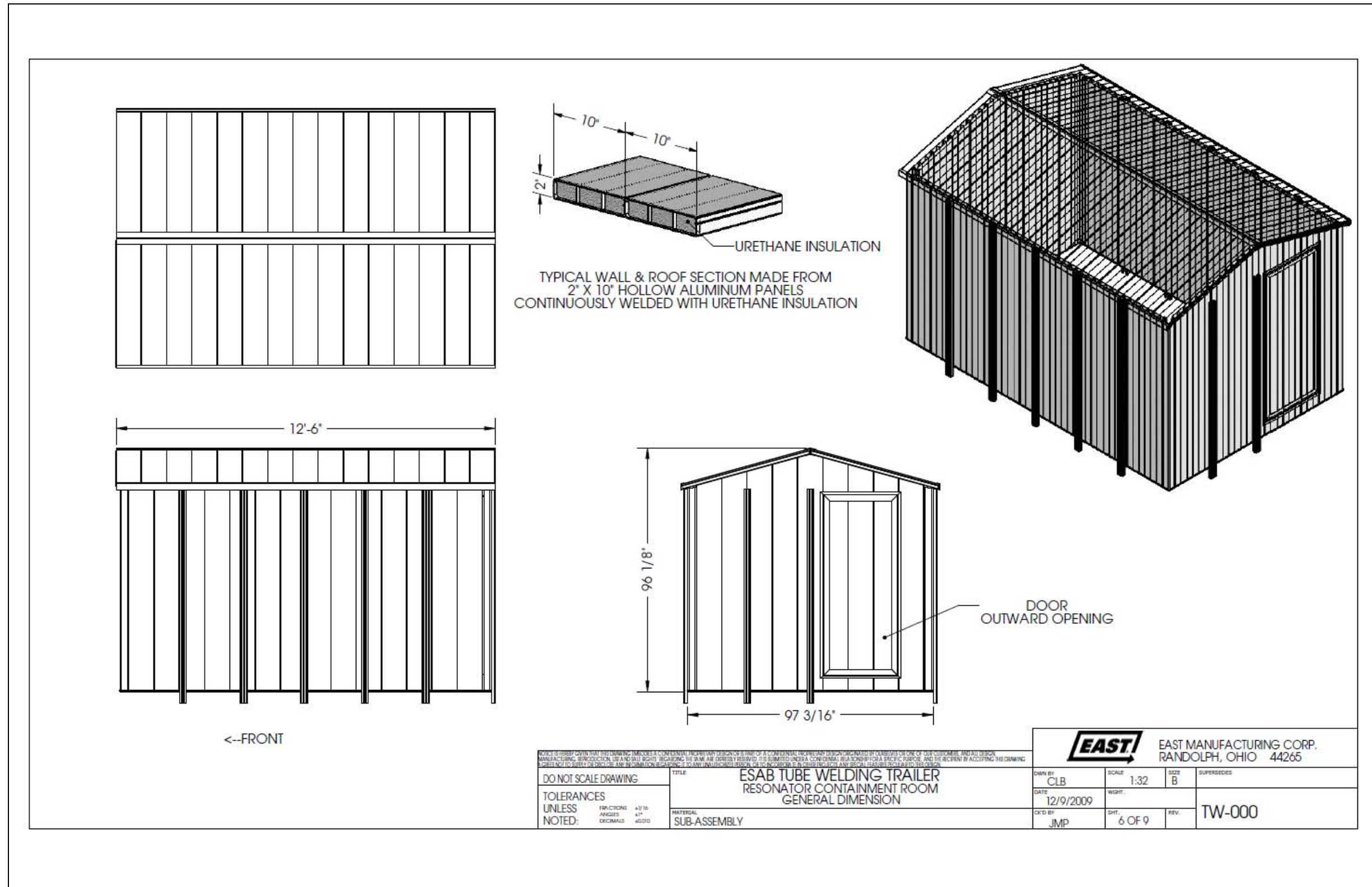


Figure 6.25: ESAB Tube Welding Trailer Resonator Containment Room General Dimension

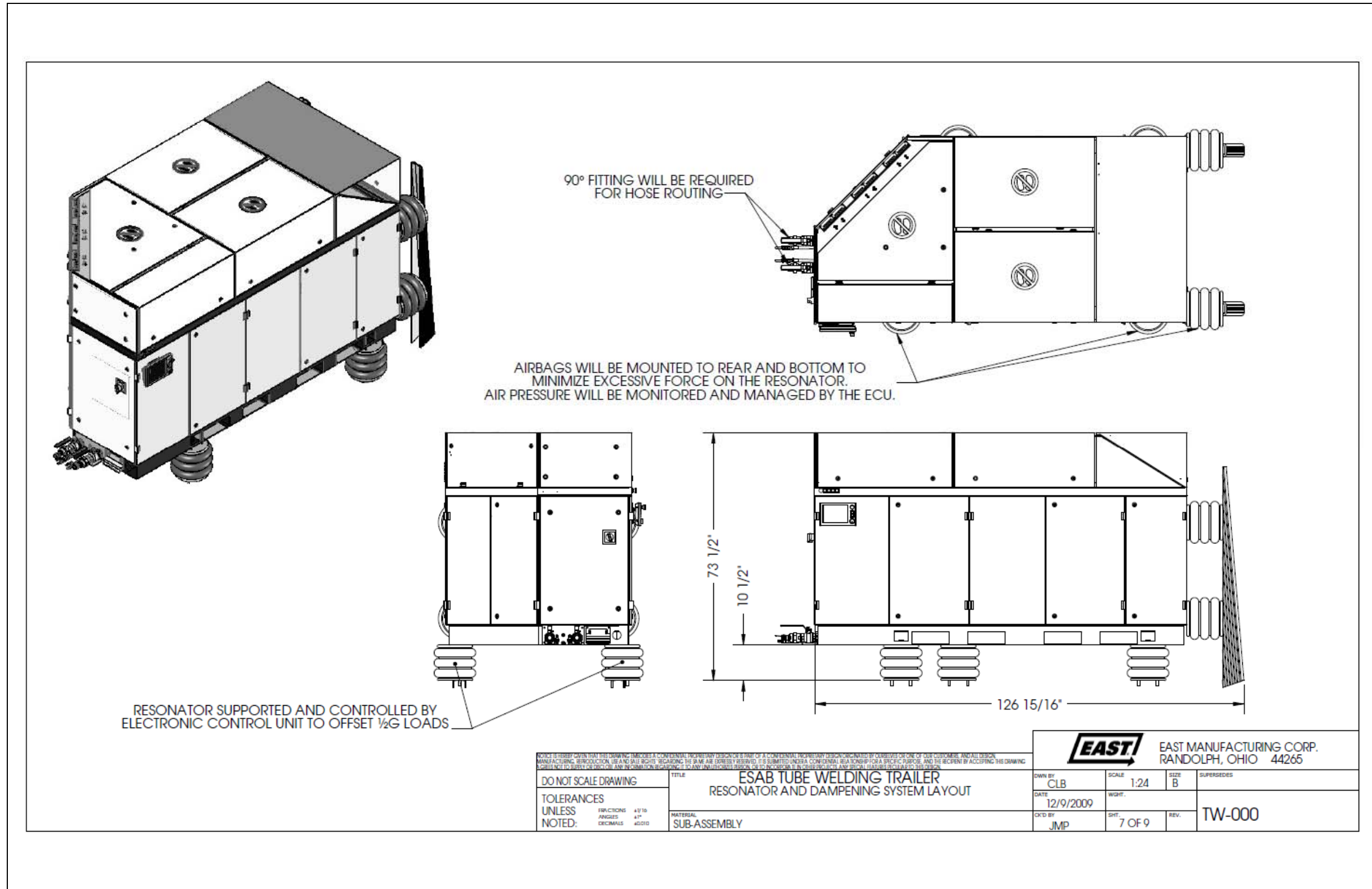


Figure 6.26: ESAB Tube Welding Trailer Resonator and Dampening System Layout

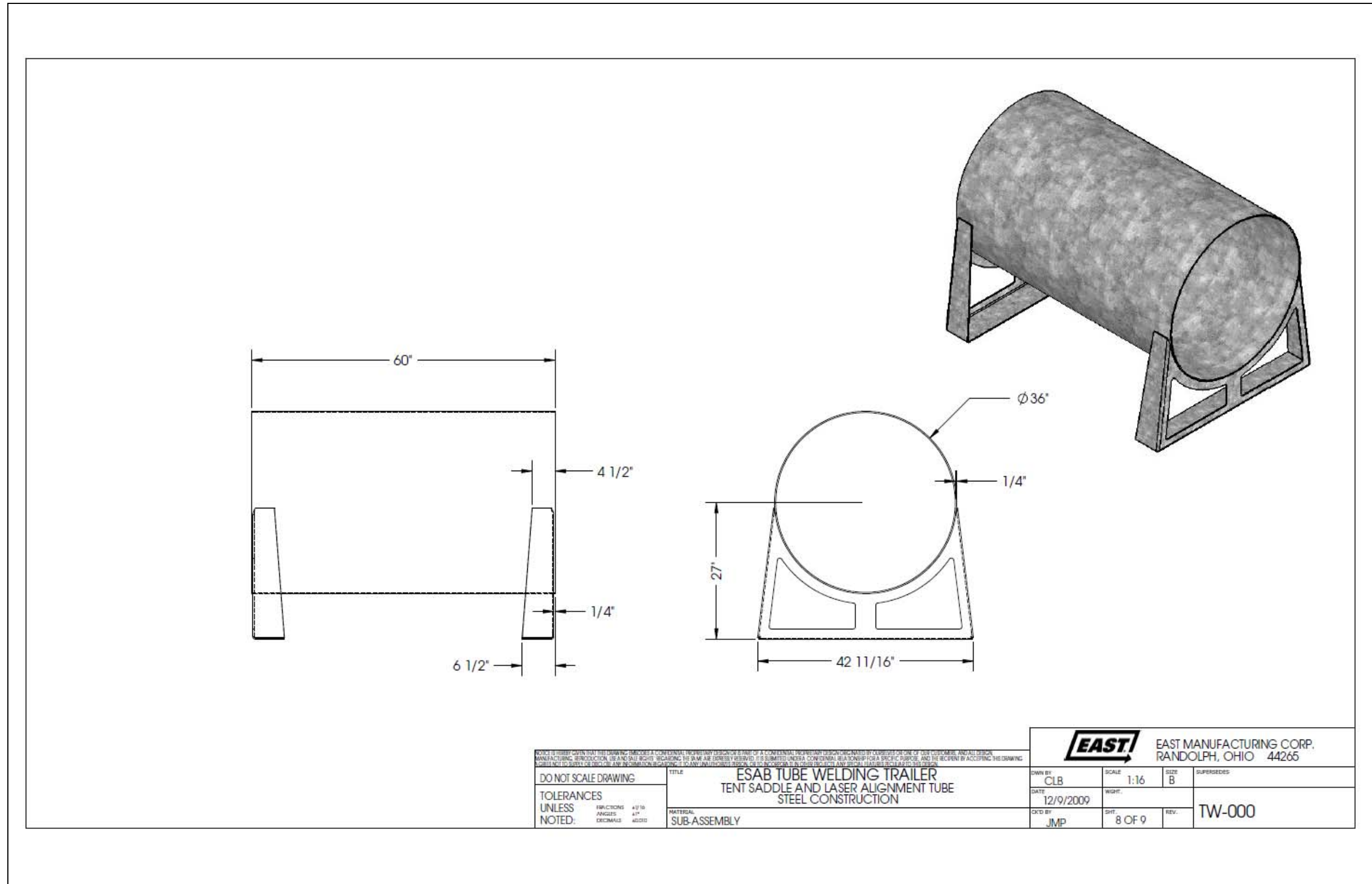


Figure 6.27: ESAB Tube Welding Trailer Tent Saddle and Laser Alignment Tube Steel Construction

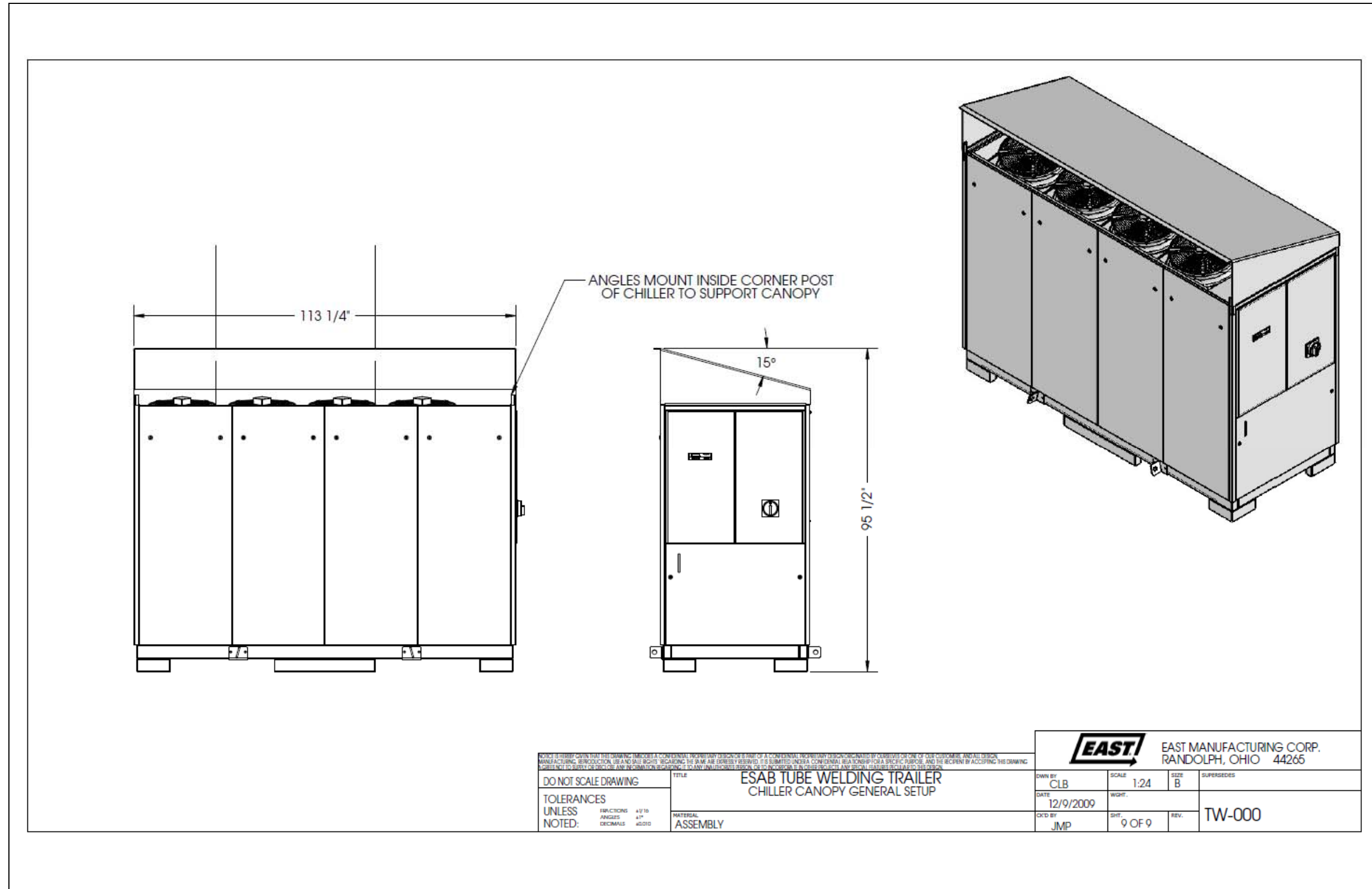


Figure 6.28: ESAB Tube Welding Trailer Chiller Canopy General Setup

6.1.13 System Activation and Testing

The integration of system software with the TriTool orbital motion system was completed. A comparison between the physical and schematic layout of the system is shown in Figure 6.29.

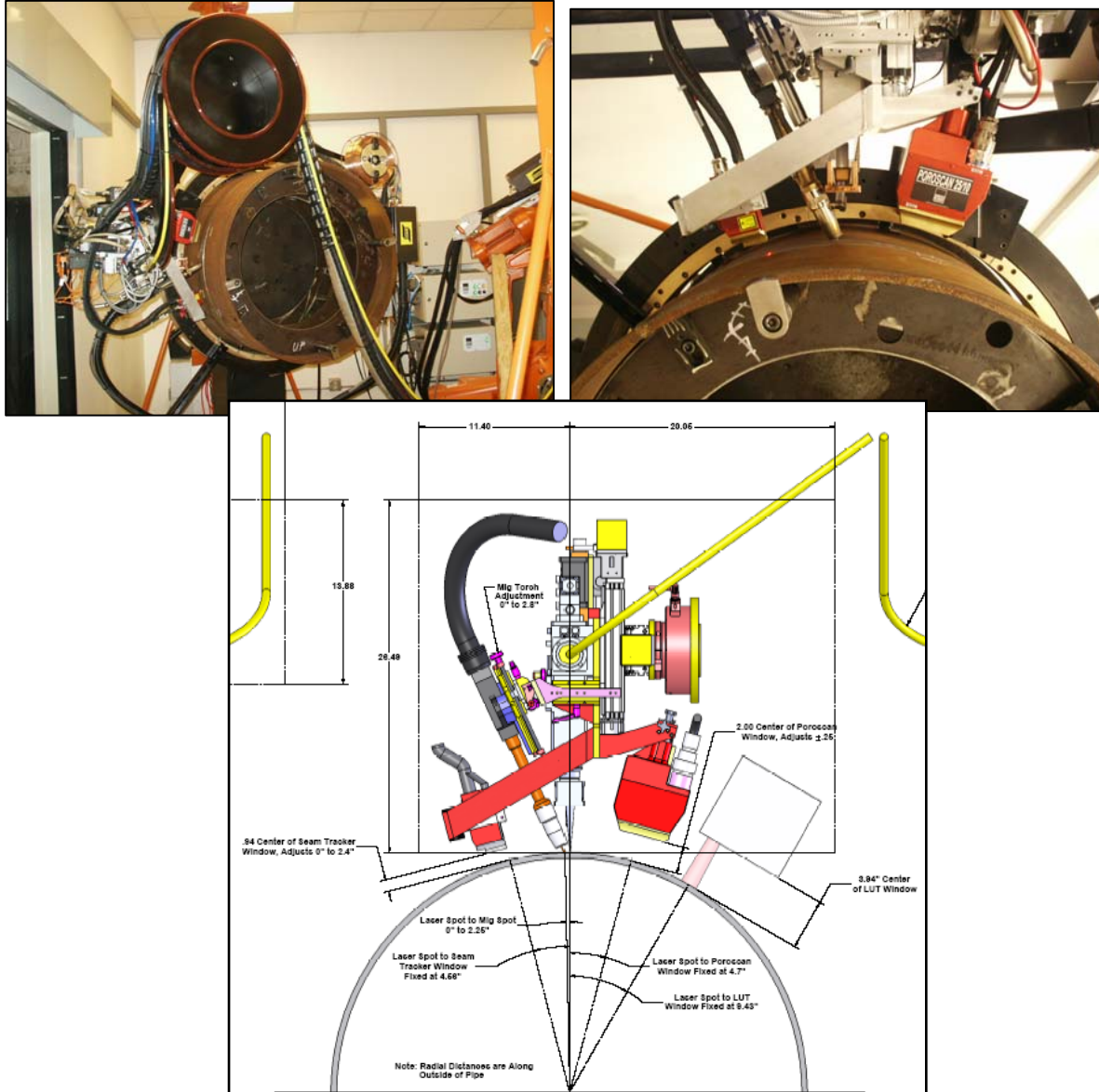


Figure 6.29: Orbital Welding Set-up

Figure 6.30 shows the same orbital system outfitted with the ALUT components.

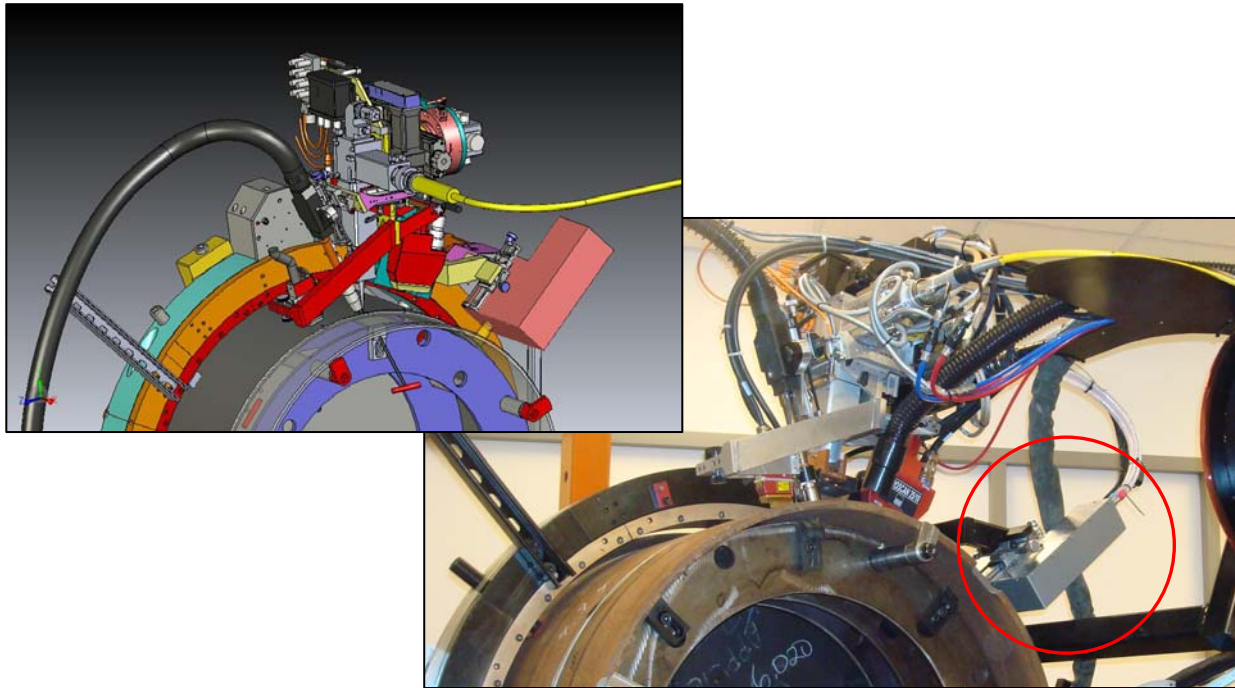


Figure 6.30: Orbital Set-up with ALUT Attachment

Final system integration and testing was successfully completed with the ALUT process. Figure 6.31 shows a sequence of pictures during a test and validation weld.

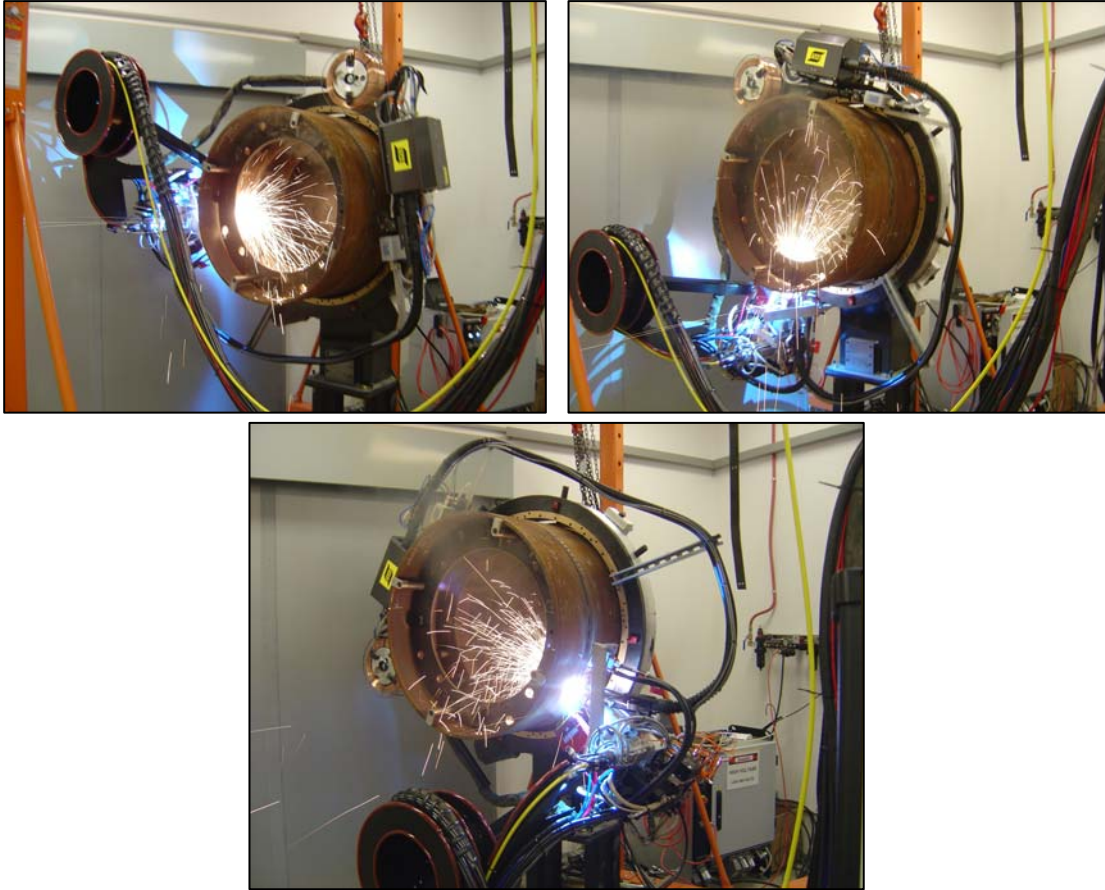


Figure 6.31: Validation Test in the Lab

6.2 Phase 2

As previously discussed, Phase 2 is broken down into the following tasks:

- Task 2.1: HLAW Process Optimization;
- Task 2.1: HLAW Procedure Qualification Testing and Research;
- Task 2.2: Implement and Validate HLAW System;
- Task 2.3: Develop Final System Specifications and Users Guide;
- Task 2.4: Calculate ROI of HLAW Compared to Current Practice; and
- Task 2.5: Prepare and Submit Draft and Final Reports.

6.2.1 Task 2.1 – HLAW Process Optimization

Parameters were developed for 5G full-orbit welding for 10.4 mm X80 and 14.3 mm X100 pipe sections. These parameters were originally based on an 8 mm root face and presented process robustness issues at the 200 degree position. There was significant land variation due to machining capabilities, which led to increasing capabilities for machining weld preparations on pipe sections. Initial trials with preheat were conducted to determine a suitable preheat for the mechanical test specimens.

Two fully welded pipe sections were sent to a local non-destructive test facility (Quality Assurance Laboratories, South Portland, Maine) for XRay analysis in accordance with API 1104 [1]. The pipes sent for Non-Destructive Evaluation (NDE) were sections fabricated at the time of the industry demo, and subsequently filled and capped. It should be noted that the parameters used in this study were for 8 mm root face and 10 mm fill height, using Thyssen NiMo80, 0.9 mm diameter. Each pipe section was radiographically inspected (RT) using single source internal, similar to procedures used in the field. RT evaluation determined that internal concavity was not observed; however, the pipes were rejectable for excessive porosity. This porosity was confirmed to be isolated to the fill/cap passes. Fill and cap pass optimization are discussed below.

RT results indicate that a dramatic improvement was achieved by reducing the laser power from 1.5 kW down to 200 W for fill and cap pass parameters. Process development for fill and cap passes had determined that at slow travel speeds with a closed root may result in porosity when using a physical setup that is ideal for high penetration open root welding. Fill pass development was concluded by selecting a weld procedure from TransCanada Pipelines Limited for NiMo80 wire using 75/25 Ar/CO₂ shield gas, augmented with laser. Weld cosmetics and weld quality had been improved and were satisfactory with the requirements of API 1104 [1].

In order to improve on process robustness the joint face dimension was reduced from 8mm down to 6 mm. The bevel angle was maintained at 25 degrees (50 degrees included). This reduction helped to stabilize the root bead at all positions. A change in vendor to machine the joint improved on root face tolerance and kept the dimension within 0.7 mm. The pipe sections as fitup were held to have joint mismatch at less than 2.0 mm, and root face gaps less than 0.5 mm.

Based on the hardness study conducted, an appropriate preheat of 100°C was selected. This preheat was used to fabricate all of the welds, with a maximum interpass temperature of 135°C.

Each root pass was completed using the specified Thyssen NiMo80 and Ar/CO₂ 85/15 process gas. Each root pass had an average 6.8 kJ/inch heat input with a travel speed of 95 inches per minute, and a weld time of 1min and 16 seconds. The weld process parameters varied around the circumference based on location. The laser power for the pipes was consistent between the X80 and X100 ranging from 6.7 kW to 7.3 kW. The wire feed started at 425 inches per minute and then at 210 degrees around the part dropped down to 350 inches per minute. The process was stable and consistent over the ten pipe sections manufactured.

A number of segment and continuous 5G welds were made on 14.3 mm X100 pipe sections to test overall system functionality. These welds were run with full HLAW process control and post weld surface inspection enabled and functioning. Welds were initiated at the 12 o'clock position and progressed counter clockwise for a full revolution. Weld rates of 95 ipm (2.4 m/min) between 3-8 o'clock and 85 ipm (2.2 m/min) from 8-3 were demonstrated. Maximum laser power was 9.5 kW and achieved a nominal 0.420 inch (10.7 mm) root pass fill. A schematic of these weld rates along with resulting macros of selected sections is shown in Figure 6.32. While these weld parameters were not yet optimized for fill or speed, they did represent nominal achievable production rates for the test conditions. In addition, system capability was also demonstrated for additional fill passes at speeds of 65 ipm (1.7 m/min). While HLAW system is capable of performing multiple fill passes, it does not have the high deposition rates of other tandem or twin systems. For this reason, it is anticipated that the HLAW system would benefit the most in root pass welding.

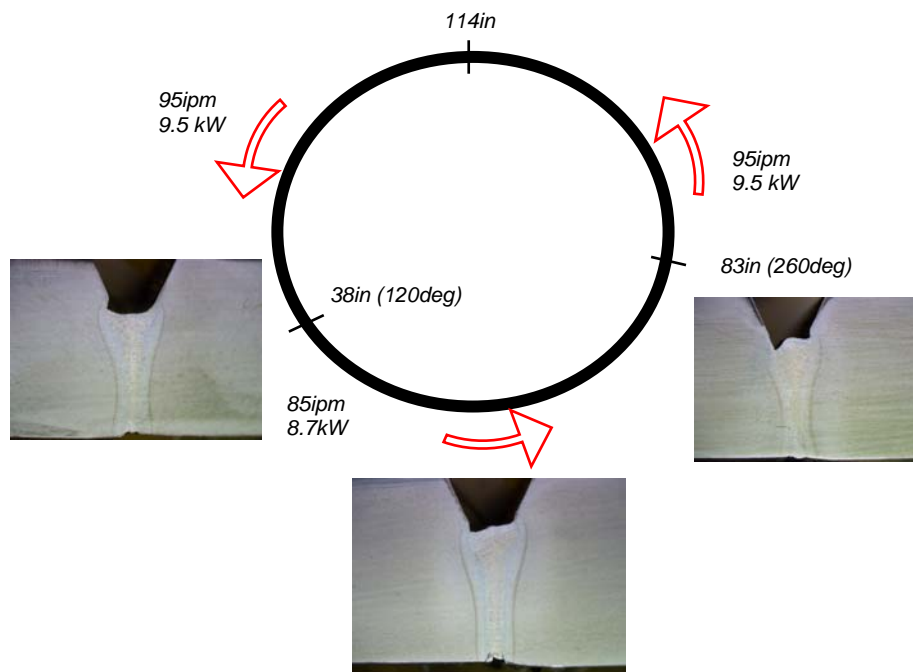


Figure 6.32: Girth Weld Development

Fill and cap passes were added in the 5G position with progression of vertical down. This was completed using the specified Thyssen NiMo80 and Ar/CO₂ 75/25 process gas. Each fill/cap pass had an average 12.3 kJ/inch heat input, at a travel speed of 20 inches per minute. The weld process was not varied during its progression.

The depth of fill for each pass was measured around the circumference of the pipe and the results for X80 and X100 are shown Figure 6.33 and Figure 6.34.

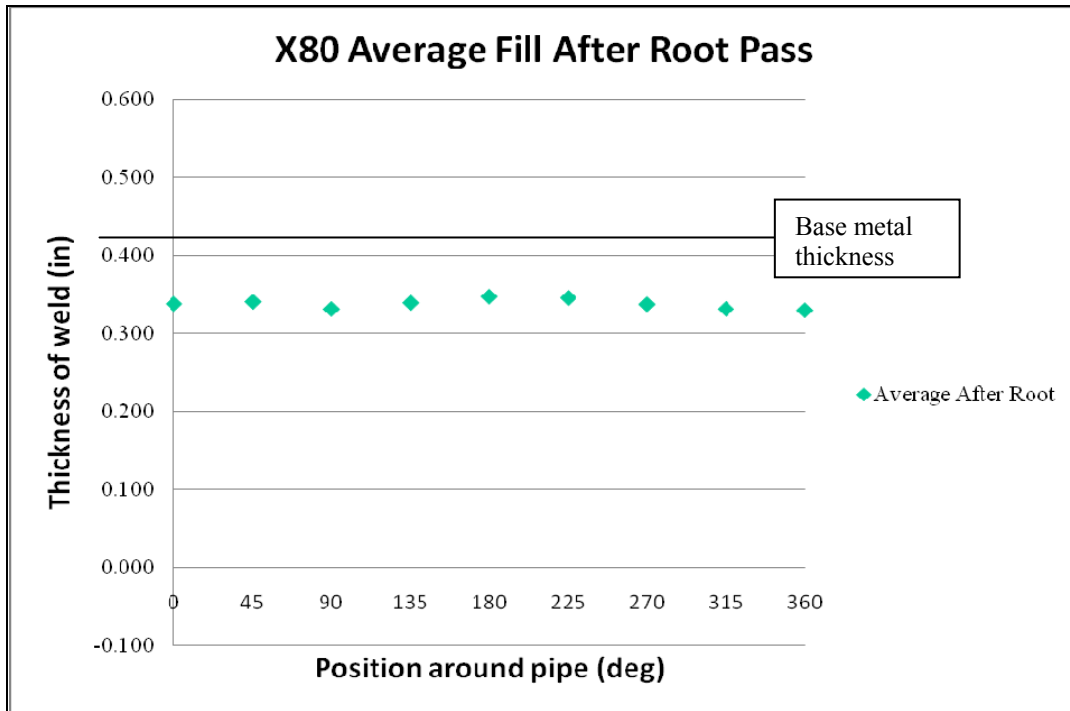


Figure 6.33: Depth of Fill per Pass for X80

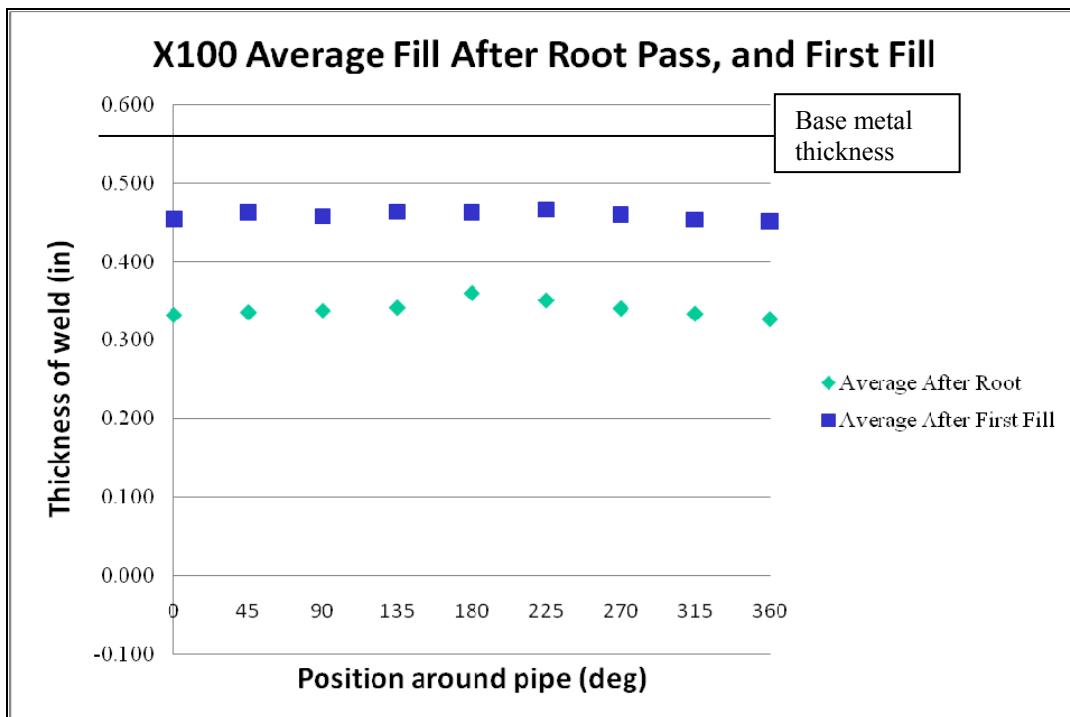


Figure 6.34: Depth of Fill per Pass for X100

The appearance of the root and cap passes for the X80 and X100 welds are shown in Figure 6.35 to Figure 6.38.



Figure 6.35: Typical Face Bead Profile for X80



Figure 6.36: Typical Root Bead Profile for X80

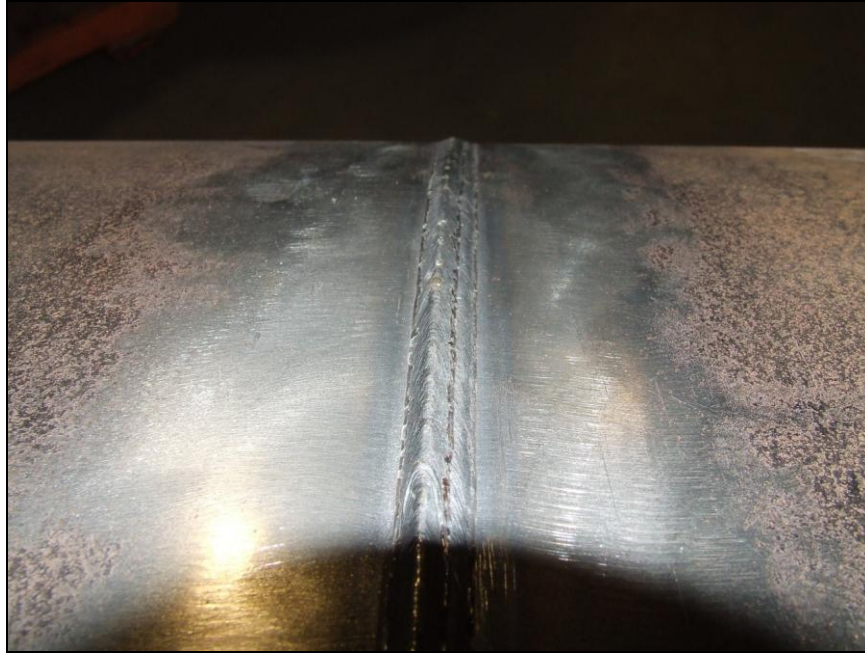


Figure 6.37: Typical Face Bead Profile for X100



Figure 6.38: Typical Root Bead Profile for X100

A total of ten welded pipe sections were fabricated to be subjected to a series of mechanical testing and investigations (see Figure 6.39).



Figure 6.39: Ten Pipe Sections Manufactured for Testing (Pipe Samples 498 to 508)

6.2.2 Task 2.1 – HLAW Procedure Qualification Testing and Research

The ten pipes manufactured were used to perform a series of standard and non-standard tests. The mechanical properties of the welds deposited in NPS36 X80 and X100 pipes were evaluated using a series of Nick Break, Side Bend, Cross Weld Tension, Charpy Impact, and CTOD testing.

All ten pipes were subjected to radiography and ultrasonic inspection in accordance with API 1104 [1]. The test results are provided in Annex B.

Mechanical test specimens were extracted and machined to size in accordance with API 1104 [1] for the welding procedure qualification of girth welds. Figure 6.40 shows the location where each test specimen was removed from.

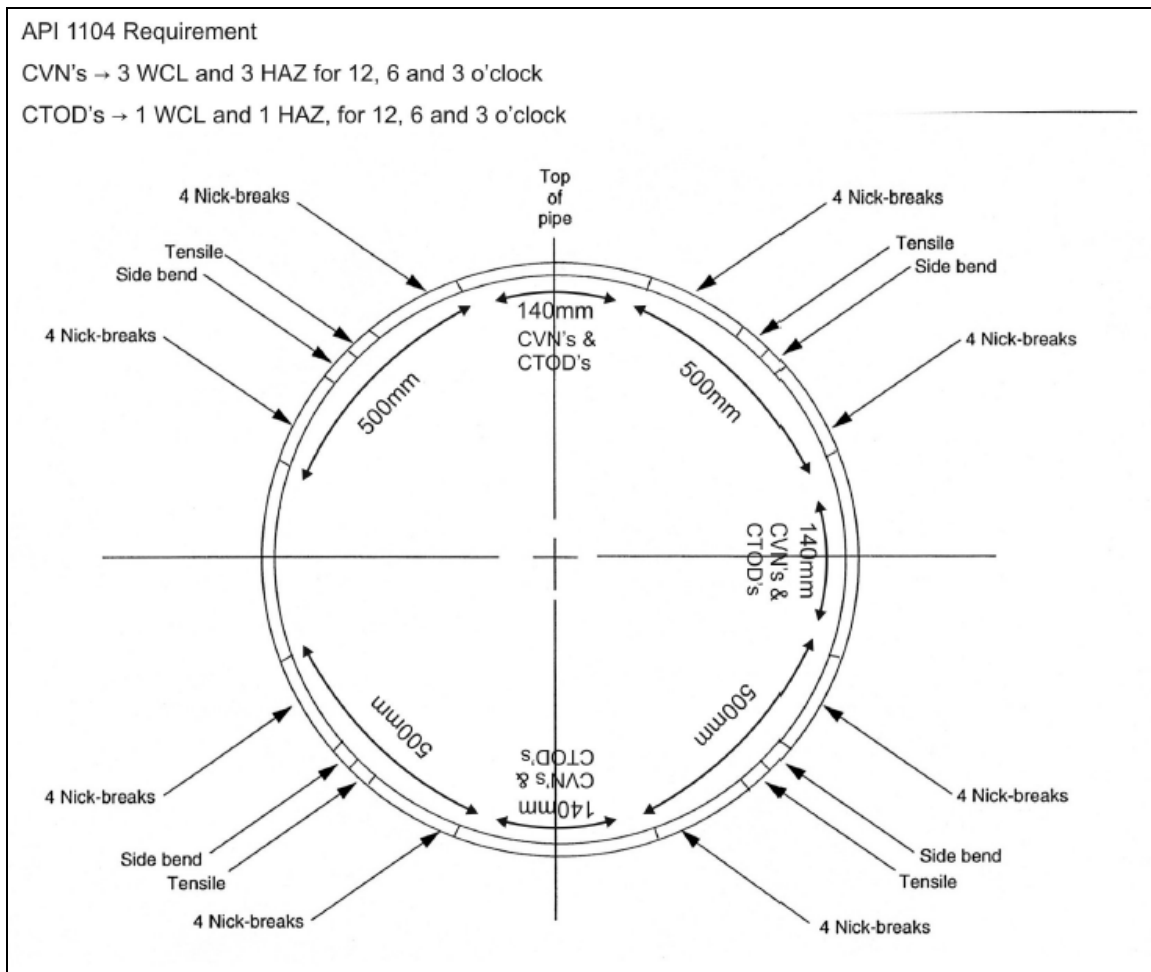


Figure 6.40: Location of Test Specimens

6.2.2.1 Nick Break Results

Nick break specimens were extracted, machined to size, notched, and tested in a Baldwin hydraulic test frame until failure. The surfaces were inspected for discontinuities in accordance with API 1104 [1]. There were no visible discontinuities on any of the tested fracture surfaces.

6.2.2.2 Side Bend Results

Side bends were extracted, machined to size, and tested in a jig with a bend mandrel diameter of 90 mm. All specimens were bent 180 degrees and were inspected for any openings that exceed 3.2 mm in size. Each of the specimens met the requirements of API 1104 [1].

6.2.2.3 Cross Weld Tensile Testing Results

Cross weld tensile specimens were extracted, machined to size, and tested in a Baldwin hydraulic test machine. The maximum load to failure was recorded. The results for each of the specimens are shown in Table 6.4.

Table 6.4: Cross Weld Tensile Results for Pipes 497 (X100) and 508 (X80)

Sample ID	Thickness		Width		Area		Ultimate Load		U.T.S.		Fracture Location
	in	(mm)	in.	(mm)	in. ²	(mm ²)	lbs.	(kN)	psi	(MPa)	
497-1	0.546	13.86	0.753	19.13	0.41	265	48,200	214	117,299	809	BM Ductile
497-2	0.548	13.92	0.753	19.12	0.41	266	47,300	210	114,680	791	BM Ductile
497-3	0.553	14.05	0.751	19.08	0.42	268	47,600	212	114,538	790	BM Ductile
497-4	0.552	14.03	0.748	19.00	0.41	267	48,200	214	116,676	804	BM Ductile

Sample ID	Thickness		Width		Area		Ultimate Load		U.T.S.		Fracture Location
	in	(mm)	in.	(mm)	in. ²	(mm ²)	lbs.	(kN)	psi	(MPa)	
508-1	0.399	10.13	0.747	18.99	0.30	192	30,500	136	102,337	706	BM Ductile
508-2	0.394	10.01	0.748	18.99	0.29	190	30,500	136	103,475	713	BM Ductile
508-3	0.399	10.13	0.750	19.06	0.30	193	31,000	138	103,550	714	BM Ductile
508-4	0.398	10.10	0.749	19.03	0.30	192	30,400	135	101,986	703	BM Ductile

6.2.2.4 All Weld Metal Tensile Testing Results

In North America, API 1104 [1] and CSA Z662 [2] are the standard test procedures used for pipeline girth weld testing. In this work, the constraints imposed by an irregular HLAW geometry were of primary consideration (see Table 6.4).

The GMAW portion of the HLAW weld is positioned on top of a hybrid pass, which combined, produces a non-typical weld profile. In this work, both X80 and X100 pipeline girth welds were evaluated, which included the testing of multi-pass cap (X100) and single pass cap (X80) specimens.

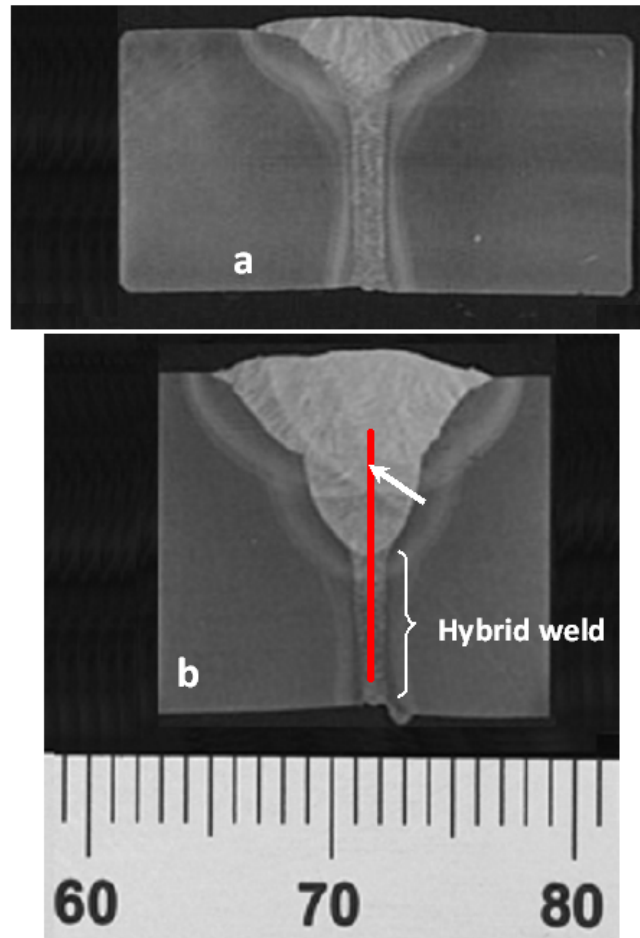


Figure 6.41: HLAW Weld Macros for (a) X80 and (b) X100 Pipe

The red vertical line represents the gauge length of the strip tensile specimens, while the white arrow indicates where the round bar specimens were extracted from.

The focus of this research was to modify current practices for extracting and testing All Weld Metal (AWM) specimens from a geometrically constrained girth weld. In a previous study [3], the strip specimen geometry was evaluated to determine the tensile properties of a GMAW cross section and it was then compared to the results obtained from the testing of a round bar Hounsfield specimen. It should also be noted that the strip specimen usually does not meet the gauge section dimensions of ASTM E8 [4] guidelines.

Two AWM specimen types were considered to be viable test configurations. These were (a) round bar and (b) strip specimens. Figure 6.42 shows the relative sizes of the dimensions of the strip tensile specimens adopted for use in this current study.

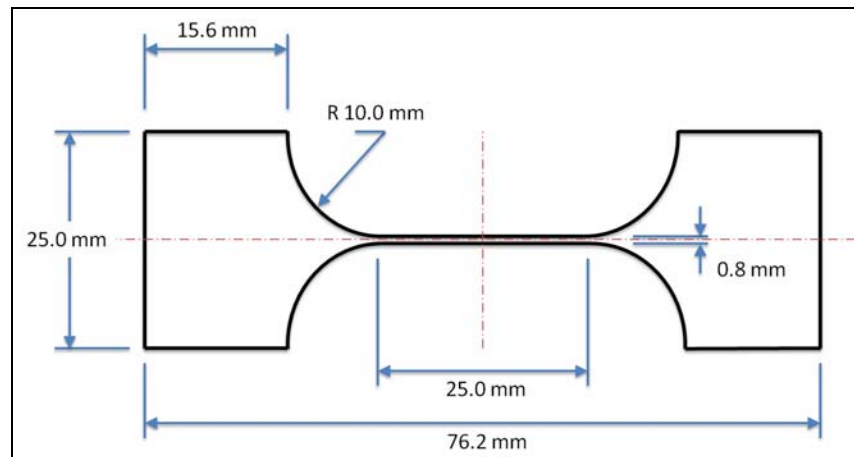


Figure 6.42: CAD drawing showing the tensile test specimen dimensions

Sample Preparation

Extraction of All Weld Metal (AWM) Tensile Specimens

Two tensile specimen types were produced for testing. The sample geometry included strip tensile (Figure 6.43) and Hounsfield tensile specimen (Figure 6.44) types. The aim was to extract all weld metal tensile coupons from pipe numbers 503 and 507 (X80) and pipe numbers 500 and 502 (X100).

For the X80 pipe, with a nominal pipe wall thickness of 10.4 mm, only strip tensile specimens were feasible. This is due to the hybrid portion of the weld being less than 3 mm wide. A 3 mm diameter Hounsfield-type specimen could realistically not be extracted.

For the X100 pipe, with a nominal pipe wall thickness of 14.3 mm, in addition to the strip tensile specimens, a 3 mm diameter Hounsfield type specimen could be extracted to sample the fill and cap passes deposited with laser assisted GMAW.

Strip Tension Specimens

Approximately 75 mm (3 inch) lengths of weld were extracted from X80 and X100 pipes. These coupons were then used to machine strip tensile specimens, illustrated in Figure 6.43. The clock locations where these coupons were extracted from are given in Table 6.4.

The extracted coupons were milled, followed by surface grinding to produce a rectangular and parallel coupon. The flat coupons were then etched using 10 percent nital on the ID side to expose the weld root. As can be seen, the weld root width is approximately 1 mm.

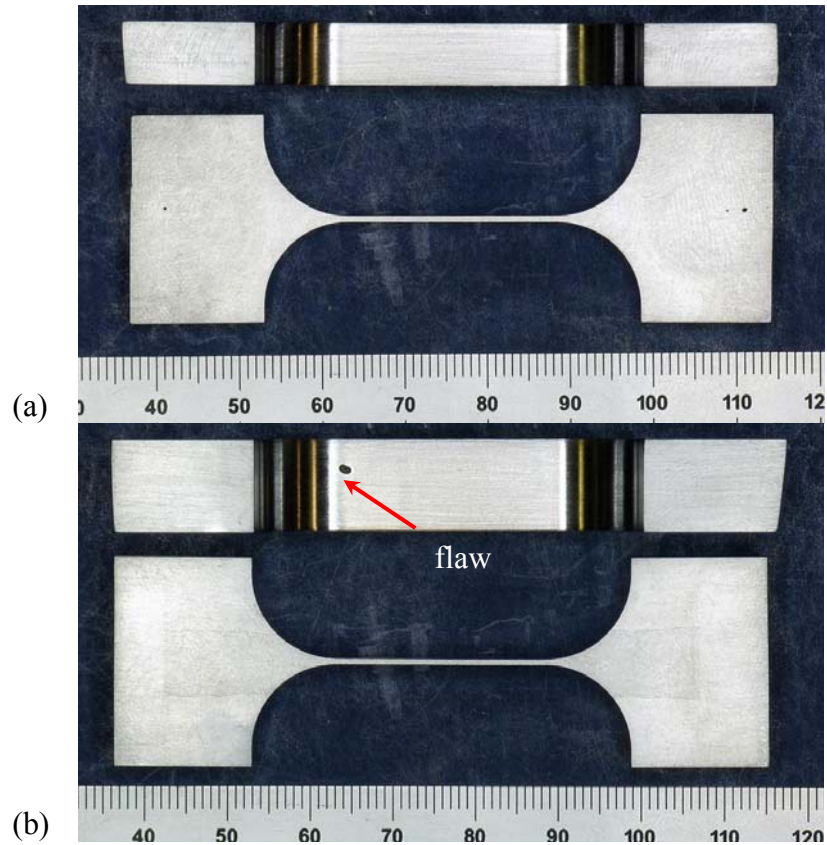


Figure 6.43: Views of Machined X80 Strip Tensile Test Specimens



Figure 6.44: Machine Hounsfield Specimen

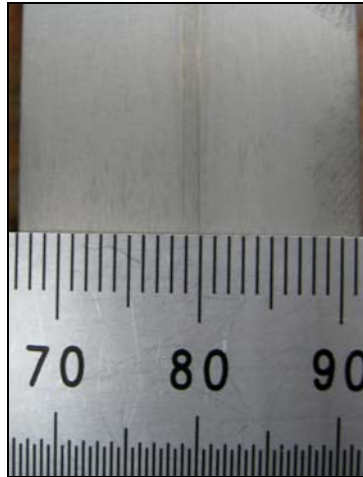


Figure 6.45: Weld Root Side of an AWM Tensile Coupon

The eventual AWM strip specimens were then profiled by Electro-Discharge Machining (EDM), based on the CAD drawing shown in Figure 6.46. The test gauge length was cleaned by polishing it with emery paper to remove any layer of material that may have been affected from the EDM process. Examples of finished specimens are displayed above in Figure 6.43. Weld metal anomalies were also observed in the finished strip tensile specimen gauge lengths as displayed in Figure 6.43 (b) and Figure 6.46.

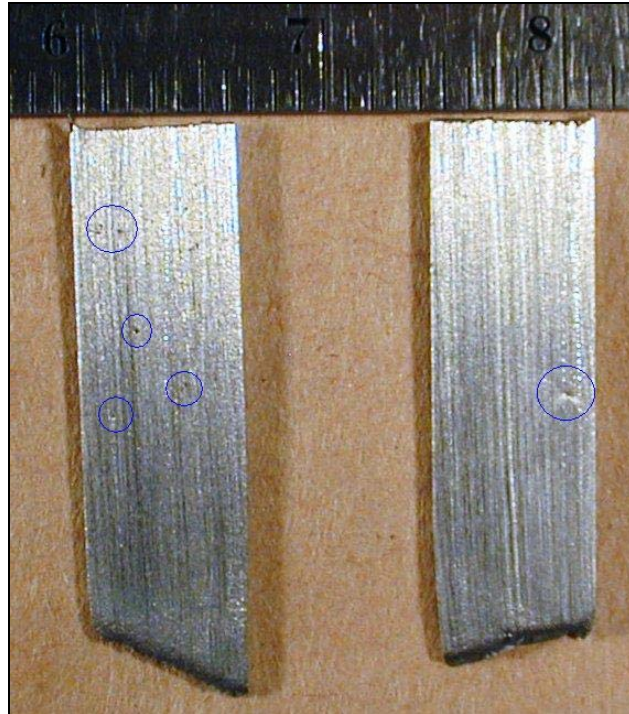


Figure 6.46: Weld Metal Anomalies Inherent in Strip Tensile Specimens

Hounsfield Tension Specimens

Approximately 25 mm (1 inch) lengths of X100 weld were sectioned from the 11:30 and 1:30 clock positions. The extracted coupons were then machined to a smooth finish and were then etched with 10 percent nital (see Figure 6.47). The cross hair mark visible in this image was used to indicate where the centre of the round bar specimen should be located during the EDM extraction process. The arrow in Figure 6.43(b) also indicates the centre of the round bar specimen. From these extracted round bars, 3 mm diameter Hounsfield specimens were then machined, as shown in Figure 6.44.

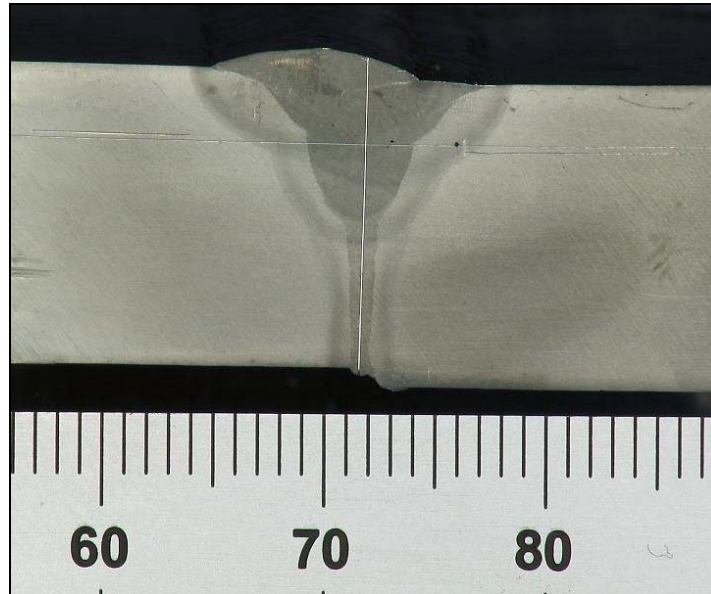


Figure 6.47: Etched End of Coupon/Hounsfield Specimen Centred Around Cross Hair

Test Procedure and Results

Test Procedure

All testing was performed at ambient temperature (23°C) using a servo-hydraulic test frame under displacement control (see Figure 6.48). The testing was conducted at The Materials Assessment Lab, CANMET, Ottawa.

The strip tensile tests were conducted using a quasi-static loading rate using a ram rate of 1 mm/min. The specimen elongation was monitored using a 25 mm gauge length extensometer.

For the round Hounsfield tensile testing, a quasi-static loading rate of 0.4 mm/min. was used. The specimen elongation was monitored using the test frame ram displacement. The specimen length (25 mm) and gauge length (approximately 10 mm) was, however, too small to mount an extensometer that could derive more accurate specimen gauge length extension.

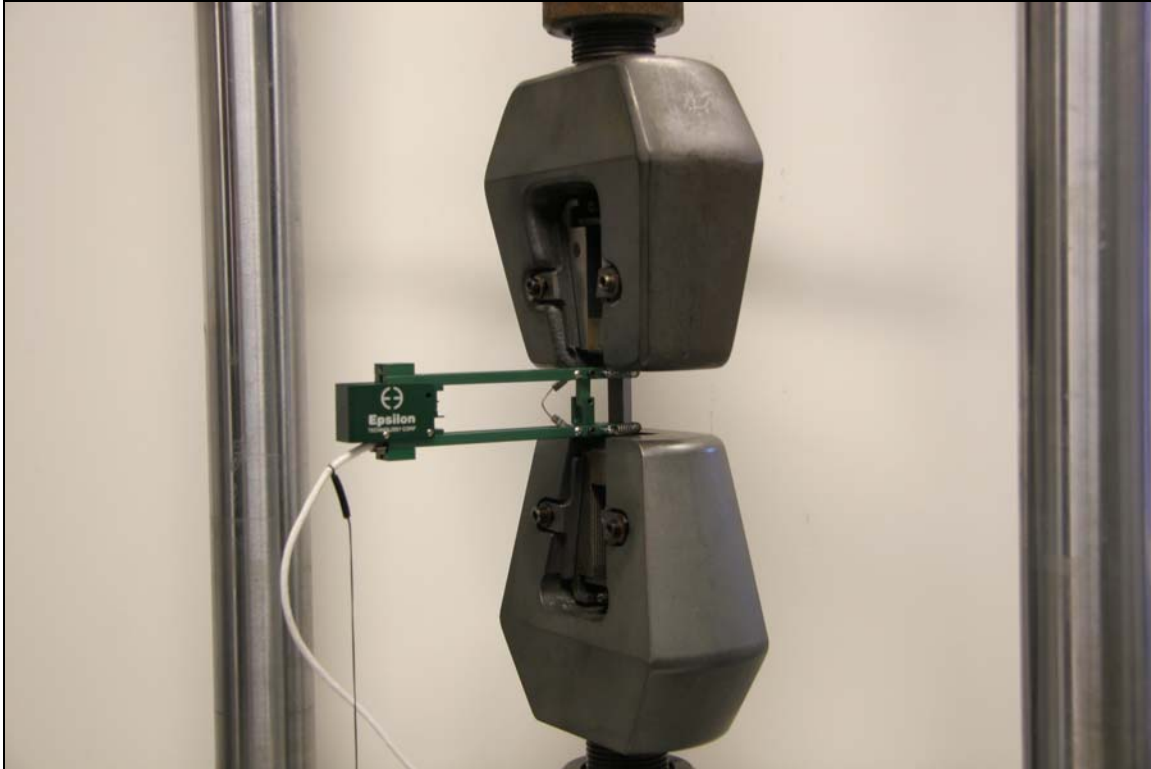


Figure 6.48: Tensile Test Configuration

Chemical Composition

Chemical analyses (ASTM E1019-08 [5] and ASTM D1076-06 [6]) was conducted on the as deposited weld coupons. The material tested was situated in the gauge section of strip tension specimens.

The chemistry at varying clock position was determined and the results for both the X80 and X100 as-deposited welds are presented in Table 6.4. The table also contains the Base Material's (BM) chemistry (X80 and X100), as supplied by the pipe manufacturers in their Materials Testing Reports (MTRs).

Table 6.5: X80 and X100 Chemical Composition

Pipe ID & Grade	Clock Location	N	O	Al	Cr	Cu	Mn	Mo	Ni	Si	Ti	V	C	S
BM X80	NA	0.0070	NA	0.029	0.16	0.22	1.65	0.30	0.12	0.25	0.11	0.005	0.05	0.004
WM X80	NA	0.0100	0.014	0.024	0.14	0.19	1.68	0.35	0.33	0.35	0.02	<0.005	0.09	<0.005
507 X80	11:00	<0.0050	0.008	0.022	0.13	0.19	1.58	0.34	0.33	0.35	0.02	<0.005	NA	NA
507 X80	9:00			0.024	0.14	0.2	1.68	0.35	0.27	0.32	0.019	<0.005	0.09	<0.005
503 X80	2:30	0.01	0.014	NA	NA	NA	NA	NA	NA	NA	NA	NA	NA	NA
BM X100	NA	0.0026	NA	0.004	0.53	0.44	1.87	0.11	0.45	0.19	0.010	0.000	0.06	0.001
WM X100	NA	0.0050	0.015	<0.005	0.33	0.30	1.70	0.27	0.78	0.43	0.028	<0.005	0.09	<0.005
500 X100	11:00	0.005	0.012	NA	NA	NA	NA	NA	NA	NA	NA	NA	NA	NA
502 X100	5:30	NA	NA	<0.005	0.29	0.27	1.65	0.27	0.78	0.43	0.028	<0.005	0.09	<0.005
502 X100	8:30	<0.0050	0.015	NA	NA	NA	NA	NA	NA	NA	NA	NA	NA	NA
502 X100	2:45	NA	NA	<0.005	0.33	0.3	1.7	0.24	0.74	0.4	0.025	<0.005	0.07	<0.005

Note: The as-deposited weld coupons sent for analysis was from the gauge section of strip tension tests

Results: Strip Tensile Testing

The results for the strip tensile testing for both the X80 and X100 are presented in Table 6.6 and show that there were minor variations in both yield and tensile strengths as the specimen location moved clockwise from the 12 o'clock position. There were also variations in the percent elongation.

Table 6.6: X80 and X100 Tensile Test Results

Pipe ID & Grade	Type	Clock Location	Specimen ID	0.2% Y.S.	U.T.S. (MPa)	% Elongation	Notes
500 X100	Strip Tensile	11:00	500-11:00	871.00	952.70	8.4	Gauge section - 10.8 x 0.75mm approx 50% each of hybrid and GMA
502 X100	Strip Tensile	2:45	502-2:45	833.50	910.00	7.4	Gauge section - 10.8 x 0.75mm approx 50% each of hybrid and GMA pass
		5:00	502-5:00	904.10	976.90	9.8	
		5:30	502-5:30	887.20	986.50	9.6	
		8:00	502-8:00	882.80	959.10	10.4	
		8:30	502-8:30	889.10	966.90	10.0	
		11:30	502-1:00	839.20	930.50	5.60	
503 X80	Strip Tensile	2:30	503-2:30	866.70	944.60	5.8	Gauge section - 10.8 x 0.75mm approx 50% each of hybrid and GMA
		5:00	507-5:00	868.00	960.60	8.6	
507 X80	Strip Tensile	5:45	507-5:45	849.20	927.70	7.9	Gauge section - 6.75 x 0.75mm approx 75% each of hybrid pass
		8:00	507-8:00	890.20	954.40	6.9	
		9:00	507-9:00	905.30	980.40	5.8	
		11:00	507-11:00	874.30	930.60	7.6	
		11:30	507-1:00	826.10	912.20	5.80	
502 X100	Hounsfeld Tensile	1:30	502-2:00	756.00	905.00	31.40	Gauge section - 3mm dia. GMA pass

Although there is no conclusive evidence, the results suggest that the bottom half of the pipe girth weld produced higher yield, Ultimate Tensile Strength (UTS), and percent elongation values when compared to the top half of the pipe.

On the lower end of the scale for the X100 welds, yield, UTS, and percent elongation of 833 MPa, 910 MPa, and 7 percent respectively was observed for specimens extracted from 2:45 o'clock.

On the higher end of the scale for the X100 welds, yield, UTS, and percent elongation of 904MPa, 976MPa, and 9.8 percent respectively and was observed for specimens extracted from 5:00 o'clock.

Example stress-strain curve for the X100 strip tensile tests are presented in Figure 6.49 for pipe number 502.

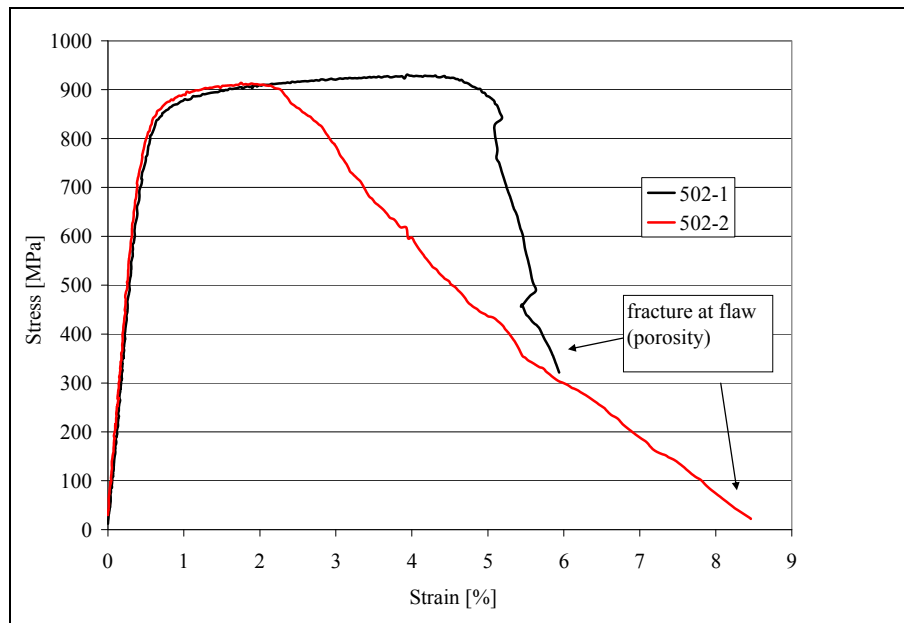


Figure 6.49: Strip Tensile Stress-strain Curves for X100 Pipe Weld

On the lower end of the scale for the X80 welds, yield, UTS, and percent elongation of 826 MPa, 912 MPa and 5.8 percent respectively was observed for specimens extracted from 11 o'clock.

On the higher end of the scale for the X100 welds, yield, UTS, and percent elongation of 905MPa, 980MPa, and 5.8 percent respectively and was observed for specimens extracted from 9:00 o'clock.

Example stress-strain curve for the X80 strip tensile tests are presented in Figure 6.49 for pipe number 507.

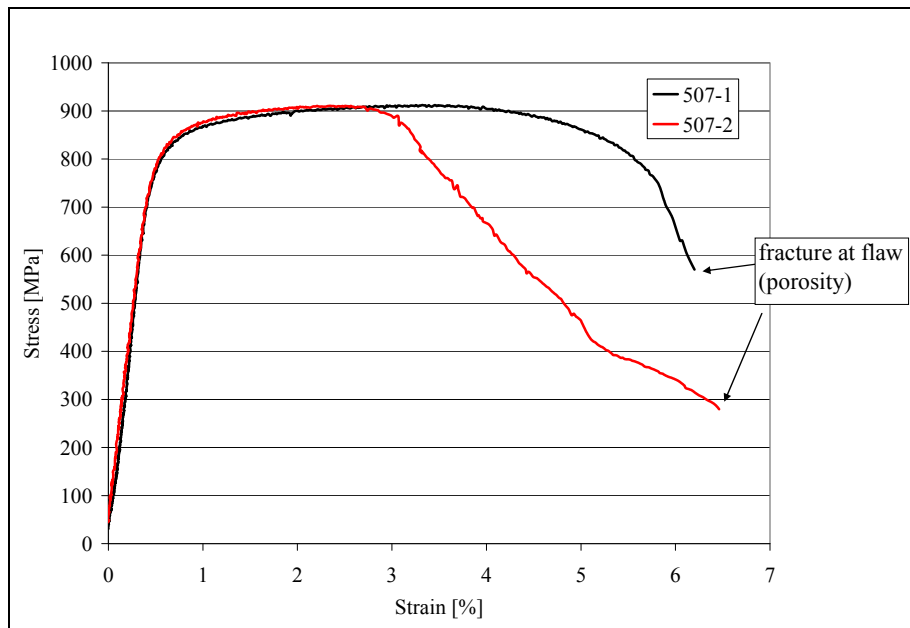


Figure 6.50: Strip Tensile Stress-strain Curves for X80 Pipe Weld

The strip tensile fracture surfaces for specimens 502-2 (X80) and 507-2 (X100) are presented in Figure 6.51 and Figure 6.52. Both fractures show porosity on the fracture surface.

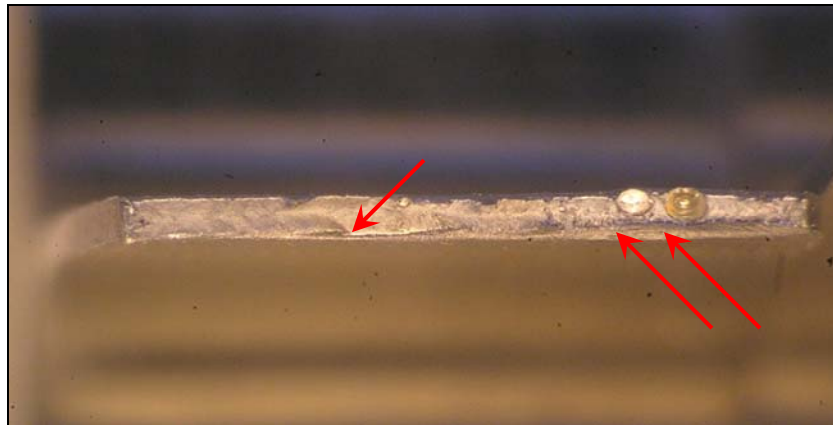


Figure 6.51: Fracture Surface of Specimen 502-2 (X100)

Note: The red arrows indicate porosity.

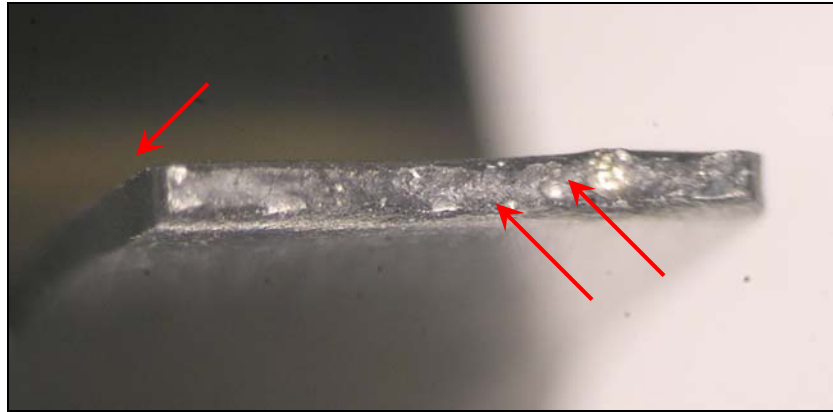


Figure 6.52: Fracture Surface of Specimen 507-2 (X80)

Note: The red arrows indicate porosity.

Results: Hounsfield Specimens

The Hounsfield tests were only conducted on the first quarter (11 to 2 o'clock) and only for the X100 girth welds. The results are presented at the bottom of Table 6.6.

When compared to the strip tensile results, a reduction in yield strength of approximately 100 MPa is noted. The results presented in Table 6.6 show that the measured percent elongation at fracture was much larger compared to the AWM strip results for X100 pipe.

It should be noted that the weld metal in the gauge section represents GMAW portion and is believed to be the likely cause for the lower yield strengths (730 and 756 MPa) compared to (839 and 849 MPa) from the strip tension test results from the same clock positions presented in Table 6.6.

Figure 6.53 displays the fracture surface of an X100 specimen and it does not have indications of porosity on the fracture surface.



Figure 6.53: Fracture Surface of X100 Hounsfield Specimen

Note: No porosity detected.

Discussion

It was possible to machine and successfully perform strip tensile tests with the specimen geometry presented previously. Accurate stress-strain curves could also be obtained from the results as the specimen extension was monitored from an extensometer. The gauge section, though extremely narrow in the weld width dimension, was found to be sufficiently rigid to perform testing in a servo-hydraulic frame.

The percent elongation at fracture from strip tension tests for both X80 and X100 welds was low, i.e., under 10 percent. The uniform elongation, i.e., elongation at maximum load during the tests was also below what is usually expected [3], i.e., under 5 percent, in the case of the stress strain curves shown in Figure 6.49 and Figure 6.50. A contributing factor for this is flaws that were present in the test gauge length, as shown in Figure 6.51 and Figure 6.52. Another contributing factor could be the non-standard gauge section dimensions of ASTM E8 [4] guidelines

The lowest yield stress in the strip tensile specimens was about 830 MPa for both the X80 and X100 pipe welds. This indicated the feasibility of producing overmatched girth welds for these grades using the HLA welding process.

When considering the Hounsfield specimens, the cap and fill region of the weld made by laser assisted GMAW had a yield stress of more than 730 MPa, thus producing a weld strength that is overmatched in terms of nominal yield strength of X100 pipe. It is, however, acknowledged that the Hounsfield specimen removed from the cap and fill region does not provide representative tensile properties for the HLA weld. Therefore, after the preliminary tests carried out on the X100 weld in the 11.30 and 1.30 clock locations, the Hounsfield specimen testing was not adopted for the remaining testing around the girth weld.

The yield and tensile strength (UTS) obtained from strip tension specimens may be compared with the predictions made from micro-hardness measurements [7]. The results from micro-hardness measurements are presented in Table 6.7. When comparing these results with those in

Table 6.6, for X100 pipe weld, most of the yield strength results in Table 6.6 fall within the mean \pm standard deviation in Table 6.7, whereas, the UTS values in Table 6.6 are mostly above the range in Table 6.7. For X80 pipe weld, both yield and UTS values in Table 6.5 fall within the range of values in Table 6.7.

Slight variations in chemical composition were detected with each change in clock position for both the X80 and the X100 welds. This was noted, but was not explored further. It is suggested that further work be conducted to clarify and analyze the relevance of these variations.

Table 6.7: X80 and X100 Yield and Tensile Strength (UTS) from Micro-hardness Measurements, (MPa)

	X80 – 1.30 clock		X100 – 4.30 clock	
	YS	UTS	YS	UTS
Mean	840	948	851	903
Standard Deviation	47	26	49	28

6.2.2.5 Charpy Impact Results – API 1104

Guidelines from API 1104 [1] were adopted in extracting coupons for machining sets from 12, 6, and 3 o'clock positions. From each coupon three specimens were to be machined.

The specimens were cooled in a temperature controlled reagent bath. The bath temperature was also measured using a calibrated digital recorder with traceability to the National Institute of Standards and Technology (NIST). The samples were tested adopting the guidelines in ASTM E23 [8] using a 300ft-lb (400J) capacity NIST-calibrated Satec Charpy impact tester. The test results are shown in Table 6.8 and Table 6.9.

Table 6.8: Weld 497 Impact Test Results – X100 (Full Size Specimens 10 mm)

WELD	SPECIMEN ID	TEST TEMP (°C)	FT. LBS	JOULES	LAT. EXP	%SHEAR
12 o'clock	497-12-1W	-5	168	228	0.074	100
	497-12-2W	-5	193	261	0.082	100
	497-12-3W	-5	187	253	0.084	100
3 o'clock	497-3-1W	-5	135	183	0.066	100
	497-3-2W	-5	137	186	0.08	100
	497-3-3W	-5	110	149	0.06	100
6 o'clock	497-6-1W	-5	181	245	0.08	100
	497-6-2W	-5	188	255	0.086	100
	497-6-3W	-5	181	245	0.074	~100
HAZ						
12 o'clock	497-12-1H	-5	186	252	0.094	100
	497-12-2H	-5	182	246	0.094	100
	497-12-3H	-5	192	260	0.096	100
3 o'clock	497-3-1H	-5	209	283	0.096	100
	497-3-2H	-5	204	276	0.09	100
	497-3-3H	-5	195	264	0.092	100
6 o'clock	497-6-1H	-5	196	266	0.094	100
	497-6-2H	-5	193	262	0.096	100
	497-6-3H	-5	215	291	0.094	100

Table 6.9: Weld 508 Impact Test Results – X80 (Subsize Specimens 8.3 mm)

WELD	SPECIMEN ID	TEST TEMP (°C)	FT. LBS	JOULES	LAT. EXP	%SHEAR
12 o'clock	508-12-1W	-5	226	306	0.084	100
	508-12-2W	-5	212	287	0.084	100
	508-12-3W	-5	>300	>400	N/A	100
3 o'clock	508-3-1W	-5	46	62	0.023	30
	508-3-2W	-5	51	68	0.034	30
	508-3-3W	-5	24	33	0.022	30
6 o'clock	508-6-1W	-5	172	233	0.077	~100
	508-6-2W	-5	31	42	0.031	40
	508-6-3W	-5	165	224	0.086	100
HAZ						
12 o'clock	508-12-1H	-5	152	206	0.093	100
	508-12-2H	-5	150	203	0.095	100
	508-12-3H	-5	141	191	0.091	100
3 o'clock	508-3-1H	-5	131	178	0.087	100
	508-3-2H	-5	142	193	0.092	100
	508-3-3H	-5	147	199	0.096	100
6 o'clock	508-6-1H	-5	150	203	0.093	100
	508-6-2H	-5	141	191	0.092	100
	508-6-3H	-5	167	226	0.098	100

Selected test specimens were sectioned at the mid-wall plane to observe the location of the root of the Charpy notch and crack propagation path. *Note that in this plane the weld ligament is the laser part of the hybrid weld (see Figure 6.54).* The results for the X100 weld (ID 497) are presented in Figure 6.55. The results indicate that for specimen on the left (from the 12 o'clock position – specimen 12/1W), the fracture propagation occurred in the weld except at the last stage. In the other two specimens, 3/1W (middle) and 6/2W (right) the fracture deviated from the

weld at the very early stages. In all three specimens the root of the Charpy notch appears in the weld metal, i.e., the notch was in the correct location.

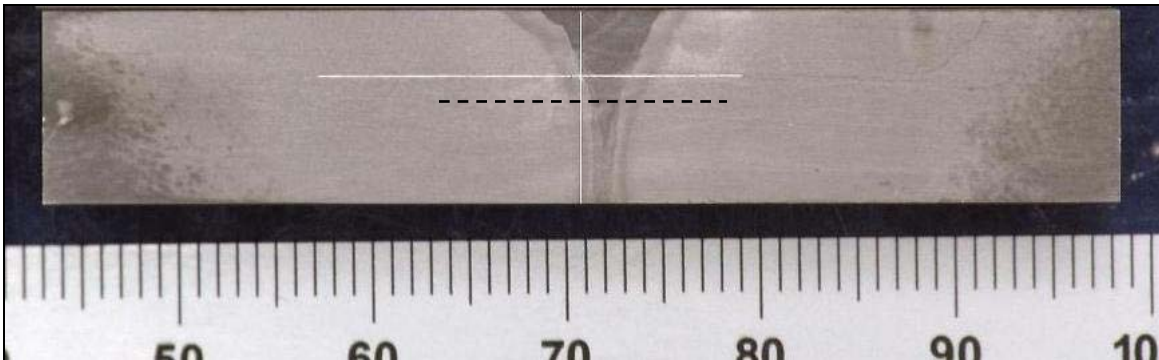


Figure 6.54: Weld 508 Impact Test Results – X80 (Subsize Specimens 8.3 mm)

Note to Figure 6.54: The cross hairs are for positioning the Charpy notch for the HAZ specimen.

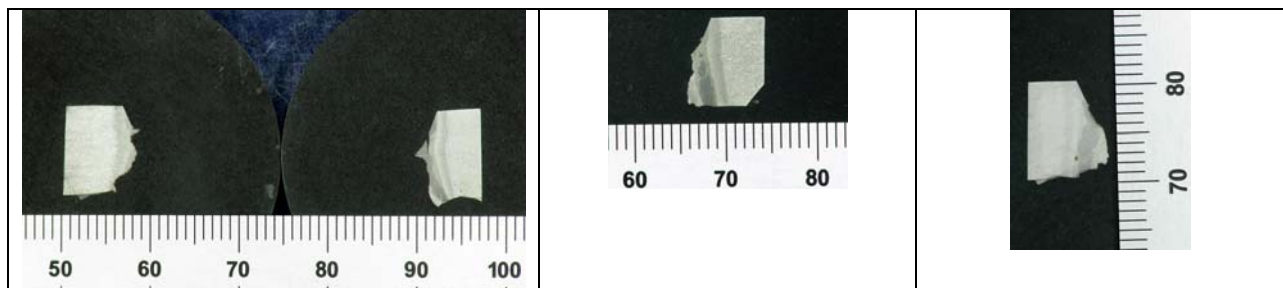


Figure 6.55: Macrographs of the Sectioned Charpy Specimens from Weld 497

Note to Figure 6.55: The sample on the left (representing 12 o'clock) show the two halves of the broken specimen. The other two samples have only one side shown, as most of the fracture propagation occurred outside the weld zone.

The results for the X80 weld (ID 508) are presented in Figure 6.56. The results indicate that in specimen 12/2W (on the left) the fracture propagation occurred in the weld except at the last stage and for specimen 3/3W (on the right) a brittle fracture was produced (30 percent shear). The fracture propagation occurred entirely in the weld.

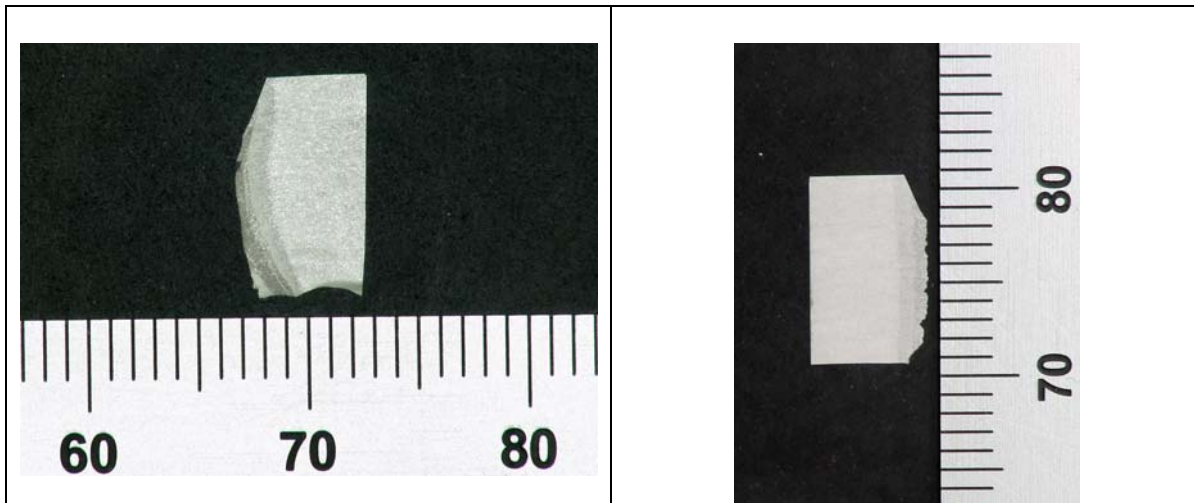


Figure 6.56: Macrographs of the Sectioned Charpy Specimen from Weld 508

Note to Figure 6.56: The sample on the left is from the 12 o'clock position (12/2W) and the sample one on the right is from the 3 o'clock position (3/3W).

The sectioning results presented in the above indicate that most of the fracture propagation occurred outside of the laser weld. One reason for this could be a result of high fracture initiation due to high energy absorption before fracture propagation. The energy is absorbed by the “large” plastic zone formed just below the Charpy notch. This increases the possibility of the ductile fracture process to commence in a “wider” region ahead of the notch. The dynamic tear test specification (ASTM 604 [9]) adopts a procedure that sharpens a machined notch.

This procedure has been found also to reduce the fracture initiation energy by causing localized strain hardening. Medium strength steels (CSA G40.21; 350WT) used in navy vessels have been evaluated by pressed notch Charpy specimens and also by standard ASTM 604 [9] dynamic tear test and shown to produce the same fracture transition temperature.

It is likely that a pressed notch Charpy option would increase the chances of the fracture propagation path occurring in the weld metal.

6.2.2.6 Non-Standard Charpy Impact Test Development and Results

This following presents the challenges and results associated with Charpy impact testing of overmatched X80 and X100 pipeline steel girth welds that were produced by HLAW. The primary objective of this task was to determine if the fracture transition temperature differed at the four quarters of the girth weld. The motivation for this work was to investigate the feasibility and accuracy of conducting Charpy v-notch impact testing on HLAW specimens and to determine whether a pressed notched approach will reduce Fracture Path Deviation (FPD) in hybrid laser arc weld deposits.

The weld profile produced by the HLAW process is characterized as having a broad GMAW cap and a narrow leg, as can be seen below. Figure 6.57 (a) illustrates a typical X80 single cap

HLAW profile and Figure 6.57(b), illustrates a typical X100 multi cap HLAW profile. At this stage, it should be noted that the geometric features and the non-uniform microstructure of the hybrid laser arc weld provide an indication of the potential challenges ahead when subjecting such samples to Charpy impact testing, particularly as the various metallurgical zones are positioned very close to one another.

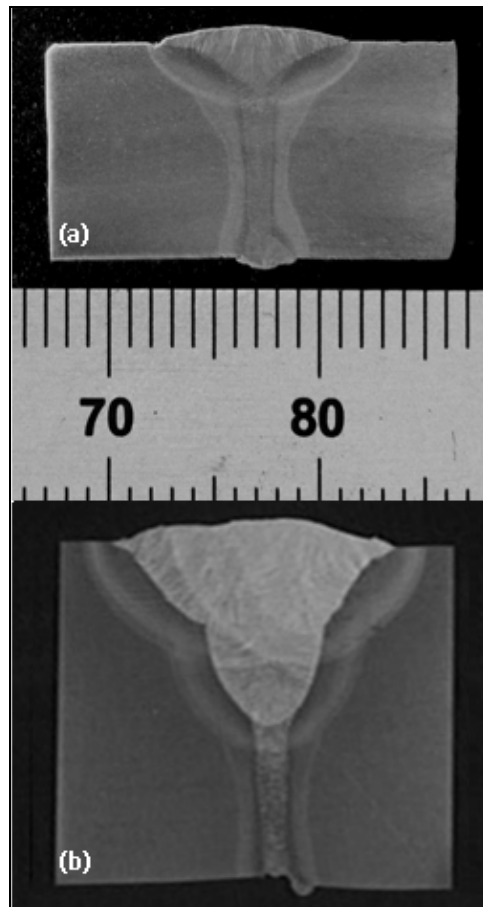


Figure 6.57: HLAW Weld Cross Section for (a) X80 and (b) X100 Sample Materials

Conventional Charpy Impact Testing

The Charpy impact test determines the total absorbed energy associated with a fracture produced at a high strain rate. This energy is then a measure of the material's toughness. The Charpy impact test is a widely used and simple test, which has been standardized in several international standards, such as ISO 148 [10], ASTM E23 [8], EN 10045 [11], and JIS Z2242 [12].

The outcome from this test is mostly used to determine the temperature-dependent brittle to ductile fracture transition of a material, as determined by the temperature at which a designated energy absorbed/percent shear occurs. In addition to the absorbed energy and percent shear, other data derived from the Charpy impact test typically also includes the lateral expansion, and may compliment the other two measures. It is typical to plot the absorbed energy or percent shear, vs. temperature to present a fracture transition curve.

Visual inspection of the fracture surface is used to determine the percent shear following guidelines in ASTM E23 [8]. Lateral expansion is measured in accordance with ASTM E23 [8]. The shiny and crystalline region indicates cleavage fracture, while the fibrous and dull region indicates region of ductile fracture by micro-void coalescence.

Usually the fracture surface of a specimen will show a combination of micro-void coalescence and cleavage on the fracture surfaces, where a greater amount of shear will designate a larger degree of ductile fracture. A typical HLAW Heat Affected Zone (HAZ) fractured impact specimen with approximately 55 percent shear is shown in Figure 6.59.

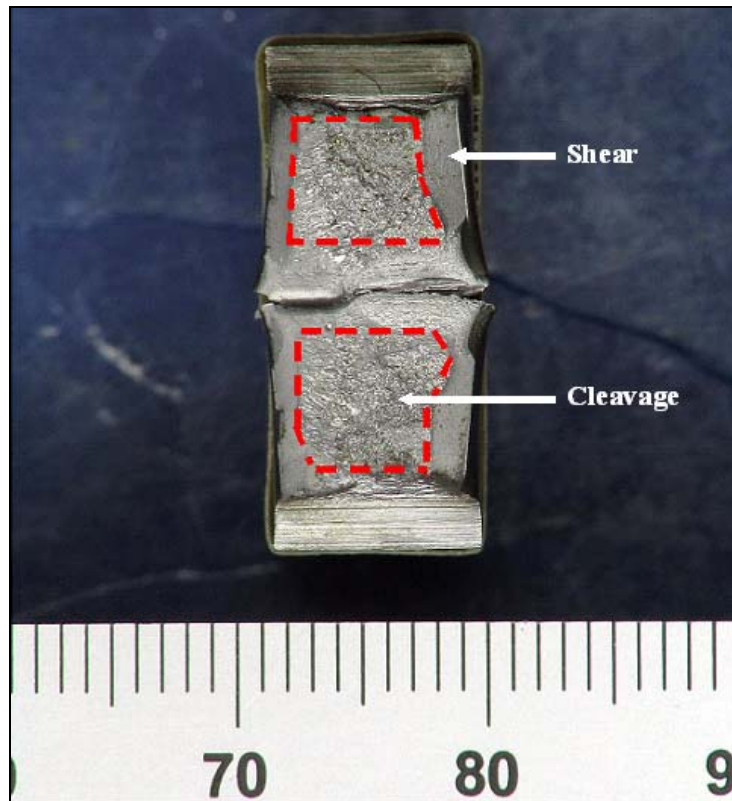


Figure 6.58: Impacted Specimen Showing Both Shear (Outside) and Cleavage (Centre)

Fracture Path Deviation (FPD)

It is generally accepted that some experimental scatter will be experienced in certain sample types, especially where the material is inhomogeneous, such as when testing the heat affected zone or the deposited weld. This scatter will occur around the fracture transition zone, when the fracture undergoes a transition from brittle to ductile behaviour as the temperature is increased. In other words, an increase in test temperature results in an increase in the amount of energy absorbed an increase in the percent shear and an increase in the lateral expansion. An increase in the value of these measures is evidence that an increase in toughness is being achieved.

In the fracture transition temperature range it is expected that the results will show scatter. The fracture transition temperature range may increase if fracture propagation path deviation occurs to regions of different microstructure than the location of the Charpy notch. Also if the notch placement is not accurate the same would occur. These two possibilities are more likely in the narrow weld profile of the hybrid laser portion shown above in Figure 6.58.

In such cases, FPD is likely to have taken place, where the fracture propagated away from the region in which the notch had initially been positioned. An example of this is when the notch is placed in the weld metal but the subsequent fracture path is through the HAZ.

There is evidence to show that the fracture path of laser welds produced under impact testing may be prone to deviation from one metallurgical region to another [13] and [14]. The deviation is typically found to occur from the weld into the base material and Nagel et al. [14] argues that the high hardness of laser weld contributes to this occurrence. The resulting values derived from impact testing then represent a mixture of the base material's and laser weld's toughness. Fracture path deviation in laser welds thereby limits the determination of accurate impact toughness for any specific region in the weldment.

Nagel et al. [14], conclude that the toughness characterization of the laser weld itself may not be possible with the conventional Charpy v-notch test procedure. Bezensek B. & Hancock [13] is in agreement and maintains that the narrow geometry of laser welds and the hardness differential between the weld and the base material could furthermore result in the concealment of low toughness weld metal when FPD occurs. This is an important consideration if one specific region of the complete weldment is evaluated, although FPD may be admissible if a specific toughness of the complete weldment is required. It should, however, be noted that for the purposes of establishing the ductile to brittle transition, FPD may limit the accuracy of the results and lead to misleading interpretation when a specific region of a narrow weld deposit is being evaluated.

Experimental Procedure

Two high strength pipeline welded joints were evaluated, namely a single cap X80 hybrid laser arc weld and a multi cap X100 hybrid laser arc weld. Pipe numbers 503 and 507 were associated with the single cap X80 welded joint, while pipe number 502 was used to test the multi-cap X100 welded joint. The cross sections of these sample test pieces have previously been provided in Figure 6.57. Consideration was also given to indications (flaws) from UT, which resulted in the exclusion of certain regions before extracting the Charpy specimens.

Conventional and pressed notch Charpy impact testing was conducted on the X80 welded joints, while the X100 joint was only evaluated through conventional Charpy impact testing. Both the HAZ and the Weld Centreline (WCL) was evaluated for the X80 and the X100. The purpose of the press notching on the X80 was to establish whether localized embrittlement would reduce or potentially eliminate fracture path deviation.

The press notching procedure first involved the placement of a conventional Charpy ASTM E23 [8] broached notch in the sample, after which a narrower and sharper indentation was made at the root of the broached notch with a hardened knife edge. The knife edge dimensions and notch tolerances from ASTM E604 [9] were adopted and incorporated into ASTM E23 [8] procedure.

A press notching procedure was then developed to ensure that the specific tolerances stipulated in ASTM E604 [9] were maintained. High speed tool steel (60 Rockwell C minimum) was used to produce each of the knife edges.

An illustration of the knife edge dimensions used for press notching purposes is shown in Figure 6.59. The subsequent testing of all Charpy impact specimens (conventional and press notched) was then performed in accordance with ASTM E23 [8], using a 400 J capacity NIST calibrated Satec Charpy impact tester.

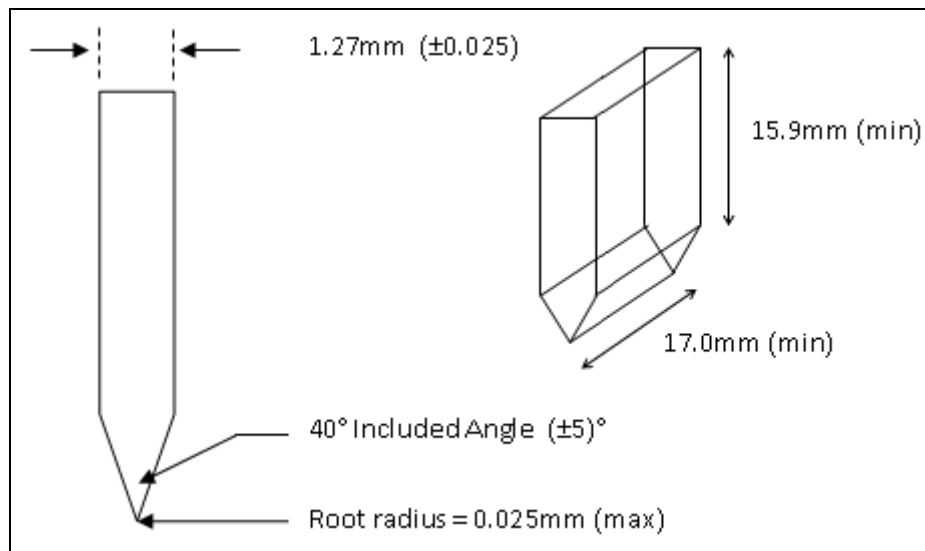


Figure 6.59: Illustration of Knife Edge Specifications for X80 Pressed Notch Trials

Due to misalignment (hi-lo), at the weld joint, in the 10.4 mm thick X80 pipe, the 4 clock positions had to be extracted from the two pipe numbers 503 and 507. Specimens from the 12 and 3 o'clock positions were extracted from pipe 507 and specimens from the 6 and 9 o'clock positions were extracted from pipe 503. It should also be noted that the relatively small wall thickness and the misalignment of the X80 pipe welds only permitted the extraction of sub-size impact specimens. The 14.2 mm wall thickness of the X100 pipe was sufficient for full sized Charpy size impact specimens.

A specific aim during the Charpy impact testing for both the X80 and X100 materials was to determine the temperature at which HLAW specimens would undergo a ductile to brittle transition. A further aim was to establish whether variations in impact toughness exist along the four quarters of the sample joints. These four quarters will be referred to as the 12, 3, 6, and 9 o'clock positions and are designated by the letters A, B, C, and D, as illustrated in Figure 6.60. It should be noted that the specimens were extracted at locations that represent the clock position showed in the image and not all specimens will, therefore, be positioned exactly at the clock positions referred to in Figure 6.60.

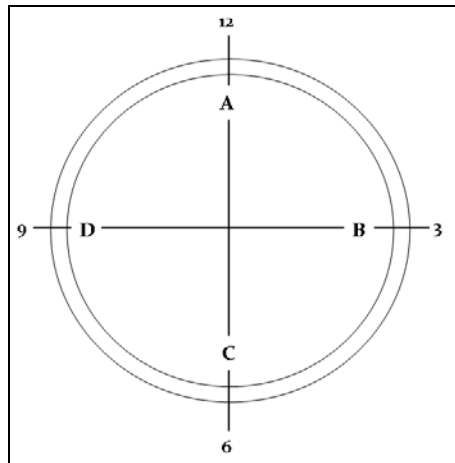


Figure 6.60: Four Clock Positions Evaluated for Both X80 and X100 HLAW Joints

Note: Individual locations are shown by the letters A, B, C, and D.

Once the specimen had been machined, pre positioning of the Charpy notch was achieved by placing a scribed line on the etched surface. Figure 6.61 displays two white parallel lines, one to show the notch location for the heat affected zone (right) and one to show the notch location for the weld centerline samples (left). The broken horizontal line illustrates the orientation and the mid thickness position of the specimens. Figure 6.62 displays broached specimens for the HAZ (left) and the WCL (right). The minimal tolerance available for notch placement can be seen in this figure for hybrid (root) pass.

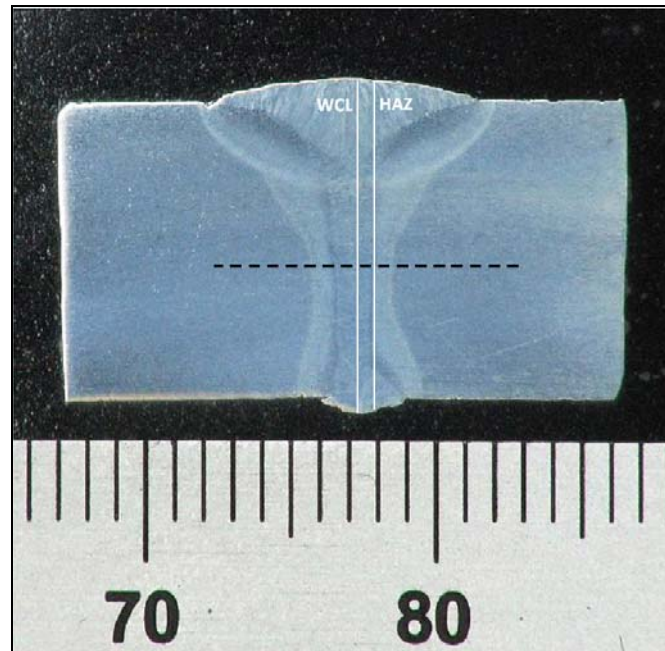


Figure 6.61: Notch Location of Weld Centreline Sample (Left) and HAZ (Right)

Note to Figure 6.61: The line on the left represents the notch position for the weld centreline, while the line on the right represents the notch location for the HAZ samples. The broken line shows the orientation and mid thickness position of the Charpy impact specimens.

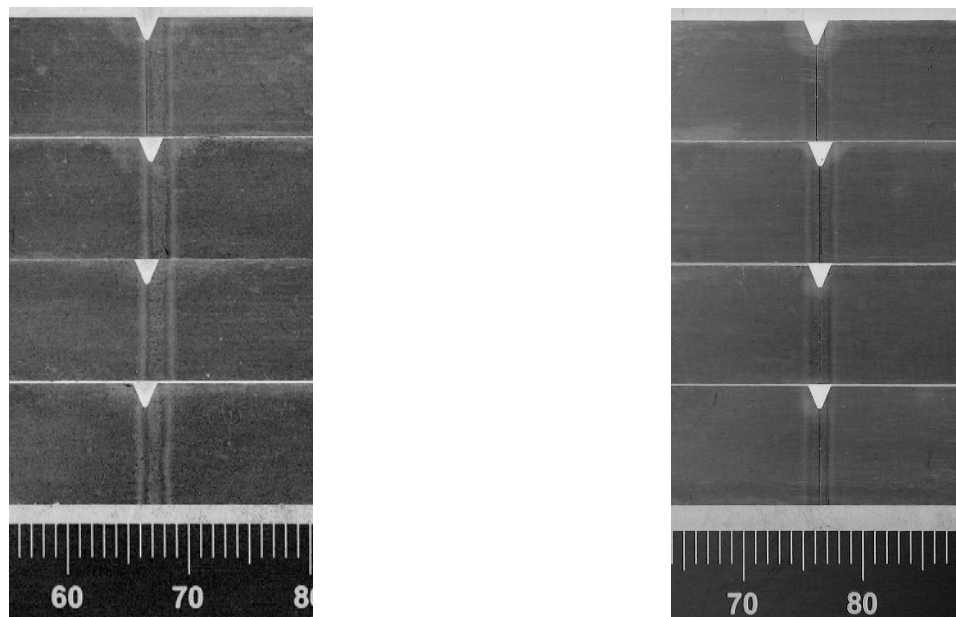


Figure 6.62: Notch Location for HAZ (Left) and Weld Centreline (Right), as Seen from Root

Charpy Impact Testing Results

The following results will display the outcomes from Charpy impact testing for the single cap X80 and the multi-cap X100 sample materials. Both conventional and pressed notch testing was conducted on the X80 sample material, while only conventional Charpy v-notch testing was conducted on the X100 sample material. The test temperature used during this study ranged from -73°C to 20°C.

The test data presented later on will include observations made of the following:

- Test temperature (°C);
- Absorbed energy (Joules);
- Percentage shear (%);
- Lateral expansion (inch x 10⁻³); and
- FPD.

From previous work [13] and [14], it was known that fracture path deviation would likely occur when laser welded specimens, with a high hardness in the weld, are subjected to impact testing. A possibility could then arise that invalid results be considered valid, thereby giving a false interpretation of the actual impact toughness.

Post-test metallography was, therefore, implemented on selected fractured specimens to qualify the test outcomes. The mounted and polished specimens were evaluated for correct notch placement and fracture path. A direct reference will be made of the unqualified results in the test outcomes to follow.

The absorbed energy versus temperature data for the X80 conventional Charpy impact testing results is plotted in Figure 6.63 and Figure 6.64, while the pressed notch data for the same sample material is plotted in Figure 6.67 and Figure 6.68. These plots include both heat affected zone and weld centerline tests.

No pressed notch testing was conducted on the X100 welded joint and the conventional Charpy impact data related to the absorbed energy for this sample material is plotted in Figure 6.71 and Figure 6.72). Both the weld centerline and heat affected zone was evaluated.

A plot to show the relationship between the absorbed energy and the percent shear for the X80 welded joint is provided in Figure 6.65, Figure 6.66, Figure 6.69, and Figure 6.70, while the same data visualization for the X100 welded joint is provided in Figure 6.73 and Figure 6.74. All data relevant to the Charpy impact testing of the X80 and the X100 is available in Table 6.10 and Table 6.11 (X80 Conventional), Table 6.12 and Table 6.13 (X80 Pressed Notch), and Table 6.14 and Table 6.15 (X100 Conventional).

The Charpy impact testing revealed an expected trend for all specimens tested, which showed that a decrease in test temperature produced a decrease in the absorbed energy, the percent shear and the lateral expansion. Both the X80 and the X100 HLAW joints, therefore, undergo a ductile to brittle transition as the test temperature decreases.

The results indicate that the introduction of a pressed notch in the X80 sample material will shift the ductile to brittle transition to higher temperature. The temperature increase due to the effects of the press notch can be approximated to be in the region of 20°C to 30°C.

Initial observations on the conventionally tested X80 specimens suggested that the 3 o'clock position could be characterized as having the lowest impact toughness or highest fracture transition temperature. This observation was, however, not reflected in the subsequent pressed notch test results, nor in the outcomes of the X100 conventional Charpy testing. Although there are suggestions of positional toughness variations along the X80 circumference, the general test outcomes when all tests are included do not provide conclusive evidence that significant Charpy impact toughness variations exist along the clock positions of materials joined with the hybrid laser arc welding process.

In terms of comparing the results between the single cap X80 and the multi-cap X100, the test results show clear distinction in impact toughness. The X100 pipe weld fracture transition occurred at a lower temperature compared to the X80 pipe weld. This means that the X100 pipe weld has superior toughness than the X80 pipe weld.

The press notched approach used in this study showed minimal reduction in scatter in the fracture transition region for the X80 sample material. From the limited conventional Charpy impact testing conducted on the X100, it would appear that more consistent results can be achieved. The multi-cap pass X100, therefore, produced less scatter than the single cap pass X80 during Charpy impact testing in this investigation.

Conventional X80 Charpy Impact Testing

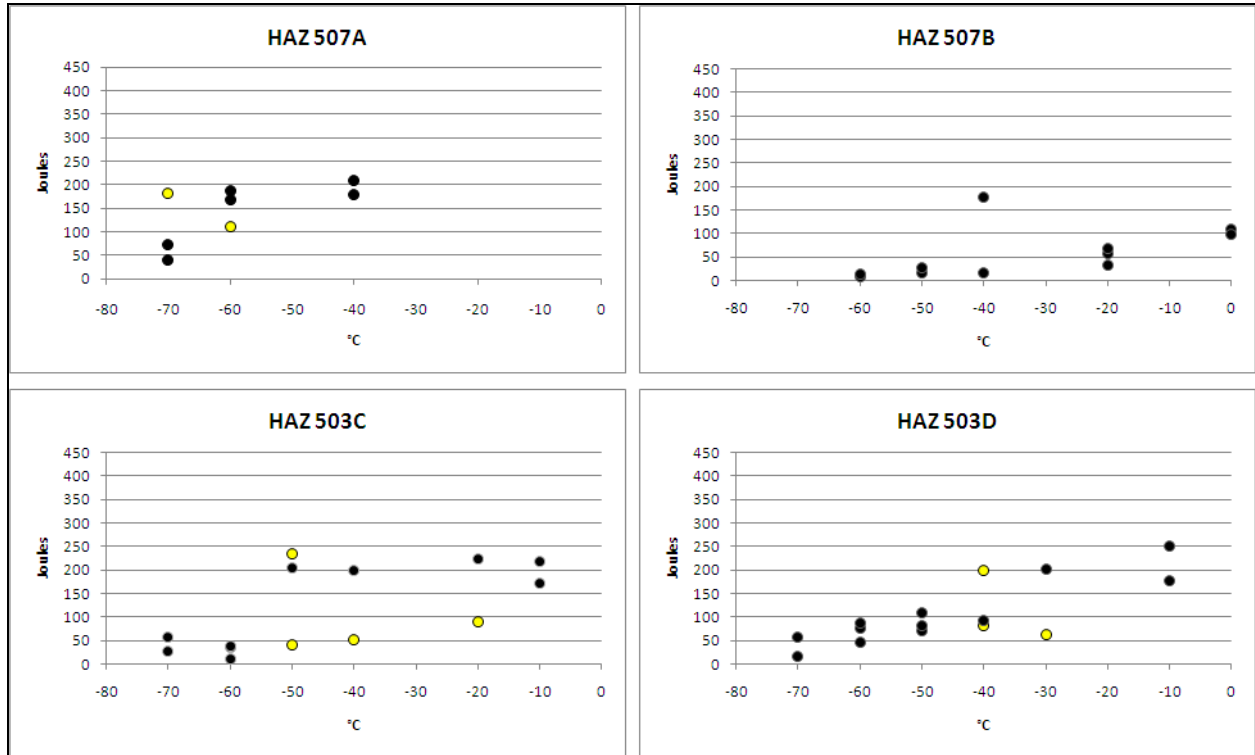


Figure 6.63: Conventional HAZ Charpy V-notch Testing

Note to Figure 6.63: The yellow data points designate invalid test results, as determined by post-test metallography.

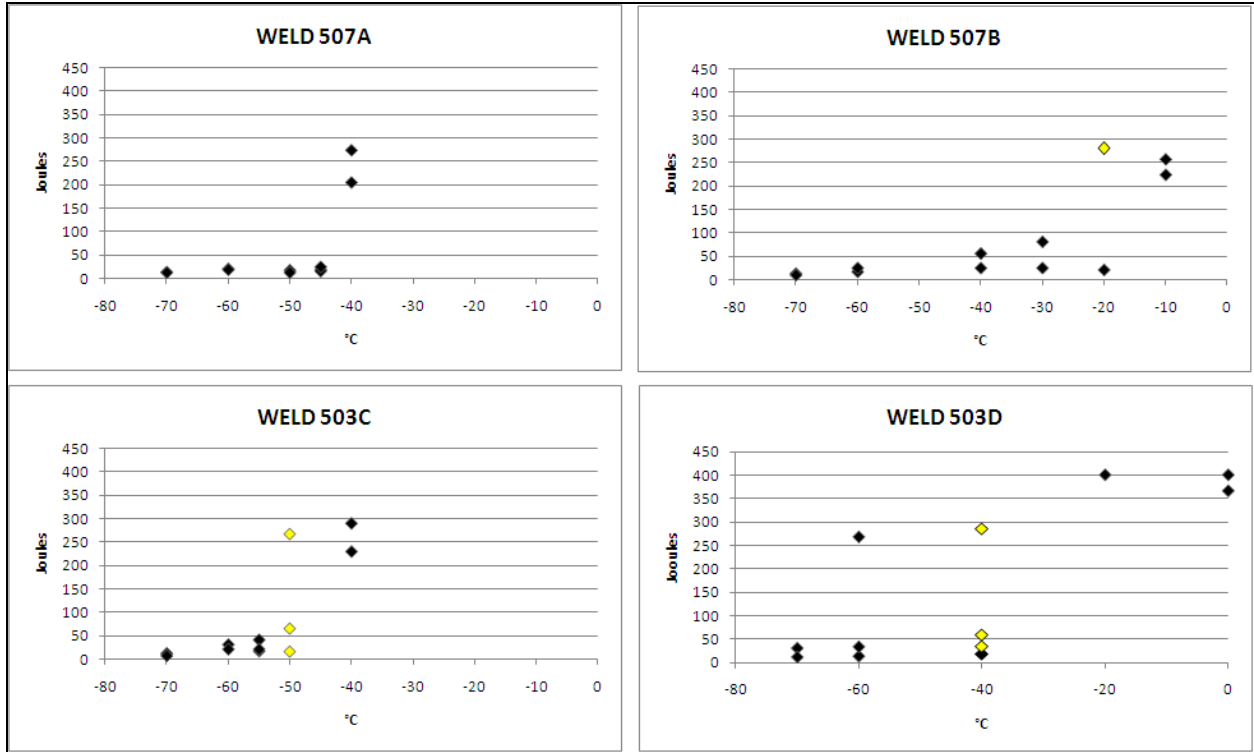


Figure 6.64: Conventional WCL Charpy V-notch Testing

Note to Figure 6.64: The yellow data points designate invalid test results, as determined by post-test metallography.

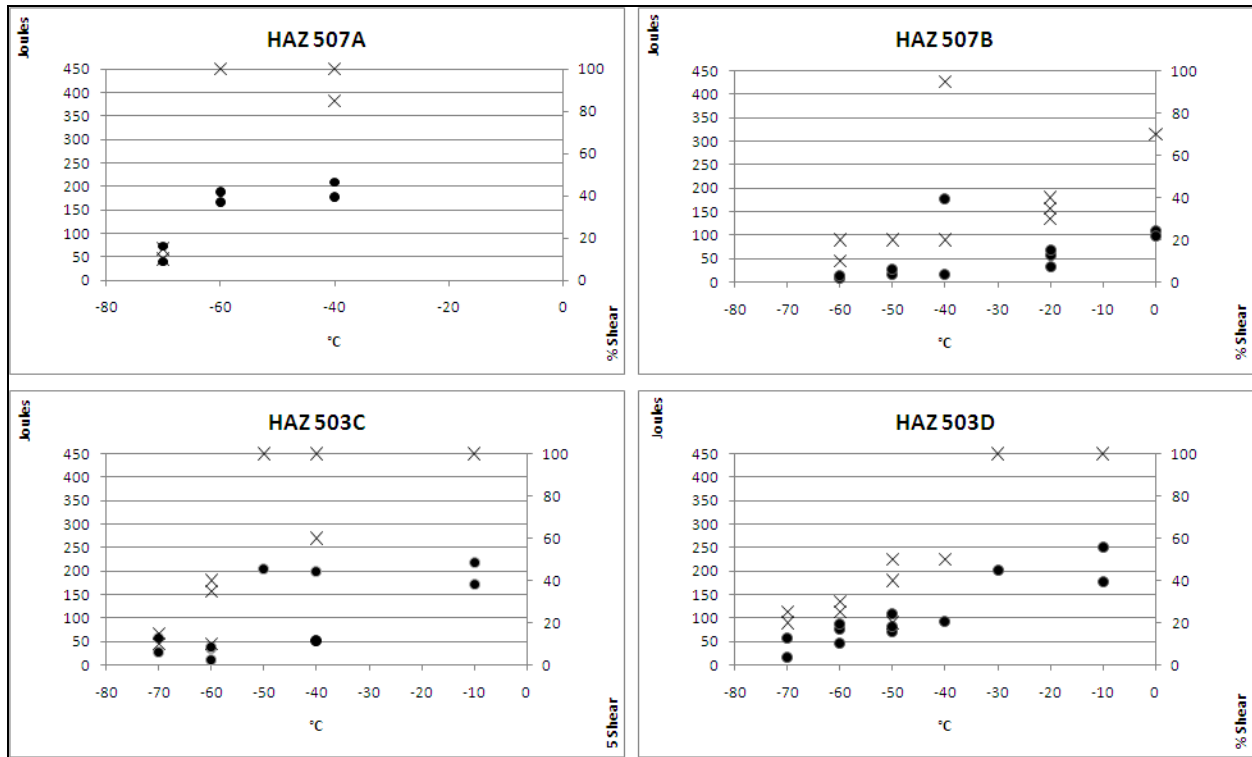


Figure 6.65: Relationship Between HAZ Absorbed Energy and Percent Shear (X) for X80 Sample Material

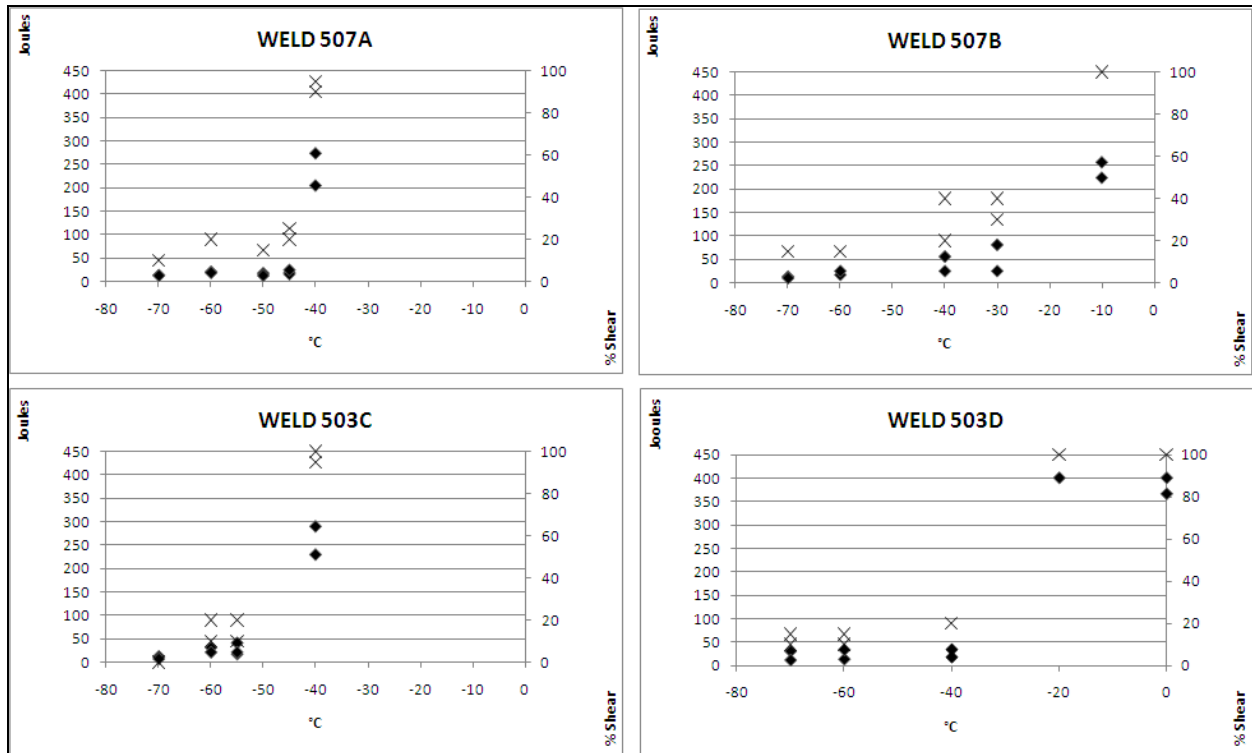


Figure 6.66: Relationship Between WCL Absorbed Energy and Percent Shear (X) for X80 Sample Material

Table 6.10: Test Results for Conventional HAZ X80 Testing

Test	Specimen No.	Temp.	Joules	Ft.lbs	Lat. Exp	% Shear	
507B HAZ	1	10	154	114	NA	100	
	2	10	112	83	NA	95	
	3	0	108	80	36	70	
	4	0	98	72	35	70	
	5	-20	58	43	23	40	
	6	-20	68	50	28	35	
	7	-20	33	24	26	30	
	8	-40	17	13	10	20	
	9	-40	178	131	48	95	
	10	-50	17	13	15	20	
	11	-50	26	19	16	20	
	12	-60	7	5	NA	10	
	13	-60	13	10	12	20	
507A HAZ	1	-40	209	154	56	100	
	2	-40	178	131	48	85	
	3	-60	188	139	51	100	
	5	-60	167	123	50	100	
	6	-70	40	30	18	10	
	7	-70	73	54	23	15	
	503C HAZ	1	-10	218	161	54	100
2		-10	173	128	45	100	
5		-40	52	38	22	60	
6		-40	200	148	52	100	
9		-50	205	151	NA	100	
10		-60	35	26	14	35	
11		-60	39	29	20	40	
12		-60	12	9	NA	10	
13		-70	56	41	22	15	
14		-70	27	20	16	10	
503D HAZ		1	-10	178	131	50	100
		2	-10	250	184	53	100
		4	-30	201	148	54	100
		7	-40	92	68	19	50
	8	-50	72	53	23	20	
	9	-50	110	81	32	50	
	10	-50	81	60	25	40	
	11	-60	77	57	22	30	
	12	-60	46	34	16	25	
	13	-60	88	65	29	25	
	14	-70	56	41	17	25	
	15	-70	16	12	12	20	

Table 6.11: Test Results for Conventional WCL X80 Testing

Test	Specimen No.	Temp.	Joules	Ft.lbs	Lat. Exp	% Shear	
507A WCL	1	-40	205	151	45	90	
	2	-40	274	202	48	95	
	3	-45	18	13	15	20	
	4	-45	15	11	15	20	
	5	-45	24	18	NA	25	
	6	-50	17	13	11	15	
	7	-50	12	9	11	15	
	8	-60	20	15	15	20	
	9	-60	18	13	12	20	
	10	-70	13	10	8	10	
	11	-70	12	9	11	10	
507B WCL	1	-10	258	190	47	100	
	2	-10	225	166	46	100	
	5	-30	26	19	17	30	
	6	-30	82	60	25	40	
	7	-40	26	19	17	40	
	8	-40	57	42	21	20	
	9	-60	18	13	12	15	
	10	-60	26	19	18	15	
	11	-70	14	10	11	15	
	12	-70	11	8	12	15	
	503C WCL	1	-40	290	214	45	100
2		-40	230	170	48	95	
6		-55	18	13	12	10	
7		-55	42	31	16	20	
8		-55	22	16	11	10	
9		-60	32	24	15	20	
10		-60	22	16	14	10	
11		-70	13	10	9	0	
12		-70	8	6	7	0	
503D WCL		1	0	400	295	NA	100
		2	0	366	270	NA	100
		3	-20	400	295	NA	100
	4	-40	18	13	15	20	
	5	-40	34	25	15	20	
	9	-60	14	10	10	10	
	10	-60	34	25	9	15	
	11	-70	31	23	16	15	
	12	-70	12	9	12	10	

Pressed Notch X80 Charpy Impact Testing

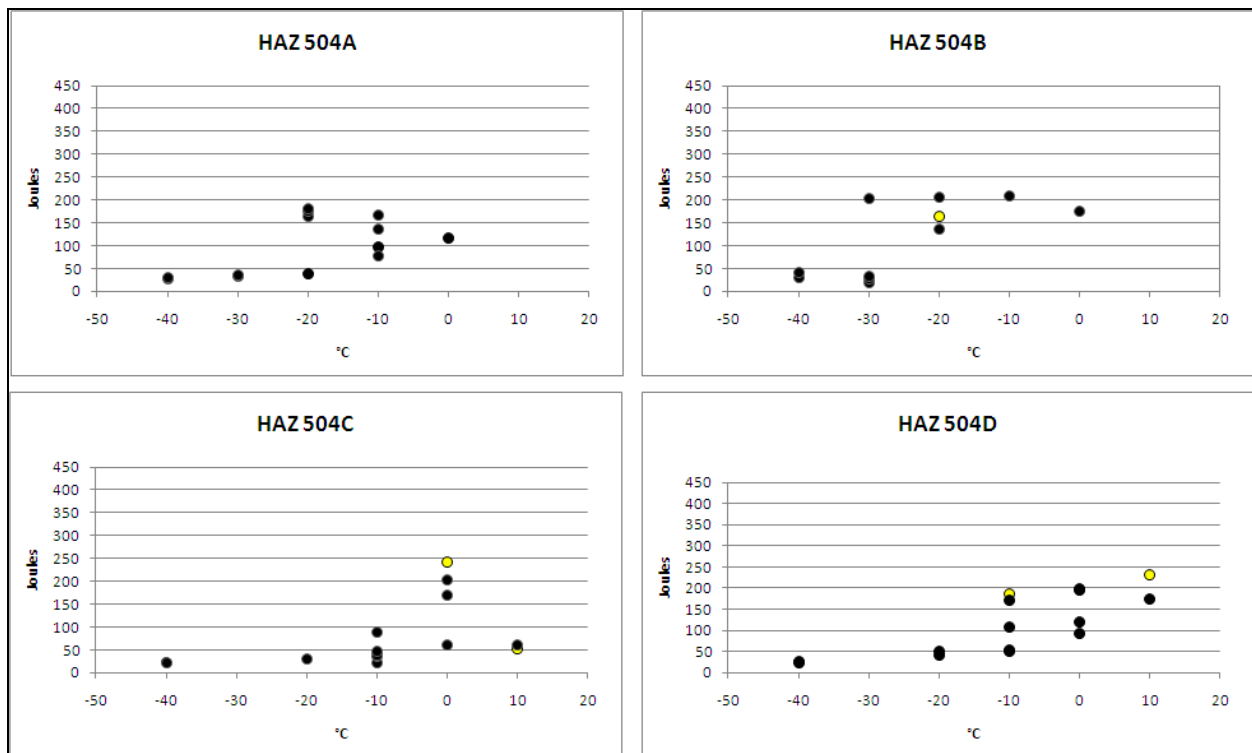


Figure 6.67: Pressed Notch HAZ Charpy V-notch Testing

Note to Figure 6.67: The yellow data points designate invalid test results, as determined by post-test metallography.

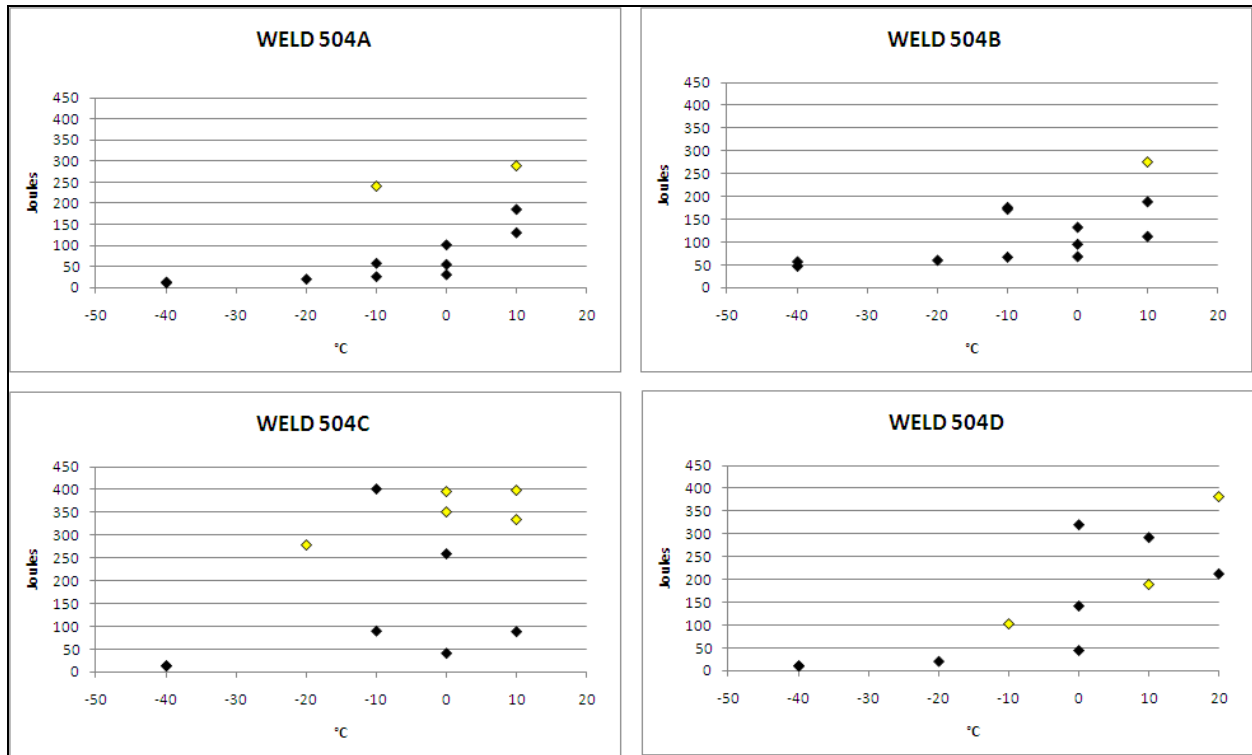


Figure 6.68: Pressed Notch WCL Charpy V-notch Testing

Note to Figure 6.68: The yellow data points designate invalid test results, as determined by post-test metallography.

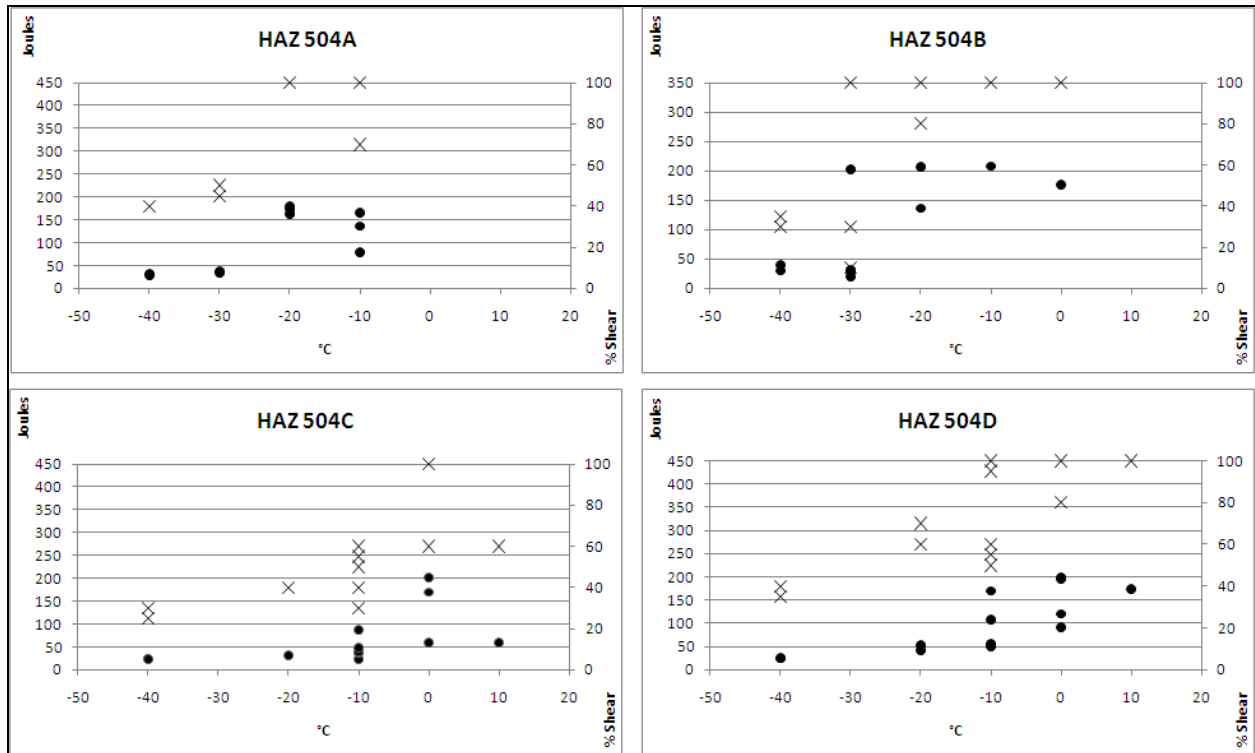


Figure 6.69: Relationship Between HAZ Absorbed Energy and Percent Shear (X) for X80 Sample Material

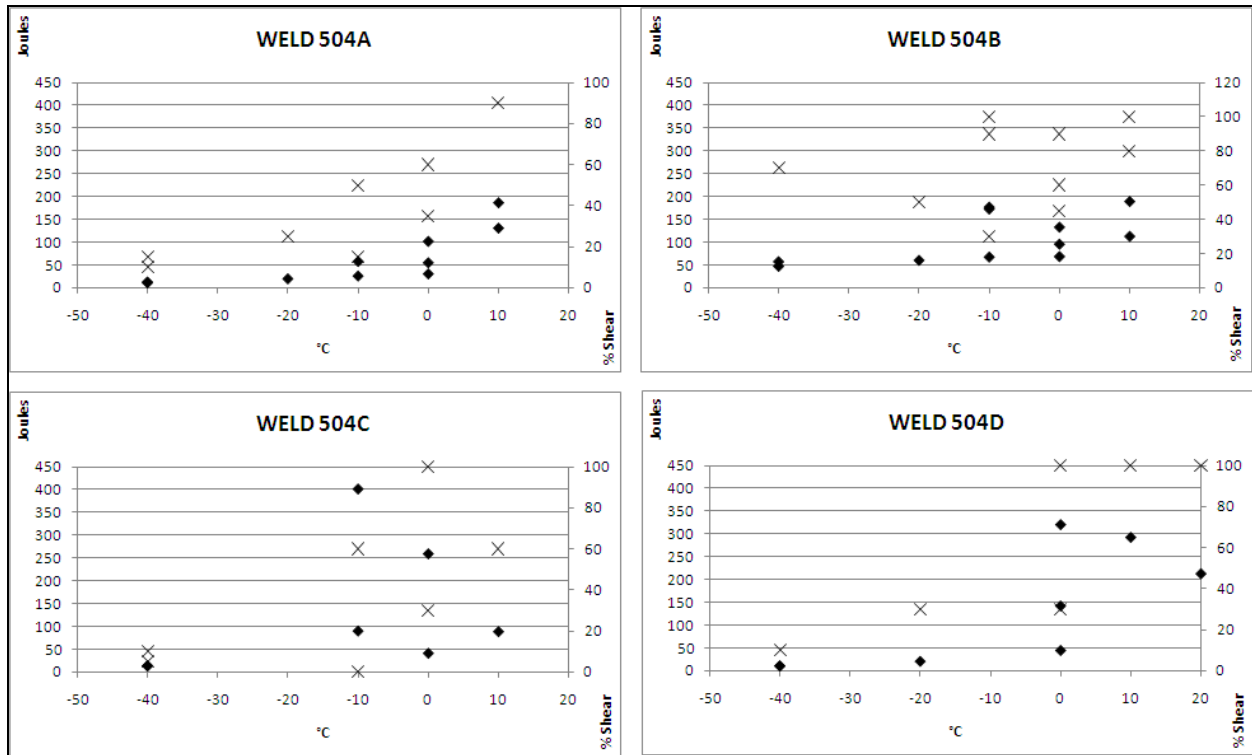


Figure 6.70: Relationship Between WCL Absorbed Energy and Percent Shear (X) for X80 Sample Material

Conventional X100 Charpy Impact Testing

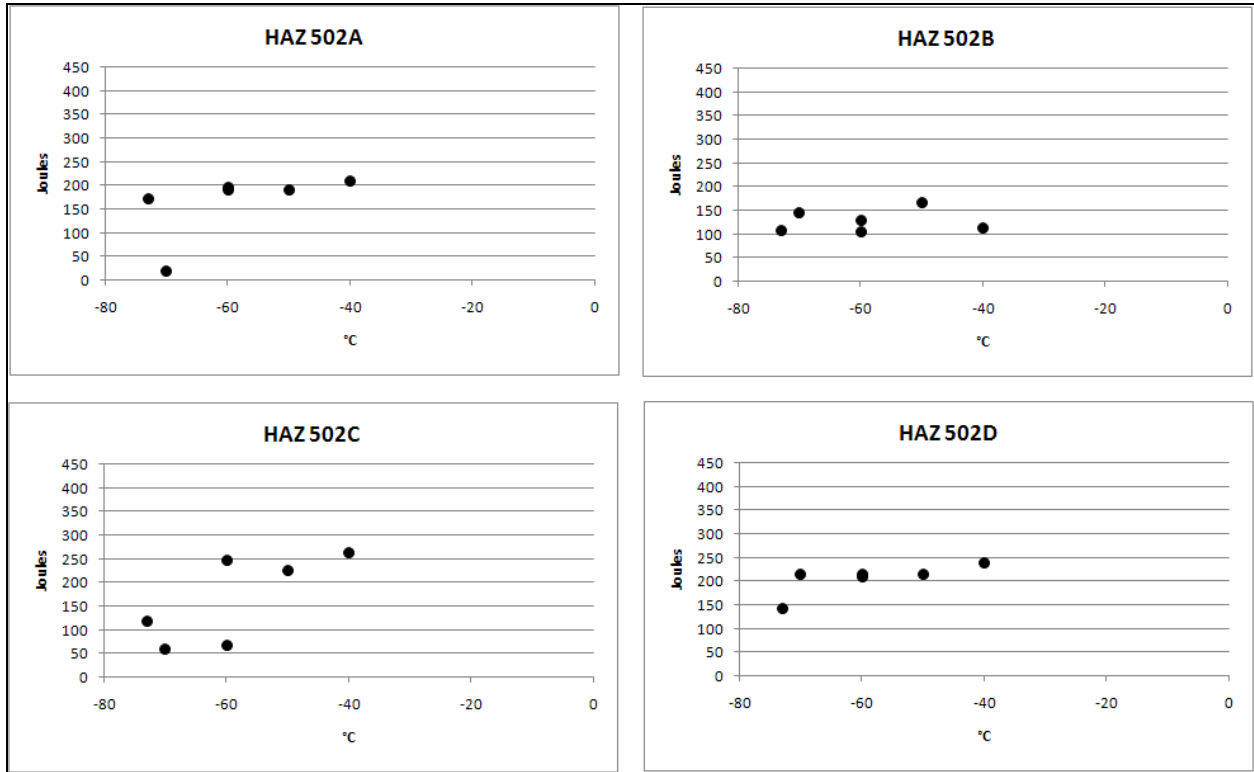


Figure 6.71: Conventional HAZ Charpy V-notch Testing for X100 HLAW

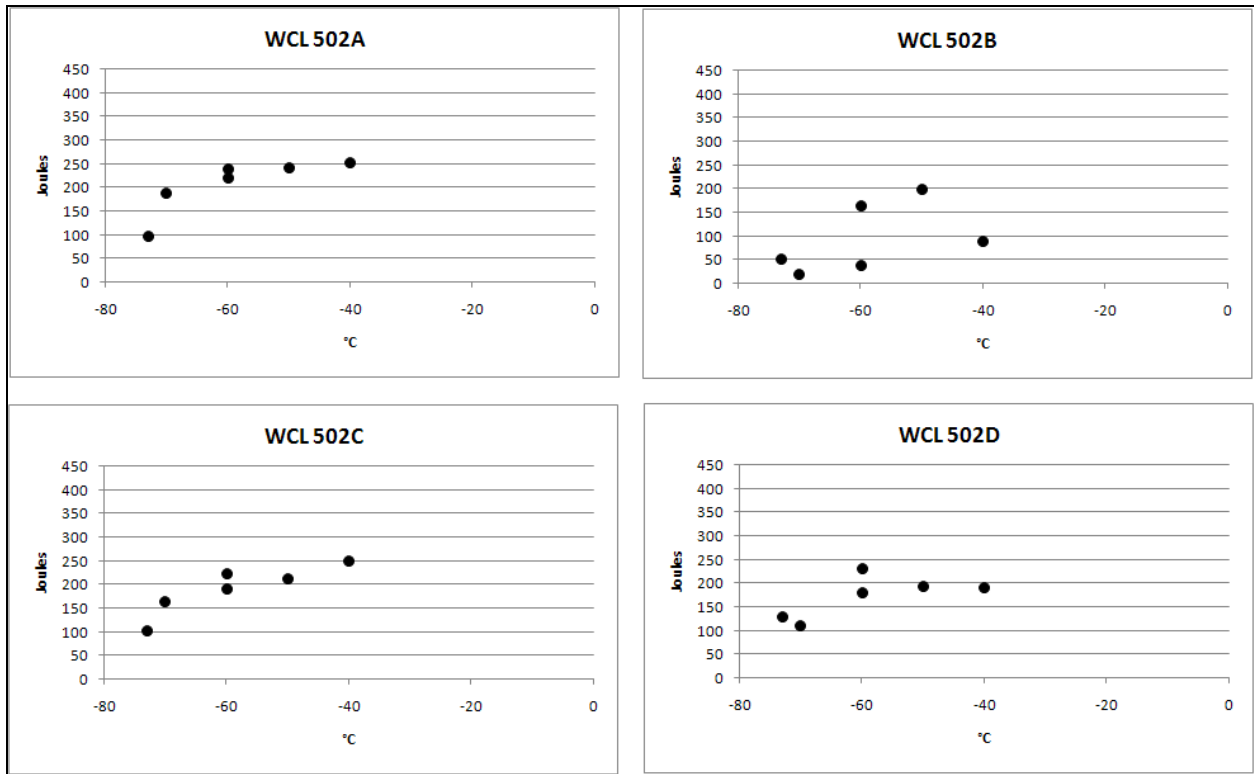


Figure 6.72: Conventional WCL Charpy V-notch Testing for X100 HLAW

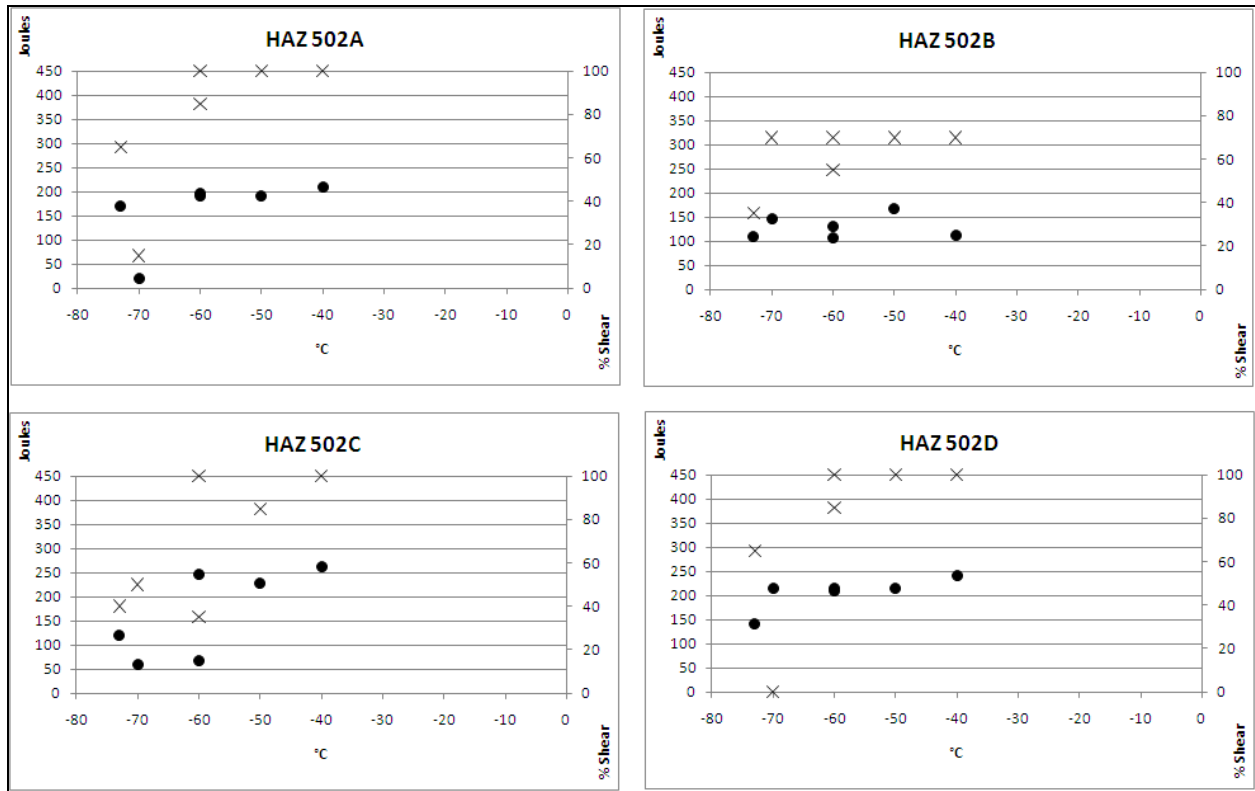


Figure 6.73: Relationship between HAZ Absorbed Energy and Percent Shear (X) for X100 Sample Material

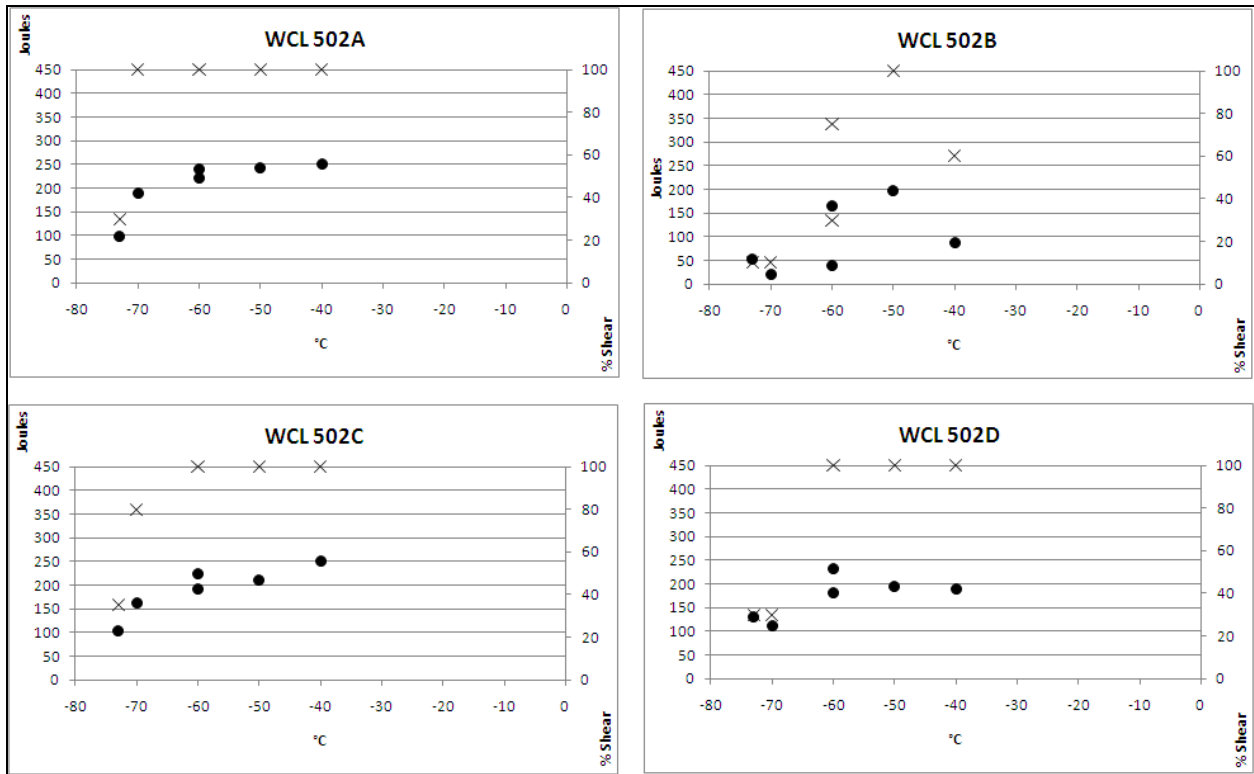


Figure 6.74: Relationship between WCL Absorbed Energy and Percent Shear (X) for X100 Sample Material

Table 6.14: Test Results for X100 HAZ Charpy Impact Testing

Test	Specimen No	Temp.	Joules	Ft.lbs	Lat. Exp	% Shear
502A HAZ	2	-73	171	126	37	65
	8	-70	20	15	14	15
	11	-60	192	142	42	85
	14	-60	195	144	42	100
	1	-50	190	140	45	100
	9	-40	210	155	43	100
Test	Specimen No	Temp.	Joules	Ft.lbs	Lat. Exp	% Shear
502B HAZ	14	-73	108	80	28	35
	9	-70	145	107	33	70
	5	-60	106	78	30	55
	1	-60	130	96	30	70
	12	-50	166	122	35	70
	2	-40	112	83	33	70
Test	Specimen No	Temp.	Joules	Ft.lbs	Lat. Exp	% Shear
502C HAZ	11	-73	119	88	28	40
	10	-70	60	44	24	50
	2	-60	67	49	24	35
	14	-60	246	181	53	100
	9	-50	227	167	45	85
	15	-40	262	193	51	100
Test	Specimen No	Temp.	Joules	Ft.lbs	Lat. Exp	% Shear
502D HAZ	15	-73	142	105	30	65
	6	-70	215	159	48	100
	8	-60	210	155	46	100
	9	-60	215	159	48	85
	16	-50	214	158	50	100
	3	-40	240	177	52	100

Table 6.15: Test Results for X100 WCL Charpy Impact Testing

Test	Specimen No	Temp.	Joules	Ft.lbs	Lat. Exp	% Shear
502A WCL	8	-73	98	72	27	30
	4	-70	188	139	42	100
	10	-60	220	162	45	100
	1	-60	240	177	51	100
	7	-50	242	178	52	100
	12	-40	252	186	51	100
Test	Specimen No	Temp.	Joules	Ft.lbs	Lat. Exp	% Shear
502B WCL	9	-73	52	38	18	10
	6	-70	20	15	12	10
	5	-60	38	28	20	30
	11	-60	164	121	35	75
	12	-50	198	146	40	100
	10	-40	88	65	30	60
Test	Specimen No	Temp.	Joules	Ft.lbs	Lat. Exp	% Shear
502C WCL	10	-73	103	76	24	35
	1	-70	163	120	36	80
	4	-60	192	142	39	100
	8	-60	223	164	46	100
	11	-50	211	156	43	100
	3	-40	251	185	47	100
Test	Specimen No	Temp.	Joules	Ft.lbs	Lat. Exp	% Shear
502D WCL	11	-73	129	95	33	30
	9	-70	111	82	29	30
	10	-60	180	133	39	100
	4	-60	232	171	44	100
	1	-50	194	143	42	100
	6	-40	190	140	42	100

Post-Test Metallography

Post-test metallography was conducted on tested specimens that ranged from the typical lower shelf, through the fracture transition zone and into the upper shelf. This exercise thereby provided visual evidence to qualify the test outcomes in terms of notch placement and the fracture path for these specimens. This was done for both the X80 and the X100 sample materials.

The broken halves of specimens were sectioned transverse to the direction of through thickness notch placement and then mounted, polished, and etched with 2 percent nital solution. The dotted line in Figure 6.75 represents the sectioning plane; and only one side, either to the left or the right of the dotted line was mounted and visually inspected through optical light microscopy.

Notch placement for a weld centerline sample is shown in Figure 6.76, while notch placement for a HAZ sample is shown in Figure 6.77. Fracture path deviation from the HAZ into the weld metal can also be observed in this image.

Additional evidence of varying FPD behaviour is shown in Figure 6.77 to Figure 6.81 where the fracture path deviated from the notch placed in the weld to the HAZ/base metal, except for Figure 6.82.

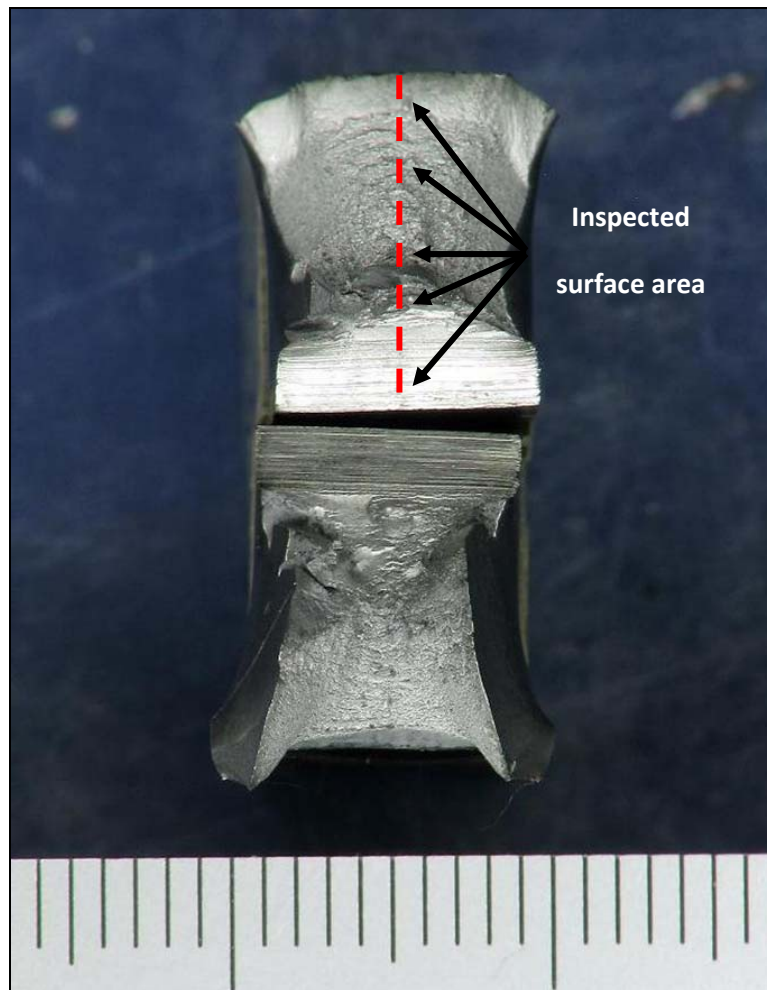


Figure 6.75: Inspected Surface Area

Note to Figure 6.75: Selected impacted specimens were sectioned along the dotted line and then one side. The surface adjacent to the sectioned plane was then mounted, polished and etched.

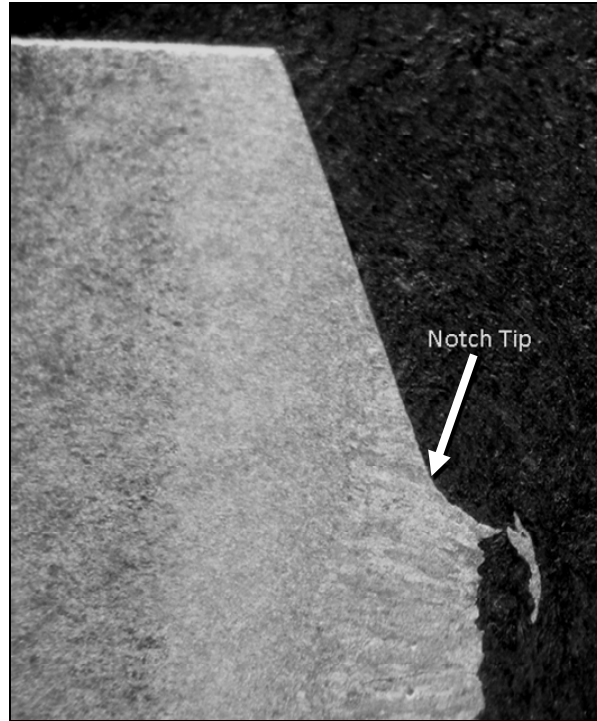


Figure 6.76: Typical Notch Placement for Weld Centreline Samples

Note to Figure 6.76: The fracture path is also in the weld.

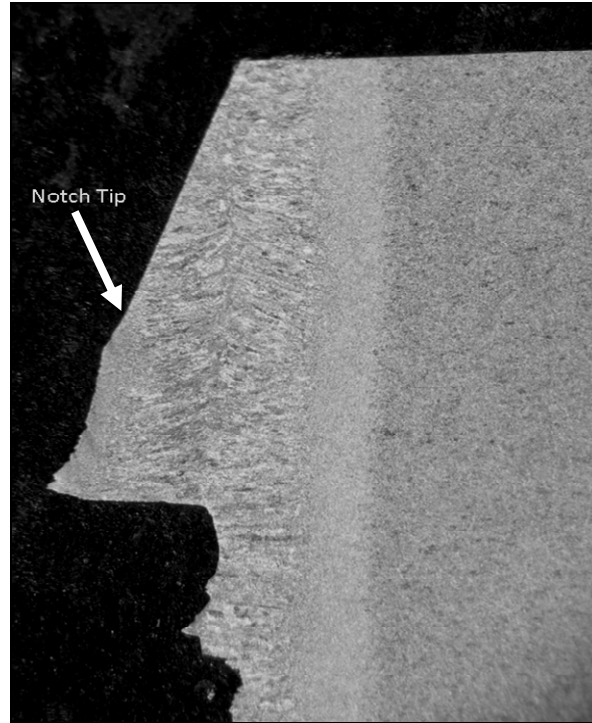


Figure 6.77: Typical Notch Placement for Heat Affected Zone Samples

Note to Figure 6.77: In this case fracture path deviated from the HAZ into the weld.

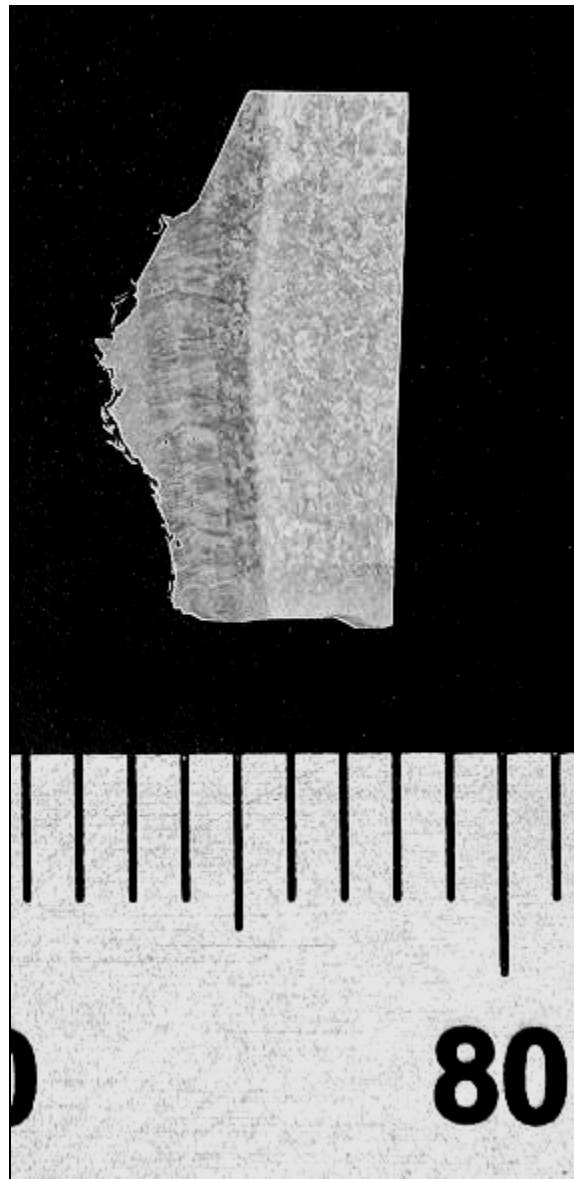


Figure 6.78: Fracture Path Deviation from Weld Metal into Heat Affected Zone

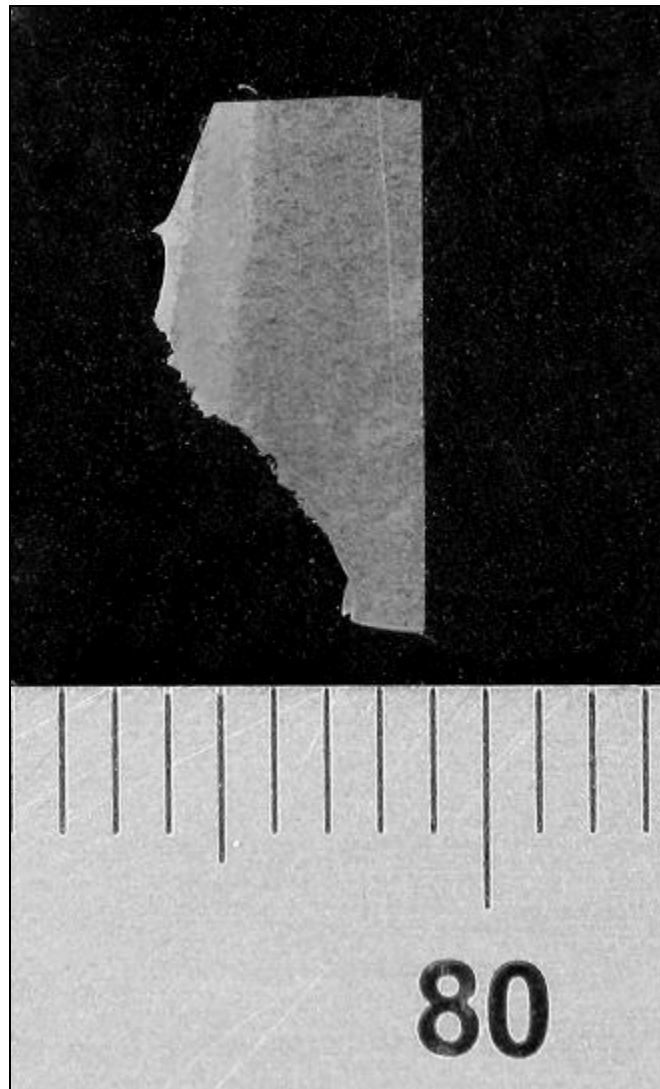


Figure 6.79: Fracture Path Deviation from Weld Metal into Base Material

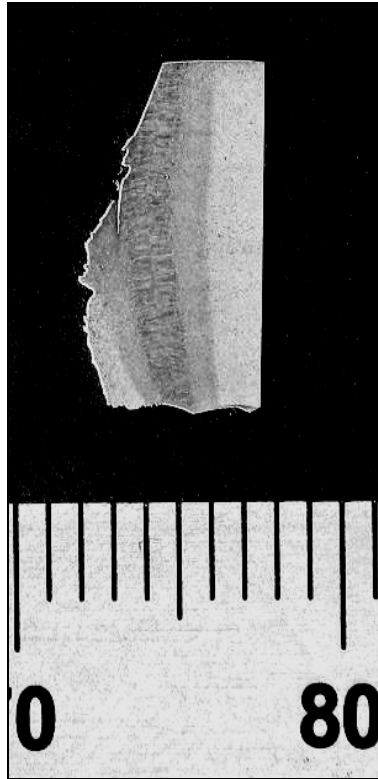


Figure 6.80: Fracture Path Deviation from Weld Metal into Heat Affected Zone and Base Metal

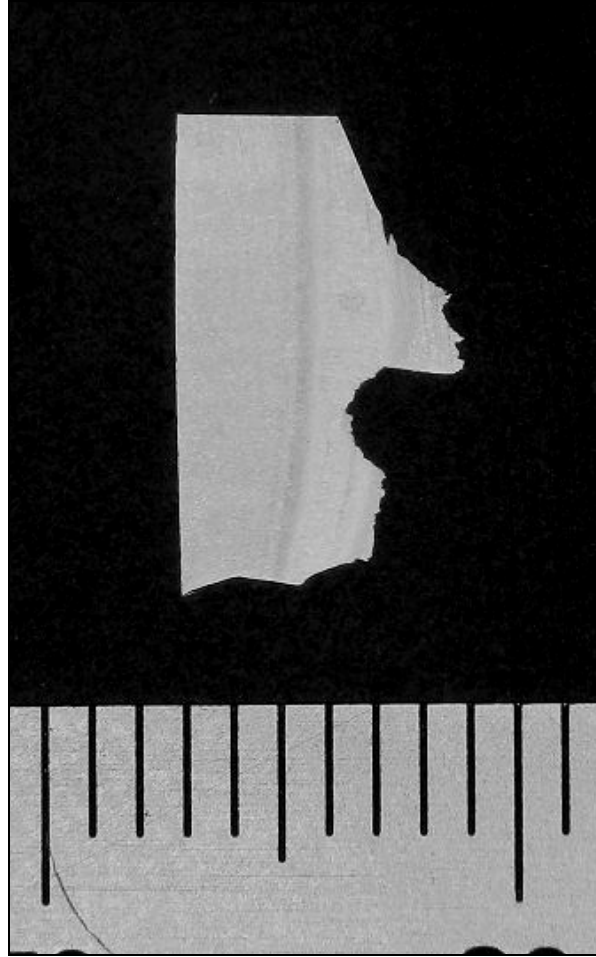


Figure 6.81: Fracture Path Deviation from Heat Affected Zone

The previous images are sample images of the FPD observed during the experimental program provided visual evidence to accept or reject the test outcomes. The disqualification of certain results would typically be associated with either (a) incorrect notch placement, (b) fracture path deviation, or (c) a combination of these. However, there were also instances where both the notch placement and the fracture path propagation occurred in the intended location, but where the test results were not consistent with the rest of the results for that material and test temperature. An example of this is illustrated in Figure 6.82, where three weld centerline specimens all display correct notch placement and fracture path propagation in the deposited weld metal. There is, however, considerable variation in the absorbed energy for these three specimens.

The weld centreline specimens shown in Figure 6.82 were taken from identical sample material (X80) and were tested at identical test temperature (-50°C). The absorbed energies of the three specimens are, however, considerably different, even though typical FPD from the weld centerline region is not observed.

It is, therefore, believed that the initial fracture propagation path determines to a large extent what the eventual absorbed energy will be, although blunting of the crack tip will also result in significant energy consumption. Supporting evidence for this argument is seen below where the arrows point to regions that show differences in the angle and horizontal distance of initial crack growth. In this example, steeper angles and longer horizontal growth equates to higher energy absorption. The direction and distance of crack growth within the intended metallurgical zone will thereby significantly influence the test results.

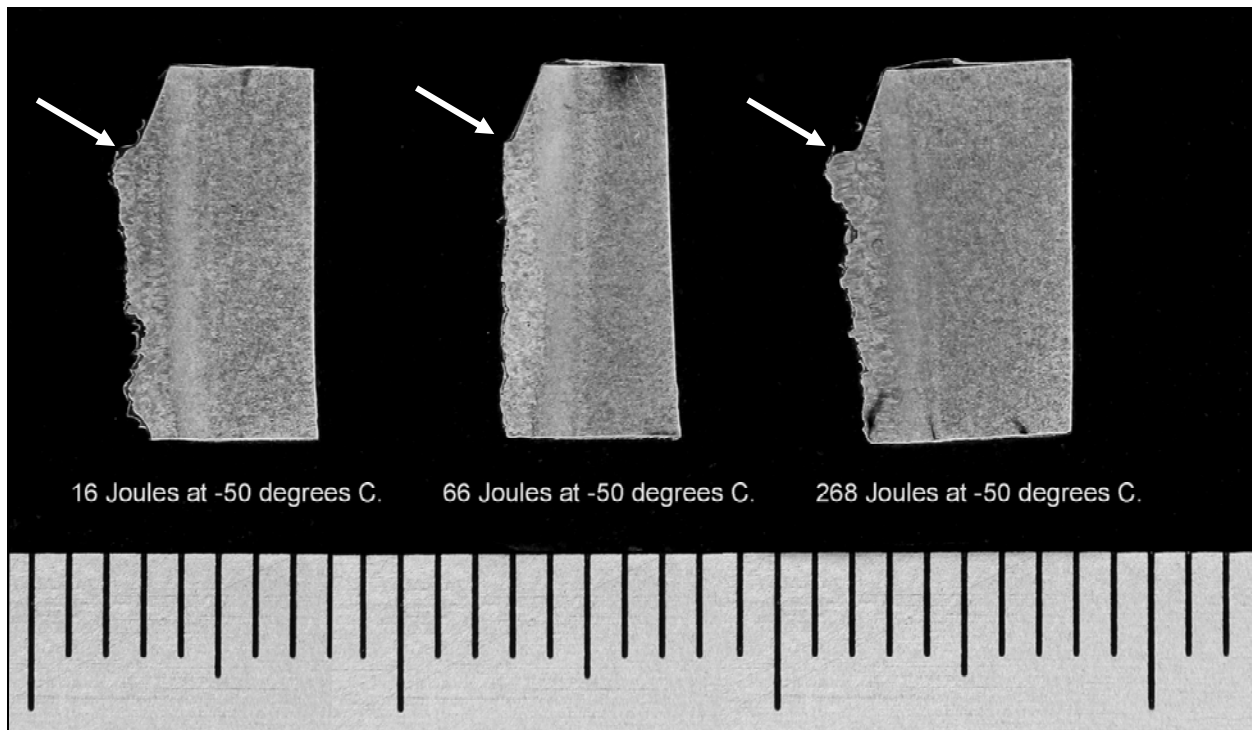


Figure 6.82: Example – Weld Centreline Specimens where Test Results Were Not Consistent with Other Results for Same Material and Test Temperature

Note to Figure 6.82: This image provides evidence to suggest that the initial energy absorbed significantly influences the test result. The arrows point to variations of the initial fracture path, where longer horizontal growth equates to higher energy absorption. Note the identical test temperatures.

Discussion

The X80 weld contained a GMAW single cap and were, therefore, considered to represent a worst case scenario in terms of toughness of the hybrid pass. This configuration did not have the benefit of tempering and refining the weld metal microstructure, which is what typically would occur under a multi-pass cap configuration.

The initial impact testing trials on the X80 welded joints displayed scatter, which was primarily due to the occurrence of fracture path deviation. An attempt was subsequently made to minimize the FPD through the placement of a pressed notch at the root of the conventional broached Charpy V-notch in the X80 specimens.

The reasoning for this approach was to create a localized brittle region at the root of the notch, which could then conceivably reduce the local toughness and ensure fracture initiation in the intended notch location for the narrow hybrid portion of the weld. It was proposed that the pressed notch would then reduce the scatter observed during initial trials as the fracture initiation energy would be more representative of the Charpy notch location.

The subsequent Charpy impact testing on pressed notched specimens, however, showed that a significant reduction in experimental scatter was not achieved. This suggested that the pressed notched approach had minimal effect on keeping the propagating crack in the intended region. The use of a pressed notch also moved the transition temperature range higher by approximately 20°C to 30°C, potentially leading to confusion when using this data to evaluate conventionally expected values. A deviation from what is traditionally expected, therefore, occurred. The pressed notch approach was, therefore, not implemented for the impact toughness testing of the X100 sample material.

There are differences between the test outcomes of conventional Charpy impact testing for the X80 and the X100 specimens. Higher impact toughness is observed for the X100 material, which also typically shows a decreased level of statistical scatter. It is probable that a reduction of microstructural hard zones due to tempering and grain refinement contributed to closer fitting data points of the X100 material.

The pressed notch apparently did not reduce the scatter in the fracture transition temperature region, while it increased the fracture transition temperature compared to the standard Charpy test results. The latter observation was expected, and the pressed notch region was locally strain hardened and, therefore, would decrease the fracture initiation portion of the total absorbed energy at a fixed test temperature. However, as the test temperature was increased, the effect of strain hardening apparently was less effective.

In terms of variations in fracture toughness along the clock positions, only the conventional X80 single cap pass Charpy impact results displayed positional variations. The results illustrate lower fracture transition temperatures for the 12 and 6 o'clock positions, when compared with the 3 and 9 o'clock positions. This suggests superior toughness for the 12 and 6 o'clock positions.

The reason for the reduction in toughness at 3 and 9 o'clock positions have not been conclusively established, although the symmetrical results, with respect to clock position, suggest that the arc, laser and shielding gas environments may have contributed to the observations along the pipe circumference. Another likely explanation is that the X80 material displayed higher total nitrogen content (100 ppm) at the 3 o'clock position, which is double the 50 ppm or less recorded at other clock locations. The effect of welding position (down hand vs. up hand) has also not been explored and may contribute to what has been observed.

Although the X80 specimens were extracted from two pipe numbers, the HLAW welding process utilized on these pipes were standardized and would have created near identical test welds. All clock positions were also examined by RT and UT prior to impact testing to ensure that defect-free test specimens were being tested.

Another factor which influences the test outcomes is related to human involvement. The narrow region of the hybrid arc weld decreases the tolerance available to place the conventional Charpy notch accurately. The ability to also position a pressed notch, consistently centred at the root of the Charpy notch will need to be considered during future work. It has not been established what effect slight variations in either conventional or pressed notch placement will have on the test outcomes. The influence of such an approach, especially if the notch is very close to a neighbouring metallurgical zone, is believed to increase the likelihood of invalid test outcomes. It will, therefore, be beneficial to determine the minimum separation distance the notch has to be from a neighbouring zone before the ensuing fracture deviates away from its origin.

FPD describes fracture propagation away from the zone in which the notch has been positioned. Our investigations reveal that FPD will occur in both HAZ and WCL hybrid laser arc welded specimens, although it has a much higher tendency to be present in the X80 WCL specimens. It is, therefore, our opinion that FPD should be expected and that the test outcomes should be qualified by post-test metallography.

Employing post-test metallography will also ensure that accurate data is used and will also remove or explain ambiguous results. An example of the latter has been shown in Figure 6.83, where variations in the absorbed energy were produced for matching specimens under identical test temperature. A satisfactory explanation would have been lacking, had post-test metallography not been employed. For this example, the variations in test data can visually be interpreted as variations during the initial stages of crack formation. This example thereby provides evidence to suggest that the energy absorbed during the initial stages of crack formation significantly influences the test result, where longer horizontal crack growth equated to higher energy absorption.

Summary

- Charpy v-notch testing can be employed on a HLAW profile.
- The impact toughness was greater for the X100 welds when compared to the X80 welds.
- Fracture path deviation is likely especially if the degree of the hardness variation in the weld zone is large.
- Post-test metallography will, therefore, be required to qualify the test outcomes.
- Multi-pass weld profiles produce less scatter in the fracture transition temperature range than the single cap pass specimens.
- The pressed notch approach will move the transition zone to higher temperatures.
- In the absence of FPD, orthogonal fracture regions equate to higher energy absorption.

6.2.2.7 Crack Tip Opening Displacement (CTOD) Testing

The fracture toughness testing program was carried out to evaluate the toughness of the overmatched X80 and X100 pipeline steel girth welds that were produced by HLAW. The weld profile produced by this process is characterized as having a broad weld cap and a narrow leg, which traverses the through thickness direction (see Figure 6.83). The welds were deposited in the 5G welding in NPS36 pipes of 10.4 mm and 14.3 mm thickness, for X80 and X100 pipes, respectively. In Figure 6.83, it can be observed that the GMAW portion of the HLAW weld is positioned on top of the hybrid pass, and forms a non-typical weld profile.

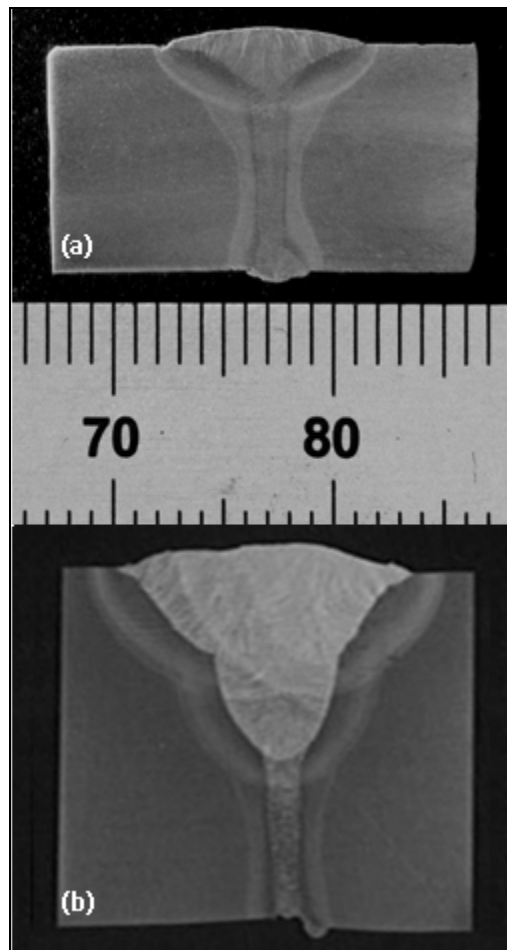


Figure 6.83: HLAW Weld Macros for (a) X80 and (b) X100 Pipes

The standard (Bx2B) size specimen geometry with a through thickness notch (BS 7448, Part 2 [15]) that was used for all CTOD testing and analysis. The specimen geometry and machine tolerances from the British Standard are shown in Figure 6.84. (Note that API 1104 [1] refers to BS 7448, Part 2 [15] for CTOD testing.)

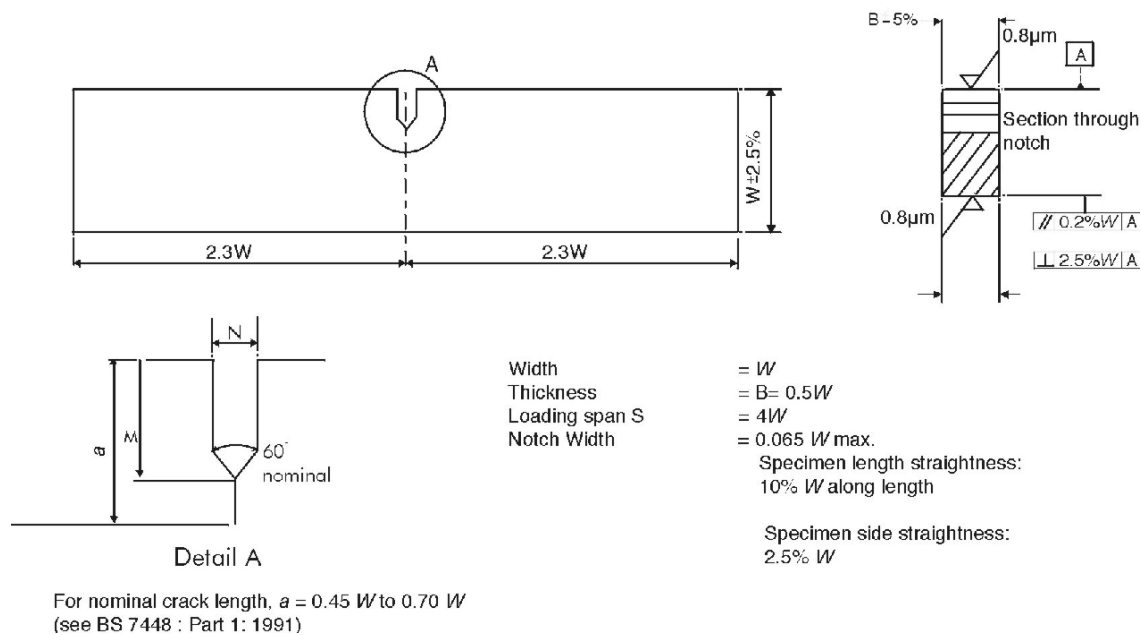


Figure 6.84: Weld Fracture Toughness Specimen Geometry

In this testing program as a baseline, specimens were extracted and machined from X80 and X100 pipe, as per API 1104 Clause A.3.2.3.2 and A.3.2.3.3 [1]. As proposed for the testing phase of this program, to reduce the likelihood of the fatigue crack deviation from the intended location in the non-typical weld profile, a task was performed, after the baseline tests. In this task, the X100 weld was subject to two series of tests to see any effect of a shorter fatigue pre-crack. The standard fatigue crack requires a minimum depth of 1.3 mm measured at both specimen surfaces. This is a requirement in the British Standard and the primary reason for this may originate from the first CTOD test standard (BS 5762 [16], Clause 5.2) where a machined notch with a 60 degree tip was specified. More recently, ASTM E1820-06 [17], Clause 7.4.5.1, allows for shorter fatigue cracks from a narrow machined notch. At BMT Fleet Technology, the narrow notch profile has been used successfully with an integral knife edge machined by EDM. The EDM slot is cut by a 0.010 mm (0.004 inch) wire and, in this case, a shorter fatigue crack (0.5 mm) would be acceptable to meet the requirement of the total included angle from the fatigue crack tip.

However the final crack tip location, i.e., the total depth crack, was to be approximately at the same location, for both standard and short pre-cracks, with respect to the specimen width (W dimension in Figure 6.84). It was assumed that the X80 HLAW will exhibit the same behaviour; and, therefore, this task was only proposed for the X100.

Specimen Preparation

Four tasks were performed under CTOD testing:

- (1) API 1104 [1] baseline tests;
- (2) Examine any effects from adopting a short fatigue crack;
- (3) Tests to determine if there is a indication of toughness variation in the four quarters of the girth weld; and
- (4) Tests to determine the CTOD fracture transition temperature at the worst clock location.

Rough blanks were extracted with a record of the o'clock position, taking care to remove material within 25 mm of any flame cut edges. The specimens were then machined to the standard geometry dimensions (Bx2B) of the British Standard BS 7448, Part 2 [15]. The machined samples had a surface ground finish on the load line and support surfaces that enabled macro-etching to reveal the weld metal and the HAZ in order to accurately mark the through thickness notch/fatigue pre-crack locations along the required weld position following guidelines in Clauses 6.1 and 8.2 in BS 7448, Part 2 [15]. Figure 6.85 displays an example of the notch location marked on the through thickness plane for the WCL and HAZ specimens. The weld centerline notch location was at the center of the hybrid portion of the weld. The heat affected zone notch was placed as to sample the HAZ at the fusion line of the HLA portion of the weld, noting that this notch location also sampled a portion of the cap pass deposited with laser assisted GMAW. This notch placement is at variance to the guidelines in API 1104, Clauses A3.2.3.2 [1] because of the non-typical weld profile. This was carried out because the objective was to determine the CTOD toughness of the HAZ of the hybrid pass. Integrated knife edges were machined into the specimens to allow for the use of an MTS clip gauge, for the measurement of Crack Mouth Opening Displacement (CMOD). An EDM notch was then placed at a pre-determined depth using a 0.01 mm wire in a direction that was opposite to the direction of welding. Figure 6.86 shows the integral knife edge geometry. Note that this is different to the machined notch geometry shown in Figure 6.84.

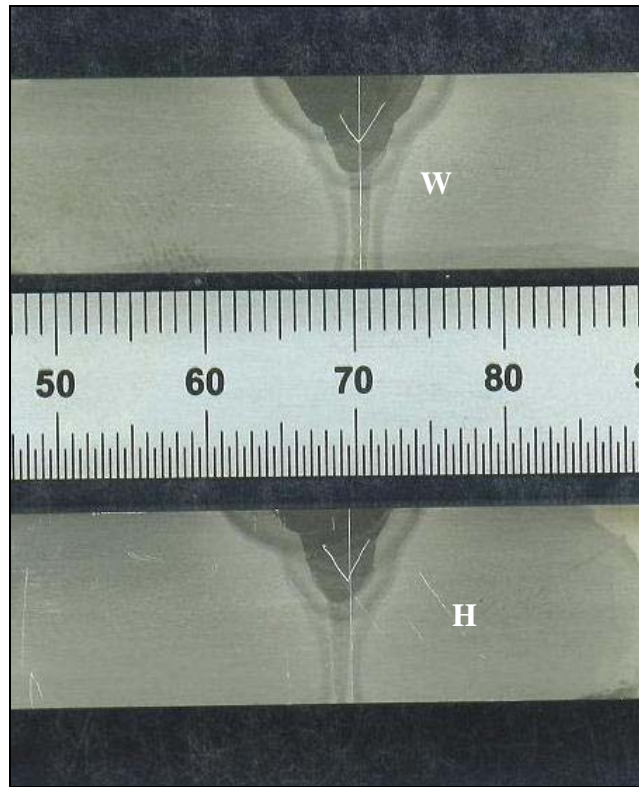


Figure 6.85: Notch Location Marked on the Through-thickness Plane of CTOD Specimen Blanks

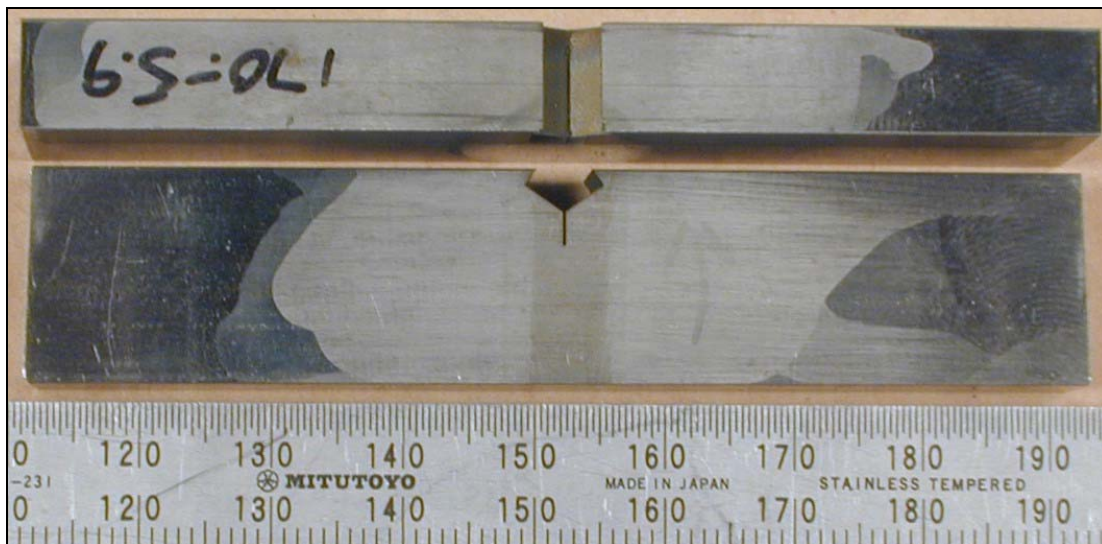


Figure 6.86: Typical EDM Notch Profile

Prior to pre-cracking, specimens extracted from X100 pipe with nominal pipe wall thickness 14.3 mm, were laterally compressed by approximately 0.5 percent of the thickness (B dimension in Figure 6.84) of the specimen. This lateral compression was conducted to alter (reduce the variation) of weld residual stresses in through-thickness direction (B) of the specimen, so as to help promote straight and even fatigue crack-front growth following the guidelines in BS 7448:Part 2, Annex D 162 [18].

Fatigue Pre-Cracking

Each of the Bx2B geometry CTOD samples were then fatigue pre-cracked to approximately half the depth of the sample (i.e., $a/W = 0.5$). For crack initiation, the maximum stress intensity factor (K_f) was kept below that allowed in BS 7448, Part 1 [15], and the minimum to maximum load ratio (R-ratio) was kept at about 0.1. After crack initiation, fatigue pre-cracking was performed in three additional stages for specimens with the maximum K_f value kept below the maximum allowed in BS 7448: Part 1 [15], as calculated from the compliance measurements during the automated pre-cracking process. This usually ensures that the final pre-cracking load is below the maximum allowed in the validity check that is performed from the average crack length measured after the completion of the CTOD test. For the specimens that had shorter pre-cracks, only two additional stages were used after crack initiation.

For the X80 grade pipe specimens with nominal pipe wall thickness 10.4 mm, where lateral pre-compression was not employed, the R-ratio was increased to 0.3 for the two intermediate pre-cracking stages. This usually helps in improving the fatigue crack straightness.

CTOD Testing

The load and CMOD were measured using a calibrated load cell and clip gauge, respectively. Both apparatus are calibrated regularly to ensure the required accuracy is achieved.

The specimens were enclosed in a chamber (as shown in Figure 6.87) and cooled by liquid nitrogen to the required temperature. Temperature control was maintained using a thermocouple attached to the specimen. After the temperature had stabilized for a minimum period that is determined from specimen thickness, they were loaded at a quasi-static rate ($\sim 1.3MPa\sqrt{m} s^{-1}$). The load and the clip gauge displacements were digitally acquired for the duration of the test. The test was ended when a fracture instability event was detected from the load-CMOD curve or a maximum load plateau was reached and surpassed.



Figure 6.87: CTOD Test Set up

The load-CMOD plot was displayed in real time on the PC screen displaying the progress of the test. Later, the acquired data was used to determine the critical CTOD from the input of specimen dimensions, measured fatigue crack length and material properties. Any audible “pop-in” detected during the progress were to be noted.

After the completion of testing, each specimen was soaked in liquid nitrogen (-196°C / -321°F) and broken open to expose the fatigue crack and any subsequent growth that may have occurred during the CTOD test. Fatigue crack depth measurements were made in accordance with BS 7448: Part 1 [15].

CTOD Results

The CTOD was calculated by adding the elastic and plastic CTOD as specified in Clause 12.1 of BS 7448, Part 2 [15]. The failure type for each test was determined by observing the crack growth as displayed on the fracture face of the specimen together with the features of the load-CMOD curve. The failure types are when a maximum load plateau is reached and surpassed (δ_m type), or when fracture instability event occurred (δ_u or δ_c type). Failure type δ_u is when some crack growth or stretch zone is observed in the fracture face and δ_c is for fracture event from the fatigue crack tip. Type δ_c^* is when a pop-in is detected as specified in BS 7448: Part 1 [18]. Finally, the required validity checks were performed in accordance with BS 7448, Part 2 [15].

API Test Results

Table 6.16 and Table 6.17 present the results for both X80 and X100 welds. The specimen number notation includes the clock position, for example, 12W is from 12 o'clock.

Table 6.16: CTOD Results for X80 Pipe at -5°C for API 1104 [1] Test Locations

Pipe # and Grade	Notch Location	Sample #	a_o/W	a_{min} [mm]	Total CTOD [mm]	Failure type	Post Test Metallography
508 X80	WCL	12W	0.527	1.39	0.123	δ_u	Fatigue crack - weld
		6W	0.513	1.44	0.228	δ_u	
		3W	0.525	1.62	0.141	δ_c	Fatigue/fracture - weld
	HAZ	12H	0.523	1.81	0.452	δ_m	
		6H	0.506	1.63	0.471	δ_m	
		3H	0.536	2.15	0.299	δ_m	

Note to Table 6.16: a_o represents average total crack length
 a_{min} represents minimum fatigue crack depth
W represents specimen width

Table 6.17: CTOD Results for X100 Pipe at -5°C for API 1104 [1] Test Locations

Pipe # and Grade	Notch Location	Sample #	a_o/W	a_{min} [mm]	Total CTOD [mm]	Failure Type	Post Test Metallography
497 X100	WCL	12W	0.496	2.01	0.243	δ_m	
		6W	0.482	1.57	0.211	δ_m	Fatigue/fracture - weld
		3W	0.492	1.74	0.181	δ_m	Fatigue/fracture - weld
	HAZ	12H	0.485	1.59	0.292	δ_m	
		6H	0.501	1.99	0.248	δ_m	Fatigue crack - HAZ
		3H	0.480	1.54	0.262	δ_m	Fatigue crack – weld/FL

Note to Table 6.16: a_o represents average total crack length
 a_{min} represents minimum fatigue crack depth
W represents specimen width

The load-CMOD curves for specimens 12W and 6W from X80 pipe weld displayed only minor load drops but need to be called a δ_u type following the procedure described in the previous section. However, it is not clear if the load drops were a result of the regions associated with discolouration at the fatigue crack front. By contrast, the specimen from the 3 o'clock location produced an “unstable” crack extension with a significant load drop that was audible. The fractures for specimens 3W and 6W from X80 pipe weld is presented in Figure 6.88 and the corresponding load-CMOD curves are in Figure 6.89. The remaining CTOD results of this set all produced ductile (upper shelf) behaviour as indicated by δ_m type.



Figure 6.88: Fracture Surface of Specimens 3W (left) and 6W (right) from X80 Pipe Weld

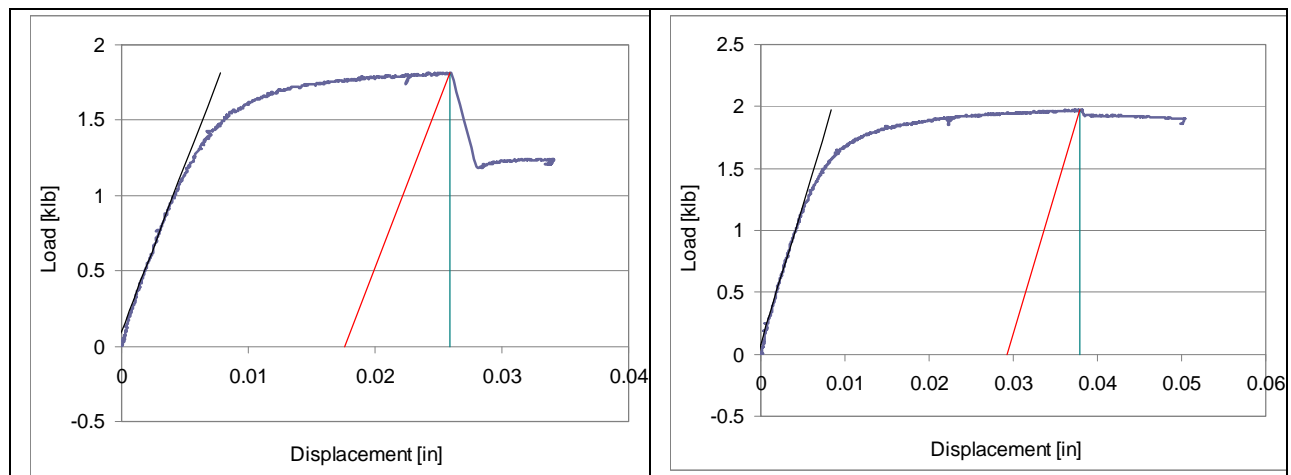


Figure 6.89: Load-CMOD Plots of Specimens 3W (Left) and 6W (Right) from X80 Pipe Weld

Selected post-test metallography was performed by sectioning the fracture following the guidelines in BS 7448, Part 2, Clause 11.2.1 [15]. The findings are also reported in Table 6.16 and Table 6.17. Typical post-test metallography macrographs are displayed in Figure 6.90. It is to be noted that, for the HAZ specimens, the EDM notch was placed very close to the fusion line of the hybrid pass and, therefore, part of the fatigue crack would be in the laser-assisted GMAW deposits.

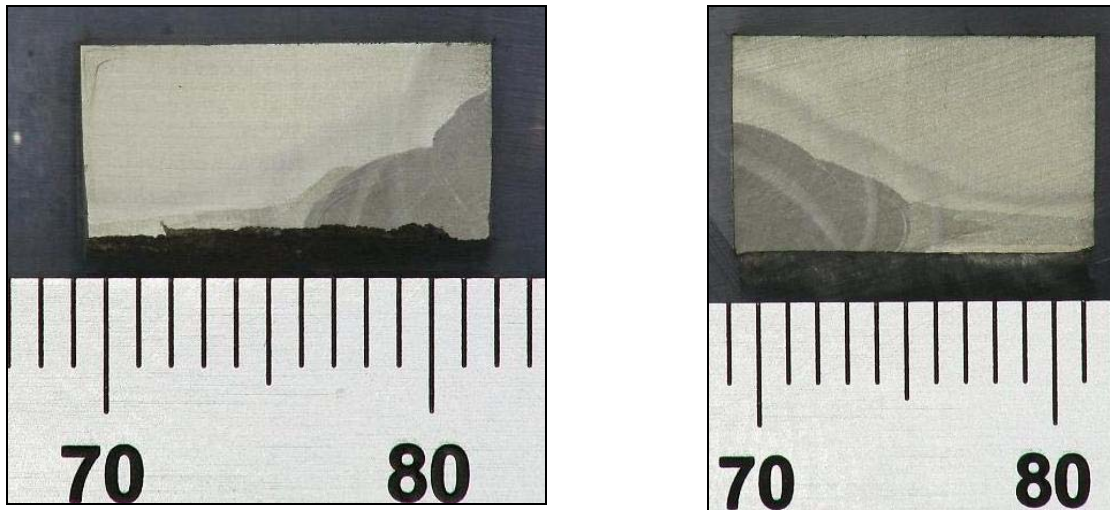


Figure 6.90: Macrographs of Specimens 3W (Left) and 6H (Right) from X100 Pipe Weld

Test Results from Evaluation of Shorter Fatigue Crack Depth

In this examination, specimens were extracted from two pipe welds, 500 and 501, in the 11 to 2 o'clock positions, representing specimens from the quarter that encompass the 12 o'clock location. The pipes were X100 grade. The specimens from pipe 500 were used to prepare the fatigue crack to meet the minimum depth of 1.3 mm as per BS 7448: Part 1 [18], whereas the specimens from pipe 501 were used for the short fatigue crack. The WCL specimens were extracted from the 12 to 1 o'clock region, while the HAZ specimens were extracted from 11 to 12 o'clock. The total crack depth averaged, i.e., the machine notch plus the fatigue crack, for all specimens from welds 500 was same as for 501 ($a_0/W = 0.482$).

Table 6.18 and Table 6.19 presents the results for pipe welds 500 and 501 testing at -5°C . The specimen number notation includes the representative clock location, for example, 12-W is from the quarter 11 to 2 o'clock positions. The results show ductile behaviour in all specimens and the shorter fatigue crack does not seem to affect the CTOD toughness behaviour. Similar observations were made from the test results at -40°C , with one exception: one HAZ specimen produced an unstable fracture of the type δ_c with a low CTOD of 0.095 mm. The fracture face of the specimen is presented in Figure 6.91. The fracture surface displays a cleavage (brittle) fracture event and is associated with the sudden load drop that occurred during the test. It is known that fracture toughness of the HAZ display more variability compared to the weld metal. Therefore this "outlier" most likely to be a result of the typical variability in toughness of the HAZ rather than the effect of the difference in fatigue crack depth. Figure 6.92 shows that the fatigue crack is in the HAZ.

Table 6.20 and Table 6.21 show the results of test carried out at -40°C . The results indicate that the short fatigue crack depth did not have an influence on the fracture toughness behaviour for the X100 weld, where specimens are extracted from the 11 to 2 o'clock quarter. The average fatigue crack depths, measured using the nine-point averaging method in BS 7448: Part 1 [18], for the specimens from pipe weld 501 were in the range of 0.93 to 1.46 mm. The minimum fatigue crack length was between 0.67 mm to 1.11 mm.

Table 6.18: CTOD Results at -5°C for WCL Test Location

Pipe #	Sample ID	a_o/W	a_{\min} [mm]	Total CTOD [mm]	Failure Type	Post Test Metallography
500	12-W1	0.480	1.58	0.222	δ_m	
	12-W2	0.491	1.84	0.199	δ_m	
	12-W3	0.490	1.85	0.221	δ_m	Fatigue crack - weld
501	12-W1	0.482	0.87	0.222	δ_m	Fatigue crack - weld
	12-W2	0.481	0.84	0.269	δ_m	
	12-W3	0.481	0.90	0.214	δ_m	

Table 6.19: CTOD Results at -5°C for HAZ Test Location

Pipe #	Sample ID	a_o/W	a_{\min} [mm]	CTOD [mm]	Failure Type	Post Test Metallography
500	12-H1	0.474	1.37	0.257	δ_m	
	12-H2	0.476	1.50	0.203	δ_m	
	12-H3	0.474	1.48	0.183	δ_m	Fatigue crack - HAZ
501	12-H1	0.481	0.87	0.213	δ_m	
	12-H2	0.482	0.98	0.232	δ_m	Fatigue crack - FL
	12-H3	0.470	0.67	0.244	δ_m	

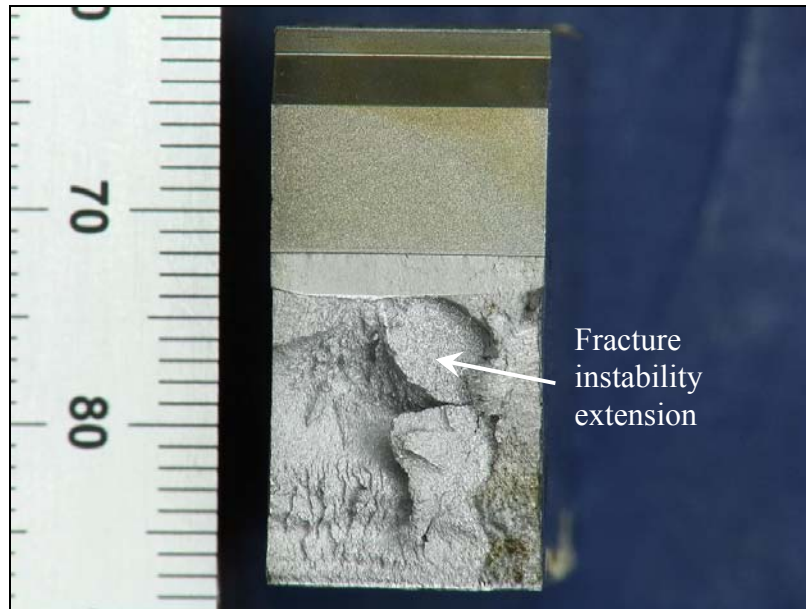


Figure 6.91: Fracture of Specimen 12-H5

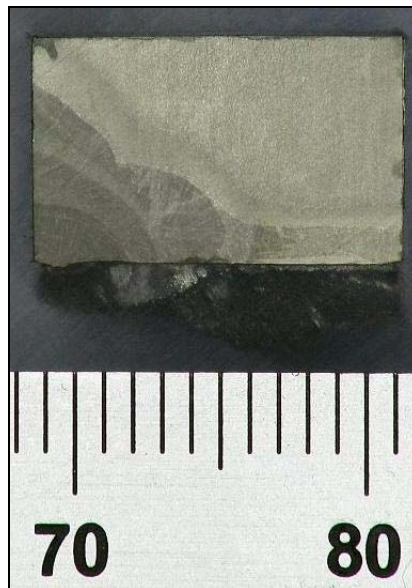


Figure 6.92: Macrograph of Specimen 12-H5 Showing Fatigue Crack Location

Table 6.20: CTOD Results at -40°C for WCL Test Location

Pipe #	Sample ID	a_o/W	a_{min} [mm]	Total CTOD [mm]	Failure type	Post Test Metallography
500	12-W4	0.491	1.82	0.242	δ_m	Fatigue crack - weld
	12-W5	0.489	1.79	0.197	δ_m	
	12-W6	0.493	1.82	0.220	δ_m	
501	12-W4	0.491	1.11	0.260	δ_m	Fatigue crack - weld
	12-W5	0.475	0.77	0.214	δ_m	
	12-W6	0.490	1.09	0.225	δ_m	

Table 6.21: CTOD Results at -40°C for HAZ Test Location

Pipe #	Sample ID	a_o/W	a_{min} [mm]	CTOD [mm]	Failure Type	Post Test Metallography
500	12-H4	0.470	1.31	0.201	δ_m	
	12-H5	0.473	1.38	0.095	δ_c	Fatigue crack - HAZ
	12-H6	0.477	1.49	0.188	δ_m	
501	12-H4	0.483	0.90	0.234	δ_m	
	12-H5	0.482	0.87	0.251	δ_m	Fatigue crack - HAZ
	12-H6	0.481	0.88	0.262	δ_m	

Toughness Variation in the Four Quarters of the Girth Weld

As the results indicated that the short fatigue crack depth did not have an influence on the fracture toughness behaviour for the X100 weld, it was decided, with the approval of DoT, to perform the remaining CTOD testing with the short fatigue crack length. In ASTM E1820-06 [17], the minimum crack length prescribed is 0.6 mm or 0.025B for a narrow notch. For specimens extracted from pipe wall thickness of 14.3 mm and 10.4 mm, the applicable crack length is 0.6 mm.

Grade X100 Pipe Weld

For the X100 welds, as the quarter encompassing the 12 o'clock was evaluated and the results presented in the previous section, the remaining clock locations encompassing the 3, 6, and 9 were evaluated by extracting specimens from 2 to 5 o'clock, 5 to 8 o'clock, and 8 to 11 o'clock, respectively. The testing was carried out at -5 and -40°C. The complete results are presented in Annex C, Table C1. (All of the specimens were extracted from pipe weld ring 500)

The weld metal tests did not clearly indicate any quarter to have inferior CTOD toughness. One test specimen produced an unstable fracture (type δ_c) at -40°C from the 3 o'clock quarter and another specimen from 9 o'clock was categorized as δ_u . The respective CTOD values were 0.174 and 0.238 mm. All the remaining tests from the weld metal produced ductile behaviour

(δ_m). Fractures that produced unstable fractures are presented in Figure 6.93 and corresponding post test macrographs are shown in Figure 6.94. The post test macrographs confirm that the fatigue crack is in the weld. The fracture of specimen 3-W6 shows a region below the root/bottom of the fatigue crack, on the right side, that is not characteristic of cleavage fracture.

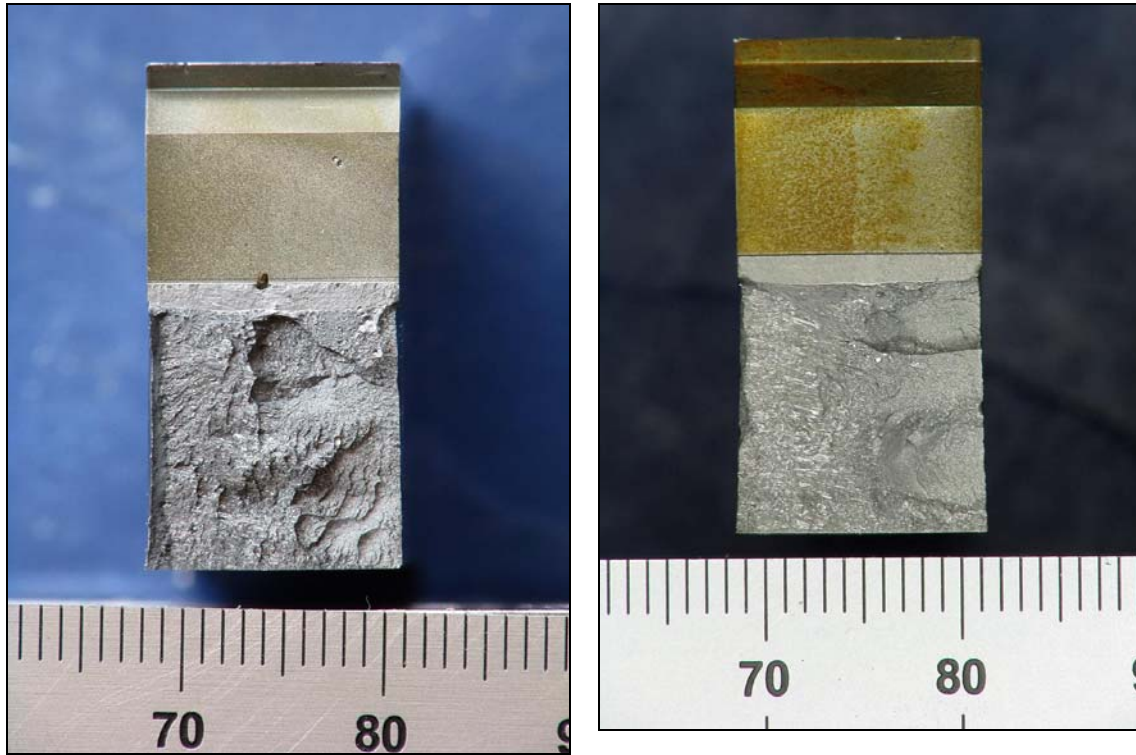


Figure 6.93: Fracture of Specimens 3-W6 (Left) and 9-W1D (Right)

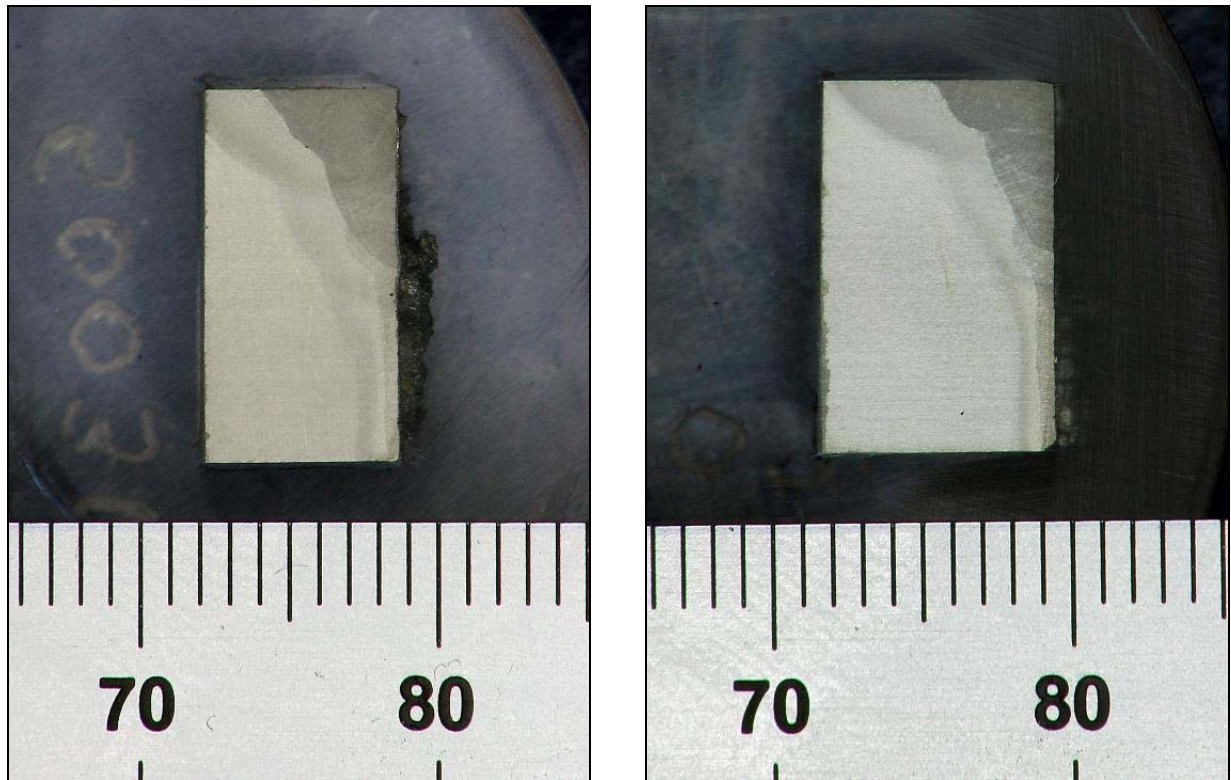


Figure 6.94: Macrographs of Specimens 3-W6 (Left) and 9-W1D (Right)

For the HAZ tests, all the three quarters produced results that have some δ_u type behaviour. Note that the specimens from 12 o'clock quarter had one δ_c type fracture at -40°C . The weld metal test results apparently indicate good CTOD toughness down to -40°C for all quarters with two tests showing fracture instability. The results for specimens from 3 o'clock location are provided in Table 6.22. In this table, the lowest CTOD value of 0.137 mm was from specimen 3-H6 tested at -40°C . The fracture face and the corresponding load-CMOD plot is shown in Figure 6.95 and the post test metallography results are presented in Figure 6.96. The crack extension occurring during the test, producing the load drop can be viewed in the fracture face. Further metallography was carried out and described in the section on discussion.

Table 6.22: CTOD Results from 3 O'clock Location from X100 Weld

Pipe #	Temp. (°C)	Sample ID	a_0/W	a_{min} [mm]	Total CTOD [mm]	Failure type	Post Test Metallography
500	-5	3-W1	0.489	0.87	0.200	δ_m	
		3-W2	0.491	0.89	0.203	δ_m	
		3-W3	0.491	0.93	0.180	δ_m	Fatigue crack - weld
		3-H1	0.495	1.07	0.181	δ_m	Fatigue crack - weld
		3-H2	0.490	0.89	0.226	δ_m	
		3-H3	0.488	0.86	0.298	δ_m	
	-40	3-W4	0.497	1.05	0.222	δ_m	Fatigue crack - weld
		3-W5	0.494	1.05	0.229	δ_m	
		3-W6	0.488	0.86	0.174	δ_c	Fatigue crack - weld
		3-H4	0.482	0.74	0.252	δ_m	Fatigue crack - FL
		3-H5	0.483	0.71	0.318	δ_m	
		3-H6	0.491	0.98	0.137	δ_u	Fatigue crack - FL

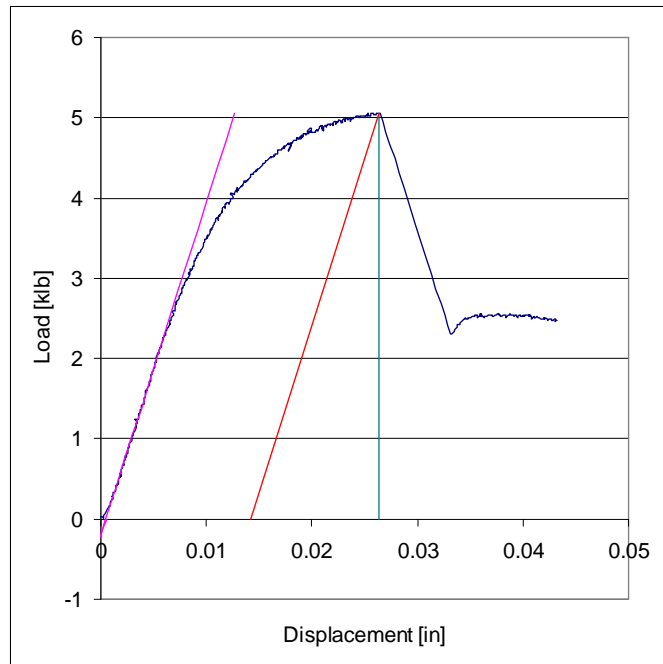
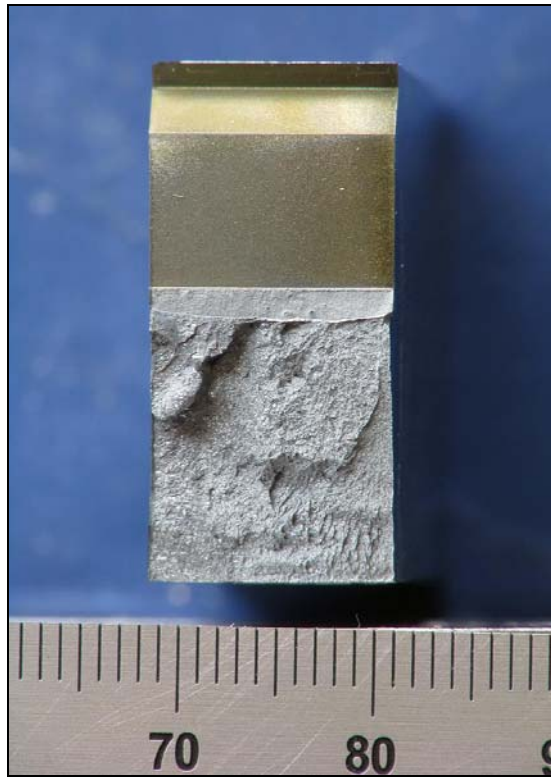


Figure 6.95: Fracture (Left) and Load-CMOD Plot (Right) of Specimen 3-H6

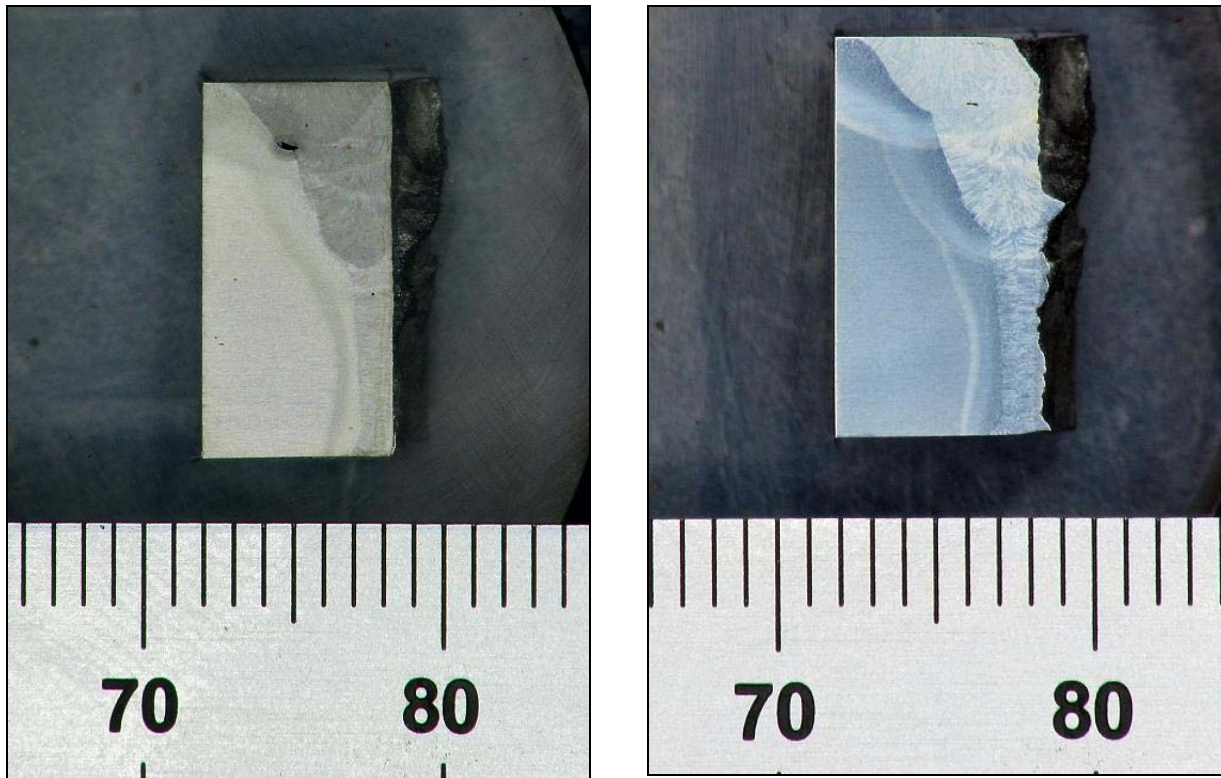


Figure 6.96: Macrographs of Specimen 3-H6 – Fatigue Crack Location (Left) and Fracture Initiation Plane (Right)

Grade X80 Pipe Weld

For the X80 welds as the quarter encompassing the 9 o'clock was not evaluated as the machined specimens showed a continuous line on one side of the specimen (see Figure 6.97 (a)). Figure 6.97 (b) shows that the line is caused by a Lack of Fusion (LOF) flaw formed between the hybrid weld and laser assisted GMA cap. When a specimen from the 3 o'clock location that had a similar line was fatigue pre-cracked, part way in the fatigue pre-cracking the fatigue crack grew on the line and not from the root of the EDM notch. As for a short fatigue pre-crack, the fatigue crack straightness as shown in Figure 6.98 would cause issues for test result validation concerning fatigue crack front straightness; it was decided to laterally compress the specimens adopting guidelines in BS 7448, Part 2, Annex D [15]. Both of these decisions were made with the approval of DoT. The specimens were extracted from each quarter as described for the X100 pipe welds. The testing was carried out at -5°C and -40°C . The complete results are presented in Annex C, Table C2. (All of the specimens were extracted from pipe weld ring 506).

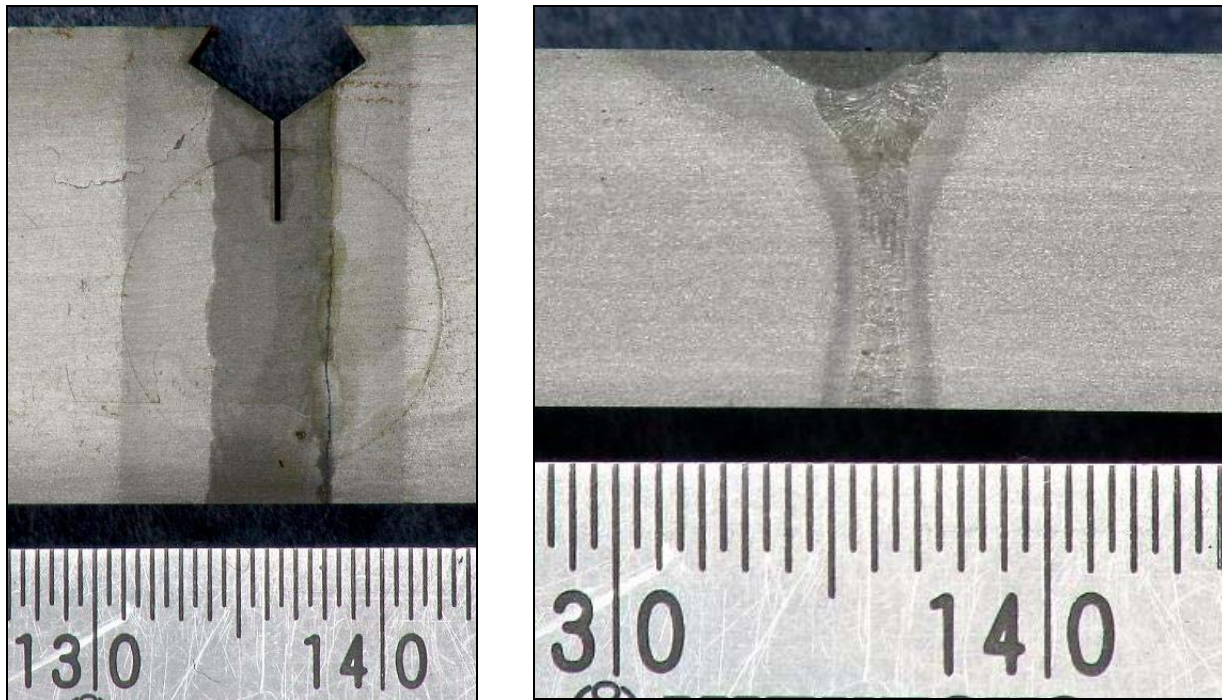
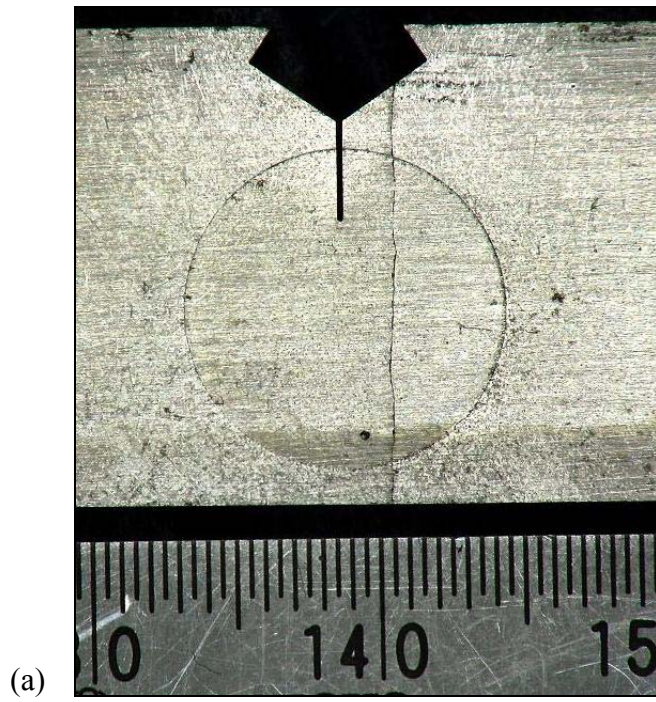


Figure 6.97: A Specimen from 9 O'clock Location

Note to Figure 6.97(b): Surface shown in Figure 6.97(b) (left) and through thickness showing weld profile (right).

The weld metal tests indicated the 3 o'clock quarter to have inferior CTOD toughness. This is based on the observation that all three specimens produced an unstable fracture of the type δ_c at -5°C , whereas specimens from 12 and 6 o'clock positions had two fractures each that were not categorized as δ_c . All of the weld metal tests at -40°C produced fracture of the type δ_c . In this way, compared to the X100 weld the X80 weld results were "very poor". The results from the specimens from the 3 o'clock position are presented in Table 6.23.

For the HAZ tests, the results from all three quarters show unstable fracture occurrences that are usually a result of cleavage fracture, except for tests done at -5°C from the 3 o'clock quarter. The latter results are in Table 6.23. Many unstable events were qualified as pop-ins (δ_c^* type) in accordance with BS 7448: Part 1 [18], Clauses 9.1 and 9.3.

Table 6.23: CTOD Results from 3 O'clock location from X80 Weld

Pipe #	Temp. (°C)	Sample ID	a_o/W	a_{min} [mm]	Total CTOD [mm]	Failure Type	Post Test Metallography
506	-5	3-W1	0.523	1.17	0.057	δ_c	Fatigue crack - weld
		3-W3	0.486	0.85	0.049	δ_c^*	Fatigue crack - weld
		3-W4	0.512	1.31	0.083	δ_c	
		3-H2	0.497	1.00	0.273	δ_m	Fatigue crack - HAZ
		3-H3	0.507	1.18	0.294	δ_m	Fatigue crack - HAZ
		3-H4	0.506	1.18	0.286	δ_m	
	-40	3-W5	0.487	0.85	0.016	δ_c^*	Fatigue crack - weld
		3-W6	0.514	1.30	0.018	δ_c^*	
		3-H4	0.481	0.81	0.094	δ_c	Fatigue crack - FL
		3-H5	0.482	0.67	0.078	δ_c	Fatigue crack - HAZ
		3-H6	0.487	0.87	0.082	δ_c	

Pop-in events are a result of a cleavage fracture occurrence recorded by a load drop and CMOD increase followed by a subsequent increase in load beyond the load at which the pop-in event occurred. A good example of the fracture face and the corresponding load-CMOD plot is presented in Figure 6.98. In the fracture face the ductile tear is clearly visible and occurred during subsequent loading after the pop-in event. The fatigue crack profile in this example is typical of the improvement that was obtained with regard to crack front straightness as a result of lateral compression before pre-cracking (compare with Figure 6.88).

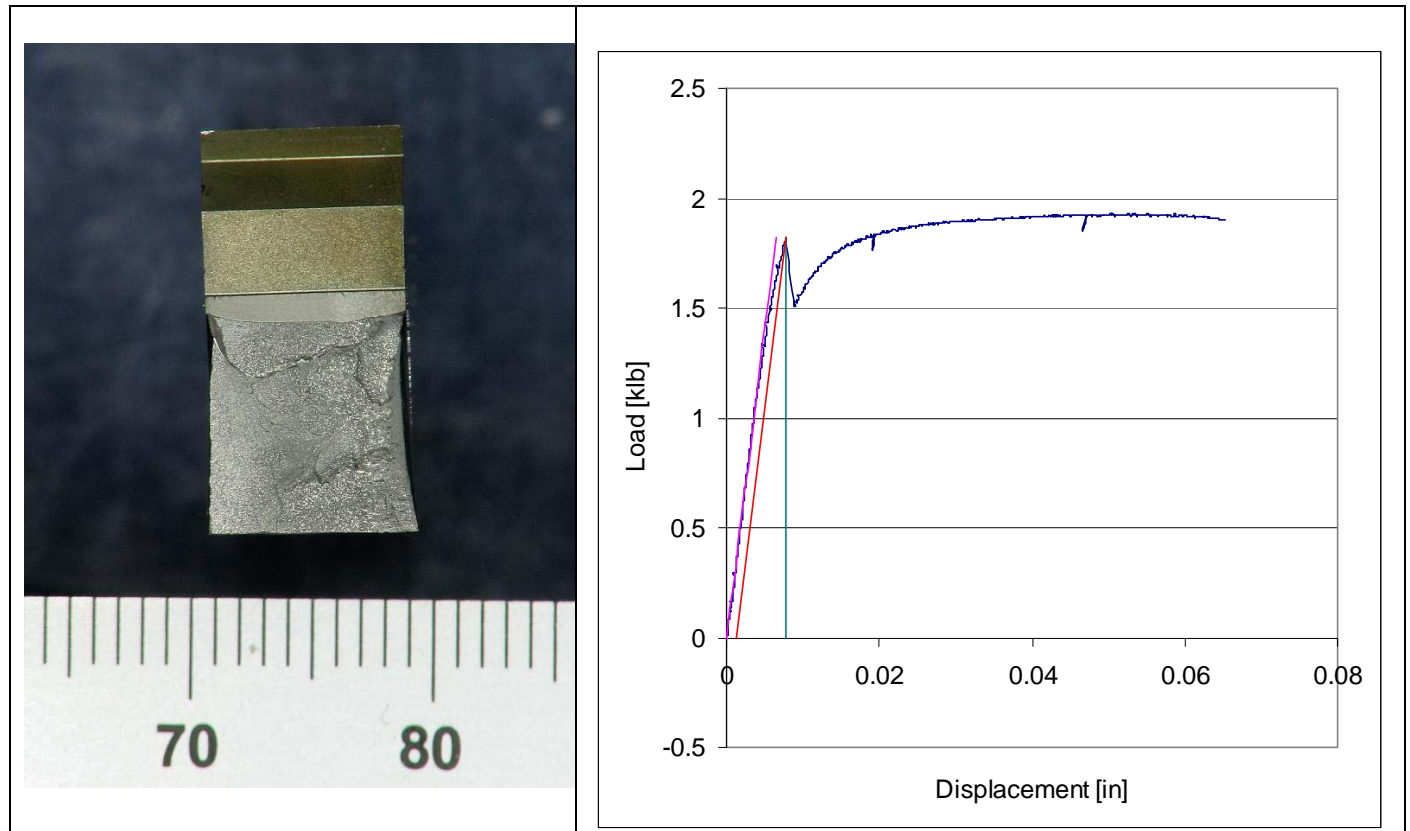


Figure 6.98: Fracture (Left) and Load-CMOD Plot (Right) of Specimen 6-H5

Determination of Fracture Transition Behaviour

Although it was decided to determine the CTOD fracture transition behaviour at the worst clock position, the test results presented for the X100 pipe weld did not give a clear indication of where this was. For the X80 pipe weld, the CTOD toughness was very poor from the three clock positions that were evaluated. Therefore, with the approval of DoT, no further testing was carried for X80 pipe weld. A contributing factor was also the continuous line on the surface of the specimens that were extracted from the 9 o'clock location for the X80 grade (see Figure 6.97). For the X100 weld it was decided to extract specimens from the 3 o'clock location. The test results are presented in Annex C, Table C3, noting that the pipe weld was 498.

The temperature versus CTOD plot for these tests is provided in Figure 6.99, together with the failure type. The results indicate that for, these tests, the CTOD fracture transition commences at about -60°C , for both the weld and HAZ. The plot in Figure 6.100 includes the CTOD results from the pipe weld 500 at the 3 o'clock position, excluding the CTOD from specimen 3-W6 that did not indicate the characteristics of cleavage fracture (see Figure 6.93). The observable change when including the results from pipe weld 500 is that, for the HAZ, there is one result, from specimen 3-H6 that is a δ_u type, indicating that for the HAZ the fracture transition begins at -40°C .

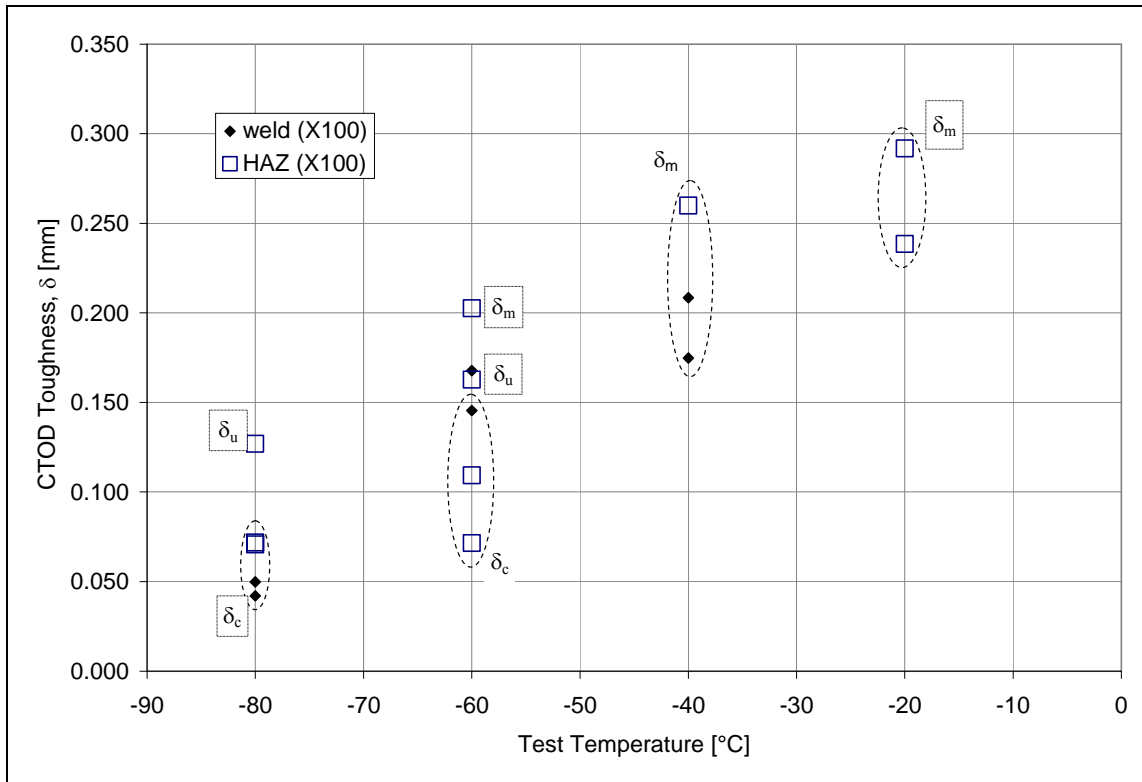


Figure 6.99: CTOD Transition Results from Pipe Weld 498 at 3 O'clock Location

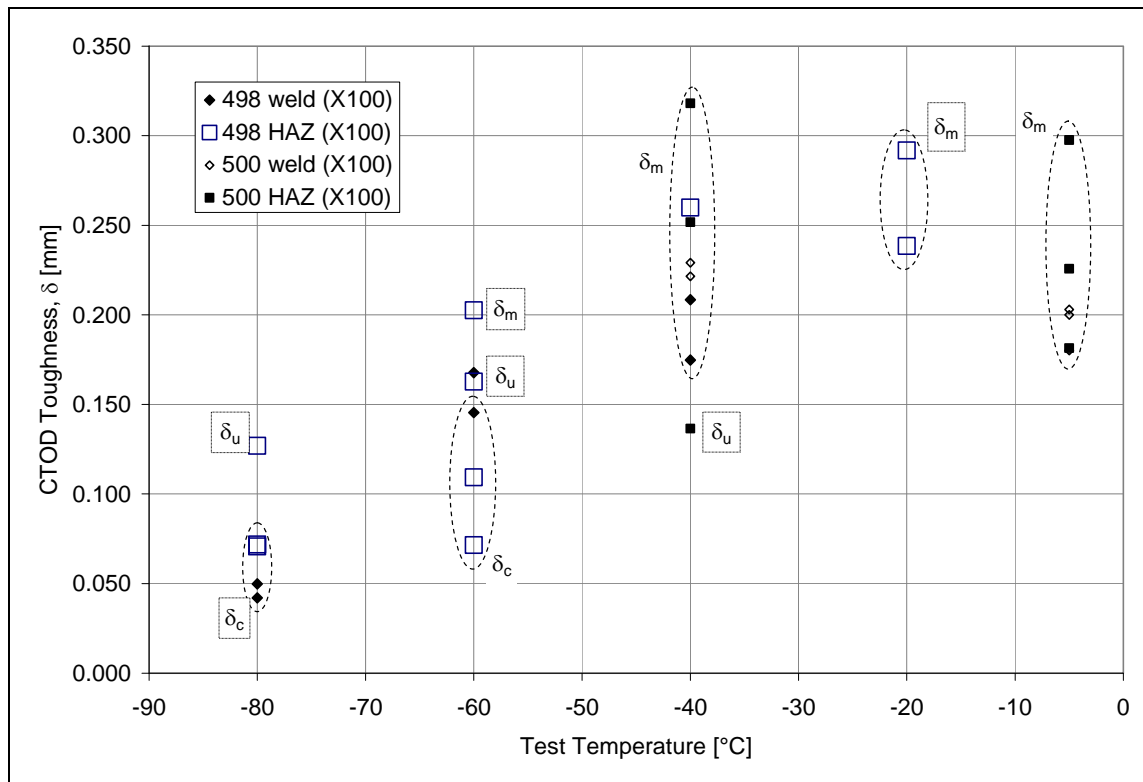


Figure 6.100: CTOD Transition Results from Pipe Welds 498 and 500 at 3 O'clock Location

Discussion

Grade X100 Pipe Welds

Comparing the results of tests carried out as per the API 1104 [1] with the rest of the tests (Annex C, Table C1) shows two results that are different for the rest. The API 1104 [1] tests were done at -5°C and the CTOD values were all type δ_m . Two test results from HAZ specimens coming from the 6 o'clock region had behaviour categorized as δ_u . The load-CMOD plots and corresponding fractures are presented in Figure 6.101 and Figure 6.102.

The fracture face in Figure 6.101 shows a dull region below the fatigue crack that is most likely to have caused the load drop displayed in the load-CMOD plot. Note that this is a gradual load drop and occurred without any audible sound and is, therefore, not typical of a brittle (cleavage) fracture. By contrast, the load-CMOD behaviour in Figure 6.103 is typical of a brittle event and corresponding sudden drop in load. The stretch zone at the root of the fatigue crack and a very small thumb nail extension before the cleavage fracture is categorized as a δ_u type. Post test metallography carried out on specimen 6H-1 showed the fatigue crack to be in the HAZ (see Figure 6.103).

As reported earlier, HAZ test at -40°C displayed δ_u type brittle events. In specimen 3-H6 the fracture initiation occurred in the HAZ (see Figure 6.95). Post test metallography performed on two other specimens, that produced brittle extensions of the δ_u type, 6-H4 and 9-H6 tested at -40°C , reported in Annex C, Table C1, also indicated fracture initiation in the HAZ. For the weld metal tests, one test specimen produced an unstable fracture (type δ_c) at -40°C from the 3 o'clock quarter and another specimen from 9 o'clock was categorized as δ_u . The respective CTOD values were 0.174 and 0.238 mm. The lower CTOD of type δ_c , can be discounted from fracture appearance. **Therefore, in summary, for the X100 pipe weld, the CTOD fracture transition apparently commences at -40°C for both the weld had HAZ, producing of δ_u type results. There is however, an exception for the HAZ in specimens 6-H3 shown in Figure 6.102 below at -5°C .**

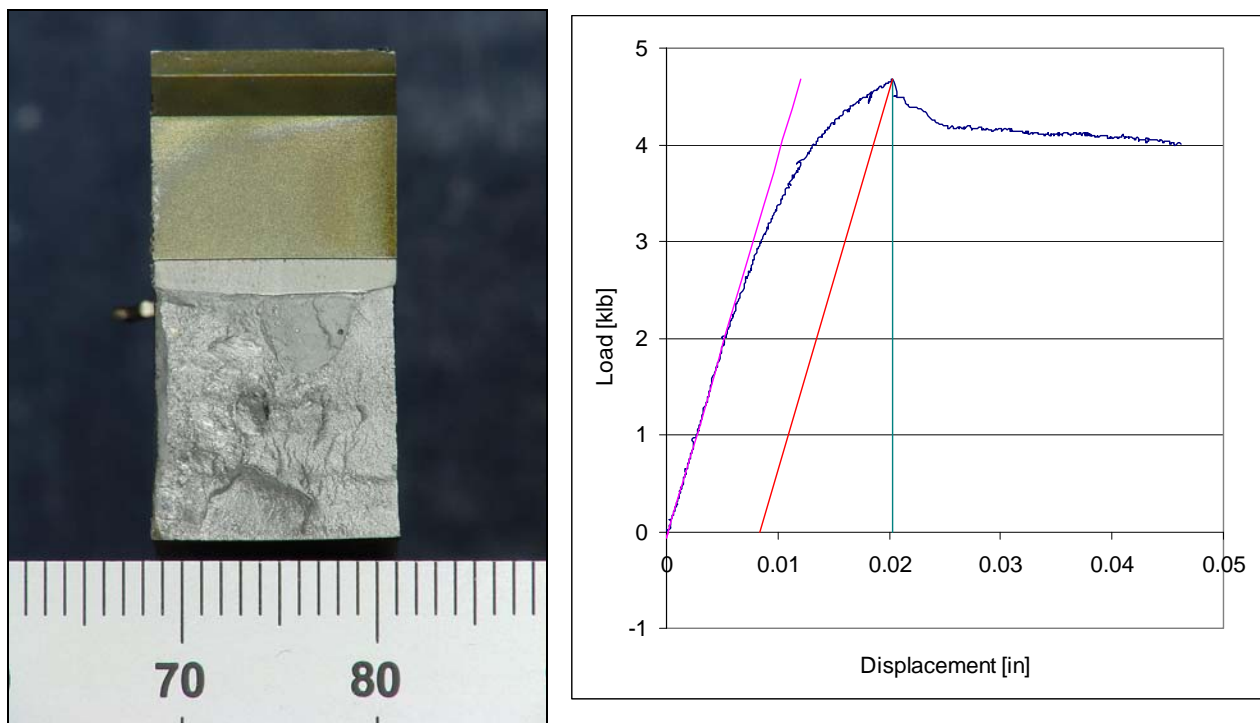


Figure 6.101: Fracture (Left) and Load-CMOD Plot (Right) of Specimen 6-H1

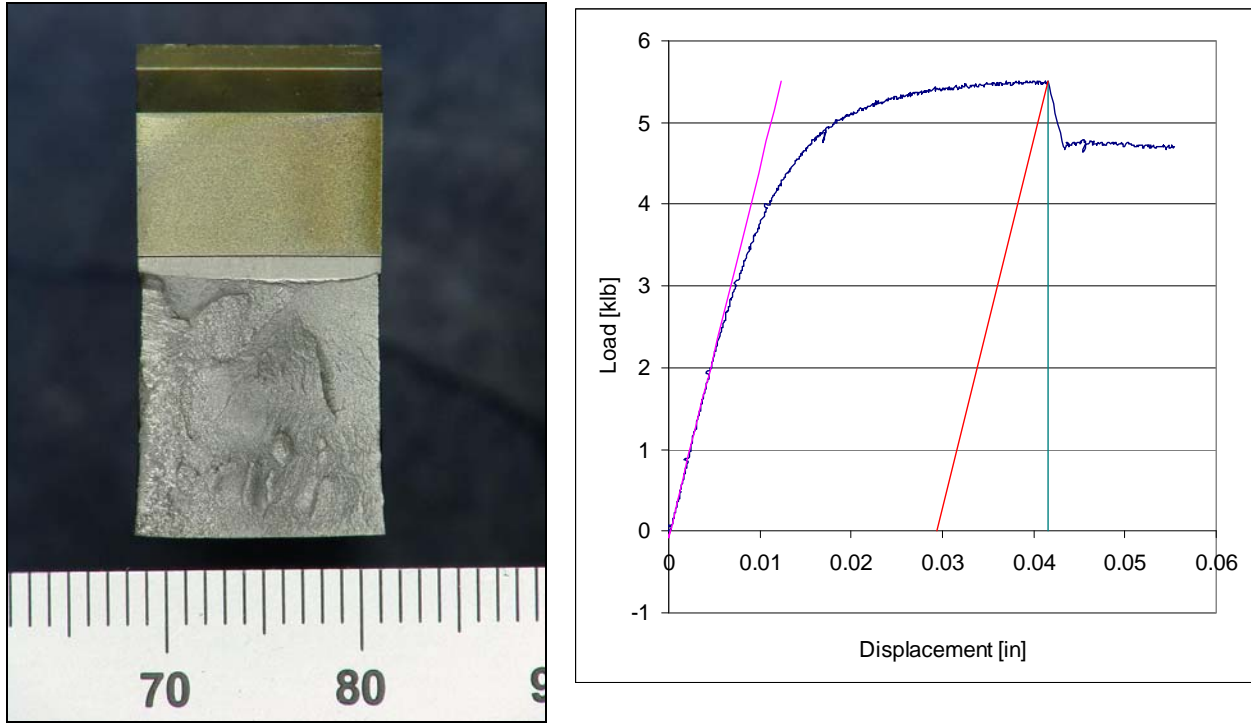


Figure 6.102: Fracture (Left) and Load-CMOD Plot (Right) of Specimen 6-H3



Figure 6.103: Macrographs of Specimen 6-H1

Grade X80 Pipe Welds

Comparing the results tests carried out as per the API 1104 [1] with those in with the rest of the tests (Annex C, Table C2) shows that for the weld metal the results indicate brittle (cleavage) fracture, except for one test result (12-3W) that produced a δ_m type failure. The API 1104 [1] tests were done at -5°C . The results from HAZ specimens tested at -5°C , indicates most behave in ductile (upper shelf) δ_m type. Two of the results, 12-H1 and 6-H2 are δ_u type and have low CTOD, 0.113 and 0.173 mm, respectively. The events corresponding to δ_u categorization are a result of a minor load drop (see Figure 6.104). Figure 6.104 displays the typical fracture face. The post test metallography performed indicated the fatigue crack is located in the fusion line of the hybrid weld (see Figure 6.105).

In the weld metal tests one of the brittle extensions may be linked to a flaw that can be viewed on the fracture face and this likely resulted in the pop in. Figure 6.106 shows the fracture and the load CMOD plot.

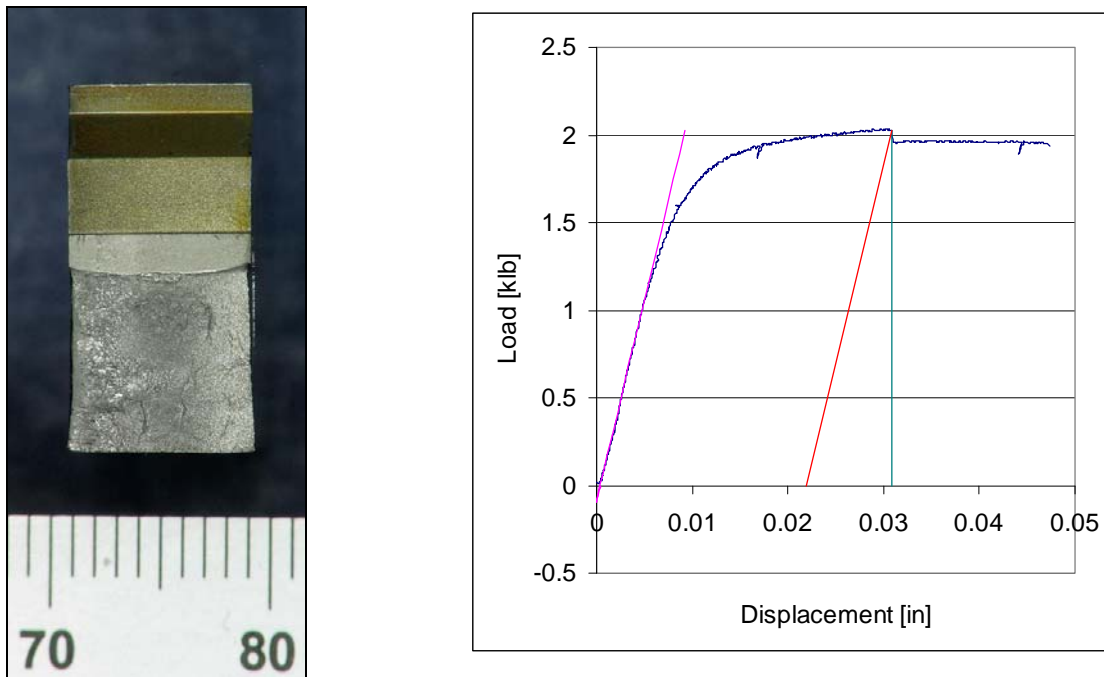


Figure 6.104: Fracture (Left) and Load-CMOD Plot (Right) of Specimen 6-H2

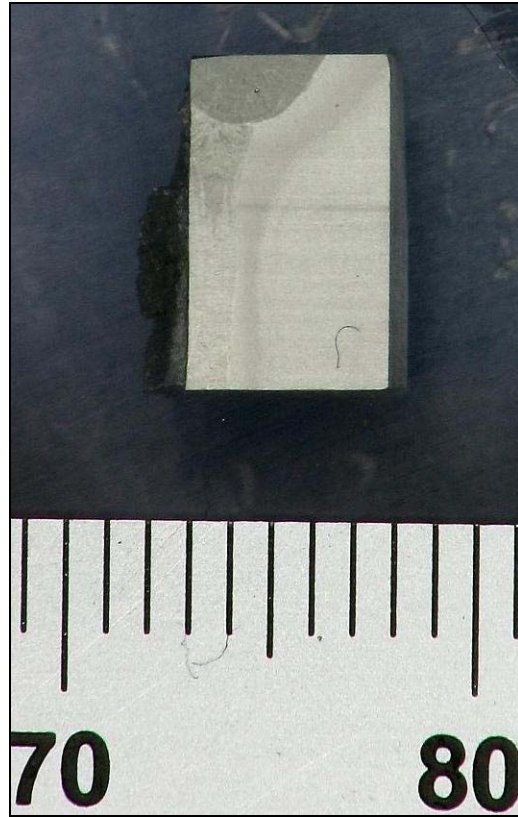


Figure 6.105: Macrographs of Specimen 6-H2

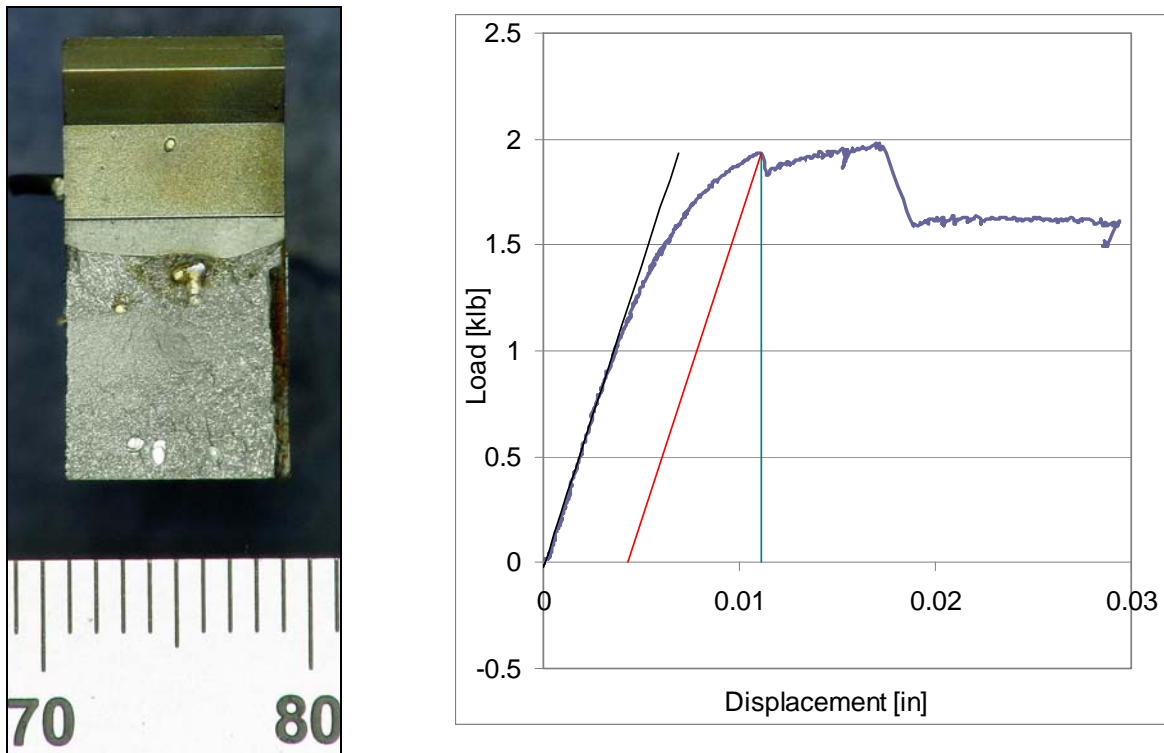


Figure 6.106: Fracture (Left) and Load-CMOD Plot (Right) of Specimen 3-W3

In tests performed at -40°C , all results indicate brittle events for both weld metal and HAZ tests. Except for three results from the HAZ, 12H-5, 6H-4 and 6H-6, all other test results were from critical CTOD categorized as δ_c or type δ_c^* . These CTOD values were less than 0.1 mm (see Annex C, Table C2). Post test metallography done on selected weld metal specimens indicated that the fatigue crack was in the weld and fracture initiation region is in the hybrid weld (see Annex C, Table C2). The low critical CTOD values obtained for the HAZ test may be associated with fracture initiation also in the hybrid weld. This inference is made from selected post test metallography done on HAZ test specimens, an example is presented in the following illustrations (Figure 6.107 through Figure 6.109) for specimen 3-H5 that is categorized as δ_c type with a CTOD of 0.078 mm. Figure 6.109 shows that the fracture is in the hybrid weld.

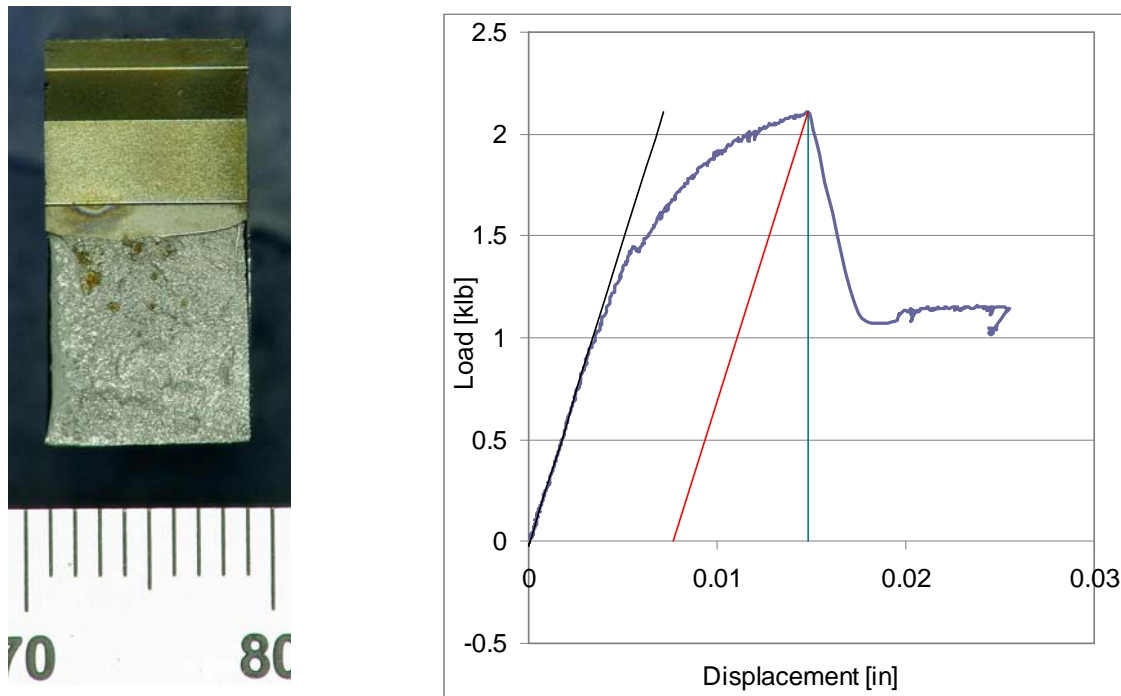


Figure 6.107: Fracture (Left) and Load-CMOD Plot (Right) of Specimen 3-H5

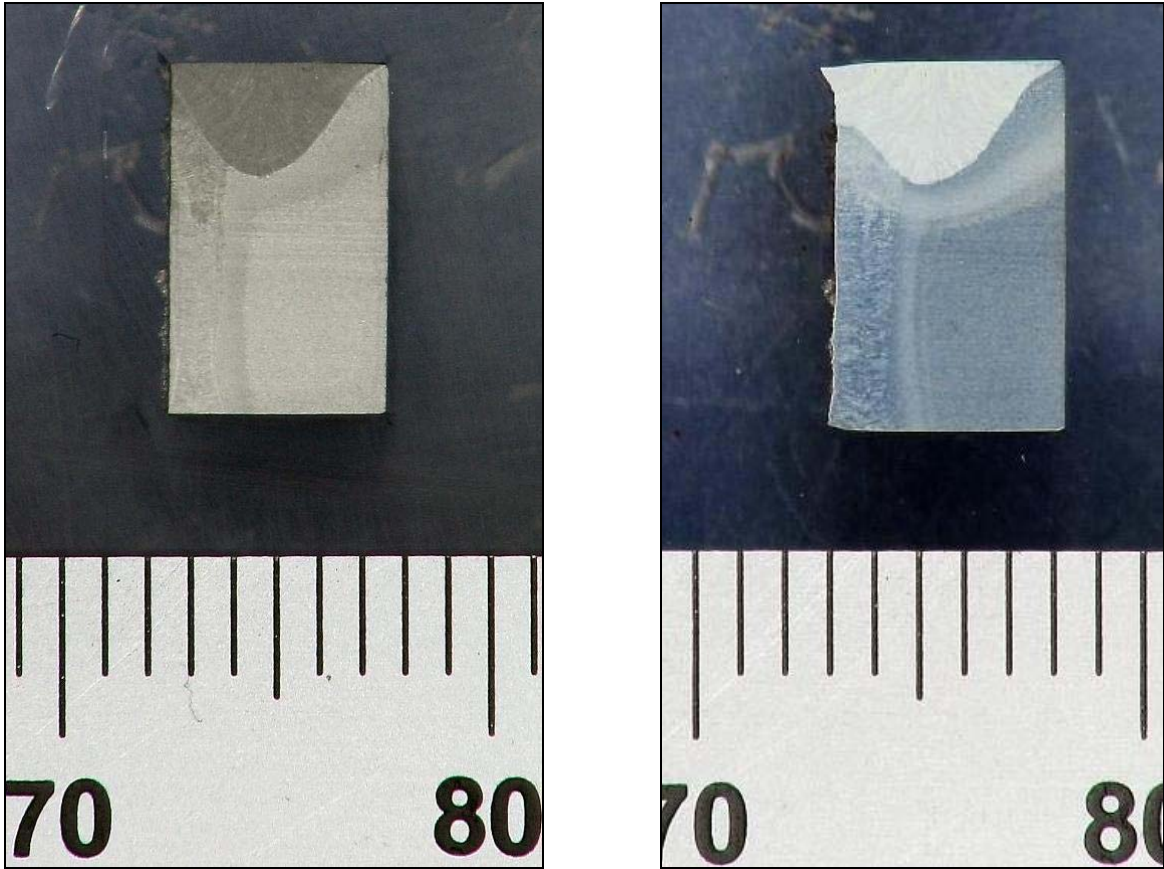


Figure 6.108: Macrographs at Fatigue Crack (Left) and Fracture Initiation (Right) Planes of Specimen 3-H5

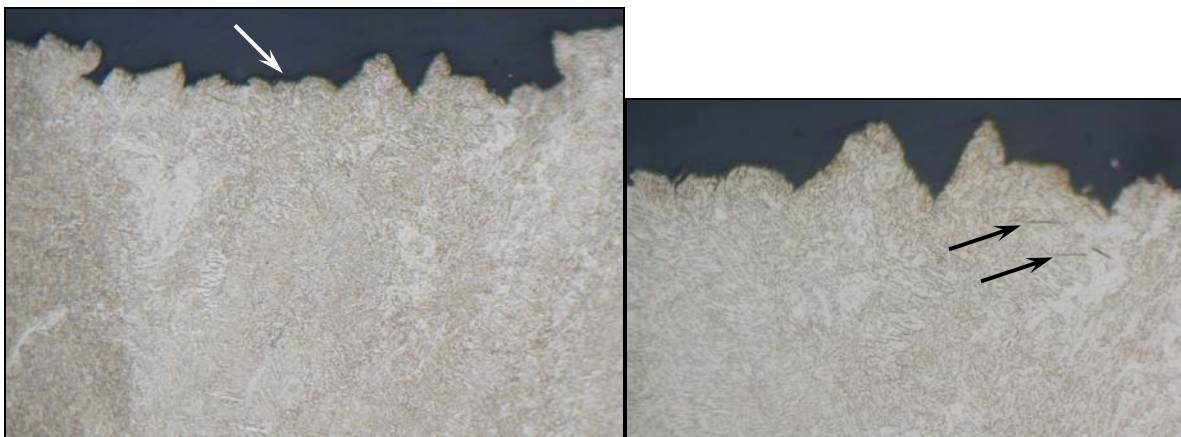


Figure 6.109: Micrographs of Fracture Initiation Location in Specimen 3-H5 at Two Magnifications

Note to Figure 6.109: The black arrow points to micro-cracks and the white arrow points to the fracture plane.

CTOD Estimation Procedures

BS7448, Part 2, Clause 12.3 [15] requires that for weld metal CTOD estimation procedures the following conditions be met:

- (1) The degree of under-match versus over-match based on the yield strength ratio of the weld metal to base metal must be in the range 0.5 to 1.5. *This criterion was met considering the weld metal yield strength of 849 MPa (from AWM strip tensile results) and pipe longitudinal yield strength of 711 MPa (from the material test report NSC). The ratio was ~1.19 for the X100 weld. It was also met for the X80 weld considering the weld metal yield strength of 831 MPa (from AWM strip tensile results) and pipe longitudinal yield strength of 612 MPa (from the material test done at BMT). The ratio was ~1.36.*
- (2) For the weld centreline (W) tests, the ratio of the weld width ($2h$) in the central 75 percent of the thickness of the specimen (see Figure 6.110), to the ligament length of the fatigue cracked specimen ($W-a_o$) needs to exceed 0.2. *This criterion was not met. The failure results from the narrow hybrid laser weld.*

These requirements are necessary for the CTOD estimate to be within a ± 10 percent error. These requirements are a result of the non-uniform material properties in the weld zone.

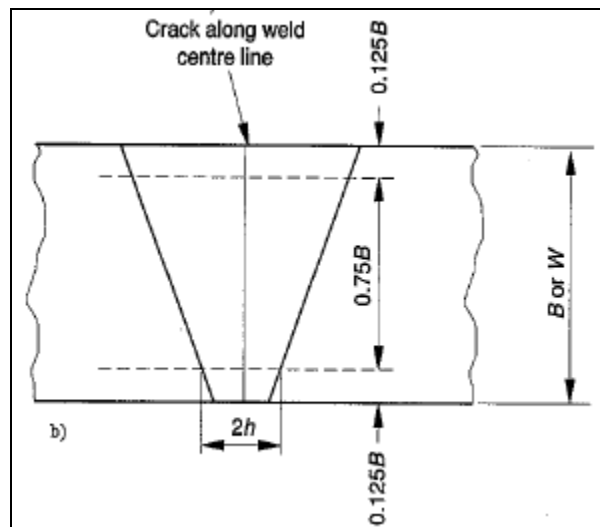


Figure 6.110: Measurement Location for $2h$ in Figure 11 [1]

Concluding Remarks

CTOD done for the non-typical weld profile of the HLAW had two modifications with respect to guidelines in API 1104 [1], Appendix A. These are as follows:

- Notch location for the HAZ test – the location was optimized to sample the HAZ of the hybrid weld portion and, therefore, the notch also sampled the laser assisted GMA weld deposit(s); and
- The minimum fatigue pre-crack depth, 1.3 mm required in BS 7448, Part 1 [18], to 0.6 mm to reduce the likelihood that the tip of the fatigue crack was not in the intended region due to deviation of the fatigue.

The observations made, considering the non-typical weld profile, indicated that the process adopted has been successful in detecting low toughness regions in the weld zone. The X100 weld zone displayed good CTOD toughness down to -40°C . The X80 weld displayed poor toughness even at -5°C . This is likely a result of the poor toughness in the weld metal.

6.2.2.8 Frontic Testing

Procedure from Joshua (ExonMobil) to be inserted here

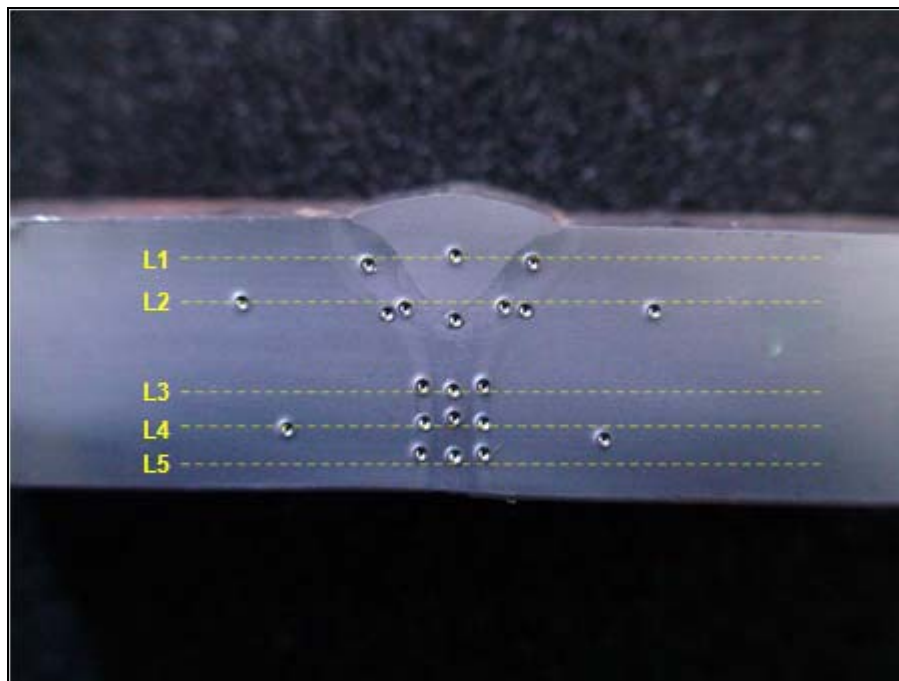


Figure 6.111: X80, 1:30 Location Macro

Table 6.24: Results for X80, 1:30 Location

Unit: MPa

		BM	GRHAZ	GCHAZ	FL	WM	FL	GCHAZ	GRHAZ	BM
L1	YS			689.2		790.5		747.2		
	UTS			788.0		937.4		859.6		
L2	YS	593.8	615.8	672.4	847.9	811.6	819.8	681.2	681.2	676.9
	UTS	737.8	813.9	788.3	918.0	917.6	902.2	785.9	780.0	734.9
L3	YS		709.6			817.5			732.2	
	UTS		803.2			934.4			798.8	
L4	YS	641.3	682.4		823.6	883.7	770.6		652.7	662.1
	UTS	748.2	788.5		875.8	969.7	855.5		798.4	739.8
L5	YS		664.8			896.7			620.2	
	UTS		790.8			981.1			777.9	

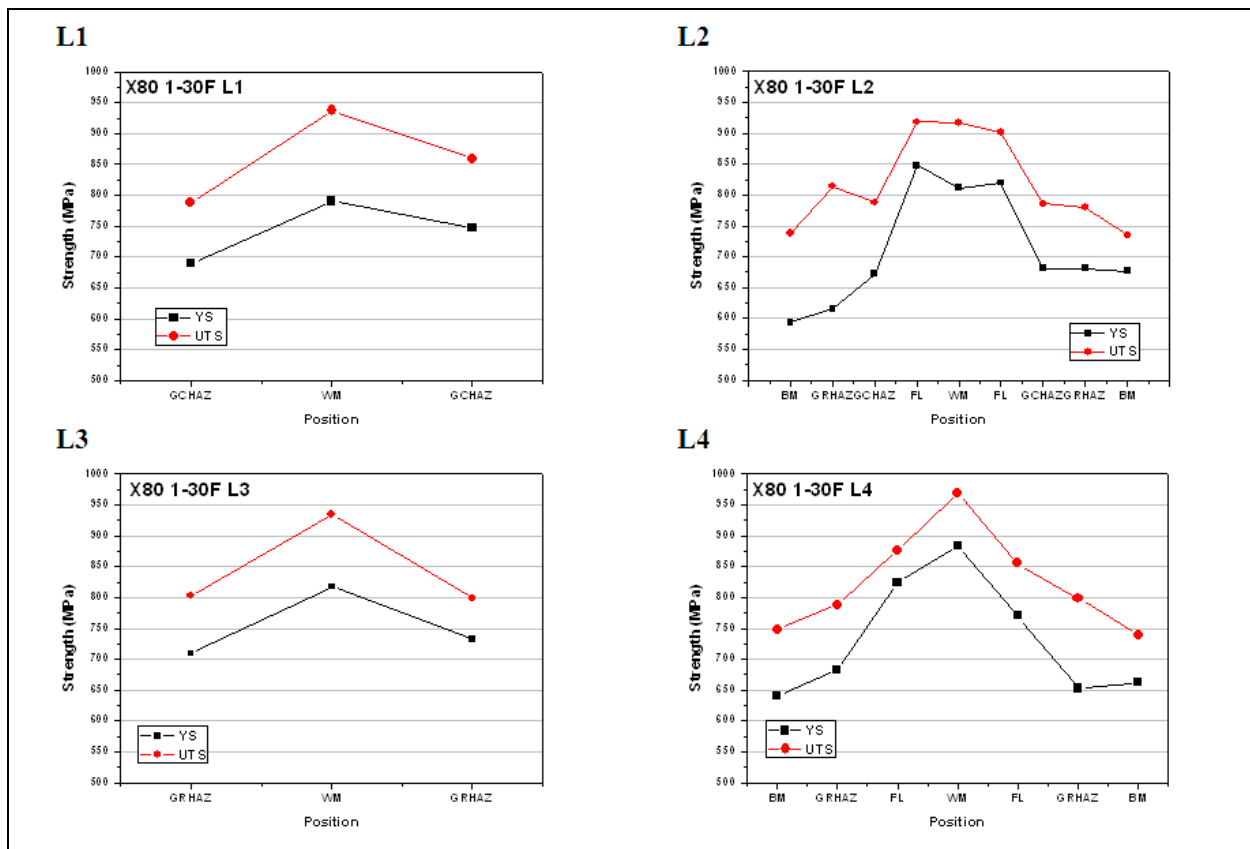


Figure 6.112: Plot for Layer 1-4, X80, 1:30 Location

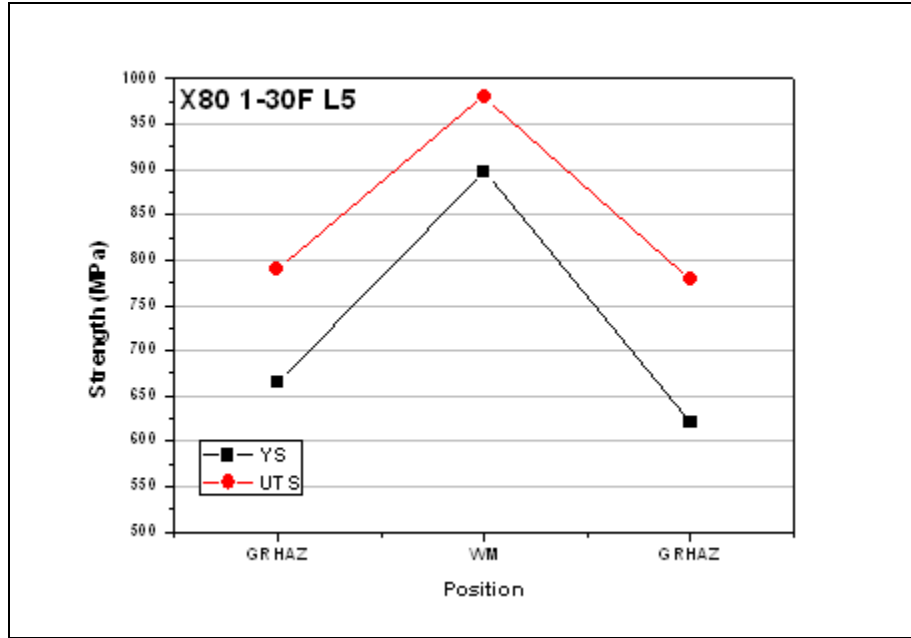


Figure 6.113: Plot for Layer 5, X80, 1:30 Location

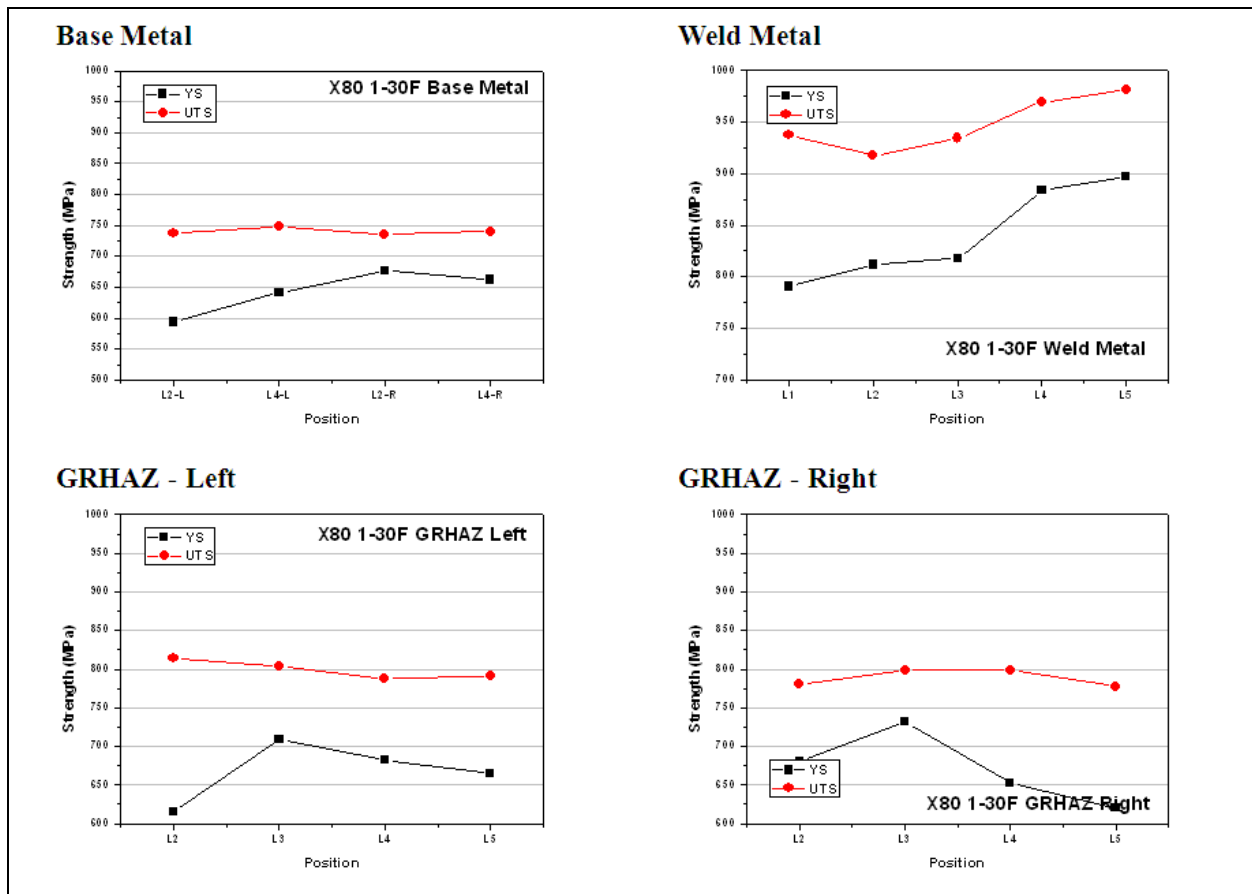


Figure 6.114: Plot for X80 BM, WM, GRHAZ, 1:30 Location

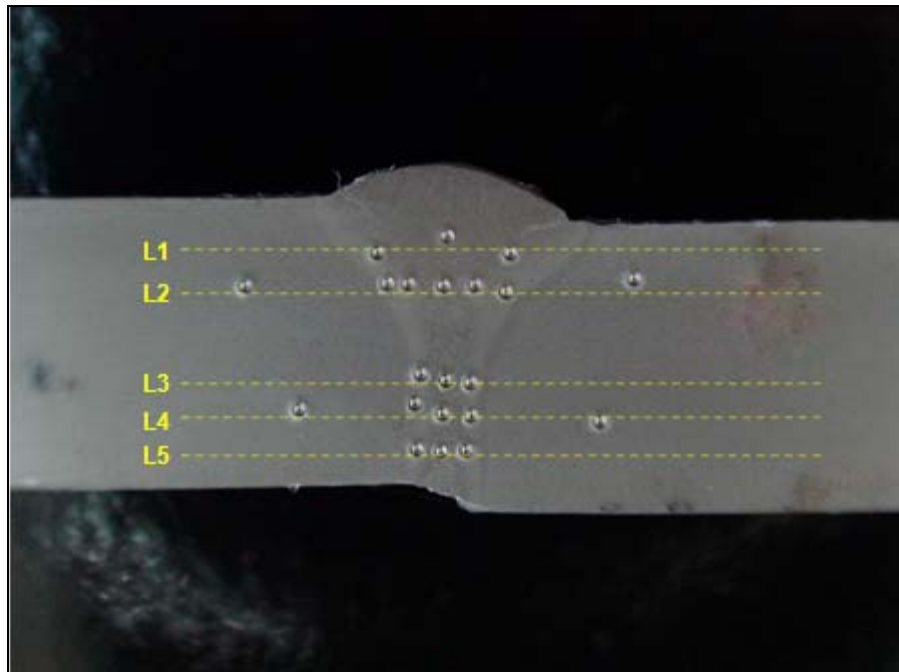


Figure 6.115: X80, 4:30 Location Macro

Table 6.25: Results of X80, 4:30 Location

Unit: MPa

		BM	GRHAZ	GCHAZ	FL	WM	FL	GCHAZ	GRHAZ	BM
L1	YS			717.0		775.2		785.3		
	UTS			805.8		896.8		863.5		
L2	YS	670.2	659.0	682.3	740.1	787.5	815.7	728.4	742.5	649.3
	UTS	736.1	777.4	772.1	829.7	894.9	888.2	845.2	800.4	724.3
L3	YS		713.9			779.7			726.3	
	UTS		780.5			872.0			806.0	
L4	YS	674.1	672.9		875.0	775.9	749.9		753.5	581.7
	UTS	735.0	779.2		908.8	904.7	797.8		821.6	702.2
L5	YS		655.6			757.3			759.9	
	UTS		769.9			879.0			814.8	

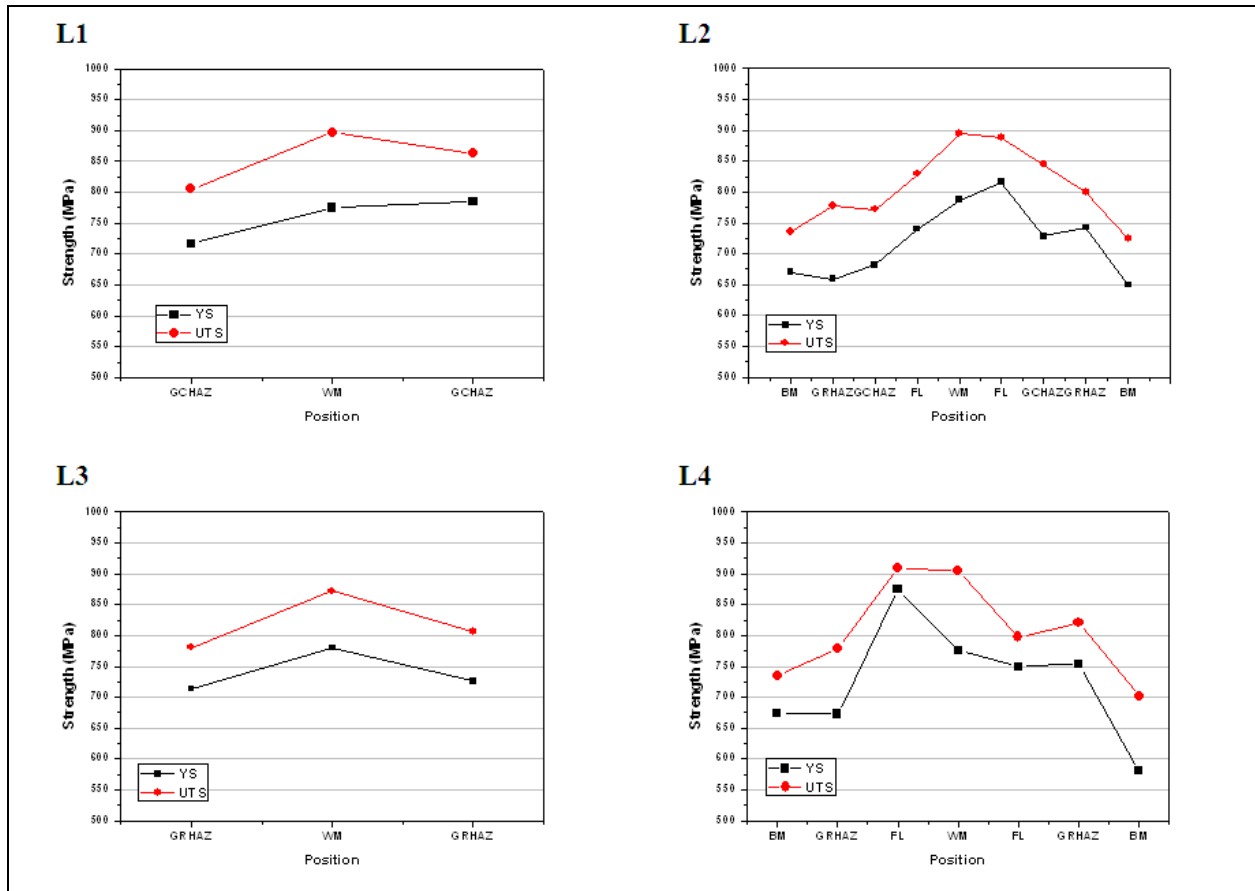


Figure 6.116: Plots of Layers 1-4, X80, 4:30 Location

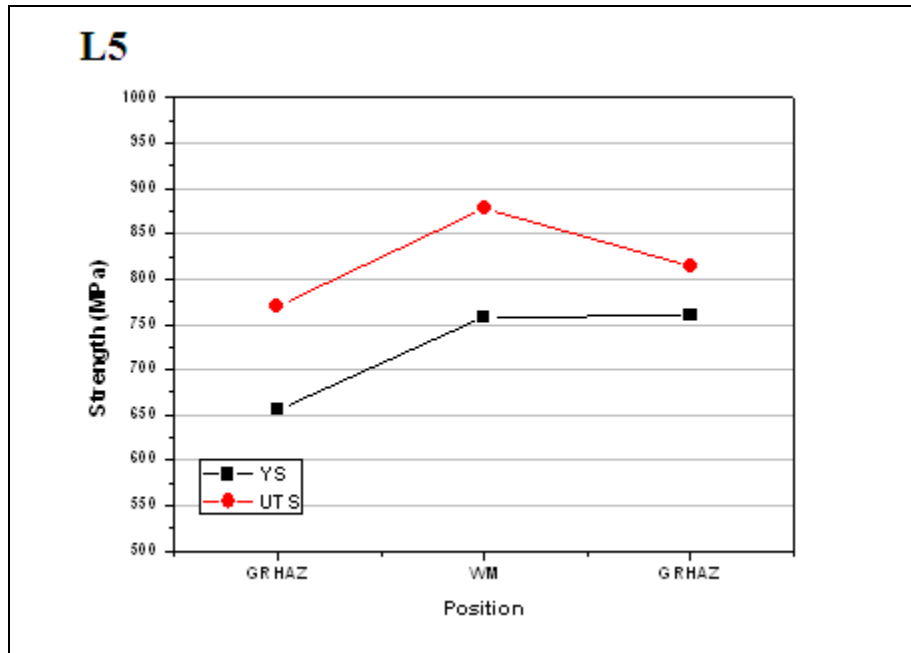


Figure 6.117: Plot for Layer 5, X80, 4:30 Location

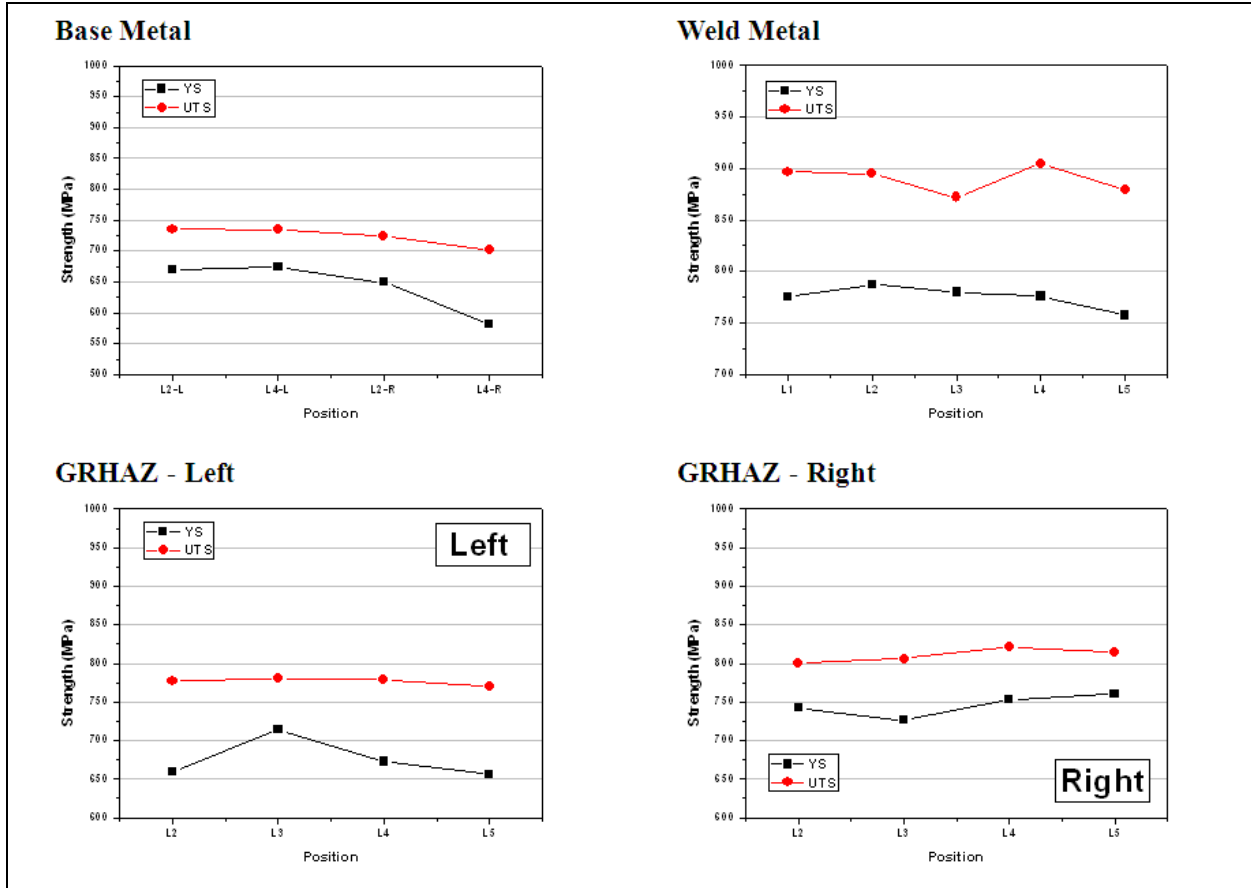


Figure 6.118: Plot for X80 BM, WM, GRHAZ, 4:30 Location

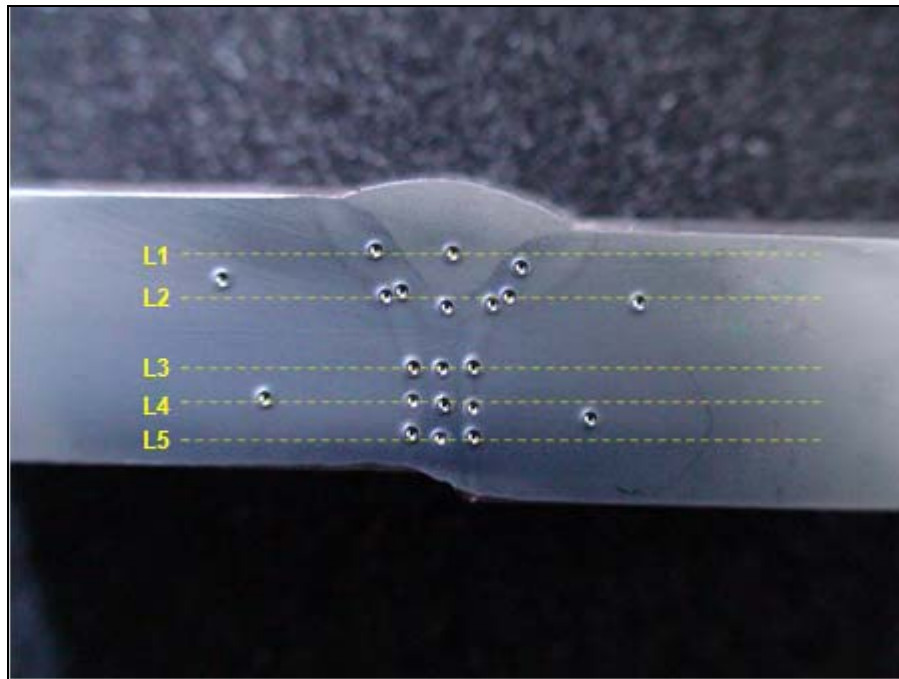


Figure 6.119: X80, 7:30 Location Macro

Table 6.26: Results of X80, 7:30 Location

Unit: MPa

		BM	GRHAZ	GCHAZ	FL	WM	FL	GCHAZ	GRHAZ	BM
L1	YS			676.5		734.0		766.4		
	UTS			793.3		886.5		859.1		
L2	YS	674.2	629.1	644.6	796.5	803.4	821.9	663.4	689.7	665.8
	UTS	738.6	767.2	779.4	877.3	879.1	873.7	772.7	768.0	744.9
L3	YS		733.3			793.4			733.2	
	UTS		805.4			897.1			794.7	
L4	YS	664.9	598.0		854.6	887.1	785.7		656.2	671.3
	UTS	745.5	774.1		876.9	951.8	829.5		771.9	738.3
L5	YS		730.6			810.4			718.6	
	UTS		808.1			940.4			791.7	

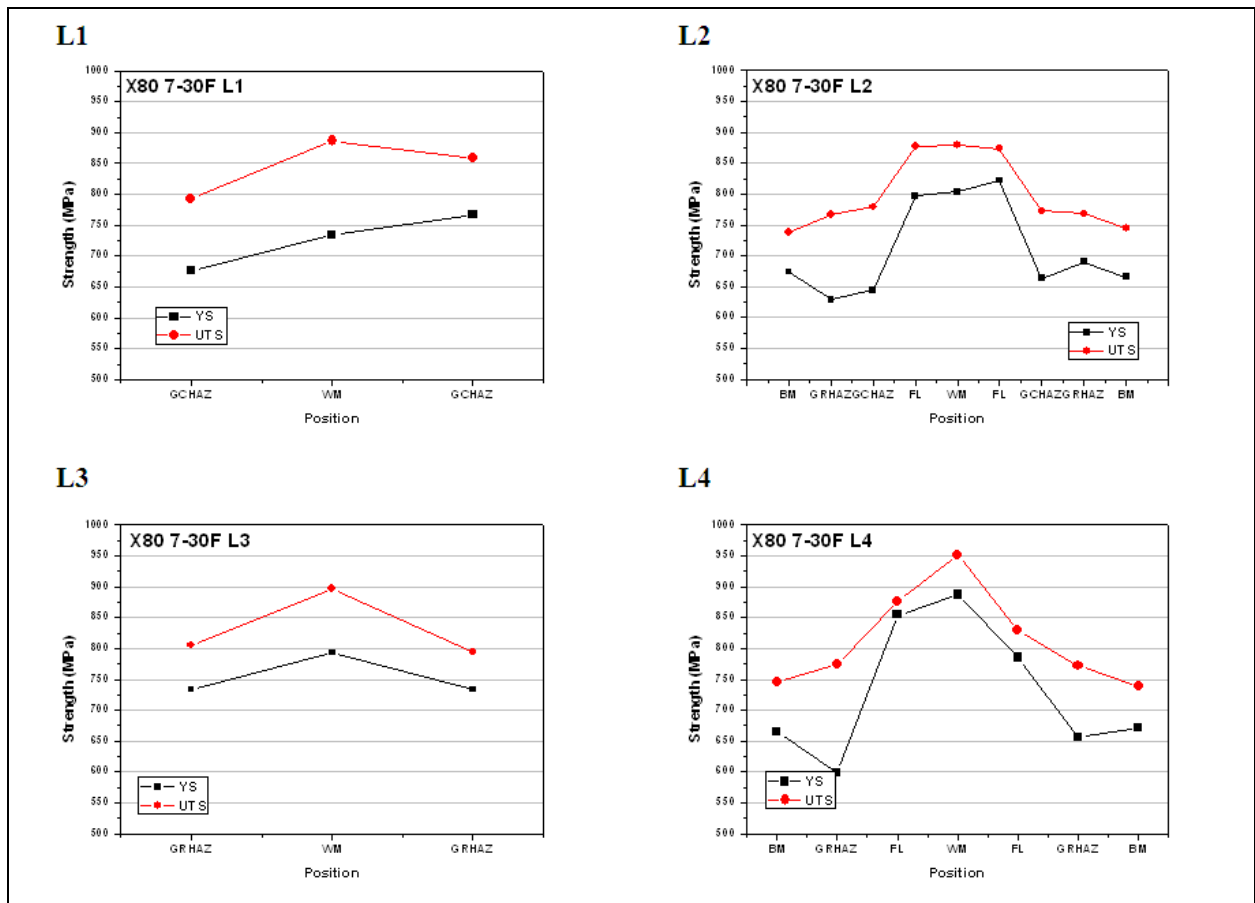


Figure 6.120: Plots for Layers 1-4, X80, 7:30 Location

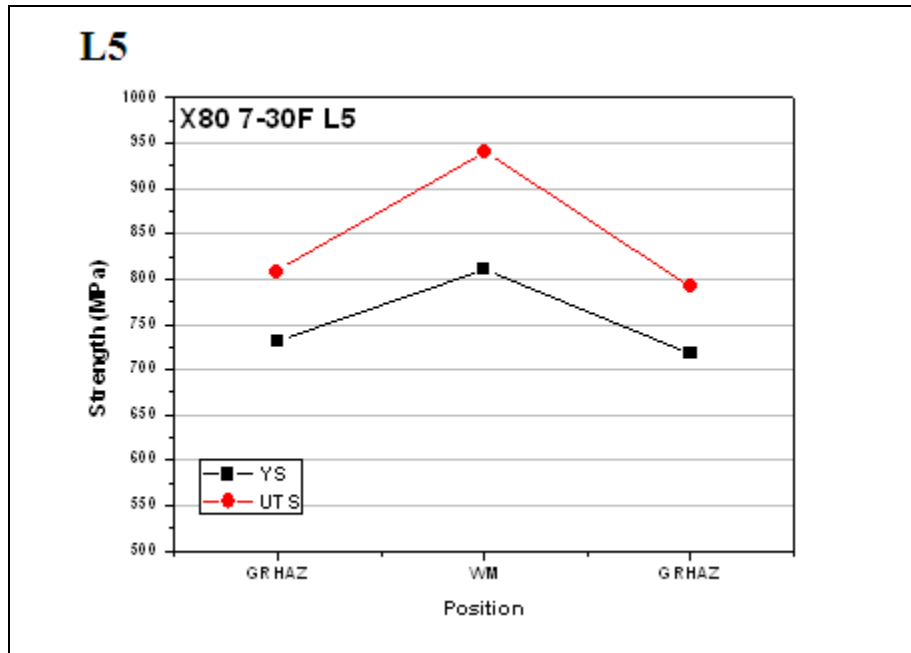


Figure 6.121: Plot for Layer 5, X80, 7:30 Location

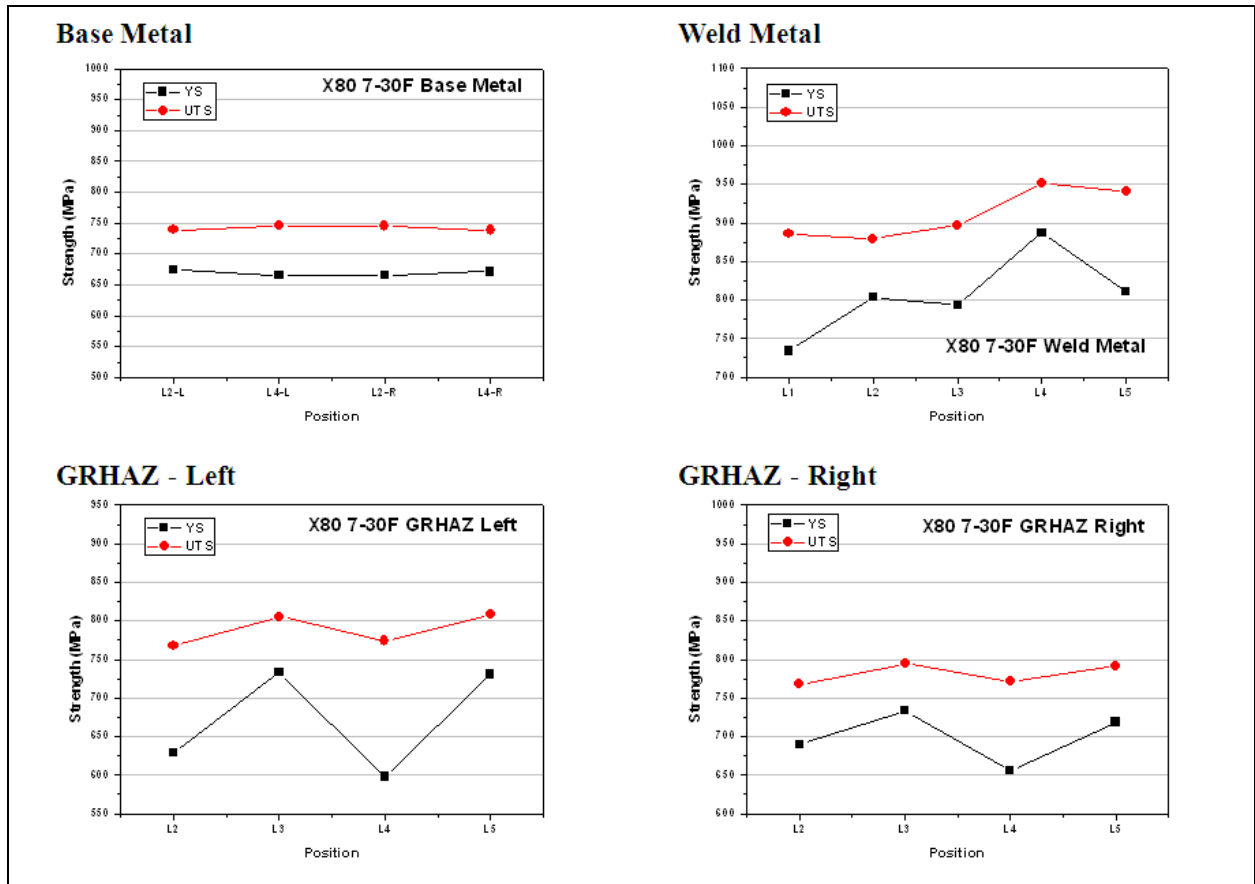


Figure 6.122: Plot for X80 BM, WM, GRHAZ, 7:30 Location

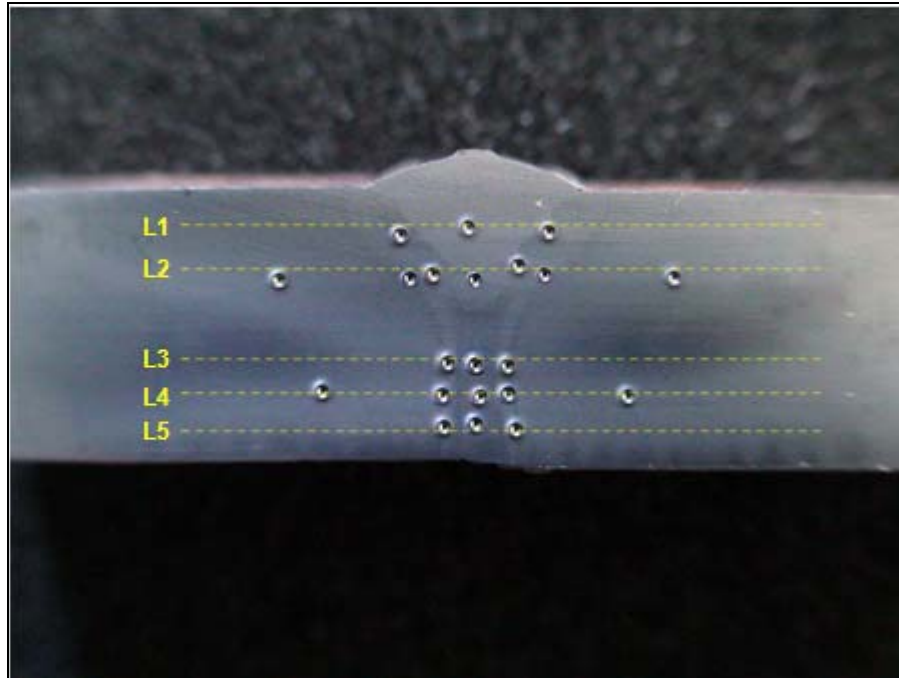


Figure 6.123: X80, 10:30 Macro

Table 6.27: Results, X80, 10:30 Location

Unit: MPa

		BM	GRHAZ	GCHAZ	FL	WM	FL	GCHAZ	GRHAZ	BM
L1	YS			714.7		766.0		733.4		
	UTS			836.8		869.7		840.1		
L2	YS	657.5	690.5	649.7	808.5	806.7	755.5	738.5	699.4	623.1
	UTS	731.5	777.7	779.8	877.6	896.0	864.1	840.1	775.4	734.7
L3	YS		746.6			937.5			665.7	
	UTS		809.5			971.1			790.2	
L4	YS	672.2	675.6		809.9	894.9	771.5		765.5	613.4
	UTS	746.5	778.7		866.6	916.5	826.2		804.1	732.1
L5	YS		715.5			917.6			700.1	
	UTS		803.4			990.5			792.8	

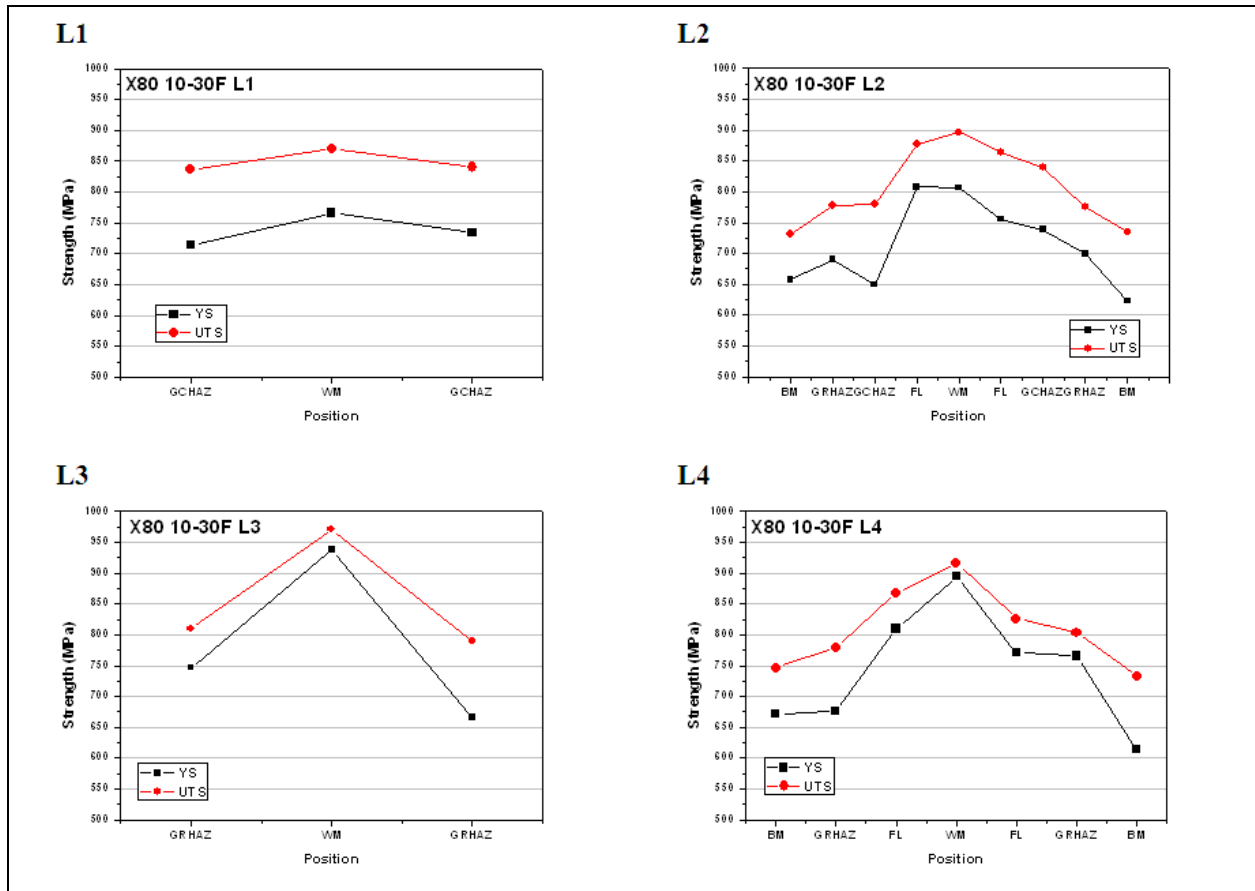


Figure 6.124: Plots for Layers 1-4, X80, 10:30 Location

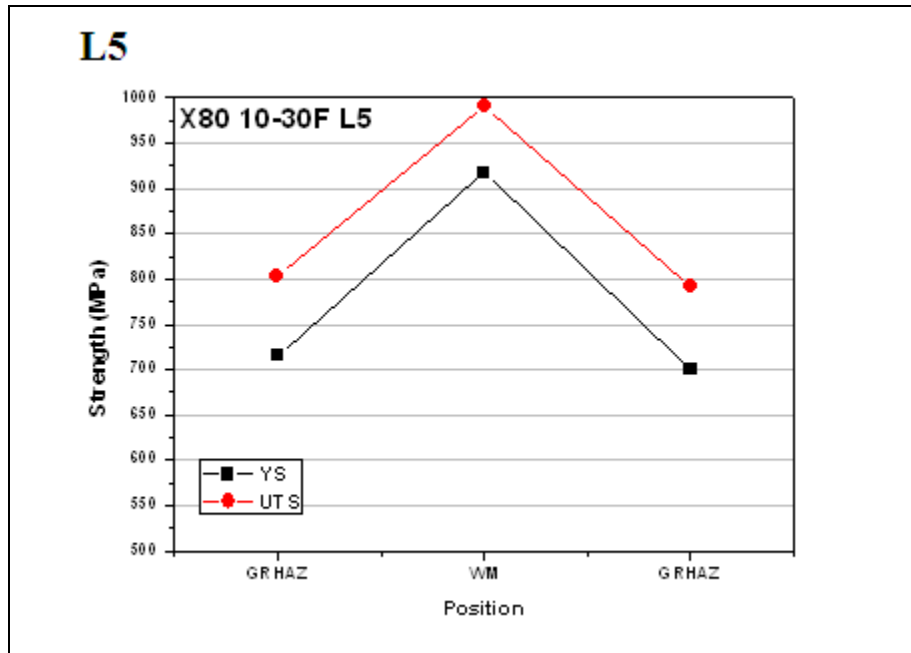


Figure 6.125: Plots for layer 5, X80, 10:30 Location

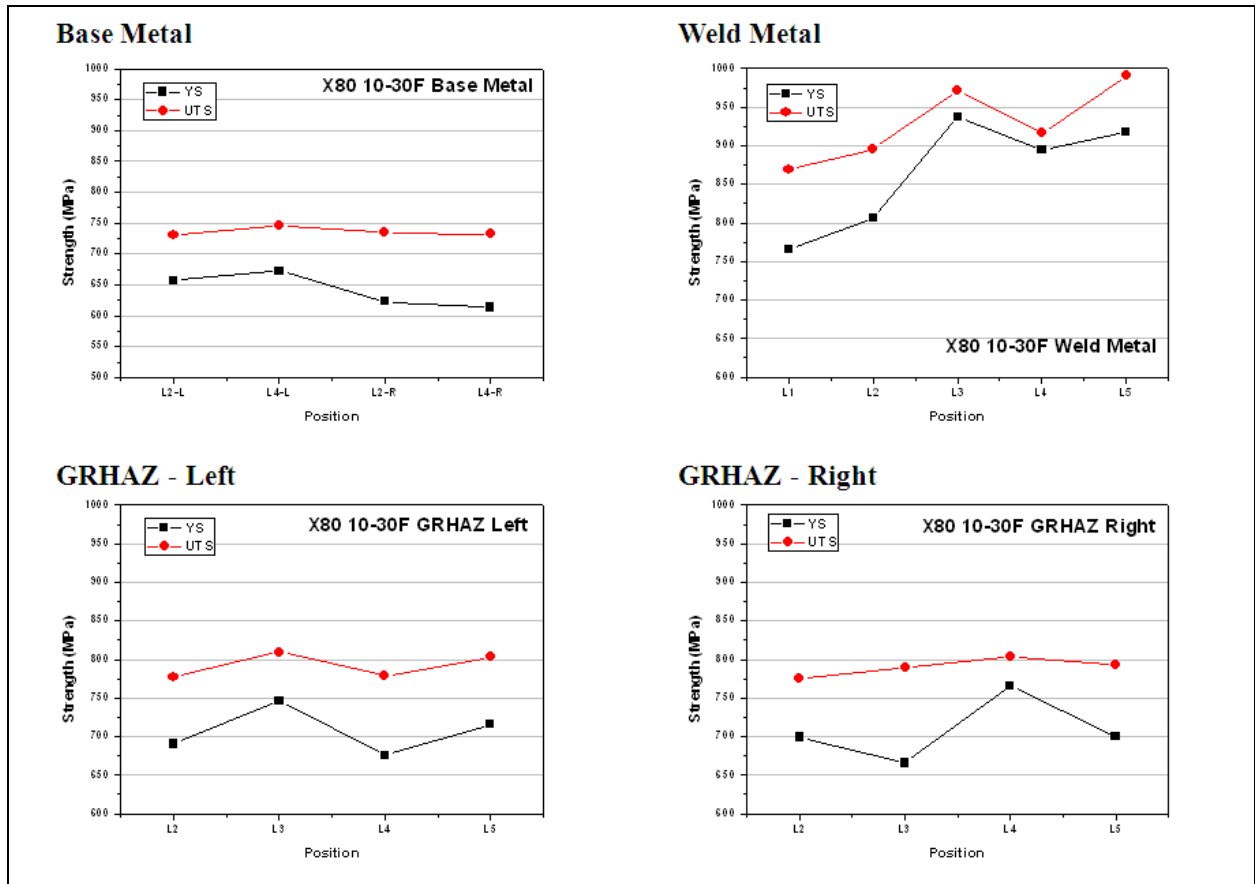


Figure 6.126: Plot for X80 BM, WM, GRHAZ, 10:30 Location

6.2.2.9 Microhardness Testing

Need a copy of the procedure from Joshua (ExonMobil) to be inserted here

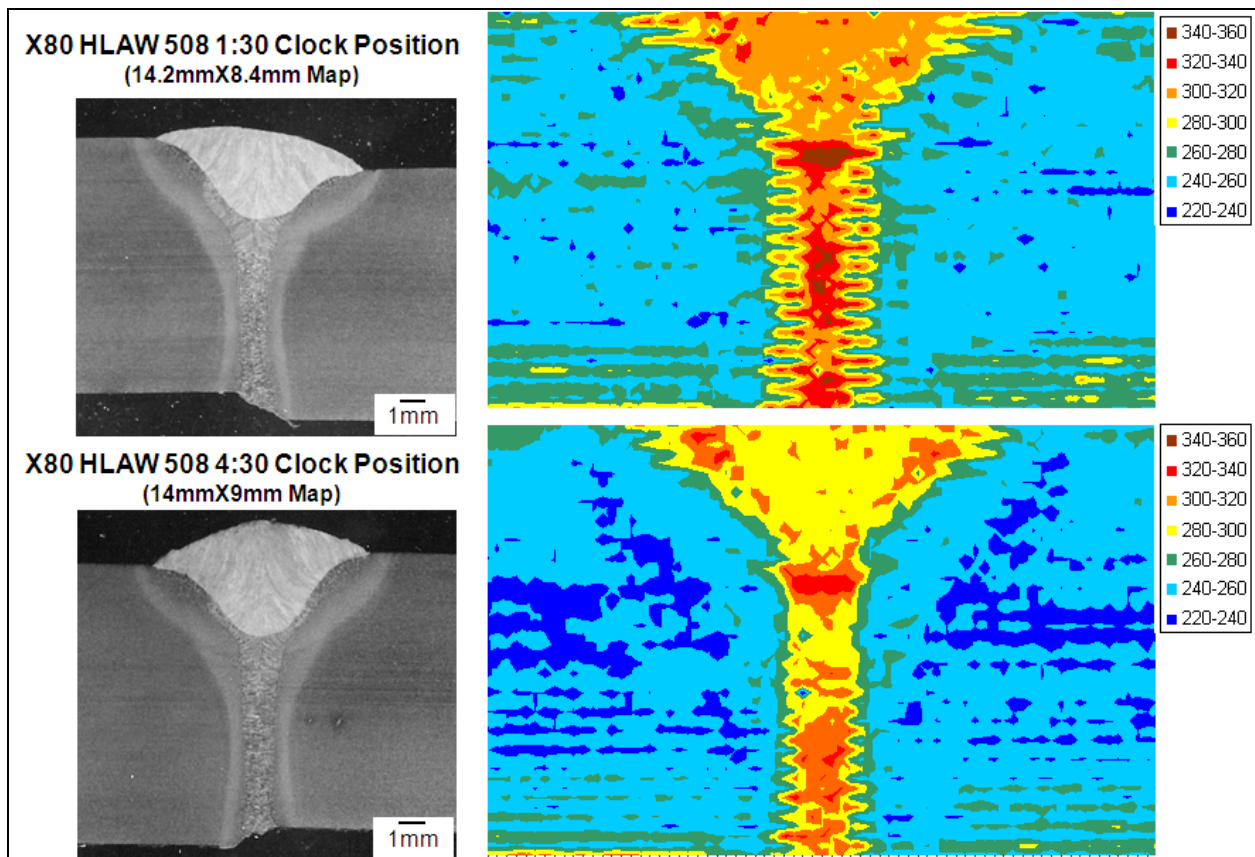


Figure 6.127: Microhardness Mapping, X80, 1:30 and 4:30 Clock Positions

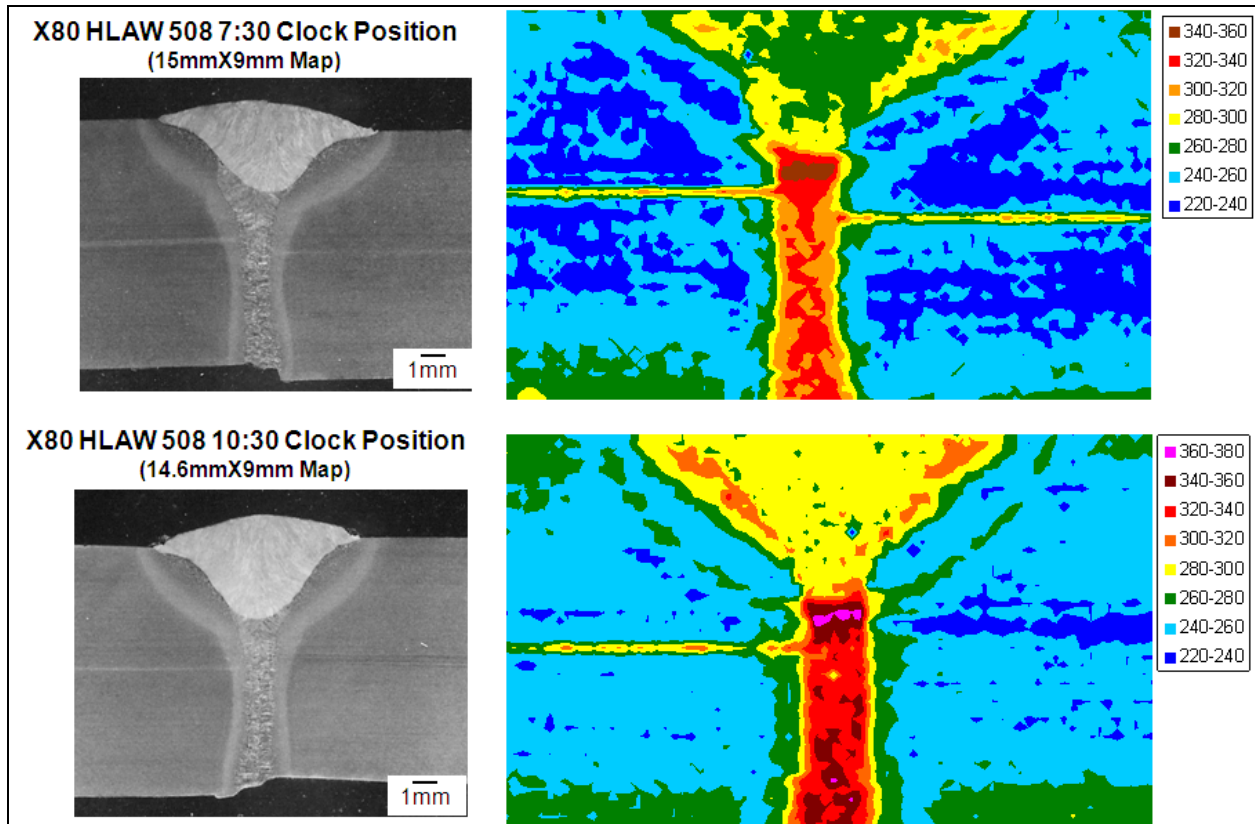


Figure 6.128: Microhardness Mapping, X80, 7:30 and 10:30 Clock Positions

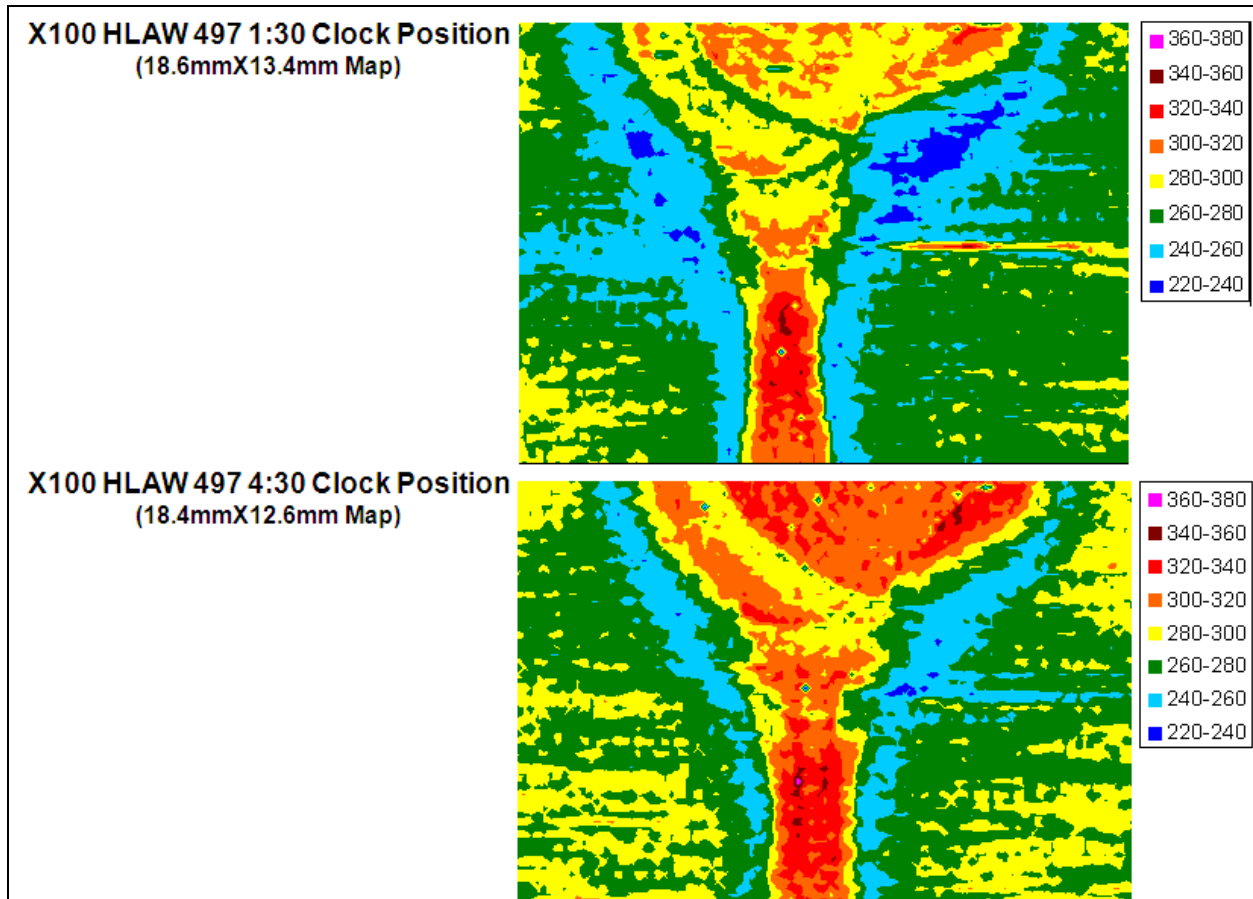


Figure 6.129: Microhardness Mapping, X100, 1:30 and 4:30 Clock Positions

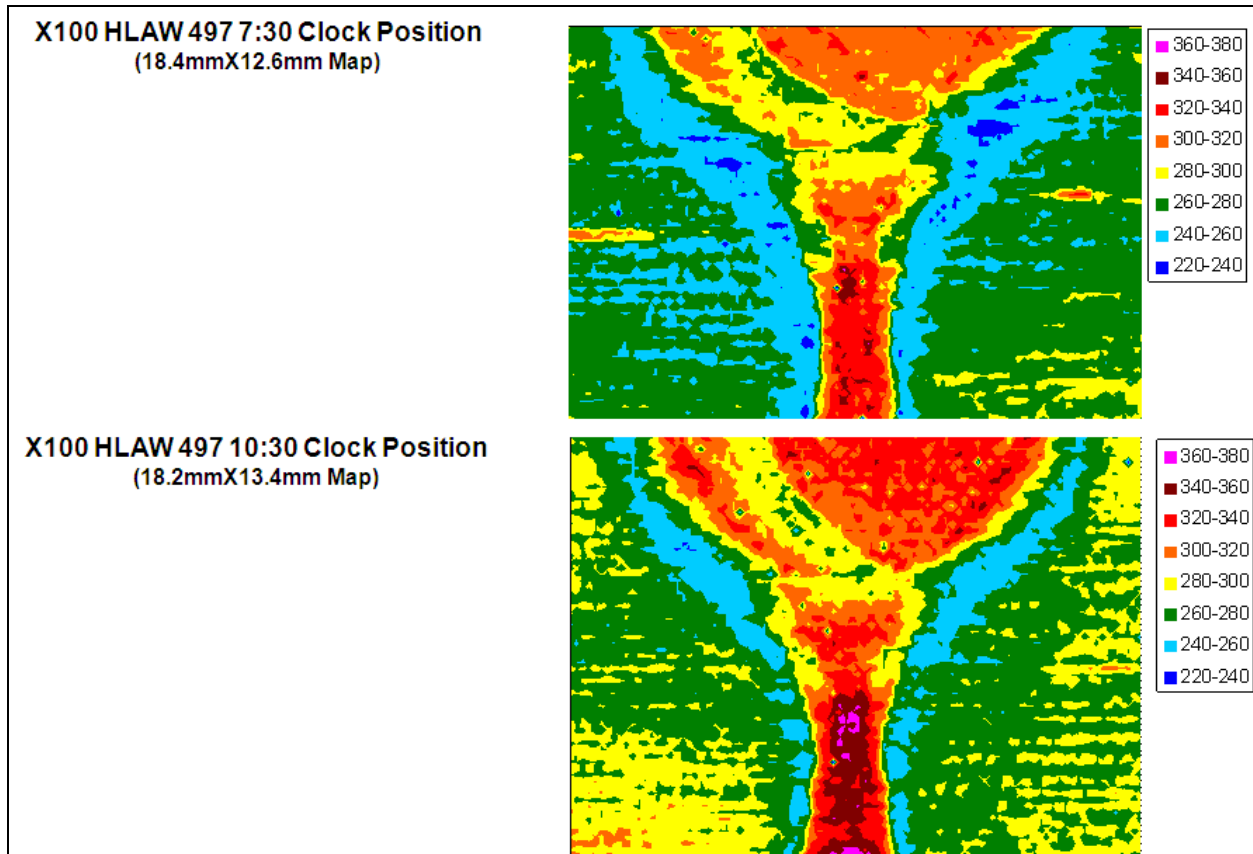


Figure 6.130: Microhardness Mapping, X100, 7:30 and 10:30 Clock Positions

6.2.2.10 Microstructure Assessment

Details to be inserted here (need input from Joshua, ExxonMobil)

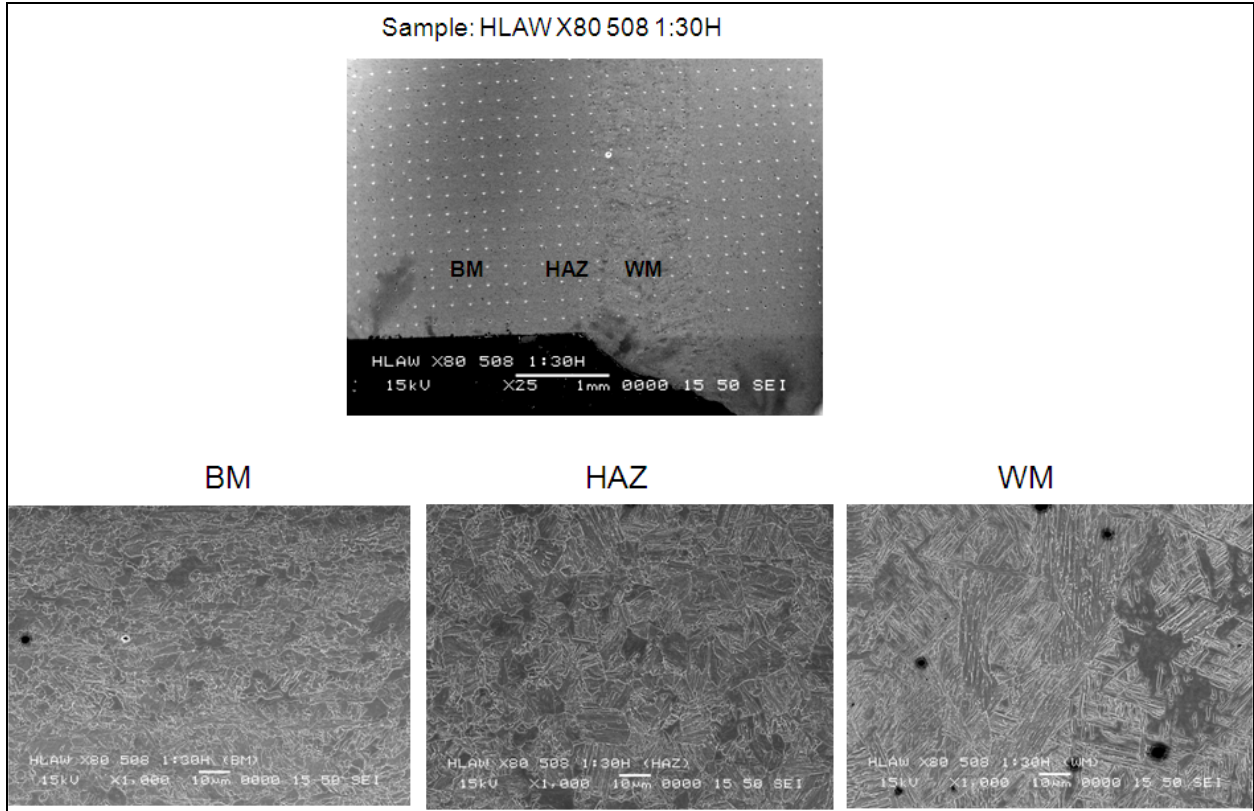


Figure 6.131: Sample X80 1:30 Location

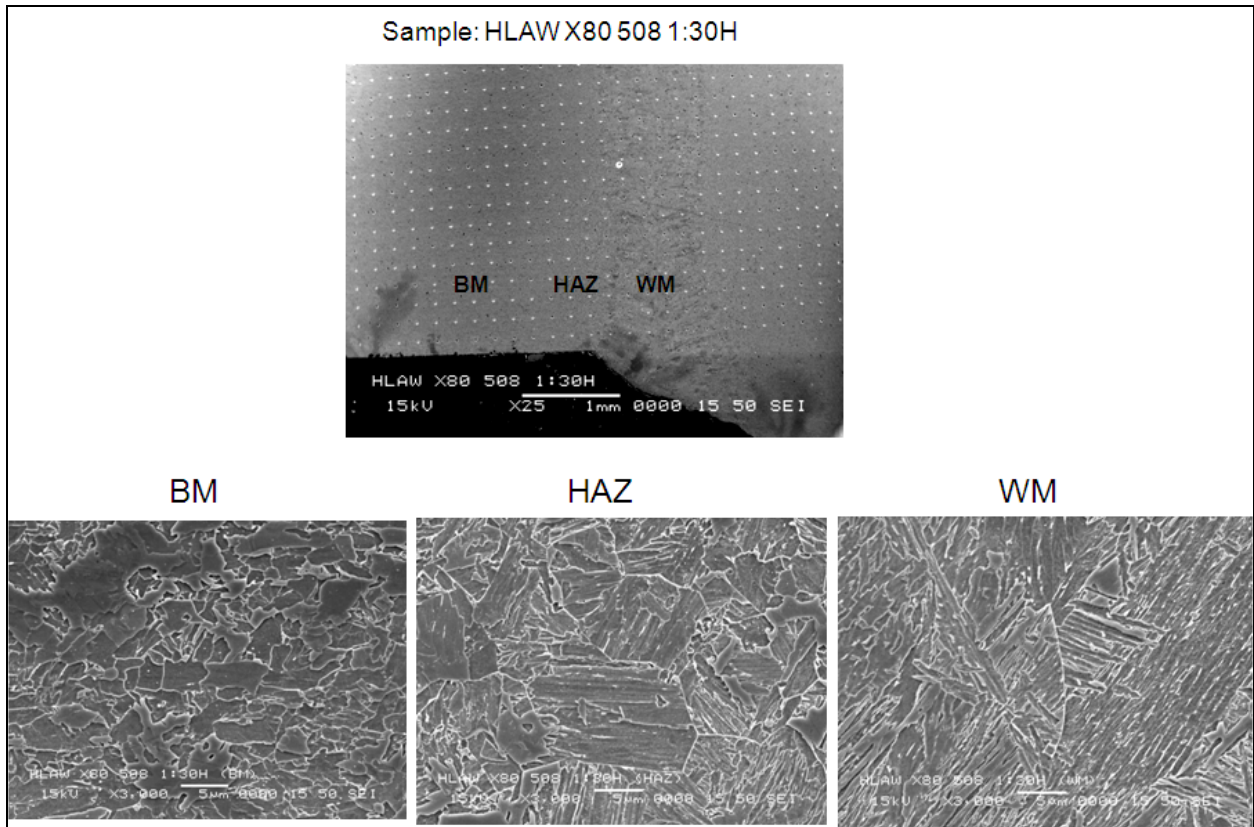


Figure 6.132: Sample X80 1:30 Location

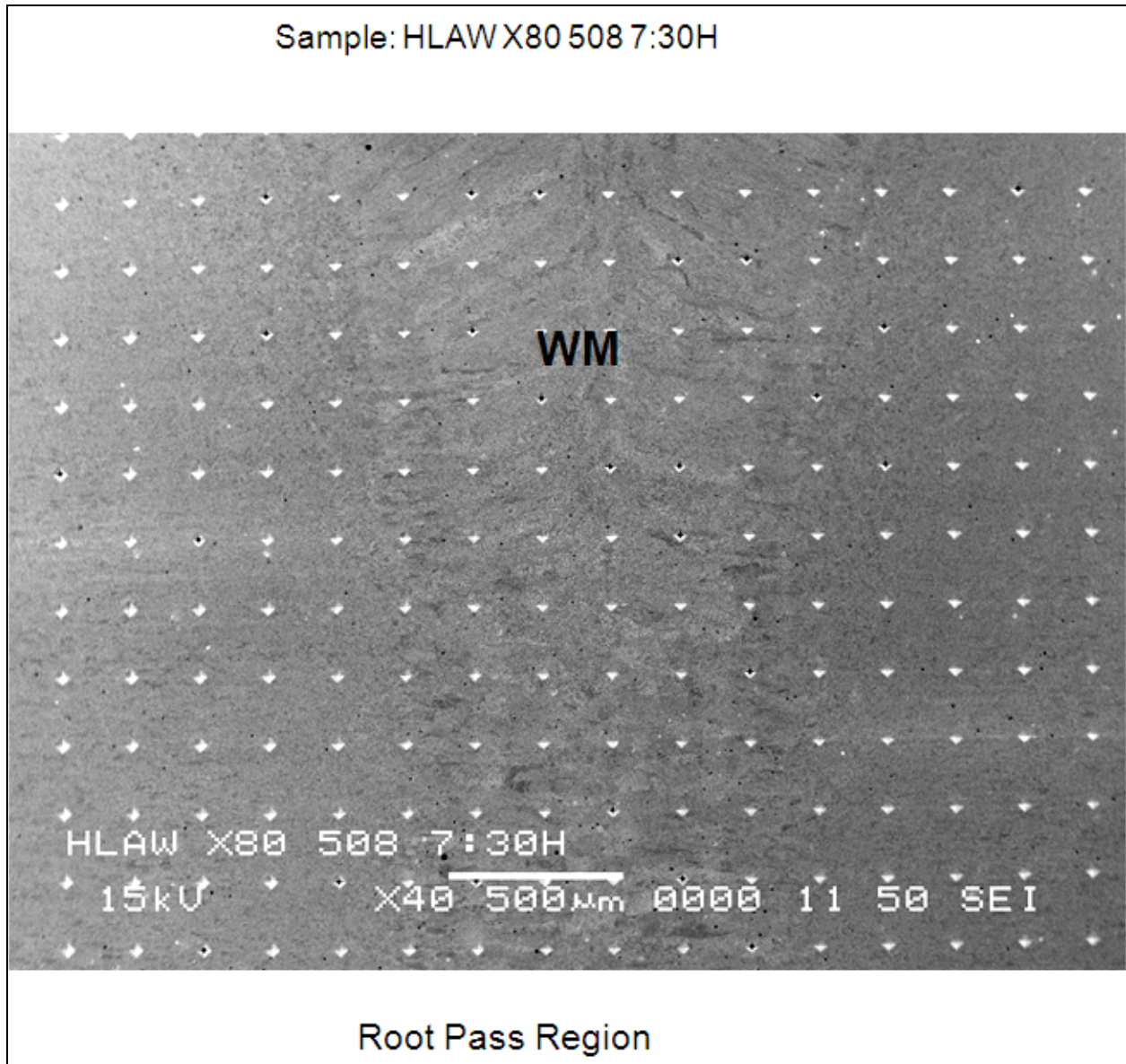


Figure 6.133: Sample X80 7:30 Location

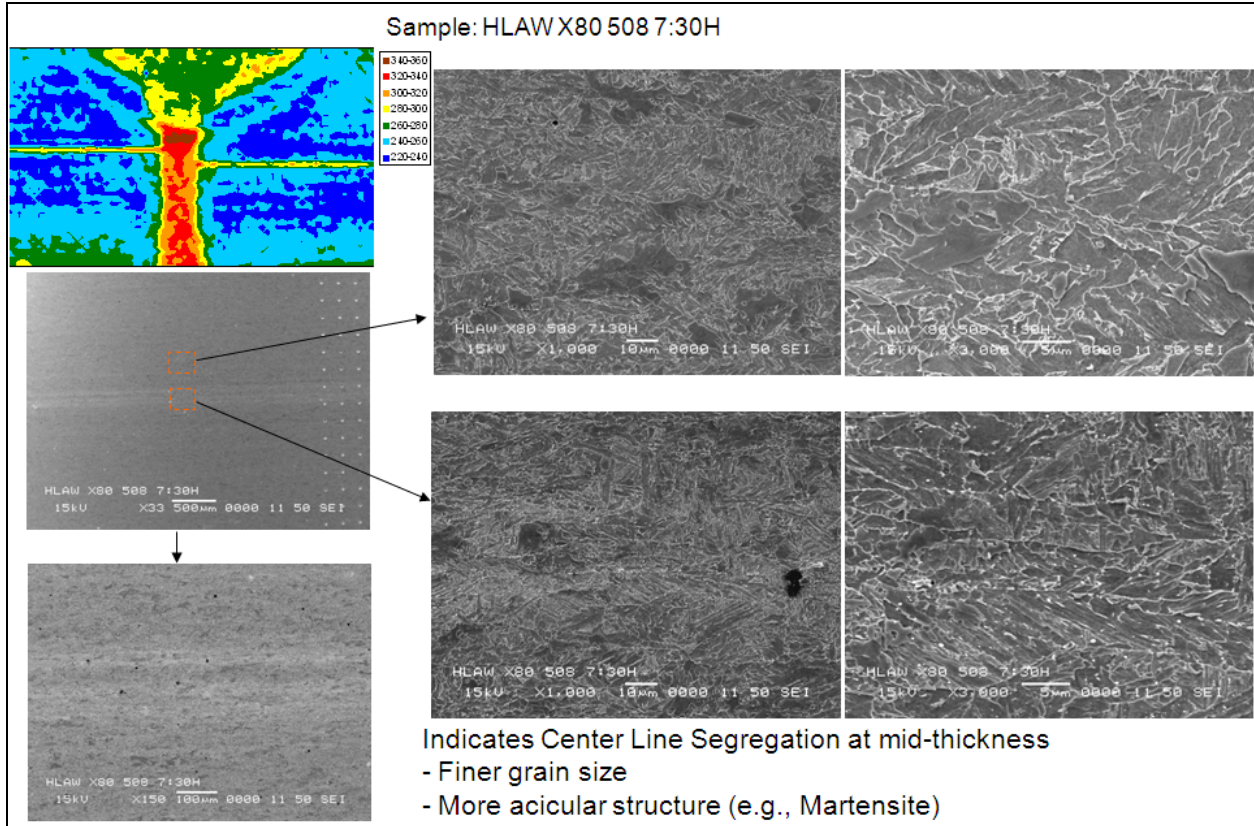


Figure 6.134: Sample X80, 7:30 Location

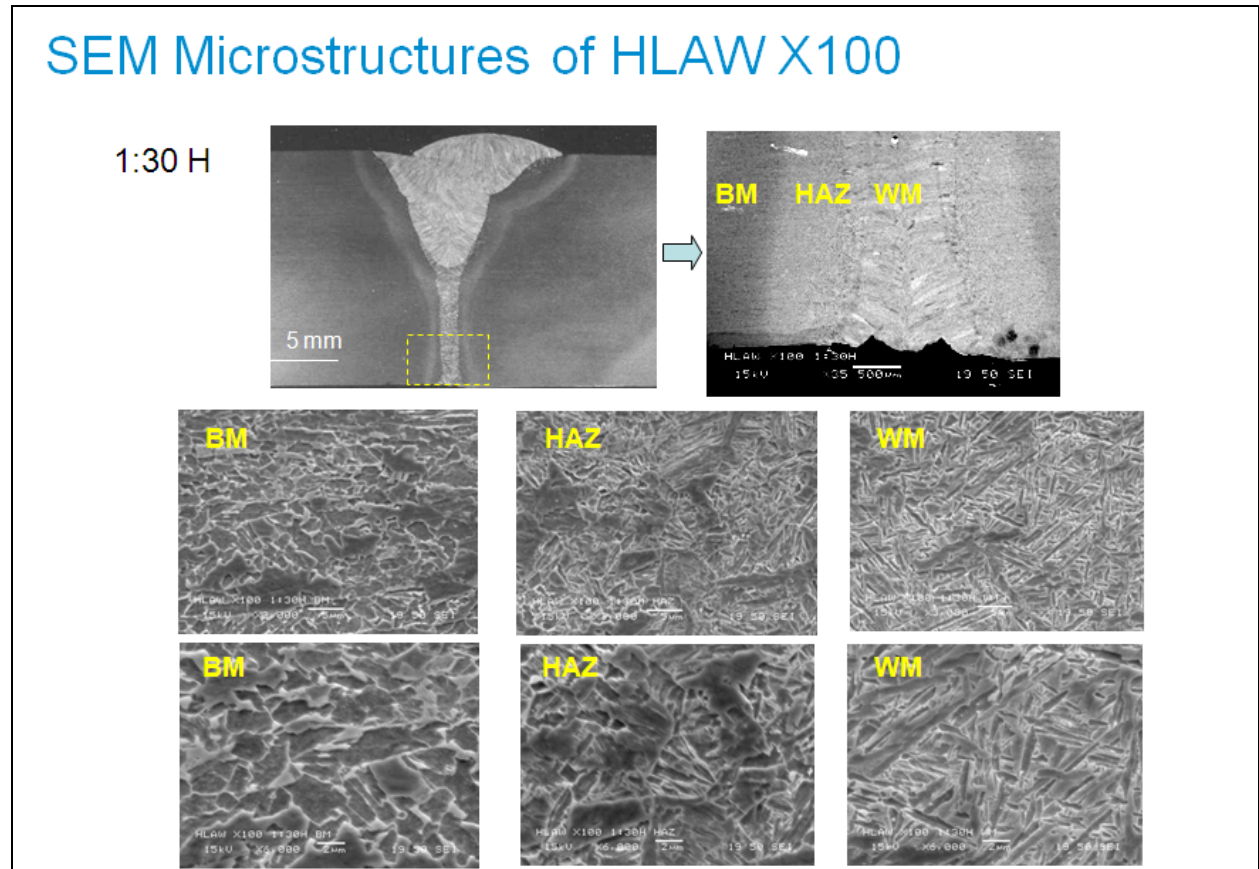


Figure 6.135: Sample X100, 1:30 Location

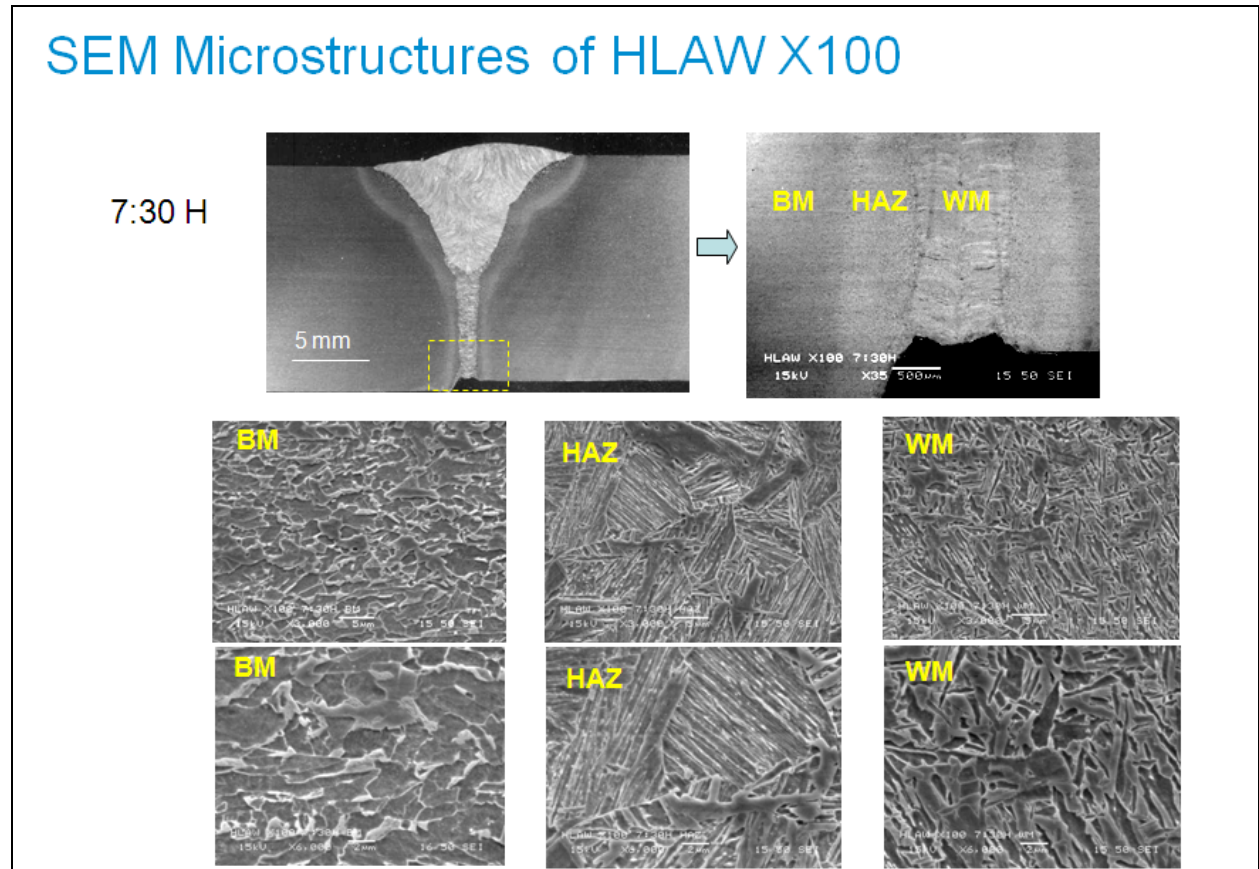


Figure 6.136: Sample X100, 7:30 Location

7 REFERENCES

- [1] API 1104, “Welding of Pipelines and Related Facilities”, American National Standards Institute (ANSI/API STD 1104, 12th edn. American Petroleum Institute, Washington DC, USA, 2005.
- [2] CSA Z662-07, “Oil and gas pipeline systems”, Canadian Standards Association, 2007.
- [3] Gianetto, J.A., Bowker, J.T., Dorling, D.V., Taylor, D., Horsley, D. and Fiore, S.R. 2008 “Overview of tensile and toughness testing protocols for assessment of X100 pipeline girth welds,” 7th International Pipeline Conference, Calgary, ASME, IPC2008-64668, pp. 1-10.
- [4] ASTM E8/E8M-09, “Standard Test Methods for Tension Testing of Metallic Materials”, ASTM International, West Conshohocken, PA, 2009, DOI: 10.1520/E0008_E0008M-09, www.astm.org.
- [5] ASTM E1019, “Standard Test Methods for Determination of Carbon, Sulfur, Nitrogen, and Oxygen in Steel, Iron, Nickel, and Cobalt Alloys by Various Combustion and Fusion Techniques”, ASTM International, West Conshohocken, PA, 2008, DOI: 10.1520/E1019-08, www.astm.org.
- [6] ASTM D1076-06, “Standard Specification for Rubber-Concentrated, Ammonia Preserved, Creamed, and Centrifuged Natural Latex”, ASTM International, West Conshohocken, PA, 2006, DOI: 10.1520/D1076-06, www.astm.org.
- [7] Communication from Exxon-Mobile.
- [8] ASTM E23-07ae1, “Standard Test Methods for Notched Bar Impact Testing of Metallic Materials”, ASTM International, West Conshohocken, PA, 2007, DOI: 10.1520/E0023-07AE01, www.astm.org.
- [9] ASTM E604-83(2008), “Standard Test Method for Dynamic Tear Testing of Metallic Materials”, ASTM International, West Conshohocken, PA, 2008, DOI: 10.1520/E0604-83R08, www.astm.org.
- [10] ISO 148, “Metallic materials – Charpy Pendulum Impact Test”, International Organization for Standardization, 2006.
- [11] EN 10045, “Charpy Impact Test on Metallic Materials”, Euronorm, 1993.
- [12] JIS Z2242, “Method for Charpy Pendulum Impact Test of Metallic Materials”, Japanese Standards Association, 2005.
- [13] Bezensek B. & Hancock J.W., “Fracture toughness and crack path deviations in laser welded joints”, Proc. Int. Conf. ASME 2004 Pressure Vessels and Piping , PVP-vol.474, Ed: PS Lam et al, San Diego, CA, USA, July 2004

- [14] M. Nagel, P. Langenberg, F. Lüder, W. Bleck and U. Dilthey., “Discussion of testing procedures for the determination of the toughness properties of laser welded joints”, European Structural Integrity Society, Volume 30, 2002, Pages 253-261
- [15] BS 7448: Part 2, “Fracture Mechanics Toughness Test; Method for Determination of K_{Ic} , Critical CTOD and Critical J Values of Welds in Metallic Materials”, BSI, London, UK, 1997
- [16] BS 5762: 1979, “Crack tip opening displacement (COD) testing”, BSI, London, UK, 1979.
- [17] ASTM 1820-06, “Standard Test Method for Measurement of Fracture Toughness”, ASTM International
- [18] BS 7448, Part 1, “Fracture Mechanics Toughness Test; Method for Determination of K_{Ic} , Critical CTOD and Critical J Values of Metallic Materials”, BSI, London, England, 1991.

ANNEX A –
HYBRID LASER ARC WELDING SYSTEM AND PROCESS SPECIFICATION

A.1 APPLICATION

A.1.1 General

The Hybrid Laser Arc Welding (HLAW) system shall be capable of operating in an environment that has a service temperature range of between -45°C to $+45^{\circ}\text{C}$. All components in this system shall be designed to withstand these conditions.

The system shall be capable of producing sound welds in high strength pipe of at least API 5L grades X80 to X120, that have a minimum specified yield strength of 80 ksi to 120 ksi, respectively.

The process shall be developed and validated to deposit single pass full penetration welds, from the outside diameter only, on pipes of 30 inches to 48 inches diameter with a wall thickness of up to 10 mm, unless sound full penetration welds can be demonstrated on pipe walls of greater thickness. Beyond 10 mm wall thickness, the process shall at least be capable of producing HLAW root passes with laser assisted Gas Metal Arc Welding (GMAW) fill and cap passes, again all from the outside diameter.

All welding shall be produced with the pipe fixed in the 5G position with a maximum clearance between the bottom of the pipe and the ground of 28 inch.

A.1.2 Tolerances on Pipe Dimensions and Mass

A.1.2.1 Tolerances on Outside Diameter – Pipe Body

Tolerances on outside diameter shall be as given in Table A-1.

Table A-1: Tolerances on Outside Diameter

Specified outside diameter, mm	Outside diameter tolerances
48.3 or smaller	+0.4 mm, -0.8 mm
Larger than 48.3 but smaller than 114.3	$\pm 1.00\%^*$
114.3 to 457 inclusive	$\pm 0.75\%^*$
Larger than 457, nonexpanded	$\pm 1.00\%^*$
Larger than 457, cold-expanded	$+0.75\%^*$, $-0.25\%^*$

**Calculated values are percentages of the specified outside diameter, rounded to the nearest 0.1 mm.*

A.1.2.2 Tolerances on Outside Diameter – Pipe Ends

- (1) Except as allowed by Clause 1.2.2(b), pipe larger than 457 mm OD shall be not more than 0.8 mm smaller or 2.4 mm larger than the specified outside diameter for a distance of 100 mm from the ends of the pipe as measured with a diameter tape.
- (2) For pipe larger than 457 mm OD, it shall be permissible for the tolerances on outside diameter at the ends of the pipe (see Clause 1.2.2(a)) to be applied to the inside diameter at the ends of the pipe.

A.1.3 Tolerances on Out-of-Roundness

For a distance of 100 mm from the ends of pipe larger than 457 mm OD, the maximum outside diameter shall be not more than 1 percent larger than the specified outside diameter and the minimum outside diameter shall be not more than 1 percent smaller than the specified outside diameter.

A.1.4 Tolerances on Wall Thickness

The tolerances on wall thickness shall be as given in Table A1.

Table A1: Tolerances on Wall Thickness

Specified outside diameter, mm	Specified wall thickness, mm	Type of pipe	Tolerances on wall thickness, %*
73.0 or smaller	Any	Any	+20.0, -12.5
Larger than 73.0 but smaller than 101.6	Any	Any	+18.0, -12.5
101.6 to 457 inclusive	Any	Any	+15.0, -12.5
Larger than 457	Any	Seamless	+17.5, -10.0
Larger than 457	9.5 or less	Welded	+17.0, -8.0
Larger than 457	9.6 to 12.6 inclusive	Welded	+15.0, -8.0
Larger than 457	12.7 or greater	Welded	+12.0, -8.0

**Calculated values shall be rounded to the nearest 0.1 mm.*

Note: *For orders where the minus tolerance on wall thickness is reduced from the applicable value given in this Table, unless otherwise specified in the purchase order, the corresponding plus tolerance on wall thickness shall be increased by the same number of percentage points.*

A.2 HLAW SYSTEM COMPONENTS

A.2.1 Laser Power Source

The laser power source for this system shall be at least 10kW as delivered to the workpiece and of a wavelength between 1,030 nm to 1,070nm. Delivery of the processing beam shall be through an XXm 300 micron fibre optic cable. An example of a compatible laser is the TruDisk 10003 manufactured by Trumpf.

A.2.2 HLAW Processing Components

The following comprises the HLAW components that make up the processing head and will be directly mounted to the motion system. The overall system height of the moving components shall be less than 710 mm (28 inches) as measured from the outer surface of the pipe.

A.2.3 Laser Focus Head

The laser beam focusing optics shall be compatible with the laser power source both optically and thermally. It shall have a free aperture that is consistent with the optical parameters of the delivery fibre and have sufficient cooling of the optical elements to sustain full power operation for the required weld process time (~2 min). It shall provide an optical magnification of 2.0 and have an effective focal length of 300 mm for enhanced standoff from the workpiece. The head will include both a pneumatic air knife and a quartz glass window that protects the lens assembly from contamination during the welding process. An example of a compatible weld head assembly is the BIMO-HP from HighYAG.

A.2.4 Seam Tracking

The seam tracking system shall be capable of discriminating and properly tracking both a square butt joint with as little as 0.25 mm gap as well as a bevelled joint. Overall, the system will provide servo driven adjustment slides for the entire weld head assembly with at least +/-25 mm of adjustment in both the transverse (Y) and height directions (Z). The system must be capable of measuring the gap in the joint and relaying that information to the Master Process Controller. An example of a compatible system is the Auto-Trac/LW with RAFAL/SSO-W camera from Servo-Robot, Inc. This particular seam tracking camera has an operating Field of View (FOV) of 16 mm wide by 10 mm in height. At weld initiation, the system is set up in the middle of these ranges thus can accommodate +/- 8 mm of transverse (Y) and +/-5mm of height (Z) variation in the joint location with respect to the weld process. This translates to a lateral seam misalignment of less than +/- 0.07 mm/mm of circumference based on the current 116 mm separation distance between the process spot and the joint image. Changes in height of the joint must be less than +/- 0.04 mm/mm of circumference.

A.2.5 Post Weld Surface Inspection

The post weld surface inspection system shall be capable of 2D imaging of the welded joint and reporting pertinent weld attributes to the Master Process Controller. Applicable weld attributes include weld profile, bead height, presence of undercut, cracks, and surface porosity. An example of a compatible system is the ROBONET/MASTER for POROSCAN with the POROSCAN 25/10 camera from Servo-Robot, Inc. This system has an overall FOV of 27 mm in width by 16 mm in height. Position of the weld joint image in this FOV will be matched with

that of the seam tracker camera to insure that the joint stays within the viewing window. Accounting for the maximum offsets due to the seam tracker, the maximum dimensions of the inspectable weld becomes 11 mm in width by 6 mm in bead height.

A.2.6 GMAW Torch

The GMAW torch shall be coolant cooled and have a 600 amp capacity. An example of a compatible torch is a Binzel AUT602 180D.

A.2.7 Crash Sensor

All the HLAW head components shall be mounted on a breakaway crash sensor that stops the process and prevents damage to the processing components in the event of a system malfunction. An example of a compatible system is the QS-800 from Applied Robotics.

A.2.8 Master Process Controller and User Interface

The master process controller provides the operator user interface and controls the various subsystems to accomplish the HLAW process. This system also provides critical feedback on weld parameters and interfaces with the inline post weld inspection equipment to provide a complete examination of the HLAW process.

A.2.9 GMAW Equipment

The overall GMAW system comprises the controller, power supply and wire feeder. The controller shall be an ESAB AristoPendant U8. The power supply is an ESAB AristoMig 500 capable of 500A @ 60 percent duty cycle or 400A continuous duty operation. The wire feed unit is an ESAB Aristo RoboFeed 30-4 capable of feeding 1.2 mm (0.045 inch) diameter wire at up to 25 m/min(1,000 ipm). The power supply also has an integrated torch cooler.

A.2.10 Orbital Motion System

The orbital motion system shall be servo controlled with external speed control input and position feedback. The system should provide smooth weld motion from 0 to 5 m/min with minimal acceleration time under load. Payload capacity of the system should be at least 40 kg at a distance of 160 mm (6.3 inches) from the mounting face.

A.2.11 Detailed Power Requirements

Table A2: Detailed Power Requirements

Device	Voltage	Current (max)	Breaker
Laser	480VAC 3 phase	93 amp	100 amp
Chiller	480VAC 3 phase	42 amp	50 amp
Welder	480VAC 3 phase	38 amp	40 amp
MPC (Includes Seam Tracker & Weld Inspection)	120VAC	22 amp	30 amp

A.2.12 Air Supply Requirements

Both the crash sensor and the laser processing head require externally supplied, compressed air that is dry, oil free and filtered. In the laser processing head this air helps to shield the optics from contamination of the welding process. Minimum supply requirements of 500 litres/min. (18 scfm) at 0.6 MPa (90 psi). Maximum overpressure cannot exceed 1.2 MPa (180 psi).

A.2.13 Safety Controls

The particular laser wavelength specified presents an eye hazard to the operator and bystanders within the nominal hazard zone. To minimize the potential exposure, the operator control station will be located outside the welding zone which will be fully enclosed and guard against stray reflections. Moving components will be interlocked to insure there will be no accidental exposure if a guard is inadvertently opened/removed.

A.3 FIELD WELDING REQUIREMENTS

A.3.1 Alignment

The alignment of abutting ends shall minimize the offset between surfaces. For pipe ends of the same nominal thickness, the offset should not exceed $\frac{1}{8}$ inch (3 mm). Larger variations of the pipe end dimensions within the pipe purchase specifications tolerances, and such variations have been distributed essentially uniformly around the circumference of the pipe. Hammering of the pipe to obtain proper lineup should be kept to a minimum.

Lineup clamps shall be used for butt welds in accordance with the procedure specifications. When it is permissible to remove the lineup clamp before the root bead is completed, the completed part of the bead shall be in similar-sized segments spaced approximately equally around the circumference of the joint. However, when an internal lineup clamp is used and conditions make it difficult to prevent movement of the pipe or if the weld will be unduly stressed, the root bead shall be completed before the clamp tension is released.

A.4 WORKMANSHIP AND NONDESTRUCTIVE TESTING REQUIREMENTS

A.4.1 Workmanship Requirements – Visual Inspection

The surfaces to be welded shall be smooth, uniform, and free from laminations, tears, scale, slag, grease, paint, and other deleterious material that might adversely affect the welding. The joint design and spacing between abutting ends shall be in accordance with the procedures specifications used.

For position welding, the number of filler and finish beads shall allow the completed weld a substantially uniform cross section around the entire circumference of the pipe. At no point shall the crown surface fall below the outside surface of the pipe, nor should it be raised above the parent metal by more than $\frac{1}{16}$ inches (1.6 mm).

Two beads shall not be started at the same location. The face of the completed weld should be approximately $\frac{1}{8}$ inch (3 mm) wider than the width of the original groove. The completed weld shall be thoroughly brushed and cleaned.

Welds shall be free from cracks, inadequate penetration, and burn-through, and must present a neat workman-like appearance. The depth of undercutting adjacent to the final bead on the outside of the pipe shall not be more than $\frac{1}{32}$ inch (0.8 mm) or 12.5 percent of the pipe wall thickness, whichever is smaller; and there shall not be more than 2 inches (50 mm) of undercutting in any continuous 12 inches (300 mm) length of weld.

Welds shall be free from any relevant indications with a maximum dimension of $\frac{1}{16}$ inch (1.6 mm). Any larger indication believed to be non-relevant shall be regarded as relevant until re-examined by magnetic particle, liquid penetrant, or another non-destructive testing method to determine whether or not an actual imperfection exists. The surface may be ground or otherwise conditioned before re-examination. After an indication is determined to be non-relevant, other non-relevant indications of the same type need not be re-examined.

Relevant indications are those caused by imperfections. Linear indications are those in which the length is three times the width or less.

Relevant indications shall be considered defects should any of the following conditions exist:

- (1) Linear indications evaluated as crater cracks or star cracks exceed $\frac{5}{32}$ inch (4 mm) in length.
- (2) Linear indications are evaluated as cracks other than crater cracks or star cracks.
- (3) Linear indications are evaluated as IF and exceed 1 inch (25 mm) in total length in a continuous 12 inches (300 mm) length of weld or 8 percent of the weld length.

A.4.2 Ultrasonic Inspection Requirements

Indications produced by ultrasonic testing are not necessarily defects. Changes in the weld geometry due to alignment offset a butting pipe ends, changes in the weld reinforcement profile of ID root and OD capping passes, internal chamfering, ultrasonic wave mode conversion due to such conditions may cause geometric indications that are similar to those caused by weld imperfections but that are not relevant to acceptability.

Linear indications are defined as indications with their greatest dimension in the weld length direction. Typical linear types may be caused by, but are not limited to, the following types of imperfections: inadequate penetration without high-low (IP), inadequate penetration due to high-low (IPD), inadequate cross penetration (ICP), incomplete fusion (IF), incomplete fusion due to cold lap (IFD), elongated slag inclusion (ESI), cracks (C), undercutting adjacent to the cover pass (EU) or root pass (IU), and hollow bead porosity (HB).

Transverse indications are defined as indications with their greatest dimension across the weld. Typical transverse indications may be caused by, but are not limited, to the following types of imperfections: cracks (C), isolated slag inclusions (ISI), and incomplete fusion due to cold lap (IFD) at starts and stops in the weld passes.

Volumetric indications are defined as three-dimensional indications. Such indications may be caused by single or multiple inclusions, voids, or pores. Partially-filled voids, pores, or small inclusions at start/stops in weld passes may cause larger indications in the transverse direction than in the weld length direction. Typical volumetric indications may be caused by, but are not limited to, the following types of imperfections: internal concavity (IC), burn-through (BT), isolated slag inclusions (ISI), porosity (P), and cluster porosity (CP).

Relevant indications are those caused by imperfections. Relevant indications shall be evaluated to API 1104 at the evaluations level given in Section 11.4.7 to the acceptance standards given in Section 9.6.2 of this Standard.

Note: When doubt exists about the type of imperfection being disclosed by an indication, verification may be obtained by using other non-destructive testing methods.

Indications shall be considered defects should any of the following condition exist:

- (1) Indication determined to be cracks (C);
- (2) Individual indications with a vertical height (through-wall) dimension determined to be greater than one quarter of the wall thickness; or
- (3) Multiple indications at the same circumferential locations with a summed vertical height (through-wall) dimension exceeding one half the wall thickness.

Linear Surface (LS) indications (other than cracks) interpreted to be open to the ID or OD surface shall be considered defects should any of the following conditions exist:

- (1) The aggregate length of LS indications in any continuous 12 inch (300 mm) length of weld exceeds 1 inch (25 mm); or
- (2) The aggregate length of LS indications exceeds 8% of the weld length.

Linear Buried (LB) indications (other than cracks) interpreted to be subsurface within the weld and not ID or OD surface-connected shall be considered defects should any of the following conditions exist:

- (1) The aggregate length of LB indications in any continuous 12 inch (300 mm) length of weld exceeds 2 inches (50 mm); or
- (2) The aggregated length of LB indications exceeds 8% of the weld length.

Transverse (T) indications (other than cracks) shall be considered volumetric and evaluated using the criteria for volumetric indications. The letter T shall be used to designate all reported transverse indications.

Volumetric Cluster (VC) indications shall be considered defects when the maximum dimension of VC indications exceeds $\frac{1}{2}$ inch (13 mm).

Volumetric Indications (VI) shall be considered defects when the maximum dimension of VI indications exceeds $\frac{1}{8}$ inch (3 mm)

Volumetric Root (VR) indications interpreted to be open to the ID surface shall be considered defects should any of the following exist:

- (1) The maximum dimension of VR indications exceeds $\frac{1}{4}$ inch (6 mm) or the nominal wall thickness, whichever is less; or
- (2) The total length of VR indications exceeds $\frac{1}{2}$ in. (13 mm) in any continuous 12 inches. (300 mm) length.

Any accumulation of relevant indications (AR) shall be considered a defect when any of the following conditions exist:

- (1) The aggregate length of indications above evaluation level exceeds 2 inches (50 mm) in any 12 inch (300 mm) length of weld.
- (2) The aggregate length of indications above evaluation level exceeds 8 percent of the weld length.

ANNEX B –
RADIOGRAPHY AND ULTRASONIC TESTING REPORTS



Radiographic Testing Report

R- 11543

Client BMT Fleet Technology Location KAWATA, ON Client Reference # 0245DB Date AUG 105/2009
 Contractor CLIENT Canspec Job/WO # 151-9-2035 DTR # E19834 Page 1 of 3

Item Inspected 36" Ø COUPONS # of Welds 5
 Acceptance Std. API-1104 Rev Date _____
 Material Type Carbon Steel Other _____
 Procedure RT0016 Other _____
 Radiation Source Ir192 X ray Curies 87 KV _____

Film Brand Agfa Kodak
 Film Type 1 2 3
 Screens Lead 0.005" Front 0.010" Back
 Focal Spot Size mm inch 0.7
 Exposure SWE DWE SWV DWV

Film Used	
17"	8 1/2"
2 3/4"	
3 1/2"	
4 1/2"	
14"	

Final film interpretation is the responsibility of the client. I am in full agreement with the details of this report, and acknowledge receipt of the film.

Client Rep (sign) [Signature]
 Technician (sign) [Signature] TLD# 311657 mR 10 CGSB 2 SNT 2
 Assistant (print) _____ TLD# _____ mR _____ CEDO Assistant
 TSSA DOL (sign) _____

1	Identification	Pipe Dia	Pipe Sch	Rein.	Pen.	Tech #	SOD (D)	OFD (t)	# Of Exp	Crk	LF	IP	P	S/T	UC	IC	EP	*	Defect Location and Remarks	Acc (✓)	Rej (X)
2	497 0 → 35	36"	14.3		D	B	176"		1				✓							✓	
3	35 → 70				S															✓	
4	70 → 105				S															✓	
5	105 → 140				S								✓							✓	
6	140 → 175				S								✓							✓	
7	175 → 210				S							X								✓	X
8	210 → 245				S								✓							✓	
9	245 → 280				S								✓							✓	
10	280 → 0				S								✓							✓	
11																					
12																					
13																					
14																					
15																					
16																					

Table Legend: 1 - Accept, 2 - Moderate, 3 - Reject, * - Welder Symbol, Acc - Acceptable, Rej - Rejected, Crk - Crack, LF - Lack of Fusion, IP - Incomplete Penetration, P - Porosity, S - Slag, T - Tungsten, UC - Undercut, IC - Internal Concavity, EP - Excessive Penetration, BT - Burn Through, HB - Hollow Bead, PH - Pinhole

Refer to opposite side for scope of services, and standard of care.

April, 05



Radiographic Testing Report

R- 11543

Client

BMT Fleet Technology

Item Inspected

36" Carbon

Canspec Job/WO#

151-9-2035

Date

Page 2 of 3
AUG-05-2009

Final film interpretation is the responsibility of the client. I am in full agreement with the details of this report, and acknowledge receipt of the film.

Client Rep (sign)

M. Peric

Technician (sign)

[Signature]

TLD #

311657

mR

10

CGSB

2

SNT

2

TSSA DOL (sign)

Identification	Pipe Dia	Pipe Sch	Rein.	Pen.	Tech #	SOD (D)	OFD (t)	# Of Exp	Crk	LF	IP	P	ST	UC	IC	EP	*	Defect Location and Remarks	Acc (✓)	Rej (X)		
498 ↓	0-35	36"	14.3	D	B	17/8"	C	1											✓			
	35-70																	✓				
	70-105																	✓				
	105-140																	✓				
	140-175																	✓				
	175-210																	✓				
	210-245																	X		@215 TO 245		X
	245-280																	X		@245 TO 255		X
280-0	✓																					
500 ↓	0-35	36"	14.3	D	B	17/8"	C	1											✓			
	35-70																	✓				
	70-105																	✓				
	105-140																	✓				
	140-175																	X		@145 TO 175		X
	175-210																	X		@183 TO 210		X
	210-245																	X		@210 TO 230		X
	245-280																	✓				
280-0	✓					@285 TO 0		X														

Table Legend: 1 - Accept, 2 - Moderate, 3 - Reject, * - Welder Symbol, Acc - Acceptable, Rej - Rejected, Crk - Crack, LF - Lack of Fusion, IP - Incomplete Penetration, P - Porosity, S - Slag, T - Tungsten, UC - Undercut, IC - Internal Concavity, EP - Excessive Penetration, BT - Burn Through, HB - Hollow Bead, PH - Pinhole

Refer to opposite side for scope of services, and standard of care.

April, 05



Radiographic Testing Report

R- 11542

Client BMT Fleet Technology Location KANATA, ON Client Reference # 0245DB Date Aug/05/2009
 Contractor CLIENT Canspec Job/WO # 151-9-2035 DTR # E19834 Page 1 of 3

Item Inspected 36" CANTONS # of Welds 5
 Acceptance Std. API-1104 Rev Date _____
 Material Type Carbon Steel Other _____
 Procedure RT0016 Other _____
 Radiation Source 1a192 X ray Curies 8.76 KV _____

Film Brand Agfa Kodak
 Film Type 1 2 3
 Screens Lead 0.005" Front 0.010" Back
 Focal Spot Size mm inch 2.7
 Exposure SWE DWE SWV DWV

	Film Used	
	17"	8 1/2"
2 3/4"		
3 1/2"		
4 1/2"		
14"		

Final film interpretation is the responsibility of the client. I am in full agreement with the details of this report, and acknowledge receipt of the film.

Client Rep (sign) [Signature]
 Technician (sign) [Signature] TLD # 311657 mR 10 CGSB 2 SNT 2
 Assistant (print) _____ TLD # _____ mR _____ CEDO Assistant
 TSSA DOL (sign) _____

	Identification	Pipe Dia	Pipe Sch	Rein.	Pen.	Tech #	SOD (D)	OFD (t)	# Of Exp	Crk	LF	IP	P	S	T	UC	IC	EP	*	Defect Location and Remarks	Acc (v)	Rej (X)
1	DM																					
2	SD3 0-35	36"	MM 104		D	B	176		1													
3	35-70				U																	
4	70-105				T						X											
5	105-140				M						X											
6	140-175				B						X											
7	175-210										X											
8	210-245																					
9	245-280																					
10	280-0																					
11																						
12																						
13																						
14																						
15																						
16																						

Table Legend: 1 - Accept, 2 - Moderate, 3 - Reject, * - Welder Symbol, Acc - Acceptable, Rej - Rejected, Crk - Crack, LF - Lack of Fusion, IP - Incomplete Penetration, P - Porosity, S - Slag, T - Tungsten, UC - Undercut, IC - Internal Concavity, EP - Excessive Penetration, BT - Burn Through, HB - Hollow Bead, PH - Pinhole

Refer to opposite side for scope of services, and standard of care.

April, 05



Radiographic Testing Report

R-11542

Page 2 of 3

Client

BMT FLEET Technology

Item Inspected

36" casings

Canspec Job/WO#

151-9-2035

Date

AUG-05-2009

Final film interpretation is the responsibility of the client. I am in full agreement with the details of this report, and acknowledge receipt of the film.

Client Rep (sign)

M. Peric

Technician (sign)

[Signature]

TLD# 311657

mR 10

CGSB

SNT

TSSA DOL (sign)

Identification	Pipe Dia	Pipe Sch	Rein.	Pen.	Tech #	SOD (D)	OFD (t)	# Of Exp	Crk	LF	IP	P	ST	UC	IC	EP	*	Defect Location and Remarks	Acc (✓)	Rej (X)
S04	0 → 35	36	0.4	2	B	17/2		1											✓	
	35 → 70			2															✓	
	70 → 105			2															✓	
	105 → 140			1															✓	
	140 → 175			3															✓	
	175 → 210			1															✓	
	210 → 245			1															✓	
	245 → 280			1															✓	
280 → 0																		✓		
S06	0 → 35																		✓	
	35 → 70																		✓	
	70 → 105																		✓	
	105 → 140																		✓	
	140 → 175																		✓	
	175 → 210																		✓	
	210 → 245																		✓	
	245 → 280																		✓	
280 → 0																		✓		

Table Legend: 1 - Accept, 2 - Moderate, 3 - Reject, * - Welder Symbol, Acc - Acceptable, Rej - Rejected, Crk - Crack, LF - Lack of Fusion, IP - Incomplete Penetration, P - Porosity, S - Slag, T - Tungsten, UC - Undercut, IC - Internal Concavity, EP - Excessive Penetration, BT - Burn Through, HB - Hollow Bead, PH - Pinhole

Refer to opposite side for scope of services, and standard of care.

April, 05



Radiographic Testing Report

R- 11542

Client BMT FLEET TECHNOLOGY Item Inspected 36" CW Coups Canspec Job/WO# 151-9-2035 Date AUG-05-2009
 Page 3 of 3

Final film interpretation is the responsibility of the client. I am in full agreement with the details of this report, and acknowledge receipt of the film.

Client Rep (sign) [Signature]

Technician (sign) [Signature]

TLD# 311657 mR 10 CGSB 2 SNT 2

TSSA DOL (sign)

Identification	Pipe Dia	Pipe Sch	Rein.	Pen.	Tech #	SOD (D)	OFD (t)	# Of Exp	Crk	LF	IP	P	S/T	UC	IC	EP	*	Defect Location and Remarks	Acc (v)	Rej (X)
507	0 → 35	36"			B	176		1											/	
	35 → 70																		/	
	70 → 105																		/	
	105 → 140										X							@114 to 121	/	X
	140 → 175										X							@175 to 185	/	X
	175 → 210																		/	
	210 → 245																		/	
	245 → 280																		/	
280 → 0																		/		
508	0 → 35																		/	
	35 → 70																		/	
	70 → 105											X						@76 to 104	/	X
	105 → 140																		/	
	140 → 175																		/	
	175 → 210																		/	
	210 → 245																		/	
	245 → 280																		/	
280 → 0																		/		

Table Legend: 1 - Accept, 2 - Moderate, 3 - Reject, * - Welder Symbol, Acc - Acceptable, Rej - Rejected, Crk - Crack, LF - Lack of Fusion, IP - Incomplete Penetration, P - Porosity, S - Slag, T - Tungsten, UC - Undercut, IC - Internal Concavity, EP - Excessive Penetration, BT - Burn Through, HB - Hollow Bead, PH - Pinhole

Refer to opposite side for scope of services, and standard of care.

April, 05

Project # 6166C Hybrid Laser Arc Welding Ultrasonic Inspection Results

Radiographic reports for the ten 36" diameter pipe girth welds revealed several indications including: lack of fusion, incomplete penetration, porosity, undercut and internal concavity in several areas on the pipes. Ultrasonic inspection was done to confirm, locate and size these and any additional anomalies in the joints. Distance measurements are as per the radiographic film positions. The 12 o'clock position (start of weld) was the "X" line zero position for all measurements and "Y" zero was the centerline of the weld.

All ten welds had reflectors at the start (12 o'clock position) of the weld and eight of the ten reflectors were rejectable defects by API 1104 quality standards. All ten joints had at least one rejectable indication in it. The majority of defects located are side wall fusion defects ranging from a few millimeters to 260 millimeters in length.

See the attached table for the length, depth and position of the recorded reflectors.

The initial inspection was done as per CSA Standard W59-03 Section 12 for Cyclically Loaded Structures. The conversion to API Standard 1104 was by amplitude comparison of the DSC Calibration Block and the API Calibration Block.



Lanny Hofmeister
CGSB # 375 Level II MT, PT & UT
CWB # 3296 Level II Welding Inspector

Pipe section	Indication	Reference	Attenuation	Indication		Sound		"X" Position		"Y"	API 1104 Conversion	
	Level	Level	Factor	Rating	Length	Path Dist.	Depth	Start	End		for API	Comments
#497			2.5		15 mm	57.3	9.0	20 mm	45 mm	0		
14.3 mm	+10.0	47.8	1.4	11.4	25 mm	43.1	6.1	190 mm	215 mm	0	-2.2	Reject
	+5.9	47.8	3.7	9.6	7 mm	72.5	4.0	228 mm	235 mm	0	-4.0	Reject
			1.2		5 mm	40.1	14.0	235 mm	240 mm	0		
#498	+8.8	49.0	0.6	9.4	15 mm	33.6	11.5	20 mm	35 mm	0	-4.2	Reject
14.3 mm	+20.0	49.0	0.8	20.8	11 mm	35.0	11.7	403 mm	414 mm	0	7.2	
	+13.8	49.0	0.8	14.6	23 mm	35.0	11.7	600 mm	623 mm	0	1.0	
	+12.0	49.0	0.9	12.9	24 mm	36.5	12.5	713 mm	737 mm	0	-0.7	Reject
	+15.4	49.0	3.7	19.1	14 mm	72.5	3.8	972 mm	986 mm	0	5.5	
	+15.1	49.0	3.7	18.8	43 mm	72.8	3.7	1168 mm	1211 mm	0	5.2	
#500	+7.4	53.3	2.8	10.2	18 mm	60.6	8.4	7 mm	25 mm	0	-3.4	Reject
14.3 mm	+10.5	49.0	4.1	14.6	53 mm	77.5	2.7	767 mm	820 mm	0	1.0	Reject
	+17.9	47.4	2.1	20.0	10 mm	51.9	11.7	900 mm	910 mm	0	6.4	
	+18.2	47.4	4.0	22.2	12 mm	76.3	3.1	1160 mm	1172 mm	0	8.6	
	+17.8	47.4	2.0	19.8	10 mm	50.6	11.7	1215 mm	1225 mm	0	6.2	
	+15.5	47.4	0.2	15.7	10 mm	27.5	9.0	1400 mm	1410 mm	0	2.1	
	+16.0	47.4	3.5	19.5	10 mm	70.0	5.2	1470 mm	1480 mm	0	5.9	
	+18.4	47.4	4.8	23.2	20 mm	86.9	0.4	2370 mm	2390 mm	0	9.6	

Pipe section	Indication	Reference	Attenuation	Indication		Sound		"X" Position		"Y"	API 1104 Conversion	
	Level	Level	Factor	Rating	Length	Path Dist.	Depth	Start	End		for API	Comments
#501	+15.1	46.8	1.6	16.7	15 mm	45.6	13	20 mm	35 mm	0	3.1	
14.3 mm	+11.5	46.8	2.0	13.5	14 mm	51.3	11.5	517 mm	531 mm	0	-0.1	Reject
	+13.7	46.8	3.9	17.6	87 mm	75.0	3.6	593 mm	680 mm	0	4.0	
	+6.2	48.2	3.9	10.1	180 mm	75.0	3.6	2030 mm	2210 mm	0	-3.5	Reject
	+4.8	48.2	3.9	8.7	260 mm	75.0	3.6	2230 mm	2490 mm	0	-4.9	Reject
#502	+9.6	47.9	2.4	12.0	18 mm	55.8	9.5	20 mm	38 mm	0	-1.6	Reject
14.3 mm	+13.7	47.9	2.7	16.4	31 mm	60.2	8.0	137 mm	168 mm	0	2.8	
	+10.7	47.9	3.8	14.5	40 mm	73.4	3.5	675 mm	715 mm	0	0.9	Reject
	+11.9	47.9	2.4	14.3	50 mm	55.8	9.5	795 mm	845 mm	0	0.7	Reject
	+13.3	47.9	4.0	17.3	7 mm	76.3	2.5	995 mm	1002 mm	0	3.7	
	+13.3	47.9	0.8	14.1	7 mm	35.1	12.0	995 mm	1002 mm	0	0.5	
	+10.8	47.9	0.5	11.3	20 mm	32.2	11.0	1080 mm	1100 mm	0	-2.3	Reject
	+16.3	47.9	3.8	20.1	30 mm	73.4	3.5	2030 mm	2060 mm	0	6.5	
	+2.9	47.9	3.8	6.7	41 mm	73.4	3.5	2197 mm	2238 mm	0	-6.9	Reject
	+11.6	47.9	3.7	15.3	185 mm	71.9	4.0	2373 mm	2558 mm	0	1.7	Reject
	+17.3	47.9	0.8	18.1	28 mm	35.1	12.0	2760 mm	2788 mm	0	4.5	

Pipe section	Indication	Reference	Attenuation	Indication		Sound		"X" Position		"Y"	API 1104 Conversion	
	Level	Level	Factor	Rating	Length	Path Dist.	Depth	Start	End		for API	Comments
#503	+8.3	48.5	1.2	9.5	13 mm	40.3	7.0	5 mm	18 mm	0	-4.1	Reject
10.4 mm	+16.6	48.5	1.5	18.1	18 mm	44.7	5.5	662 mm	580 mm	0	4.5	
	+16.3	48.5	2.7	19.0	20 mm	59.4	3.5	2145 mm	2165 mm	0	5.4	
#504	+6.9	48.2	0.8	7.7	11 mm	35.6	9.0	10 mm	21 mm	0	-5.9	Reject
10.4 mm	+14.4	48.2	0.6	15.0	30 mm	32.5	10.0	590 mm	620 mm	0	1.4	
	+16.8	48.5	2.5	19.3	30 mm	56.9	1.8	2175 mm	2205 mm	0	5.7	
#506	5.5	48.5	0.6	6.1	10 mm	33.1	9.8	75 mm	85 mm	0	-7.5	Reject
10.4 mm	+10.7	48.5	2.1	12.8	15 mm	51.9	3.5	345 mm	360 mm	0	-0.8	Reject
	+8.2	48.5	2.3	10.5	20 mm	55.0	2.5	430 mm	450 mm	0	-3.1	Reject
	+7.5	48.5	2.0	9.5	52 mm	50.6	3.9	465 mm	517 mm	0	-4.1	Reject
	+12.7	48.5	2.5	15.2	39 mm	57.5	1.4	862 mm	907 mm	0	1.6	
	+13.8	48.5	2.3	16.1	10 mm	54.4	2.7	1145 mm	1155 mm	0	2.5	
	+14.8	48.5	2.1	16.9	90 mm	52.5	3.3	1177 mm	1267 mm	0	3.3	
	+18.0	48.5	2.6	20.6	18 mm	58.8	1.8	1580 mm	1598 mm	0	7.0	
	+13.2	48.5	2.0	15.2	10 mm	51.3	3.7	1775 mm	1785 mm	0	1.6	
	+9.9	48.5	2.6	12.5	33 mm	58.1	1.4	1852 mm	1885 mm	0	-1.1	Reject
	+9.6	48.5	2.6	12.2	32 mm	58.1	1.4	1920 mm	1952 mm	0	-1.4	Reject

Pipe section	Indication	Reference	Attenuation	Indication		Sound		"X" Position		"Y"	API 1104 Conversion	
	Level	Level	Factor	Rating	Length	Path Dist.	Depth	Start	End		for API	Comments
	+9.3	48.5	2.6	11.9	34 mm	58.3	1.2	1958 mm	1992 mm	0	-1.7	Reject
	8.9	48.5	2.6	11.5	38 mm	58.1	1.4	2025 mm	2463 mm	0	-2.1	Reject
#507	+13.6	48.3	0.8	14.4	15 mm	36.0	8.5	10 mm	35 mm	0	0.8	Reject
10.4 mm	+16.8	48.3	1.5	18.3	94 mm	44.7	5.5	1871 mm	1955 mm	0	4.7	
#508	+7.9	47.8	1.1	9.0	15 mm	38.9	7.5	20 mm	35 mm	0	-4.6	Reject
10.4 mm	+10.0	47.8	0.6	10.6	3 mm	33.1	9.0	126 mm	129 mm	0	-3.0	Reject
	+10.1	47.8	0.6	10.7	3 mm	33.1	9.0	132 mm	135 mm	0	-2.9	Reject

ANNEX C –
PIPE WELD TEST RESULTS

Table C1: Grade X100 Pipe Weld CTOD Test Results

Pipe ID & Grade	Clock Location	Notch Location & Test Temp	Specimen ID	a/W	a _{min} (mm)	Elastic CTOD (mm)	Plastic CTOD (mm)	Total CTOD (mm)	Failure Type	NOTES	post test metallography - location w.r.t. hybrid weld (60% of thickness)	
500 X100	3 o'clock 2 to 5 sector	Weld Centerline (W) -5°C (23°F)	W1	0.489	0.870	0.036	0.164	0.200	δ _{III}			
			W2	0.491	0.890	0.036	0.167	0.203	δ _{III}			
			W3	0.491	0.930	0.032	0.148	0.180	δ _{III}		fatigue crack in weld	
		HAZ (H) - 5°C (23°F)	H1	0.495	1.070	0.035	0.146	0.181	δ _{III}			
			H2	0.490	0.890	0.039	0.187	0.226	δ _{III}			
			H3	0.488	0.860	0.037	0.261	0.298	δ _{III}			
		Weld Centerline (W) -40°C (-40°F)	W4	0.497	1.050	0.033	0.188	0.222	δ _{III}		flaw below fatigue crack - insignificant pop-in	fatigue crack in weld
			W5	0.494	1.050	0.034	0.195	0.229	δ _{III}			
			W6	0.488	0.860	0.036	0.138	0.174	δ _c		flaw below fatigue crack	fatigue crack in weld
		HAZ(H) - 40°C (-40°F)	H4	0.482	0.740	0.041	0.211	0.252	δ _{III}			fatigue crack in FL
			H5	0.483	0.710	0.040	0.278	0.318	δ _{III}			
			H6	0.491	0.980	0.035	0.102	0.137	δ _{III}		fracture in HAZ	fatigue crack in FL
500 X100	6 o'clock 5 to 8 sector	Weld Centerline (W) -5°C (23°F)	W1	0.508	1.450	0.035	0.152	0.187	δ _{III}		fatigue crack in weld	
			W2	0.507	1.370	0.036	0.131	0.166	δ _{III}			
			W3	0.491	1.040	0.038	0.175	0.213	δ _{III}			
		HAZ (H) - 5°C (23°F)	H1	0.504	1.340	0.035	0.059	0.094	δ _c		ductile extension	fatigue crack in HAZ
			H2	0.506	1.330	0.040	0.242	0.282	δ _{III}			fatigue crack in HAZ
			H3	0.480	0.790	0.041	0.225	0.266	δ _{III}		instability with sudden load drop	
		Weld Centerline (W) -40°C (-40°F)	W4	0.483	0.790	0.039	0.182	0.221	δ _{III}			
			W5	0.492	1.040	0.039	0.205	0.244	δ _{III}			fatigue crack in weld
			W6	0.487	0.850	0.039	0.187	0.226	δ _{III}			
		HAZ(H) - 40°C (-40°F)	H4	0.489	0.970	0.041	0.288	0.328	δ _c		instability with sudden load drop - ductile tear in HAZ - fracture in HAZ	fatigue crack in HAZ
			H5	0.484	0.820	0.042	0.247	0.289	δ _{III}			
			H6	0.500	1.160	0.042	0.355	0.397	δ _c		instability with sudden load drop	
500 X100	9 o'clock 8 to 11 sector	Weld Centerline (W) -5°C (23°F)	W1	0.494	1.150	0.038	0.153	0.191	δ _{III}			
			W2	0.486	0.910	0.037	0.172	0.209	δ _{III}			
			W3	0.482	0.790	0.037	0.183	0.220	δ _{III}		fatigue crack in weld	
		HAZ (H) - 5°C (23°F)	H2	0.495	1.070	0.039	0.317	0.356	δ _{III}			
			H3	0.481	0.780	0.039	0.278	0.317	δ _{III}			fatigue crack in FL
			H4	0.479	0.760	0.038	0.210	0.248	δ _{III}			
		Weld Centerline (W) -40°C (-40°F)	W4	0.499	1.150	0.037	0.165	0.202	δ _{III}			
			W5	0.486	0.900	0.039	0.193	0.232	δ _{III}			
			W1D	0.494	1.170	0.038	0.200	0.238	δ _c		instability with sudden load drop - initiation in weld	fatigue crack in weld
		HAZ(H) - 40°C (-40°F)	H5	0.500	1.290	0.039	0.299	0.338	δ _{III}			fatigue crack in FL
			H6	0.507	1.430	0.037	0.303	0.340	δ _c		instability with sudden load drop - fatigue crack/ductile tear in weld - fracture in HAZ	fatigue crack in FL
			H6D	0.485	0.910	0.039	0.319	0.358	δ _c			
500 X100	12 o'clock 11 to 2 sector	Weld Centerline (W) -5°C (23°F)	W1	0.480	1.580	0.034	0.188	0.222	δ _{III}			
			W2	0.491	1.840	0.034	0.165	0.199	δ _{III}			
			W3	0.490	1.850	0.034	0.186	0.221	δ _{III}		fatigue crack in weld	
		HAZ (H) - 5°C (23°F)	H1	0.474	1.370	0.035	0.221	0.257	δ _{III}			
			H2	0.476	1.500	0.035	0.168	0.203	δ _{III}			
			H3	0.474	1.480	0.034	0.149	0.183	δ _{III}	0.482		fatigue crack in HAZ
		Weld Centerline (W) -40°C (-40°F)	W4	0.491	1.820	0.036	0.206	0.242	δ _{III}			fatigue crack in weld
			W5	0.489	1.790	0.034	0.163	0.197	δ _{III}			
			W6	0.493	1.820	0.034	0.186	0.220	δ _{III}			
		HAZ(H) - 40°C (-40°F)	H4	0.470	1.310	0.035	0.166	0.201	δ _{III}			
			H5	0.473	1.380	0.031	0.064	0.095	δ _c		instability with sudden load drop	fatigue crack in HAZ
			H6	0.477	1.490	0.034	0.153	0.188	δ _{III}			
501 X100	12 o'clock 11 to 2 sector	Weld Centerline (W) -5°C (23°F)	W1	0.482	0.870	0.036	0.186	0.222	δ _{III}		fatigue crack in weld	
			W2	0.481	0.840	0.035	0.233	0.268	δ _{III}			
			W3	0.481	0.900	0.035	0.179	0.214	δ _{III}			
		HAZ (H) - 5°C (23°F)	H1	0.481	0.870	0.037	0.176	0.213	δ _{III}			
			H2	0.482	0.980	0.035	0.197	0.232	δ _{III}			fatigue crack in FL
			H3	0.470	0.670	0.036	0.208	0.244	δ _{III}	0.482		
		Weld Centerline (W) -40°C (-40°F)	W4	0.491	1.110	0.036	0.224	0.260	δ _{III}			fatigue crack in weld
			W5	0.475	0.770	0.035	0.180	0.214	δ _{III}			
			W6	0.490	1.090	0.034	0.178	0.212	δ _{III}			
		HAZ(H) - 40°C (-40°F)	H4	0.483	0.900	0.036	0.198	0.234	δ _{III}			
			H5	0.482	0.870	0.037	0.214	0.251	δ _{III}			fatigue crack in HAZ
			H6	0.481	0.880	0.037	0.225	0.262	δ _{III}			

Notes
a₀ - average total crack length
W - Specimen width
a_{min} - minimum fatigue crack size

Table C2: Grade X80 Pipe Weld CTOD Test Results

Pipe ID & Grade	Clock Location	Notch Location & Test Temp	Specimen ID	a/W	a _{min} (mm)	Elastic CTOD (mm)	Plastic CTOD (mm)	Total CTOD (mm)	Failure Type	Notes	post test metallography - location w.r.t. hybrid weld (70-80% of thickness)	
506 X80	12 o'clock 11 to 2 sector	Weld Centerline (W) -5°C (23°F)	W1	0.491	0.910	0.022	0.095	0.117	δ ₂	sudden load drop		
			W2	0.492	0.940	0.016	0.026	0.042	δ ₂ *	metallography-fracture region hybrid weld closer to root side	fatigue crack in weld	
			W3	0.497	1.020	0.022	0.256	0.278	δ _{2m}		fatigue crack in weld	
		HAZ(H) - 5°C (23°F)	H1	0.476	0.810	0.023	0.090	0.113	δ ₂	small load drop		
			H2	0.480	0.930	0.026	0.353	0.379	δ _{2m}	fatigue crack in HAZ		fatigue crack in HAZ
			H3	0.483	0.960	0.025	0.293	0.318	δ ₂	small load drop - fatigue crack in FL		fatigue crack in FL
		Weld Centerline (W) -40°C (-40°F)	W4	0.480	0.730	0.010	0.003	0.013	δ ₂ *			
			W5	0.493	0.980	0.014	0.011	0.025	δ ₂			
			W6A	0.480	0.850	0.012	0.006	0.018	δ ₂ *	metallography-fracture region hybrid weld closer to root side		fatigue crack in weld
		HAZ(H) - 40°C (-40°F)	H4	0.475	0.790	0.020	0.042	0.062	δ ₂	metallography-fracture region hybrid weld		fatigue crack in HAZ
			H5	0.483	0.970	0.024	0.158	0.182	δ ₂	sudden load drop; fatigue crack in FL		fatigue crack in FL
			H6	0.481	0.940	0.018	0.025	0.043	δ ₂			
506 X80	3 o'clock 2 to 5 sector	Weld Centerline (W) -5°C (23°F)	W1	0.523	1.170	0.019	0.038	0.057	δ ₂	metallography-fracture region hybrid weld		fatigue crack in weld
			W3	0.486	0.850	0.017	0.032	0.049	δ ₂ *	flaw in fracture initiation region		fatigue crack in weld
			W4	0.512	1.310	0.020	0.062	0.083	δ ₂			
		HAZ(H) - 5°C (23°F)	H2	0.497	1.090	0.023	0.250	0.273	δ _{2m}	fatigue crack in HAZ		fatigue crack in HAZ
			H3	0.507	1.180	0.023	0.271	0.294	δ _{2m}			fatigue crack in HAZ
			H4	0.506	1.180	0.022	0.244	0.266	δ _{2m}			
		Weld Centerline (W) -40°C (-40°F)	W5	0.487	0.950	0.009	0.007	0.016	δ ₂ *			fatigue crack in weld
			W6	0.514	1.300	0.011	0.007	0.018	δ ₂ *			
			H1	0.481	0.810	0.021	0.073	0.094	δ ₂			fatigue crack in FL
		HAZ(H) - 40°C (-40°F)	H5	0.482	0.670	0.020	0.058	0.078	δ ₂	metallography-fracture region hybrid weld/FL		fatigue crack in HAZ
H6	0.487		0.870	0.020	0.062	0.082	δ ₂					
506 X80	6 o'clock 5 to 8 sector	Weld Centerline (W) -5°C (23°F)	W1	0.483	0.810	0.021	0.080	0.101	δ ₂			
			W2	0.484	0.790	0.022	0.186	0.208	δ ₂			
			W3	0.487	0.910	0.020	0.114	0.134	δ ₂	insignificant pop-in + small load drop give δ ₂		fatigue crack in weld
		HAZ(H) - 5°C (23°F)	H1	0.485	0.810	0.025	0.457	0.482	δ _{2m}			
			H2	0.511	1.340	0.022	0.151	0.173	δ ₂	small load drop - fatigue crack in FL		fatigue crack in FL
			H3	0.475	0.640	0.024	0.311	0.334	δ _{2m}			fatigue crack in HAZ
		Weld Centerline (W) -40°C (-40°F)	W4	0.481	0.880	0.015	0.019	0.033	δ ₂ *			
			W5	0.484	0.940	0.014	0.013	0.027	δ ₂	metallography-fracture region hybrid weld		fatigue crack in weld
			W6	0.482	0.810	0.016	0.021	0.038	δ ₂			
		HAZ(H) - 40°C (-40°F)	H4	0.478	0.750	0.020	0.102	0.122	δ ₂			
H5	0.474		0.690	0.013	0.010	0.024	δ ₂ *	metallography-fracture region hybrid weld/HAZ		fatigue crack in HAZ		
H6	0.493		1.010	0.025	0.201	0.226	δ ₂					
Notes												
a ₂ - average total crack length												
W - Specimen width												
a _{min} - minimum fatigue crack size												
δ ₂ * - pop in												

Table C3: Fracture Transition Behaviour Test Results

Pipe ID & Grade	Clock Location	Notch Location & Test Temp	Specimen ID	a_i/W	a_{min} (mm)	Elastic CTOD (mm)	Plastic CTOD (mm)	Total CTOD (mm)	Failure Type	NOTES	post test metallography - location w.r.t. hybrid weld (60% of thickness)	
498 X100	3 o'clock 2 to 5 sector	Weld Centerline -80°C	00	0.490	0.900	0.024	0.018	0.042	δ_c			
			01	0.487	0.820	0.026	0.024	0.050	δ_c			
		Weld Centerline -60°C	1	0.488	0.780	0.032	0.114	0.145	δ_c			fatigue crack in weld
			2	0.488	0.660	0.033	0.135	0.168	δ_u	fracture weld		fatigue crack in weld
		Weld Centerline -40°C	02	0.486	0.860	0.037	0.137	0.175	δ_m	ductile tear in weld		fatigue crack in weld
			3	0.491	0.850	0.039	0.170	0.208	δ_m			
498 X100	3 o'clock 2 to 5 sector	HAZ -80°C	12	0.492	0.890	0.033	0.038	0.071	δ_c			
			10	0.489	0.690	0.032	0.040	0.072	δ_c	fracture in HAZ		fatigue crack in HAZ
			4	0.492	0.010	0.038	0.089	0.127	δ_u			
		HAZ -60°C	13	0.490	0.890	0.033	0.039	0.072	δ_c			
			9	0.490	0.920	0.037	0.072	0.109	δ_c	fracture FL/HAZ		fatigue crack in FL
			5	0.491	0.960	0.037	0.126	0.163	δ_u			
			6	0.508	1.040	0.042	0.161	0.203	δ_m			
		HAZ -40°C	11	0.487	0.860	0.043	0.217	0.260	δ_m			
		HAZ -20°C	7	0.491	0.800	0.042	0.196	0.238	δ_m			fatigue crack in FL/HAZ
			8	0.489	0.820	0.042	0.250	0.292	δ_m			

BMT Fleet Technology is an innovative leader in providing through-life engineering support from concept development through design, construction, operations, life extension/upgrade and disposal. The company employs its technological expertise and practical experience to provide services to clients in the Marine, Defence, Energy & Environment, Civil & Industrial Infrastructure, and Transport industry sectors. We are committed to retaining and applying practical knowledge of sector-specific factors in developing responsive solutions to customer's needs. The company's hallmark of engineering excellence involves the provision of leading edge structural and mechanical system damage assessment, materials and welding engineering, inspection and maintenance management, naval architecture and marine engineering, environmental and cold regions engineering services.

Head Office - Ottawa

311 Legget Drive
Kanata, ON, Canada, K2K 1Z8
Tel: 613-592-2830

St. John's

25 Kenmount Road
St. John's, NL, Canada, A1B 1W1
Tel: 709-753-5690

Vancouver

611 Alexander Street, Suite 412
Vancouver, BC, Canada, V6A 1E1
Tel: 604-253-0955

Victoria

Shoal Point, 101-19 Dallas Road
Victoria, BC, Canada, V8V 5A6
Tel: 250-598-5150

Email: fleet@fleetech.com

Web: www.fleetech.com

United Kingdom - Loughborough

The Point, Granite Way, Mountsorrel
Loughborough, Leicestershire, LE12 7TZ, UK
Tel: +44 (0)1509 621814
Email: uk@fleetech.com

United Kingdom - Fareham

12 Little Park Farm Road
Fareham, Hampshire, PO15 5SU, UK
Tel: +44 (0)1489 553 200
Email: uk@fleetech.com

Or contact us through any of our sister BMT companies with over 60 offices worldwide to serve you.



Canadian offices certified to ISO 9001:2000. We are dedicated to ongoing quality and management systems.